UNIVERSITY OF CALIFORNIA, SAN DIEGO

Progress Towards the Total Synthesis of the Hasubanan Alkaloids and Acutumine

A dissertation submitted in partial satisfaction of the
requirements for the degree Doctor of Philosophy

in

Chemistry

by

Thong Xuan Nguyen

Committee in charge:

Professor Yoshihisa Kobayashi, Chair
Professor Daniel Donoghue
Professor William Fenical
Professor Kyriacos Nicolaou
Professor Joseph O'Connor

2009

The Dissertation of Thong Xuan Nguyen is approved, and it is
acceptable in quality and form for publication on microfilm and electronically:

_____

_____

_____

_____

_____
chair

University of California, San Diego

2009

To my family and friends

TABLE OF CONTENTS

LIST OF ABBREVIATIONS

Ac	acetyl, acetate
AcOH	acetic acid
i-Am	*iso*-Amyl
aq.	aqueous
Ar	aryl
Bn	benzyl
BOC	*tert*-butyloxycarbonyl
bp	boiling point
br	broad
n-Bu	*normal*-butyl
t-Bu	*tertiary*-butyl
calcd	calculated
CAN	ceric ammonium nitrate
cat.	catalytic amount
CSA	camphorsulfonic acid
d	doublet
dr	diastereomeric ratio
DCM	dichloromethane
DMAP	4-dimethylaminopyridine
DMF	*N,N*-dimethylformamide
DMP	dess-martin periodinane
DMS	dimethylsulfide
DMSO	dimethylsulfoxide
EI	electron impact
equiv. (eq.)	equivalent
Et	ethyl
h	hour

Hz	hertz
IBX	2-iodoxybenzoic acid
IC	inhibitor concentration
IR	infrared (spectrum)
KHMDS	potassium bis(trimethylsilyl)amide
LDA	lithium diisopropylamine
LHMDS	lithium bis(trimethylsilyl)amide
m	multiplet
μm	micromolar
Me	methyl
min	minutes
mol	mole
MOM	methoxymethyl
mp	melting point
Ms	methanesulfonyl (mesyl)
nM	nanomolar
NMR	nuclear magnetic resonance
[O]	oxidation
Pd/C	palladium on charcoal
Ph	phenyl
PhH	benzene
Piv	pivaloyl
PMB	*para*-methyoxybenzyl
PMP	*para*-methyoxyphenyl
ppm	parts per million
PPTs	pyridinium *para*-toluenesulfonate
i-Pr	*iso*-propyl
Pro	proline
Py	pyridine
Quant.	quantitative

rt	room temperature
s	singlet
t	triplet
TBAF	tetrabutylammonium fluoride
TBAI	tetrabutylammonium iodide
TBDPS	*tertiary*-butyldiphenylsilyl
TBS	*tertiary*-butyldimethylsilyl
Tf	trifluoromethanesulfonyl
TFA	trifloroacetic acid
TFAA	trifloroacetic anhydride
TFE	2,2,2-trifluoroethanol
THF	tetrahydrofuran
TLC	thin-layer chromatography
TMS	trimethylsilyl
(*p*-)TsOH	*para*-toluenesulfonic acid
UV-Vis	Ultraviolet-Visible
Δ	heat to reflux

LIST OF FIGURES

LIST OF SCHEMES

LIST OF TABLES

ACKNOWLEDGEMENTS

I would like to thank my advisor, Yoshihisa Kobayashi. I began working for Yoshi in the summer of 2005. My first impression of Yoshi was that he was an intense boss. He expected the best from his graduate students and was not willing to accept anything less. I appreciate all his efforts to provide for all his graduate students a challenging learning experience. I will forever be grateful of the guidance that Yoshi has given me throughout my graduate career.

I would like to thank my committee members. Thank you for taking your time to meet with me whenever I needed a different perspective on my chemistry. Your critiques and encouragements show your devotion to higher learning and quality research.

I would like to thank my family for all their support. I know that I have been missed by my entire family and I know the sacrifices we all have made. I have immense love for all my family members and deeply grateful for your understanding of the choices I have made in my lifetime. I hope to have brought pride to you.

I would like to thank my friends for cracking my shell. I am a different person than I was four years ago when I first started. I have experienced a profound personal transformation because of all of you beautiful people. For that, I am eternally grateful for this wonderful experience.

CHAPTER TWO, in part, is a reprint of the material as it appears in (1) Nguyen, T. X.; Kobayashi, Y. "Synthesis of the Common Propellane Core Structure of the Hasubanan Alkaloids" *J. Org. Chem.* 2008, *73*, 5536-5541.

VITA

2005	B.S. Chemistry University of California, Irvine Irvine, CA
2005-2009	Teaching Assistant Department of Chemistry and Biochemistry University of California, San Diego
2005-2009	Research Assistant University of California, San Diego
2007	M.S. Chemistry University of California, San Diego La Jolla, CA
2009	Ph.D. Chemistry University of California, San Diego La Jolla, CA

PUBLICATIONS

Nguyen, T. X.; Kobayashi, Y. "Synthesis of the Common Propellane Core Structure of the Hasubanan Alkaloids" *J. Org. Chem.* **2008**, *73*, 5536-5541.

Nguyen, T. X.; Kobayashi, Y. "Diphenyl Diselenide" *Encyclopedia of Reagents for Organic Synthesis* [*Online (e-EROS*)]. *John Wiley & Sons Ltd.* **2007**.

Buchner, K.; Clark, T. B.; Loy, J. M.; Nguyen, T. X.; Woerpel, K. A. "Alkylidenesilacyclopropanes Derived from Allenes: Applications to the Selective Synthesis of Triols and Homoallylic Alcohols" *Org. Lett.* **2009**, *11*, 2173-2175.

ABSTRACT OF THE DISSERTATION

Progress Towards the Total Synthesis of the
Hasubanan Alkaloids and Acutumine

by

Thong Xuan Nguyen

Doctor of Philosophy in Chemistry

University of California, San Diego, 2009

Professor Yoshihisa Kobayashi, Chair

Acutumine, a chlorine containing natural product has recently been rediscovered to inhibit T-cell growth, and aid in memory by enhancing memorisation and anti-amnesic properties in mice and rats. These studies reveal the promising benefits of acutumine in alleviating conditions that are related to loss of memory such as Alzheimer's, Parkinson's and Pick's disease. We have developed a synthetic strategy that allows access to the common [4.4.3.0] propellane core structure, including 2,3-dimethoxycyclohexenone and *N*-methylpyrrolidine moieties, among the hasubanan alkaloids featuring a facile conversion of a sterically hindered amide to ester via *N*-acylbenzotriazole and a

Dieckmann cyclization of *cis*-fused bicycle to install the propellane framework. It is envisioned that a strategy towards the common propellane core skeleton found in the hasubanan alkaloids can be applied towards the synthesis of acutumine. Progress towards the total synthesis of acutumine is reported, featuring photo[2+2]cycloaddition reactions to install spiro[5.5]ring stereoselectively.

CHAPTER ONE

Background to the Hasubanan Alkaloids and Acutumine

1.1 Background on the Hasubanan Alkaloids

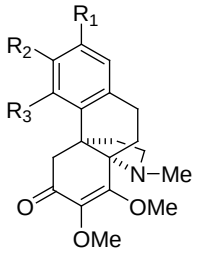

R_1 = H, R_2 = R_3 = OMe	Hasubanonine (**1**)
R_1 = R_2 = OMe, R_3 = H	Runanine (**2**)
R_1 = R_2 = -OCH_2O-, R_3 = H	Delavanine (**3**)
R_1 = H, R_2 = OMe, R_3 = OH	Aknadinine (**4**)
R_1 = H, R_2 = OH, R_3 = OMe	Homostephanoline (**5**)
R_1 = H, R_2 = OEt, R_3 = OMe	*O*-Ethylhomostephanone (**6**)
R_1 = OH, R_2 = OMe, R_3 = H	Cephatonine (**7**)

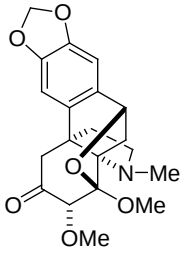

Periglaucine A (**8**)
(Yan 2007)

Figure 1.1.1 Structures of the hasubanan family of alkaloids **1-7** and periglaucine A (**8**)

A number of natural products bearing the unique propellane [4.4.3.0] core structure have been reported from plant sources (Figure 1.1.1).[1-11] Hasubanonine (**1**) was the first hasubanan alkaloid discovered in the early 1950s by Kondo and it is

representative of this class of alkaloids. Due to its close structural resemblance to the morphinan alkaloids, initially its structure was incorrectly assigned as a morphinan framework.[12] The structure of hasubanonine (**1**) was elucidated by Tomita in 1965, over a decade after its discovery.[4] To date, over 40 members of this family has been reported. The hasubanan alkaloids **1-7** share the 2,3-dimethoxycyclohexenone and *N*-methylpyrrolidine ring as a component of the hasubanan framework differing only in the substitution pattern on the aromatic ring (Figure 1.1.1). These hasubanan alkaloids have initially received attention due to their close resemblance to the morphine alkaloids, although no reported analgesic bioactivities have been disclosed. The skeletal structure of the hasubanan alkaloids is different from morphinan alkaloids in forming a five membered pyrrolidine ring as opposed to a six membered piperidine ring, and its absolute configuration is antipodal to that of morphinan (Figure 1.1.2). This has led Schultz to note that the unnatural enantiomers of these alkaloids may possess analgesic activities.[13] Toward this effort, the unnatural enantiomer of cepharamine (**9**) was synthesized; however, no biological activities have been disclosed.

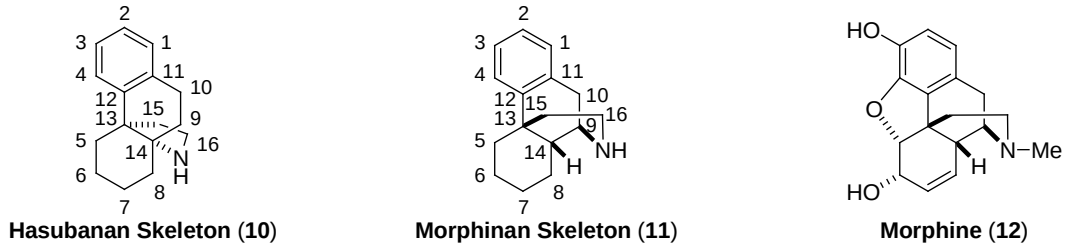

Hasubanan Skeleton (**10**) **Morphinan Skeleton** (**11**) **Morphine** (**12**)

Figure 1.1.2 Structure of the hasubanan and morphinan skeleton

Recently in 2007, Yan isolated four new hasubanan-type alkaloids, the periglaucines.[14,15] It was reported that these alkaloids possess anti-hepatitis B virus activity with IC_{50} values ranging from 0.47–1.72 mM. These new findings have increased our interest in a general synthetic strategy towards the common propellane core structure of the hasubanan alkaloids. It is interesting to note that long after the first discovery of the hasubanan alkaloids in the 1950's, it still remains a relevant topic in the scientific community. It is envisioned that a strategy towards the common propellane core skeleton found in the hasubanan alkaloids can be applied towards the synthesis of the alkaloids **1-7** starting from common precursors differing only in the substituent on the aromatic ring.

In addition to the synthesis of the hasubanan alkaloids, we also propose the synthesis of the periglaucine A (**8**) from delavanine (**3**) as shown in Scheme 1.1.1. It is envisioned that benzylic oxidation of **3** using DDQ should provide the 1-tetralone **13**. Reduction of the following ketone to reveal alcohol **14**, followed by acid catalyzed conjugate addition toward the dimethoxycyclohexenone moiety should allow an entry into periglaucine A (**8**).

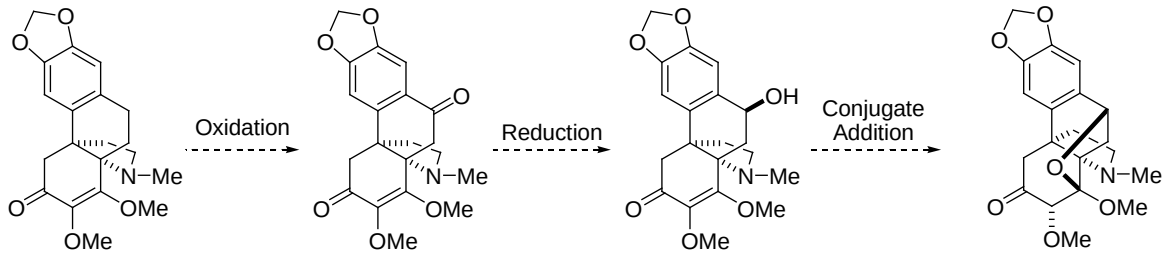

Delavanine (**3**) **13** **14** Periglaucine A (**8**)

Scheme 1.1.1 Suggested conversion of the delavanine (**3**) to periglaucine A (**8**)

1.2 Biosynthesis of Morphine

Considering the structural resemblance of hasubanonine (**1**) to morphine (**12**), some parallels can be made about the alkaloids. Extensive studies on the biosynthesis of morphine have shown that morphine is derived from two simple building blocks of tyrosine.[16] The intermediate 1-benzylisoquinoline, (*R*)-reticuline **15**, has been established as the precursor of morphine in the biosynthetic pathway (Scheme 1.2.1). The concept of phenolic oxidative radical coupling is a central theme in the synthesis of the morphinan alkaloids. One-electron oxidation of the phenol groups gives resonance stabilized radicals at the *ortho* position of the phenol group and *para* position of the benzyl group. Coupling of the intermediate radicals leads to dienone salutaridine (**16**) after rearomatization. Once the major framework of the morphinan has been established, subsequent cyclization, demethylation and reduction will lead to morphine (**12**). Early studies into the biosynthesis of the hasubanan alkaloids were first directed by the

knowledge established by the investigations into the biosynthesis of morphine (**12**). Indeed, Battersby who conducted research on hasubanonine (**1**) proposed a similar oxidative coupling mechanism in the biosynthetic pathway.

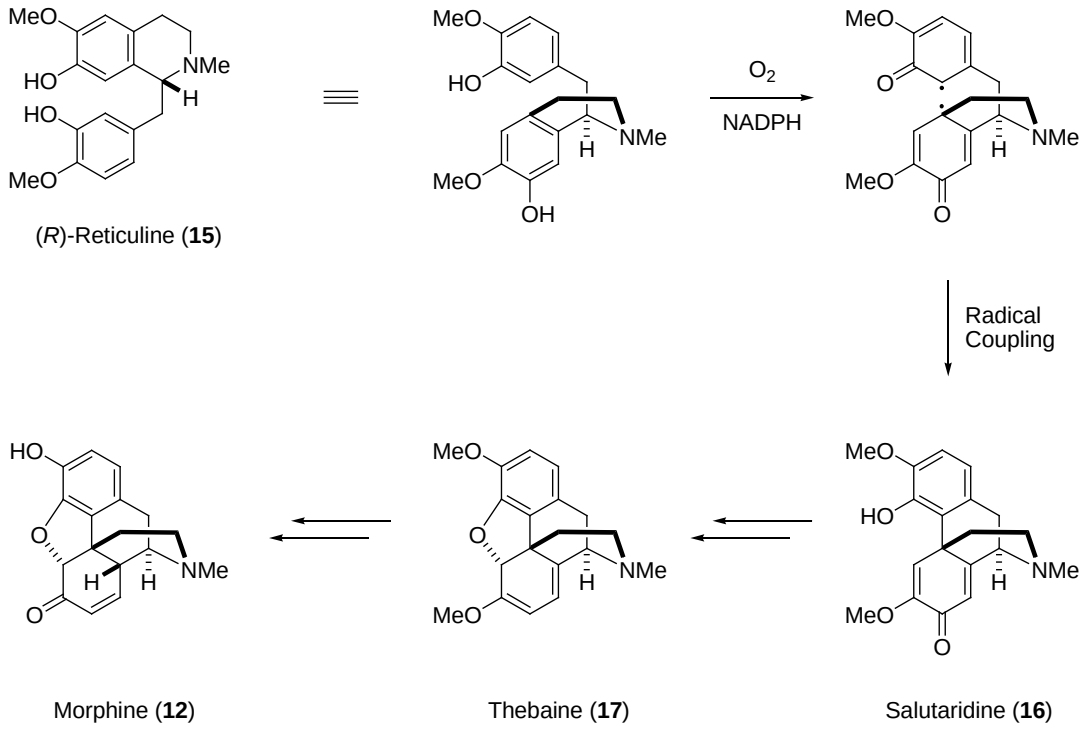

Scheme 1.2.1 The biosynthesis of morphine (**12**)

1.3 Biosynthesis of Hasubanonine

Initial investigations into the biosynthesis of hasubanonine (**1**) have shown that it is derived from the relatively simple precursor tyrosine (Scheme 1.3.1). Based on the extensive studies on the biosynthesis of morphine, several inferences have been made for

the biosynthesis of the hasubanan alkaloids. Due to its structural resemblance to the morphinan alkaloids, initial investigations into their biosynthesis employed 1-benzylisoquinoline framework in feeding experiments.[17-19] Six ^{14}C-labelled isoquinolines were prepared by Battersby and fed to *Stephania japonica* plants whereupon the labelled carbon was traced to see if they had been incorporated into the alkaloid. It was proposed that oxidative radical coupling of isoquinoline **19** led to hasubanonine (**1**), which is in accordance with the oxidative radical coupling theory in the biosynthesis of morphine. However, these isoquinolines are distinct from that of the morphinan alkaloid biosynthesis in that it requires two phenolic hydroxyl groups in one of the rings undergoing oxidative coupling. It was also discovered that isoquinolines in their secondary amino or *N*-methylated form led to incorporation into the alkaloid. Battersby concluded that the timing of *N*-methylation is not pivotal. Later stages in the biosynthetic pathway are not clearly defined. One of the proposals for the final stages of the biosynthetic pathway suggests that the resulting morphinandienone **21** undergoes a Michael-type addition and reduction of the aziridinium intermediate **22** to provide hasubanonine (**1**). There is evidence that shows the morphinan skeleton can be converted into the hasubanan skeleton via an aziridinium ion intermediate.

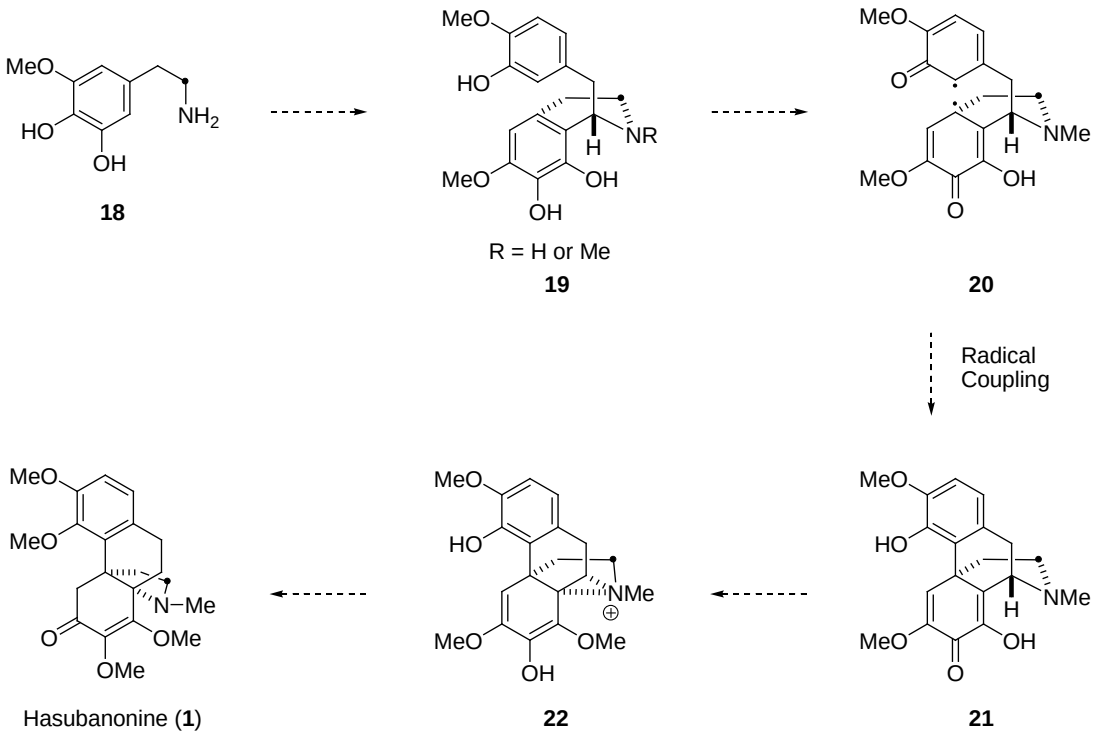

Scheme 1.3.1 The proposed biosynthesis of hasubanonine (**1**) by Battersby

1.4 Chemical Conversion of the Morphinan to the Hasubanan Alkaloids

Little is known about the late stages of the biosynthesis of the hasubanan alkaloids. Early investigations by Battersby have shown that several 1-benzylisoquinolines are precursors for the synthesis of hasubanonine (**1**). Since similar isoquinolines have been established as precursors for the synthesis of the morphinan alkaloids, it has been suggested that the same mechanism pathway is shared by both alkaloids; the major difference is that the different enzymes generate the antipodal,

"enantiomeric" substrates **16** and **21**. One speculation on the fragmentation-rearrangement of the morphinan skeleton into the hasubanan skeleton is the formation of an intermediate aziridinium ion followed by enzymatic reduction. There is evidence that suggests the hasubanan alkaloids proceed through an aziridinium ion intermediate in their biosynthesis (Scheme 1.4.1).[20] Synthetic investigations by Kirby have shown that the alkaloid **23**, bearing the morphinan framework is converted to the hasubanan framework, by treatment with silver acetate. Presumably, the coordination of the allylic iodide to the silver metal generates a transient allylic carbocation. The proximal tertiary amine undergoes an intramolecular S_N2'-type substitution to give an aziridinium ion **24** which is opened by the acetate anion at the less substituted position to provide **25** in 33% yield.

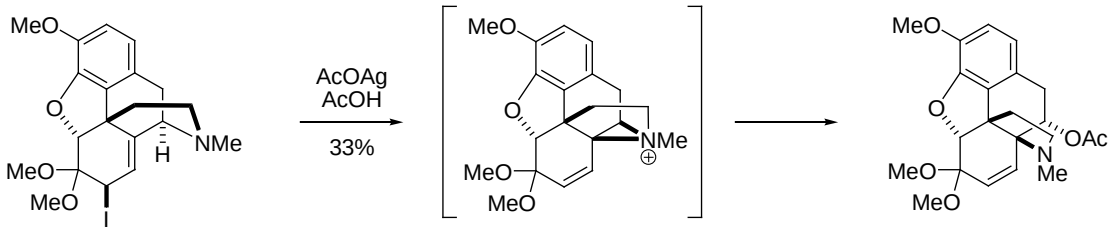

23 **24** **25**

Scheme 1.4.1 Conversion of the morphinan to the hasubanan skeleton

1.5 Ibuka Synthesis of Hasubanonine

The first and only synthesis of hasubanonine was reported by Ibuka in 1974.[10] The partial description of the synthesis of hasubanonine (**1**) is shown in Scheme 1.5.1.

The synthesis began with the alkylation of 7,8-dimethoxy-2-tetralone (**26**) with chloroacetonitrile followed by regioselective conjugate addition with methyl vinyl ketone. The intermediate 1,1-disubstituted-2-tetralone product (not shown) cyclized under the alkaline conditions to provide the bicycle **27**. Treatment of **27** with sodium ethoxide in ethanol gave the hasubanan propellane core. Presumably, under the basic conditions fragmentation of the tertiary alcohol gave the retro-Aldol product **28** which equilibrates to enolate **29**.[21] Intramolecular aldol reaction with **29** gave β-alkoxylketone **30**. The resulting alkoxide captures the tethered nitrile moiety in its *cis*-fused bicyclic form to provide **31**. Elimination of **31** with base followed by conjugate addition of carboxamide **32** gave the hasubanan propellane core structure. Further chemical manipulations provided (±)-hasubanonine (**1**) in 15 additional steps. The first total synthesis of hasubanonine (**1**) proved to be interesting in forming the hasubanan framework in 3 steps. However, one drawback is the exhaustive protocol in subsequent steps to access the correct oxygenated functionality.

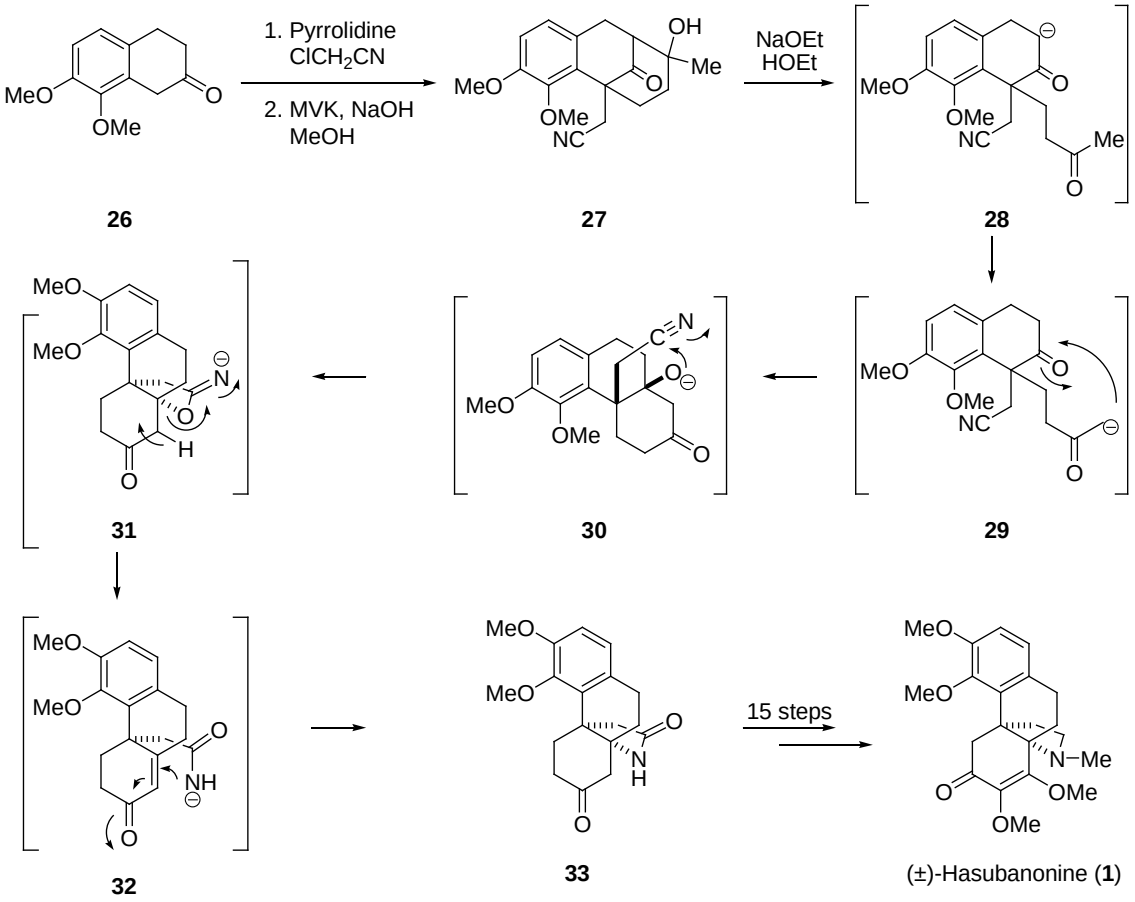

Scheme 1.5.1 Ibuka synthesis of (±)-hasubanonine (**1**)

1.6 Castle Attempted Synthesis of Hasubanonine

In 2006, Castle reported the total synthesis of (±)-hasubanonine (**1**) that employed a Lewis acid catalyzed conjugate substitution of a tethered ethylamine side chain **36** to provide hasubanonine (**1**) in racemic form (Scheme 1.6.1).[9] However, in 2008 it was reported that their product had been misassigned.[22] Under the Lewis acidic conditions, **35** rearranged to an *N,O*-acetal "isohasubanan" alkaloid **37**. It was during the synthetic

investigations into the total synthesis of runanine (**2**) and aknadinine (**4**), that it was discovered that the ^{13}C-NMR signal did not match with the reported values of those natural products. After further ^{13}C-NMR comparative studies it was revealed that the isohasubanan alkaloid **37** was indeed the isolated product of the Lewis acid catalyzed reaction conditions. Therefore, Castle never achieved the total synthesis of these hasubanan alkaloids.

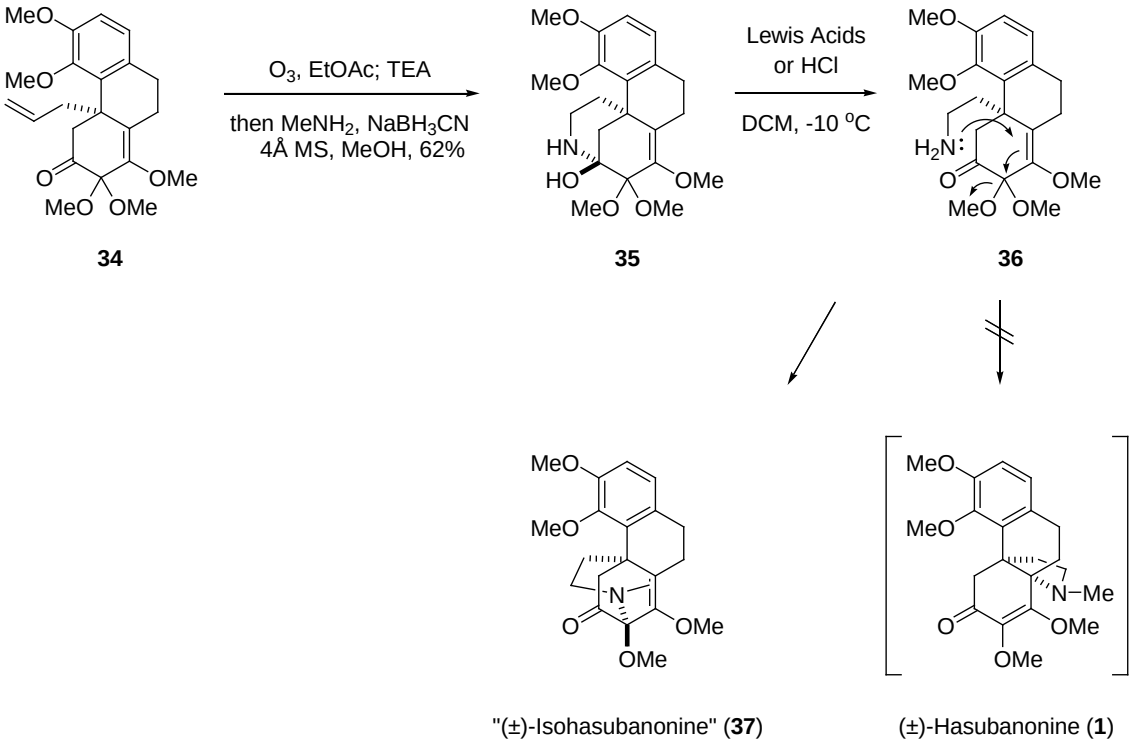

Scheme 1.6.1 Castle's synthesis of "(±)-isohasubanonine" (**37**)

1.7 Background on Acutumine

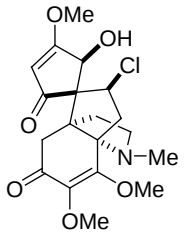

(-)-Acutumine (**38**)

Figure 1.7.1 Structure of (-)-acutumine (**38**)

Acutumine (**38**) is a chlorine containing natural product that was first isolated by Goto and Sudzuki in 1929 from the climbing plant *Sinomenium acutum* (Figure 1.7.1).[23] However, its structure was not completely assigned until 1967 by Tomita, almost 40 years after its discovery.[24] Acutumine (**38**) is structurally interesting in bearing five contiguous stereocenters in a congested framework including two adjacent quaternary carbons and a spirocycle and a stereogenic alkyl chloride next to the spirocenter. In light of the molecular complexity of acutumine (**38**), several groups have reported efforts toward the total synthesis of the alkaloid.[25,26] To date, there has been one reported total synthesis of acutumine (**38**).[27]

Chinese folk medicines have used the stems and root vines from which acutumine was isolated to treat fevers, rheumatic arthritis, articular swelling and pain.[28] Almost a century has passed since its discovery; some studies have begun to emerge showing biological benefits of acutumine (**38**). It has recently been reported that acutumine (**38**) inhibits T-cell growth with an IC_{50} value of 13.2 μM.[29] The newly reported biological activities as well as its structural complexity has garnered acutumine much attention from

the synthetic community. To our knowledge two other groups have reported efforts toward the total synthesis of acutumine in the literature.[25,26,30]

In addition, early investigations revealed that it can also aid in memory by enhancing memorisation and anti-amnesic properties in mice and rats.[31] In several animal models, acutumine (**38**) has shown to be effective as an anti-amnesic agent. In the Morris water maze test, mice were trained to find the platform under a specified time. Once the mice have been trained, scopolamine, which is known to induce memory impairments, was administered (Figure 1.7.2). Mice with treatments of acutumine (**38**) and its derivatives have shown to possess anti-amnesic properties by counteracting the effects of scopolamine in a dose dependent manner.

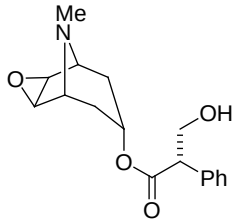

Scopolamine (**39**)

Figure 1.7.2 Structure of scopolamine (**39**)

In the object recognition test, the rats are introduced to two identical objects and they are allowed to explore the objects. In a later session, the rats are introduced to the previous object and a new object. The time the rats use to explore the previous object is indicative of their memory ability. Early investigations have shown rats with treatments of acutumine (**38**) and its derivatives preferably explored the new object compared to rats

under the control conditions. These rats apparently retained the memory of the previous object. In the natural course of life, memory loss is a normal process in the late stages of life. With the rise in life expectancy, there is an increased demand and interest in medicine with mnemocognition facilitating properties. These studies reveal the promising benefits of acutumine in alleviating conditions that are related to loss of memory such as Alzheimer's, Parkinson's and Pick's disease.

1.8 Biosynthesis of Acutumine

Due to its structural similarities with the hasubanan and morphinan alkaloids, Barton proposed that acutumine may originate from the phenolic oxidative coupling reaction of 1-benzylisoquinoline **40** (Scheme 1.8.1).[32] Oxidation of **41** followed by hydrolytic cleavage that entails a Favorskii rearrangement is predicted to give the cyclopentenone spirocycle **45**. Conjugate addition by the secondary amine in **45** provides the aziridinium ion intermediate. Ring-opening reaction followed by addition of a chloride ion is expected to give the chlorinated framework. Preliminary results from the Sugimoto group has confirmed that acutumine is derived from two simple units of tyrosine.[33] The proposed biosynthetic pathway via benzylisoquinoline intermediate **40** is not surprising considering the knowledge accrued from extensive studies of alkaloids; however, efforts to support the subsequent Favorskii rearrangement have been fruitless.

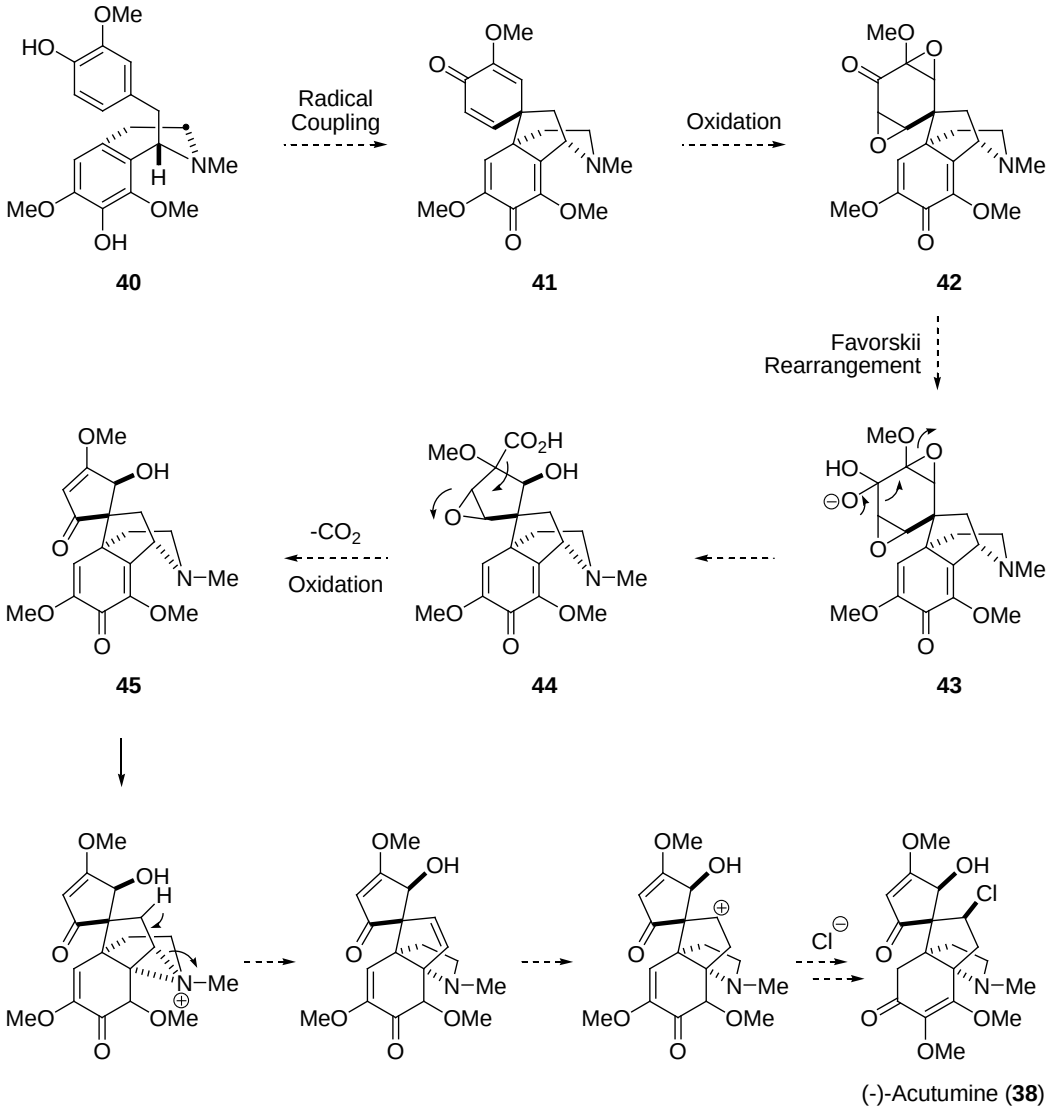

Scheme 1.8.1 Barton's proposal for the biosynthesis of acutumine (**38**)

Wipf attempted to test the feasibility of Barton's proposed biosynthesis of the spirocycle-fused methoxycyclopentenone **45** in the laboratory.[34] Oxidation of dienone **46** with basic hydrogen peroxide gave mono-epoxide **47** in 67% yield (Scheme 1.8.2). Subsequent oxidation with *m*-CPBA gave the highly oxygenated cyclohexanone **48**; however, Barton's proposed cascade reaction was not observed. Instead the highly

strained epoxyacetal **48** fragmented to give a transient oxocarbenium ion that was captured by the peracid to give **50**. A methyl ether mediated acyl shift of **50** gave the ring-expansion product. Subsequent acyl transfer provided the lactone **52**. Wipf showed that chemically epoxyether **47** prefer an alternative rearrangement than that of Barton's Favorskii rearrangement. It was noted that an enzyme might have taken a different course allowing for a Favorskii-type fragmentation to generate the spirocycle.

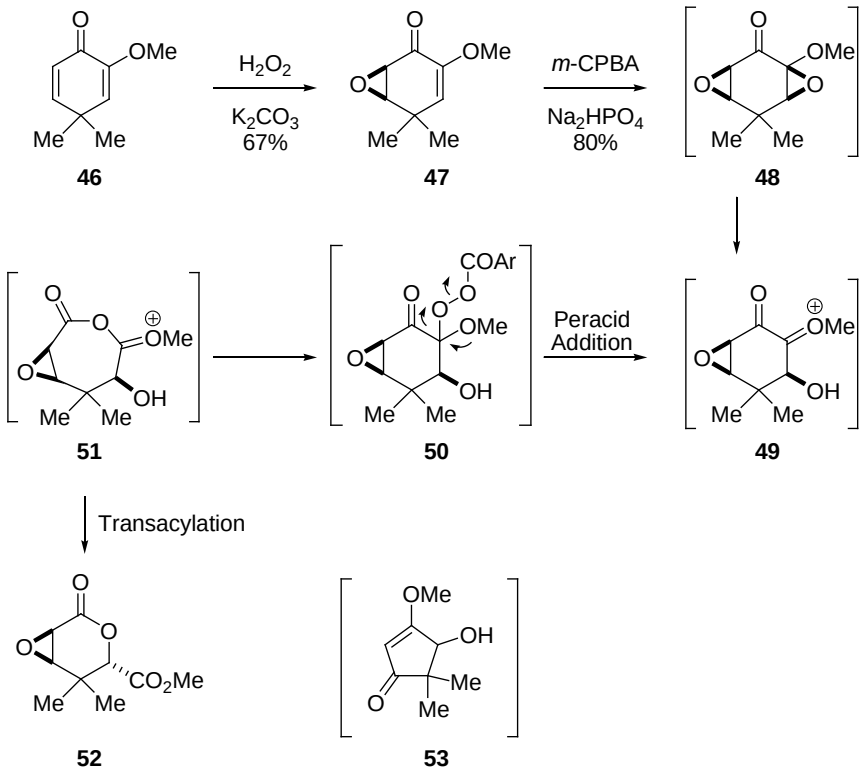

Scheme 1.8.2 Wipf attempted model of Barton's proposed biosynthetic route

Following the isolation of acutudaurin (**58**),[35] Wipf proposed an alternative biosynthetic pathway for acutumine (**38**). Oxidation of **54** followed by hydrolytic

cleavage and skeletal rearrangement is expected to give **56** (Scheme 1.8.3). Decarboxylation of **56** should give the cyclopentenone core of the spirocycle.

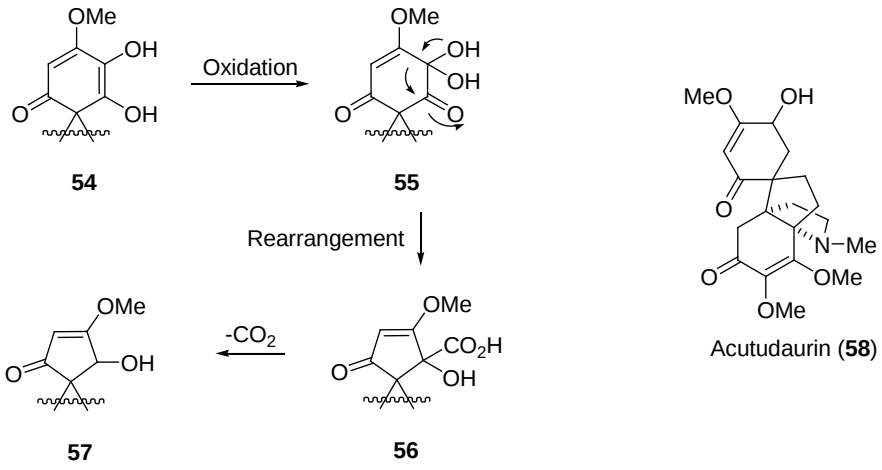

Scheme 1.8.3 Wipf's proposal for the biosynthesis of the northern fragment of acutumine

Naturally occurring organohalogen compounds are typically derived from bacteria, fungi, and marine algae.[36] Natural products containing halogens in higher plants are rare and their biosynthesis has yet to be fully understood. Barton proposed that the chlorination of acutumine (**38**) proceeded by way of an aziridinium ion intermediate, which upon ring opening would provide the framework (Scheme 1.8.1).[32] Subsequent chloride addition would provide the chlorinated framework. There is evidence that suggests the production of acutumine is highly dependent upon the concentration of chloride ion in the environment.[33] However, an increasing amount of evidence is directing a different pathway for chlorination. Early investigations into the biosynthesis of acutumine by Sugimoto have revealed some clues into the halogenation process. It was discovered that dechloroacutumine was a biosynthetic precursor of acutumine;

however, a low production rate of acutumine (**38**) was observed when ^{3}H-labelled dechloroacutumine (**62**) was fed to the roots.[37] This suggested that dechloroacutumine was on the pathway to acutumine but not its immediate precursor. In addition, investigations into feeding experiments using ^{36}Cl gave four chlorinated alkaloids as shown in Scheme 1.8.4.[38-40] These alkaloids were separated and independently fed into the root cultures. Mutual interconversion between ^{36}Cl-labelled acutumine (**38**) and its *N*-demethylated isomer acutumidine (**59**) showed that similar to the biosynthesis of hasubanonine (**1**), the *N*-methylation step is not critical. Interestingly, dauricumine (**60**) is converted to both acutumine (**38**) and acutumidine (**59**). However, epimerization of acutumidine (**59**) to dauricumidine (**60**) was not observed. This led Sugimoto to conclude that dauricumine (**60**) was the first chlorinated alkaloid to be synthesized and subsequent epimerization at the hydroxyl position should provide acutumine (**38**). Therefore, the precursor for the chlorination step should be epi-dechloroacutumine (**63**) (Scheme 1.8.5). For further investigation into the chlorination enzyme, it would also be important to supply dechloro and epi-dechloro substrates by total synthesis.

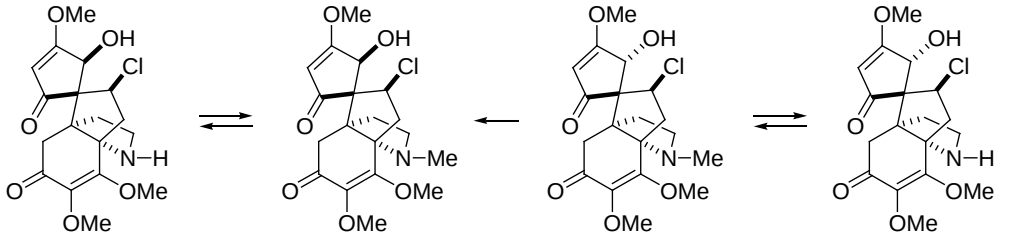

Scheme 1.8.4 The biosynthetic relationship between the chlorinated alkaloids

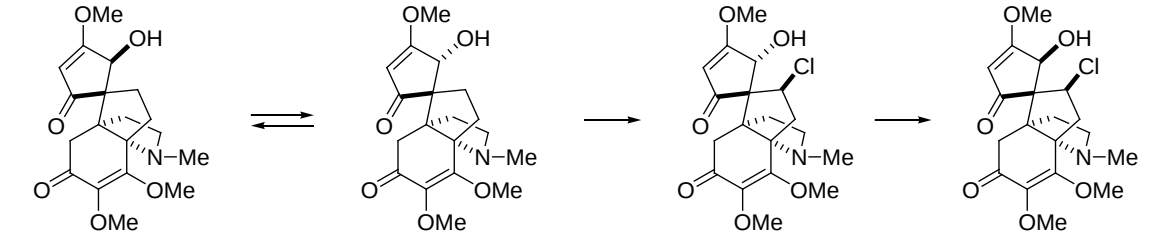

Dechloroacutumine (**62**) Epi-dechloroacutumine (**63**) Dauricumidine (**61**) (-)-Acutumine (**38**)

Scheme 1.8.5 The chlorination pathway in the biosynthesis of acutumine

1.9 Castle's Synthesis of Acutumine

There are two key reactions in the synthesis of the northern fragment of acutumine reported by the Castle group (Scheme 1.9.1).[25,26] First, the chlorine atom is installed by an S_N2 of allylic alcohol **65** with methanesulfonyl chloride and triethylamine. The alcohol **66** was derived from a diastereoselective reduction of ketone **64** using the Corey-Bakshi-Shibata catalyst. The TES ether moiety was selectively deprotected in the presence of the TBS group to provide the desired cyclopentenone **67**. Second, Castle employed a radical-polar crossover reaction to construct the spirocycle fragment of acutumine. Treatment of **67** to photochemical conditions and oxaziridine oxidant gave the spirocycle **68** in 62% yield. Presumably the aryl radical was directed to the opposite face of the alkene by the bulky silyloxy group. The resulting α-keto radical captured the oxaziridine oxidant to provide **68** as a single diastereomer. It was postulated that the aryl hydrogen directed the approach of the oxidant to the *si* face of the enolate. The radical-

polar crossover reaction allowed access to the congested spirocycle containing four contiguous stereocenters. There are several aspects of the investigations that are noteworthy: (1) The chlorospirocycle was successfully installed with the correct relative stereochemistry. (2) Installation of the propellane core to hydroindane moiety will furnish acutumine, although further manipulation with alkyl chloride functional group can be difficult to be carried out through the total synthesis due to the compatibility under the reaction conditions.

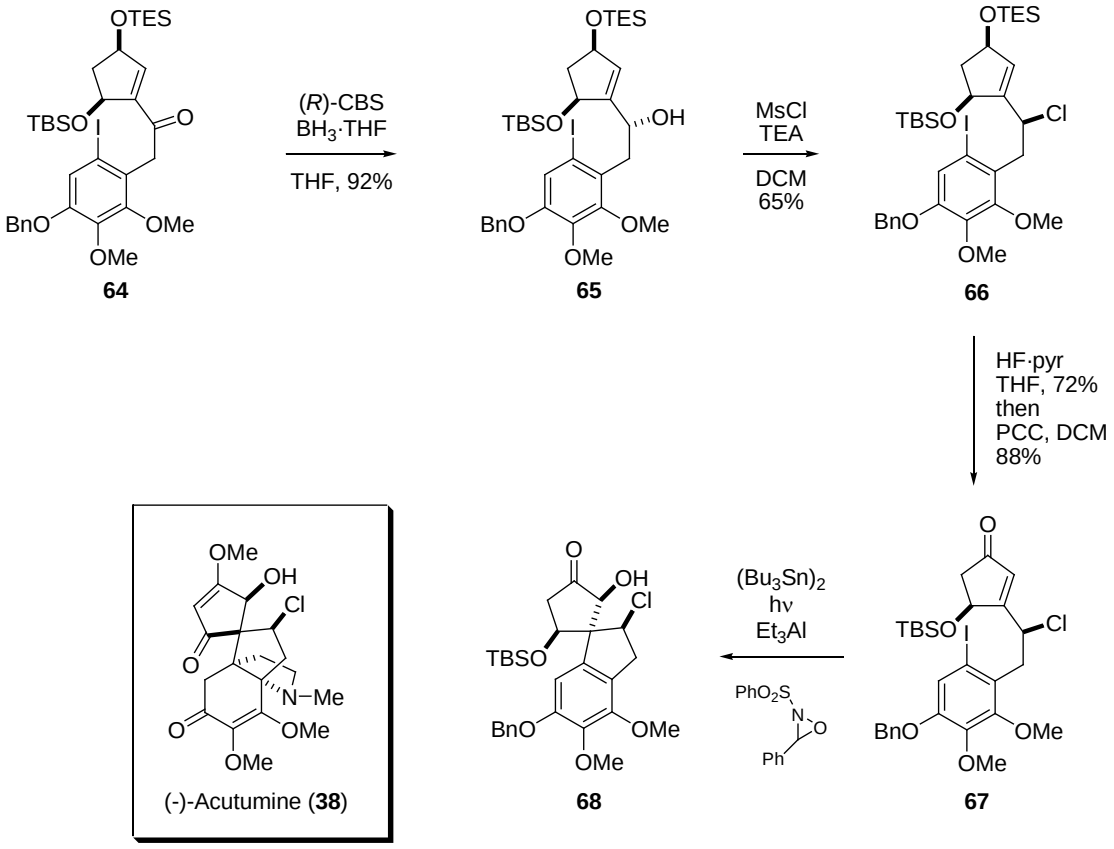

Scheme 1.9.1 Castle's synthesis of the spirocycle of acutumine

The Castle synthesis of the southern fragment of acutumine is demonstrated on a model compound **73** (Scheme 1.9.2). Castle employed a key anionic oxy-Cope rearrangement of **70** to provide the requisite quaternary carbon center in a congested site. Clearly the stereoselective allylation could be challenging in the presence of the spiro stereocenter. Subsequently, the propellane core structure is constructed by a Lewis acid promoted conjugate substitution of a secondary amine onto an α,β-unsaturated ketal **72**. Surprisingly, the model compound existed as the more stable enol tautomer.

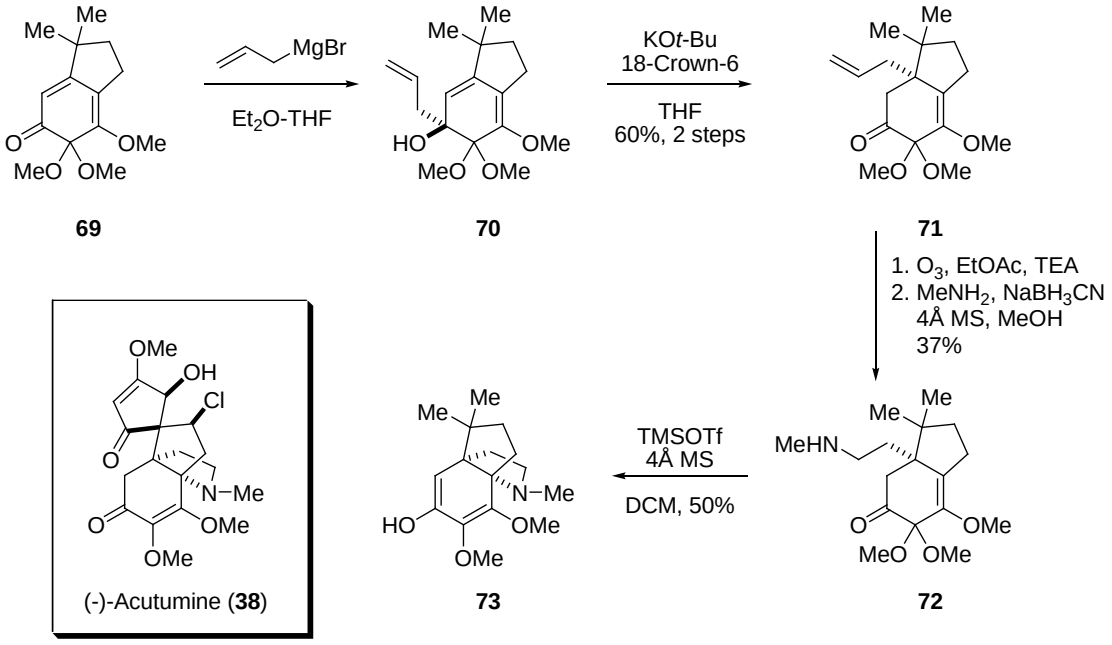

Scheme 1.9.2 Castle's synthesis of the southern core structure of acutumine

With a synthetic strategy for the creation of the southern propellane core structure **73** in hand, Castle employed it towards the synthesis of acutumine (**38**) from spirocycle **68**. In 9 steps with an overall 17% yield, spirocycle **68** could be converted to masked *o*-benzoquinone **74**, which is set up to do a similar Lewis acid promoted conjugate

substitution as **72**. Treatment with BCl_3 gave the cyclization product **75**. The TBS-ethers in **75** were deprotected and oxidized, followed by removal of the benzyl group gave dione **77**. Methylation of **77** with $TiCl_4$ in MeOH gave acutumine (**38**) in 52% followed with 14% of the undesired methyl enol ether regioisomer **78**.

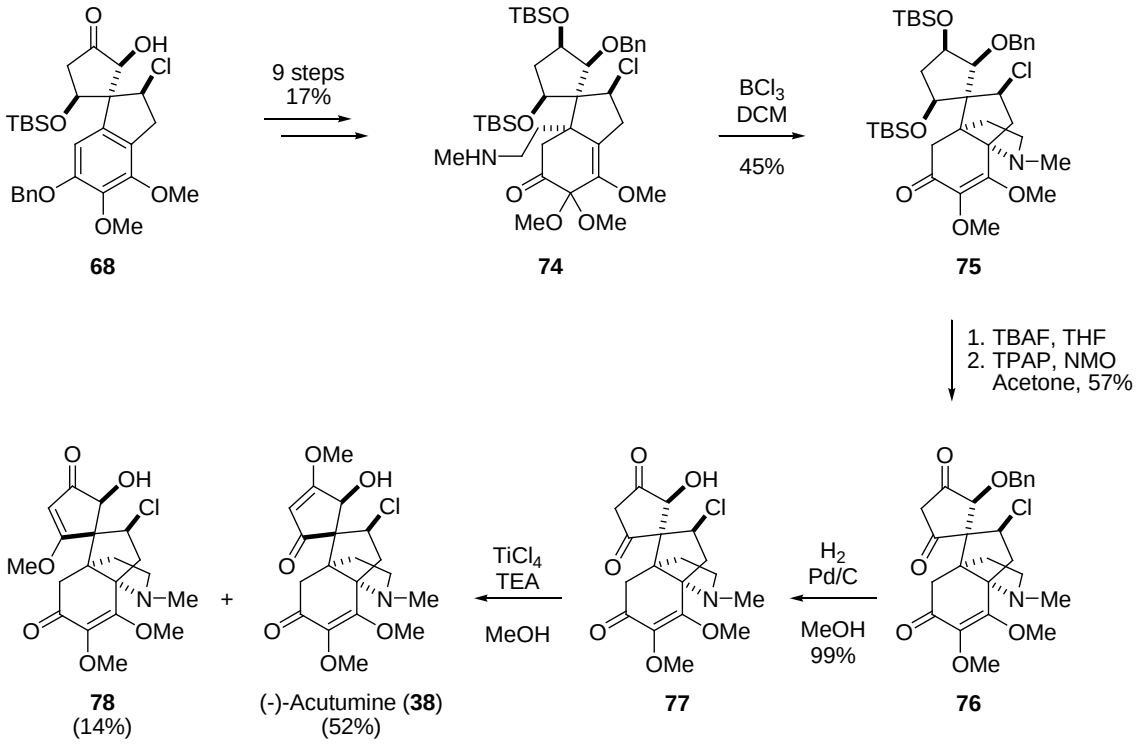

Scheme 1.9.3 Castle's total synthesis of (-)-acutumine (**38**)

1.10 Sorensen Synthesis of the Propellane Core Structure of (-)-Acutumine

Sorensen approached the spirocycle of acutumine by a classical carbonyl approach (Scheme 1.10.1).[30] Initially it was postulated that the vinylogous carbonate **79** can be converted to the tricyclic β-ketoester **83** in one step by treatment with base. Unfortunately, treatment of **79** to strong, non-nucleophilic bases led to a low conversion and the reaction was accompanied by many side products. To circumvent this problem, a more gentle reaction condition was explored. Enolization of vinylogous carbonate **80** with *n*-Bu_4NOAc gave enolate **81**, which underwent Michael cyclization to provide the bicyclic **82**. A subsequent kinetic enolization gave the Dieckmann cyclized **83**.

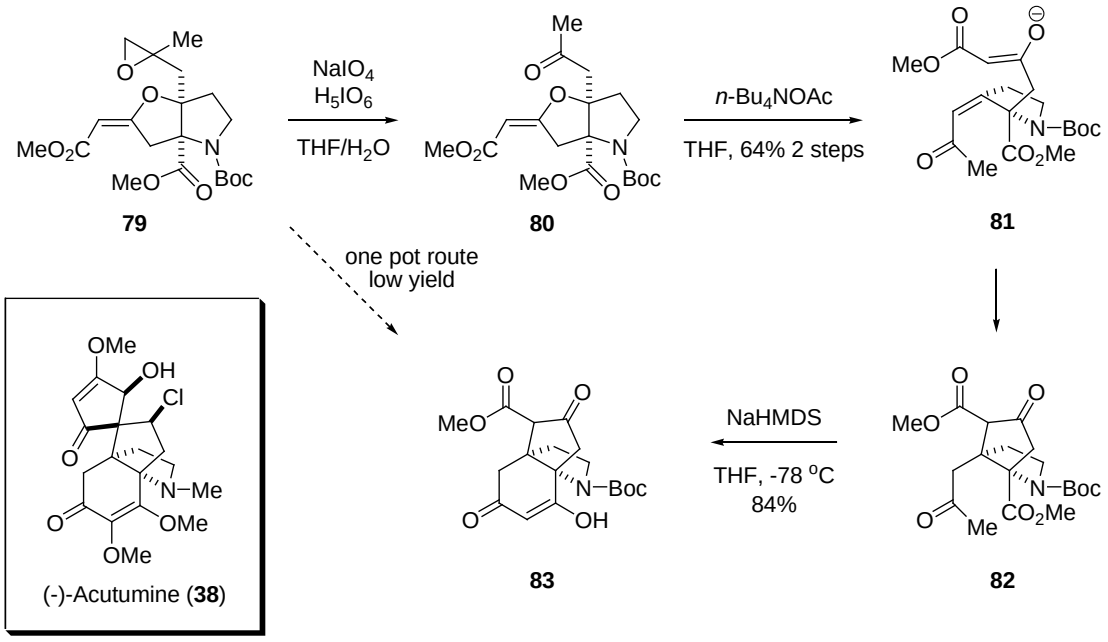

Scheme 1.10.1 Sorensen's racemic synthesis of the propellane core structure of acutumine

1.11 Conclusion

Since its first discovery, the hasubanan alkaloids have garnered much interest into their chemical and biosynthesis. Their structural resemblance to the morphinan alkaloids have initially provided increased intrigued. This culminated in the total synthesis of several hasubanan alkaloids. Interests waned, however, as their limited biological activities were reported. With the recent discovery of the biological benefits of acutumine and the periglaucines, once more the hasubanan alkaloids have accrued attention from the scientific community. We are driven by the need to develop a strategy toward the total synthesis of the hasubanan alkaloids. It is envisioned that such a strategy is also applicable to the synthesis of acutumine (**38**). Our proposed investigations include: (1) A unified strategy which allows for the stereocontrolled total synthesis of the hasubanan alkaloids as a model system of acutumine (**38**). (2) The conversion of delavanine (**3**) to periglaucine A (**8**). (3) The stereocontrolled synthesis of acutumine – the challenging part will be the chlorospirocycle. (4) The synthesis of dechlorinated derivatives for the investigation of enzymatic chlorination steps. Toward these goals, our efforts are reported in chapters 2 and 3. We have accomplished the synthesis of the common hasubanan propellane core structure and our progress towards the synthesis of acutumine is also reported.

1.12 Notes and References

(1) Kupchan, S. M.; Suffness, M. I.; White, D. N. J.; McPhail, A. T.; Sim, G. A. *J. Org. Chem.* **1968**, *33*, 4529-4532.

(2) Kondo, H.; Sanada, T. *Yakugaku Zasshi* **1928**, *48*, 1141-1156.

(3) Ibuka, T.; Kitano, M. *Chem. Pharm. Bull. (Tokyo)* **1967**, *15*, 1939-1943.

(4) Tomita, M.; Ibuka, T.; Inubushi, Y.; Watanabe, Y.; Matsui, M. *Chem. Pharm. Bull. (Tokyo)* **1965**, *13*, 538-545.

(5) Tomita, M.; Ibuka, T.; Inubushi, Y.; Watanabe, Y.; Matsui, M. *Tetrahedron Lett.* **1964**, *5*, 2937-2944.

(6) Tomita, M.; Kato, A.; Ibuka, T. *Tetrahedron Lett.* **1965**, *6*, 1019-1030.

(7) Zhi-Da, M.; Ge, L.; Guang-Xi, X.; Iinuma, M.; Tanaka, T.; Mizuno, M. *Phytochemistry* **1985**, *24*, 3084-3085.

(8) Jin, H.-Z.; Wang, H.-B.; Wang, Y.-B.; Lin, L.-P.; Ding, J.; Qin, G.-W. *Zhongguo Tianran Yaowu* **2007**, *5*, 112-114.

(9) Jones, S. B.; He, L.; Castle, S. L. *Org. Lett.* **2006**, *8*, 3757-3760.

(10) Ibuka, T.; Tanaka, K.; Inubushi, Y. *Chem. Pharm. Bull.* **1974**, *22*, 782-798.

(11) Ibuka, T.; Tanaka, K.; Inubushi, Y. *Tetrahedron Lett.* **1970**, *11*, 4811-4814.

(12) Kondo, H.; Satomi, M.; Odera, T. *Ann. Rept. ITSUU Lab.* **1951**, *2*, 35-43.

(13) Schultz, A. G.; Wang, A. *J. Am. Chem. Soc.* **1998**, *120*, 8259-8260.

(14) Cheng, P.; Ma, Y.-b.; Yao, S.-y.; Zhang, Q.; Wang, E.-j.; Yan, M.-h.; Zhang, X.-m.; Zhang, F.-x.; Chen, J.-j. *Bioorg. Med. Chem. Lett.* **2007**, *17*, 5316-5320.

(15) Yan, M.-H.; Cheng, P.; Jiang, Z.-Y.; Ma, Y.-B.; Zhang, X.-M.; Zhang, F.-X.; Yang, L.-M.; Zheng, Y.-T.; Chen, J.-J. *J. Nat. Prod.* **2007**, *71*, 760-763.

(16) Bentley, K. W. *Nat. Prod. Rep.* **2000**, *17*, 247-268.

(17) Battersby, A. R.; Jones, R. C. F.; Minta, A.; Ottridge, A. P.; Staunton, J. *J. Chem. Soc., Perkin Trans. 1* **1981**, 2030-2039.

(18) Battersby, A. R.; Jones, R. C. F.; Kazlauskas, R.; Ottridge, A. P.; Staunton, J.; Poupat, C. *J. Chem. Soc., Perkin Trans. 1* **1981**, 2010-2015.

(19) Battersby, A. R.; Jones, R. C. F.; Kazlauskas, R.; Thornber, C. W.; Ruchirawat, S.; Staunton, J. *J. Chem. Soc., Perkin Trans. 1* **1981**, 2016-2029.

(20) Allen, R. M.; Kirby, G. W. *J. Chem. Soc., Chem. Commun.* **1971**, *18*, 1121-1122.

(21) Ibuka, T.; Kitano, M.; Inubushi, Y. *Tetrahedron Lett.* **1969**, *10*, 1611-1614.

(22) Nielsen, D. K.; Nielsen, L. L.; Jones, S. B.; Toll, L.; Asplund, M. C.; Castle, S. L. *J. Org. Chem.* **2009**, *74*, 1187-1199.

(23) Goto, K.; Sudzuki, H. *Bull. Chem. Soc. Jpn.* **1929**, *4*, 220-224.

(24) Goto, K.; Tomita, M.; Okamoto, Y.; Kikuchi, T.; Osaki, K.; Nishikawa, M.; Kamiya, K.; Sasaki, Y.; Matoba, K. *Proc. Jap. Acad.* **1967**, *43*, 499-504.

(25) Reeder, M. D.; Srikanth, G. S. C.; Jones, S. B.; Castle, S. L. *Org. Lett.* **2005**, *7*, 1089-1092.

(26) Li, F.; Castle, S. L. *Org. Lett.* **2007**, *9*, 4033-4036.

(27) Li, F.; Tartakoff, S. S.; Castle, S. L. *J. Am. Chem. Soc.* **2009**, *131*, 6674-6675.

(28) Min, Y. D.; Choi, S. U.; Lee, K. R. *Arch. Pharmacal Res.* **2006**, *29*, 627-632.

(29) Yu, B.-W.; Chen, J.-Y.; Wang, Y.-P.; Cheng, K.-F.; Li, X.-Y.; Qin, G.-W. *Phytochemistry* **2002**, *61*, 439-442.

(30) Moreau, R. J.; Sorensen, E. J. *Tetrahedron* **2007**, *63*, 6446-6453.

(31) Qin, G.-W.; Tang, X.-C.; Lestage, P.; Caignard, D.-H.; Renard, P.; (Shanghai Institute of Materia Medica, Peop. Rep. China; Les Laboratoires Servier). Application: WO
WO, 2003, p 37 pp.

(32) Barton, D. H. R.; Kirby, A. J.; Kirby, G. W. *J. Chem. Soc.* **1968**, 929-936.

(33) Babiker, H. A. A.; Sugimoto, Y.; Saisho, T.; Inanaga, S. *Phytochemistry* **1999**, *50*, 775-779.

(34) Waller, D. L.; Stephenson, C. R. J.; Wipf, P. *Org. Biomol. Chem.* **2007**, *5*, 58-60.

(35) Furumoto, T.; Sugimoto, Y. *Planta Med.* **2001**, *67*, 194-195.

(36) Yarnell, A. *C&EN* **2006**, *84*, 12-18.

(37) Babiker, H. A. A.; Sugimoto, Y.; Saisho, T.; Inanaga, S.; Hashimoto, M.; Isogai, A. *Biosci., Biotechnol., Biochem.* **1999**, *63*, 515-518.

(38) Sugimoto, Y.; Matsui, M.; Babiker, H. A. A. *Phytochemistry (Elsevier)* **2007**, *68*, 493-498.

(39) Sugimoto, Y.; Babiker, H. A. A.; Saisho, T.; Furumoto, T.; Inanaga, S.; Kato, M. *J. Org. Chem.* **2001**, *66*, 3299-3302.

(40) Sugimoto, Y.; Matsui, M.; Takikawa, H.; Sasaki, M.; Kato, M. *Phytochemistry (Elsevier)* **2005**, *66*, 2627-2631.

CHAPTER TWO

Synthesis of the Common Propellane Core Structure of the Hasubanan Alkaloids

2.1 Retrosynthetic Analysis

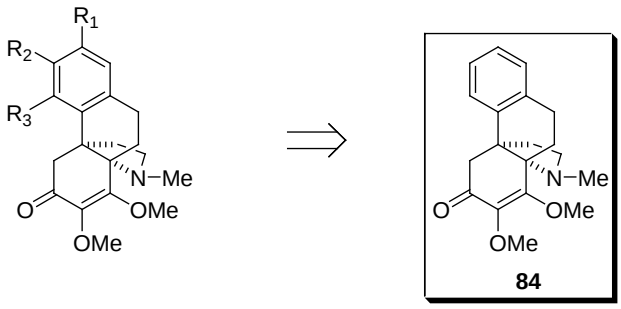

R_1 = H, R_2 = R_3 = OMe	Hasubanonine (**1**)
R_1 = R_2 = OMe, R_3 = H	Runanine (**2**)
R_1 = R_2 = -OCH_2O-, R_3 = H	Delavanine (**3**)
R_1 = H, R_2 = OMe, R_3 = OH	Aknadinine (**4**)
R_1 = H, R_2 = OH, R_3 = OMe	Homostephanoline (**5**)
R_1 = H, R_2 = OEt, R_3 = OMe	*O*-Ethylhomostephanone (**6**)
R_1 = OH, R_2 = OMe, R_3 = H	Cephatonine (**7**)

Figure 2.1.1 Structures of the hasubanan alkaloids (**1-7**) and the common propellane **84**

We chose 3,4-bisdesmethoxyhasubanonine **84** as the synthetic target due to its shared tetracyclic core structure with the series of hasubanan alkaloids **1-7**, differed only

in the positions of hydroxyl groups on the aromatic ring (Figure 2.1.1). The retrosynthetic analysis for the hasubanan skeleton **84** is shown in Scheme 2.1.1.

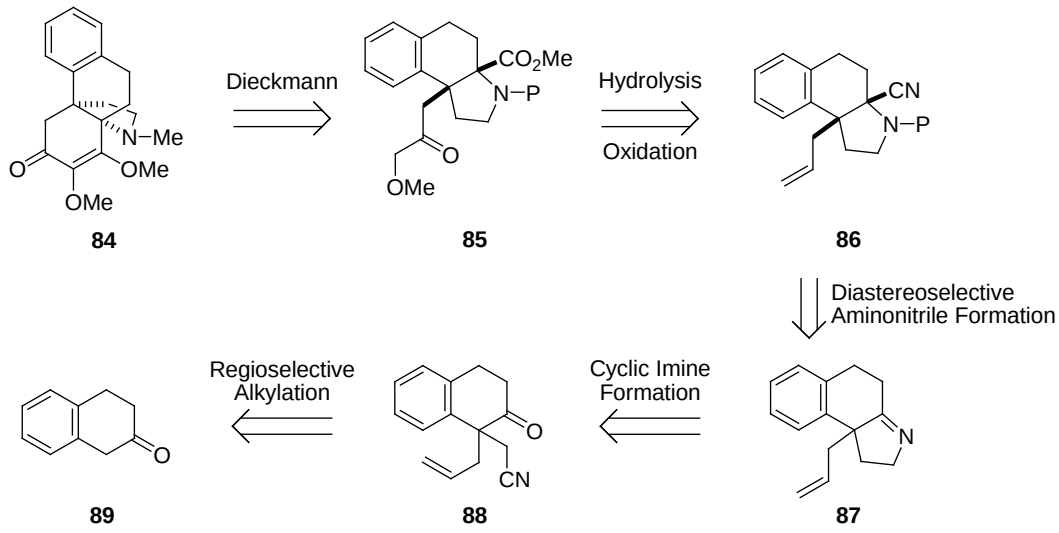

Scheme 2.1.1 Retrosynthetic analysis of hasubanan propellane core

It is envisioned that the propellane core could be constructed from a Dieckmann cyclization by the two substituents at the angular positions of *cis*-fused heterobicycle **85**. The most reasonable cyclization has never been realized as a synthetic route of the hasubanan alkaloids. Therefore, the *cis*-substituted heterocycle and similar structures have never been reported. Each substituent, e.g., the α–methoxy ketone and the ester, must be installed in an appropriate order from precursor **86** under compatible conditions during each manipulation. We wanted to apply the direct regioselective oxidation of an olefin to α–hydroxyl ketone reported by Lee. We have foreseen the difficulty of hydrolysis of the sterically hindered cyano group at the angular position of the heterobicycle to the corresponding ester although the cyano group will be converted to

the corresponding carboxamide relatively easily. The Dieckmann cyclization to obtain the propellane core hinged upon the successful diastereoselective construction of aminonitrile **86** from the cyclic imine **87**. We expected thermodynamic controlled conditions of cyanide addition will preferably give the more stable *cis*-5-6-fused ring system over *trans*-5,6-fused ring system in **86**.[1,2] The cyclic imine could ideally be formed by chemoselective reduction of the cyano group in ketone **88**. The regioselective consecutive alkylation of 2-tetralone (**89**) will give chiral 1,1-alkylated teralone **88**. For the alkylation sequence we chose to start with 1-allyl-2-tetralone due to the propensity of 2-tetralone (**89**) to undergo di-alkylation reactions under basic conditions. In addition to the reason described, mild alkylation procedures are known, the allyl group is chemically stable and a versatile synthon. The cyano methyl moiety is installed second because the acidic α-proton may promote undesired reactions under basic conditions. We chose to alkylate with an allyl moiety to install the α-methoxy ketone side chain because it provided the requisite three carbon unit for Dieckmann cyclization in **85**, and also because of the various literature precedents for regioselectively transforming a tethered terminal olefin into the desired hydroxyl ketone.[3-7]

However, while this plan is easily draw, there are issues with its laboratory operation: (1) The completion of the synthesis relied heavily on the synthesis of the *cis*-fused heterobicycle **86**. Although simple *cis*-indolindine is more stable than the *trans* isomer, our proposed intermediate has two stereocenters at angular positions and also the benzene ring is additionally fused. Formation of the *trans*-fused heterobicycle would render the subsequent Dieckmann cyclization inexecutable. (2) Although the sequence is straightforward and logical, there has been no reported synthesis using the proposed

route, i.e., construction of propellane core by Dieckmann condensation from *cis*-fused bicycle. We anticipated that our strategy could be in vain. It was in the course of this investigation that we found a difficulty of hydrolysis of sterically hindered amide at angular position of bicyclic intermediate, and also it was revealed that multiple intermediates are highly unstable under SiO_2 purifications. We believe that this could possibly be the reason why such schemes might have been abandoned by other research groups.

For the synthesis of the hasubanan alkaloids, we envisioned that the enantioselective alkylation of 2-tetralone could be achieved by using a chiral phase transfer catalyst.[8-11] To obtain each hasubanan alkaloid **1-7** in Figure 2.1.1, the same synthetic route would be applicable starting from the corresponding 2-tetralone derivatives. According to this synthetic strategy, 7,8-dimethoxy-2-tetralone (**26**) and 6,7-dimethoxy-2-tetralone (**90**) would be the precursors for the synthesis of hasubanonine (**1**) and runanine (**2**), respectively (Scheme 2.1.2). Conveniently, 7,8-dimethoxy-2-tetralone is a known compound in the literature and 6,7-dimethoxy-2-tetralone is even commercially available.[12,13]

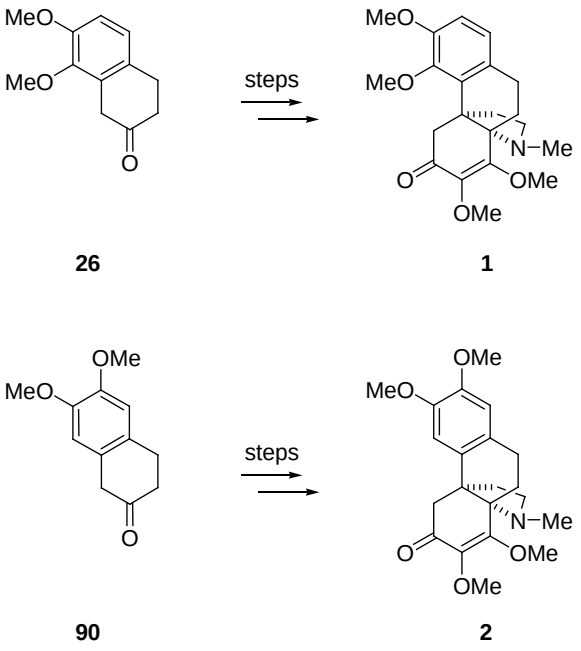

Scheme 2.1.2 Proposed synthesis of hasubanonine (**1**) and runanine (**2**) from 2-tetralone derivatives

For acutumine, we also expected the cyclopentanone derivative of **91** could be converted stereoselectively to the *cis*-5,5-fused ring system corresponding to **92** (Scheme 2.1.3). Then, the following intramolecular Dieckmann condensation could provide the skeleton of propellane [4.3.3.0] core structure of acutumine.

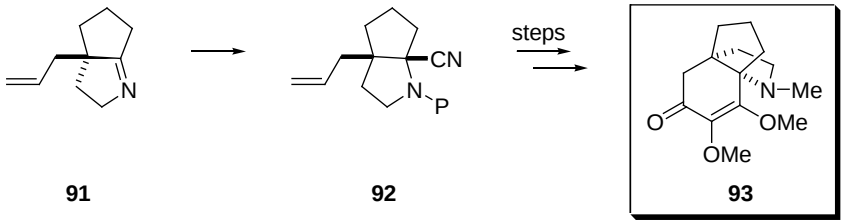

Scheme 2.1.3 Proposed synthesis from *cis*-5,5-fused heterocycle **93** in the synthesis of propellane core of acutumine

2.2 Synthesis of Cyclic Imine

In our initial synthetic planning, we focused our attention on the construction of the cyclic imine **87** by chemoselective reduction of the cyano group in 1,1-disubstituted-2-tetralone **88**.[14] We were inspired by the Evans group in their total synthesis of clavolonine.[15] In the synthesis, it was reported that a tethered nitrile moiety can be reduced using Raney Ni hydrogenation conditions (Scheme 2.2.1). The adjacent quaternary center effectively retarded the reduction of the imine group to prevent over-reduction to give saturated pyrrolidine ring.

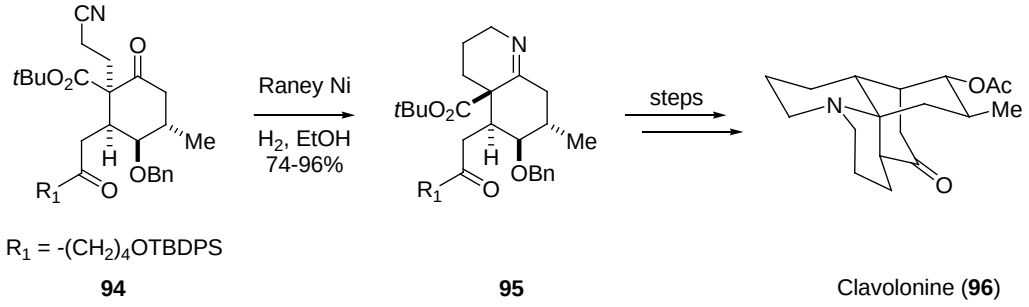

Scheme 2.2.1 Formation of a cyclic imine by chemoselective reduction of cyano group in Evans' synthesis of clavolonine (**96**)

With this precedent in hand, we began our synthesis with regioselective mono-allylation of commercially available 2-tetralone (**89**) by Tsuji-Trost procedures.[16,17] Regioselective deprotonation of 2-tetralone (**89**) with NaH and subsequent treatment with allyl chloroformate gave the stable allyl carbonate **97** in 97% yield (Scheme 2.2.2). Tsuji-Trost rearrangement of allyl carbonate **97** gave the known, unstable (±)-1-allyl-2-tetralone (**98**). During the Tsuji-Trost rearrangement, it was noticed that the dioxane

solvent required degassing prior to use. Reactions performed without degassing the solvent led to poor yields of the product. In addition, allyl carbonate solution **97** must be added to the palladium/triphenyl phosphine solution rapidly (<10 seconds). Slow addition gave a higher yield of the di-allylated side product with recovered starting material, 2-tetralone (**89**). Regioselective second alkylation of 1-allyl-2-tetralone (**98**) with bromoacetonitrile gave the stable 1,1-disubstituted-2-tetralone **88** as a racemic mixture. In an attempt to directly access cyclic imine **87** from **88**, chemoselective reduction of the nitrile group using Raney Ni was explored. Initial attempts cleanly gave the cyclic imine. The adjacent quaternary center effectively retarded the over-reduction of the cyclic imine. Unfortunately, the tethered olefin was saturated under the hydrogenation conditions. Although this could be avoided by protection of the terminal olefin as an epoxide or 1,2-diol, we decided to chase an alternative route to reach the cyclic imine.

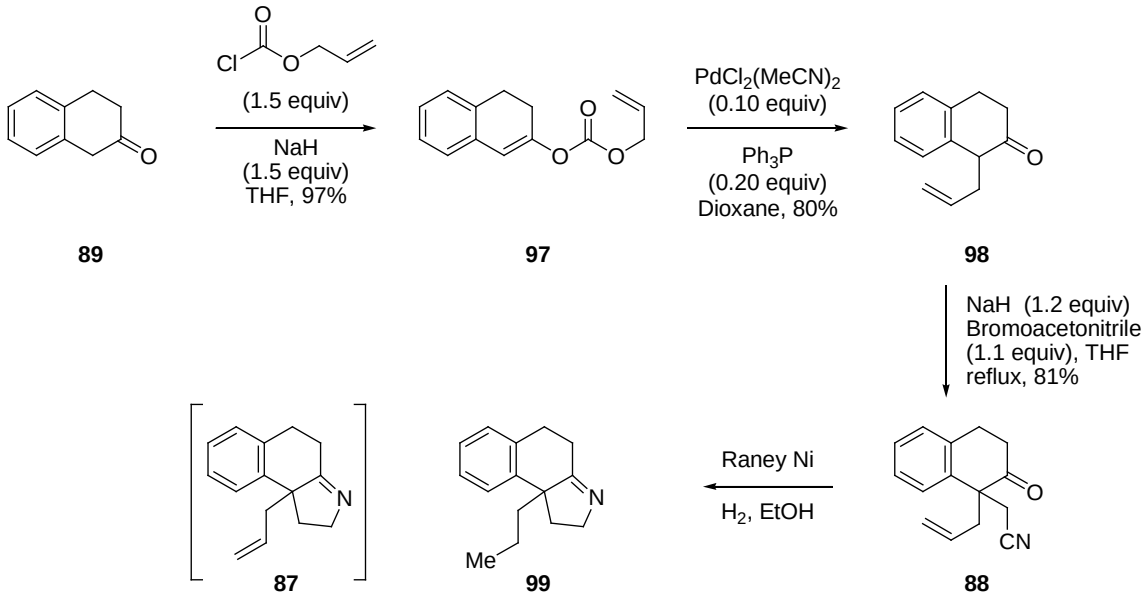

Scheme 2.2.2 Synthesis of cyclic imine **87** by chemoselective reduction of cyano group

2.3 Alternative Path to Reduce Cyano Group

Initial attempts toward the cyclic imine using Raney Ni proved to be unsuccessful due to incompatibility with the olefin moiety. We then sought an alternative stepwise strategy for the synthesis of the cyclic imine by way of a protected aminoketone **102** via a protected aminoalcohol **100** (Scheme 2.3.1). Under those reaction conditions, we expected the terminal olefin to be inert. Reduction of tetralone **88** with LAH and concomitant chemoselective protection of the resulting aminoalcohol **100** with Boc_2O gave carbamate **101** in 89% yield over two steps as an inconsequential 4:1 mixture of diastereomers.[18] The diastereomeric mixture is inconsequential because in the following

step the alcohol stereocenter will lose stereochemical information upon oxidation to the ketone.

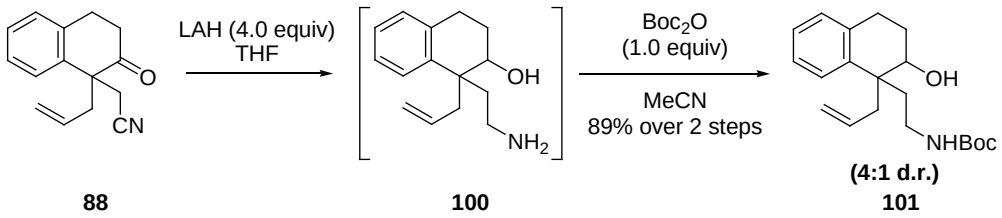

Scheme 2.3.1 LAH reduction of cyano and carbonyl groups in dialkylated tetralone **88**

2.4 Diastereoselective Construction of Cis-Fused Indolidine

With aminoalcohol **101** in hand, we attempted to synthesize the cyclic imine **87**. Swern oxidation of the diastereomixture of **101** cleanly gave tetralone **102**, although the attempt of purification by SiO_2 induced formation of several compounds including a cyclic *N*,*O*-hemiketal (Scheme 2.4.1). The ^{1}H-NMR of the crude mixture was clean, indicating the formation of **102** as a sole product. Therefore, the crude mixture was subjected to the following cyclic imine formation without purification. Deprotection of the Boc group of tetralone **102** under acidic conditions allowed an entry into the cyclic imine **87**, which was also unstable under SiO_2 purification. Again, ^{1}H-NMR of the crude mixture was clean, indicating the formation of **87**. The crude mixture was subjected to aminonitrile formation reaction without purification.

Hydro-cyanation of crude mixture of cyclic imine **87** was employed with KCN and AcOH in DMF. Isolation of the hydro-cyanation product (structure not shown) of the cyclic imine **87** proved to be difficult as the cyanide anion is extruded upon work-up and purification, presumably due to the steric hindrance of the *cis*-5-6-fused ring juncture. Our efforts then focused on finding conditions that allowed the capture of the unstable aminonitrile *in situ*. Hydro-cyanation of the cyclic imine **87** followed by *in situ* treatment with acetyl chloride allowed for the capture of the unstable intermediate in an unoptimized 56% yield over 4 steps. ^{1}H-NMR spectrum of the acetamide indicated the secondary amide existed as a single stereoisomer. The *cis*-substitution pattern of acetamide **103** was confirmed by X-ray crystal structure analysis (Figure 2.4.1) and the cyano group existed in a pseudo-equatorial while the allyl group existed in a pseudo-axial position on the cyclohexane ring. We reasoned that the diastereoselective addition of hydrogen cyanide was due to the better stability of a *cis*-5,6-fused ring than a *trans*-5,6-fused ring juncture.

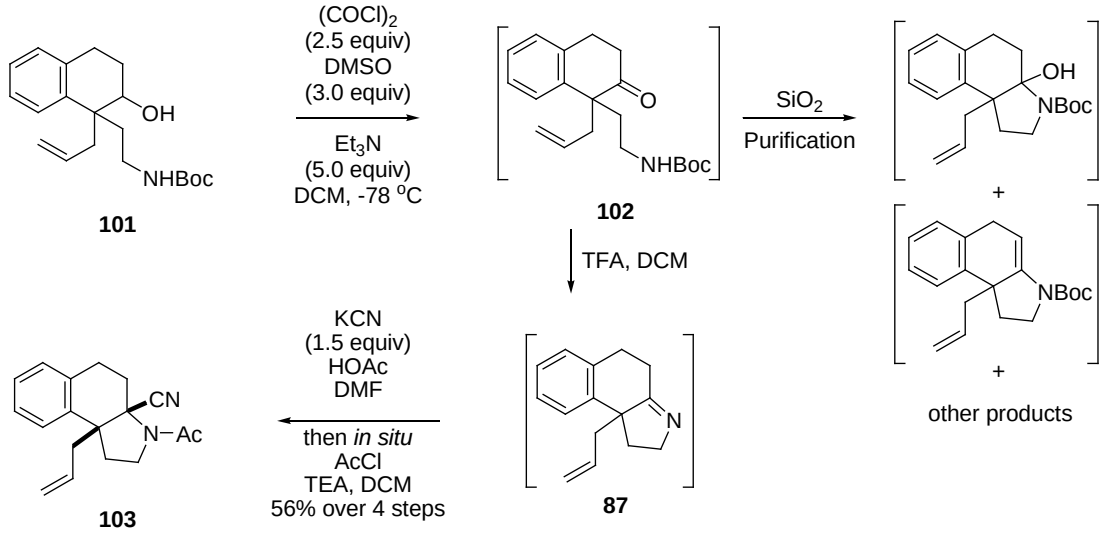

Scheme 2.4.1 Formation of cyclic imine **87** and the diastereoselective Strecker reaction to obtain *cis*-fused acetamide **103**

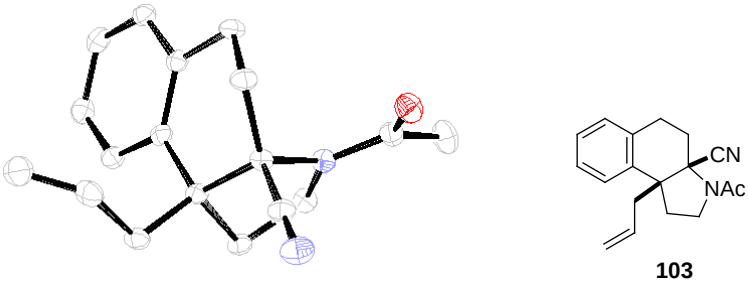

Figure 2.4.1 ORTEP figure of *cis*-acetamide **103**

2.5 Initial Attempts at Dieckmann Cyclization

With the complete carbon skeleton in hand, we attempted our proposed Dieckmann (or in the case of a nitrile moiety, the Thorpe) cyclization to construct the propellane core skeleton (Scheme 2.5.1). To this end, we first chose to install α-

methoxylketone moiety of allyl side chain. Then, we planned to try the Thorpe cyclization of the hydroxyketone toward the nitrile to give a cyclic enamine.

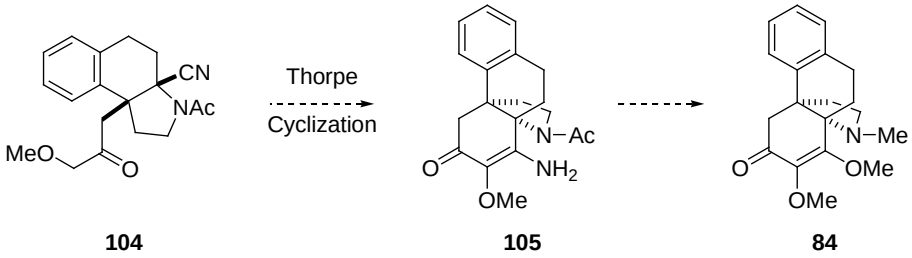

104 **105** **84**

Scheme 2.5.1 Synthetic strategy toward propellane structure **84** bearing a cyclic enamine by Thorpe reaction

Hydroxy-carbonylation of **103** using $KMnO_4$ in AcOH proved to be a reliable method for regioselective oxidation of a terminal olefin to the corresponding hydroxyl-ketone **106** in an unoptimized 46% yield (Scheme 2.5.2). It is unclear if the oxidation is regioselective or if the regioisomeric hydroxyl-aldehyde tautomerized to the more stable hydroxyl-ketone. Methylation of the resulting alcohol **106** gave the Thorpe cyclization precursor **104** in 55% yield. Unfortunately, initial investigations into the Thorpe cyclization reaction proved to be unsuccessful. There are two possible reasons why we believe that the Thorpe cyclization failed. First, the acidic proton of the acetamide moiety might have interfered with the basic conditions and lead to decomposition products. Second, the large bulky acetamide moiety did not allow the cyclization to proceed effectively. For the aforementioned reasons, we chose to continue with our synthesis using a formyl protecting group on the unstable aminonitrile. The formyl group contains no acidic hydrogen and smaller in size than an acetamide group.

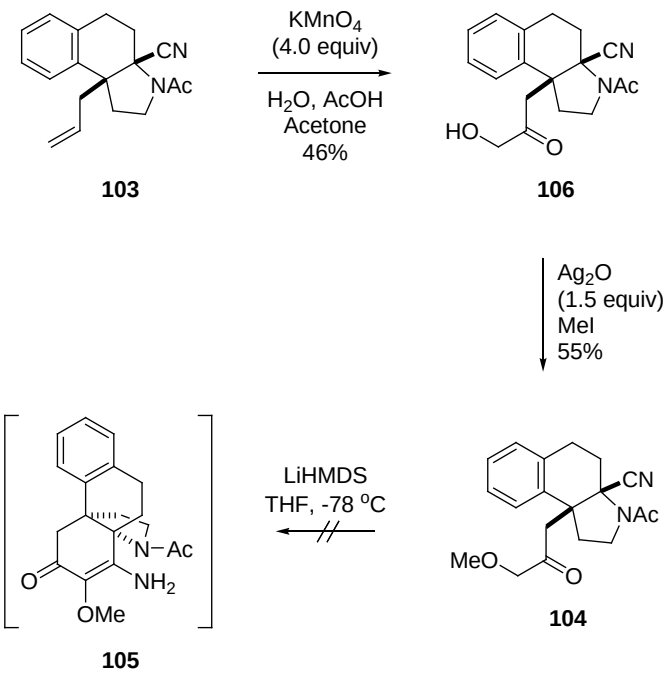

Scheme 2.5.2 Initial attempts at Thorpe cyclization to obtain propellane structure

2.6 Diastereoselective Construction of Cis-Fused Aminonitrile

Having determined that the acetamide **104** did not provide the Thorpe cyclized product, we turned our attention on constructing the *cis*-fused aminonitrile **107**. Following the similar sequence for the synthesis of the *cis*-fused acetamide **103**, Swern oxidation of the diastereomixture of **101** cleanly gave tetralone **102** (Scheme 2.6.1). The ^{1}H-NMR of the crude mixture was clean, indicating the formation of **102** as a sole product. Deprotection of the Boc group of tetralone **102** allowed an entry into the cyclic imine **87**, which was also unstable under SiO_2. Again, ^{1}H-NMR of the crude mixture was clean, indicating the formation of **87**. Hydro-cyanation of the cyclic imine **87** followed

by *in situ* treatment with acetic formic anhydride allowed for the capture of the unstable intermediate in an optimized 87% yield over 4 steps.[19] The *cis*-substitution pattern of formamide **107** was assumed by the X-ray crystal structure analysis of previously synthesized acetamide **103**. Based on the behavior of ^{1}H-NMR, the formamide existed in a mixture of rotational stereoisomers. This led to a more complex ^{1}H-NMR spectrum and made it difficult to obtain a good crystal for X-ray analysis; otherwise, the formamide proved to be inert to many reaction conditions.

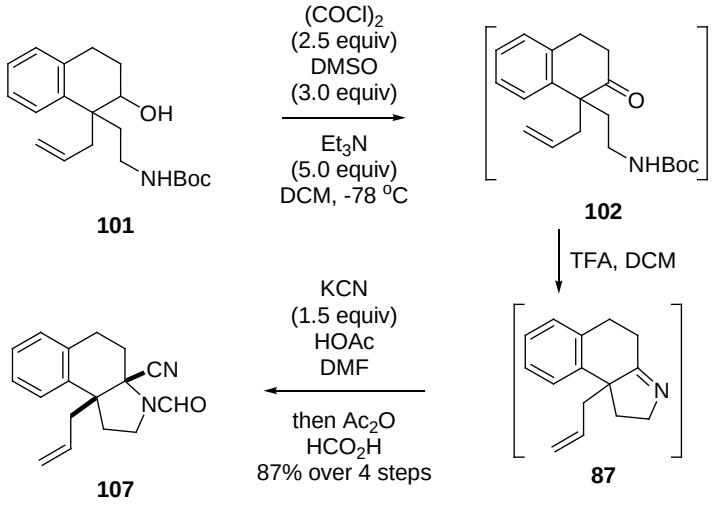

Scheme 2.6.1 Synthesis of cis-fused formamide **107** by diastereoselective Strecker reaction followed by formylation of the resulting aminonitrile

2.7 Dieckmann Cyclization with Formamide of Aminonitrile

With the complete carbon skeleton in hand, once more we attempted our proposed Thorpe cyclization to construct the propellane core skeleton (Scheme 2.7.1). We

expected there to be no difficulty in modifying the allyl side chain of formamide **107** to α-methoxylketone by following the exact same reaction condition as used for acetamide. As the formamide group did not contain acidic hydrogens and is less sterically hindered than an acetamide group, we investigated conditions for the Thorpe cyclization reaction. Hydroxy-carbonylation of the tethered olefin gave the α-hydroxyketone **108** in 58% yield. Methylation with MeI and silver oxide gave the methyl ether **109**. Subsequent treatment with potassium carbonate without purification of ether **109** smoothly gave the Thorpe cyclized product **110** in 83% over 2 steps. This might indicate the steric factor was dominant when we encountered a difficulty of the Thorpe cyclization of acetamide **104**. The Thorpe cyclization also worked with stronger bases such as LDA and NaHMDS albeit in lower yields. The formation of cyclic enamine was confirmed unambiguously by X-ray crystal structure analysis as shown in Figure 2.7.1.

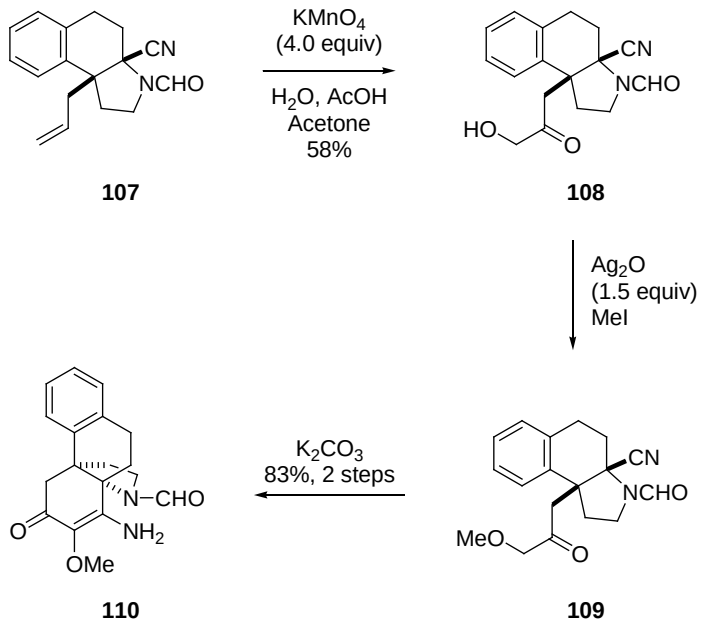

Scheme 2.7.1 Thorpe cyclization with formamide **109**

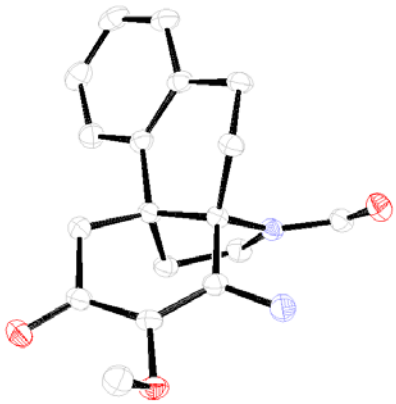

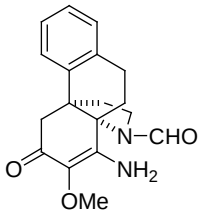

110

Figure 2.7.1 ORTEP figure of enamine **110**

Further manipulations of enamine **110** to reach to the target molecule **113** proved to be difficult (Scheme 2.7.2). Treatment of **110** in HCl and methanol only gave the de-formylated product **111**. The enamine functionality was retained under the harsh acidic conditions. This is a testament to the steric hindrance around the propellane core center. Treatment of **110** with sodium nitrite in acid and methanol once more gave recovered starting material. We envisaged that the resulting diazonium ion will be substituted with methanol to provide our desired hasubanan propellane core structure. However, nucleophilic approach toward the α-position of the fully substituted carbon of the propellane core center proved to be difficult. Then we turn our attention to prior hydrolysis of the cyano group.

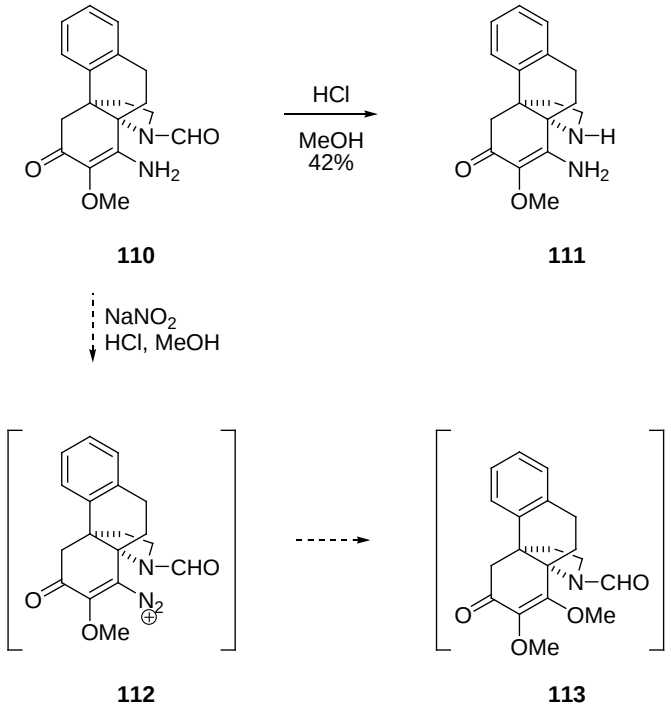

Scheme 2.7.2 Attempted functionalization of enamine **112** toward target molecule **113**

2.8 The Hydrolysis of Sterically Hindered Carboxamide

Central to our design plan is the Dieckmann cyclization from *cis*-fused bicycle to provide the common propellane core structure of the hasubanan alkaloids. We showed that the cyclization is feasible on the model substrate aminonitrile **109**. Although the resulting cyclic enamine of propellane was not converted to the desired methyl enol ether, we were encouraged to seek a protocol for the conversion of the nitrile functionality into the corresponding methyl ester prior to installation of α-methoxylketone on allyl side chain as shown in Scheme 2.8.1. The remaining agenda before the final ring closure to

form the propellane core are the following: (1) to convert a sterically hindered nitrile into a methyl ester moiety under mild reaction conditions and (2) oxidation of allylic side chain to α-methoxyketone **115**. Dieckmann cyclization between α-methoxyketone **115** and ester will afford the desired enol ether.

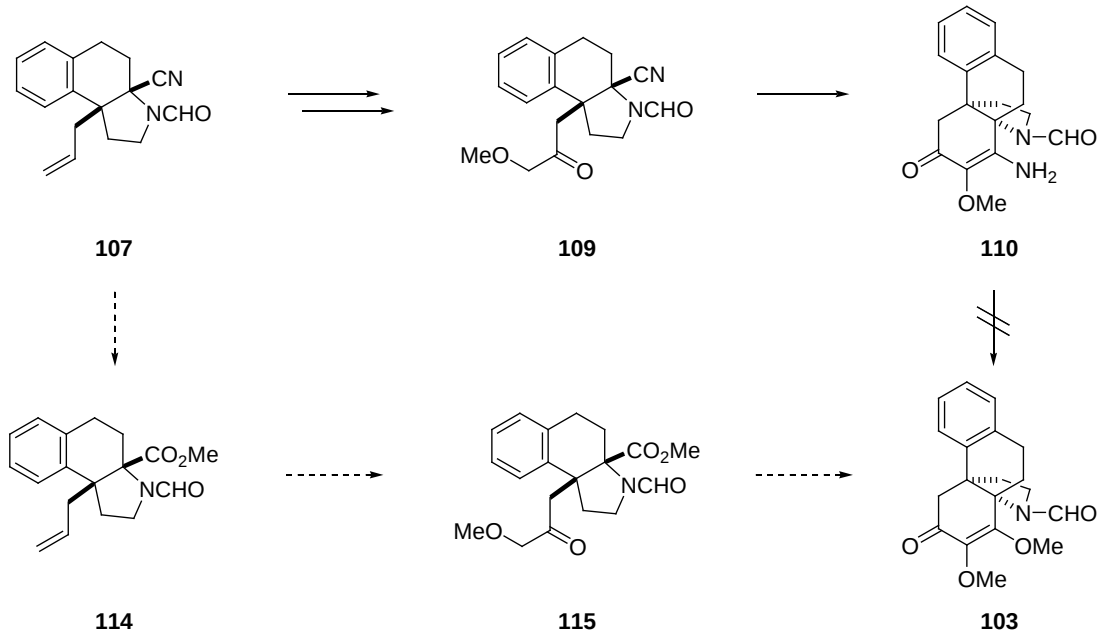

Scheme 2.8.1 Synthetic strategy toward propellane core structure **113**

The cyanide ion is commonly used as a one carbon synthon in organic synthesis. The versatility of the nitrile functional group has allowed for a facile entry into various carboxylic acid derivatives. However, one drawback to these conversions is the required harsh acidic or basic conditions. Reactions of aminonitrile **107** under acidic or basic conditions only gave recovered starting material due to the steric hindrance around the ring juncture. Subjecting the aminonitrile **107** to more stringent conditions such as adding excess reagent or heating conditions only led to decomposition of aminonitrile

moiety after deformylation. In our investigations, the sterically hindered cyano group was smoothly converted to carboxamide **116** by treatment with alkaline H_2O_2, but the simple hydrolysis of carboxamide **116** proved to be a stumbling block, presumably due to its proximity to two fully substituted carbon centers.

We sought a procedure to transform a sterically hindered carboxamide functional group to the corresponding carboxylic acid derivative under mild conditions without cleavage of the formamide moiety. In the course of our synthetic studies on proteasome inhibitor omuralide, we recently reported 2-nitrophenyl isocyanide as a convertible isocyanide in Ugi reaction (route A in Scheme 2.8.2).[20] The hydrolysis of the resulting 2-nitroanilide was facilitated by its derivatization to *N*-acylbenzotriazole, which functioned as an acid chloride synthetic equivalent.[21,22] We realized the formation of 2-nitroanilide could be possible by metal-catalyzed *N*-arylation (Goldberg reaction) of a carboxamide derived from a nitrile (route B in Scheme 2.8.2). The conditions to convert nitroanilide to *N*-acylbenzotriazole are very mild and therefore would be compatible with formamide. We foresaw the nitrogen atom of the carboxamide **116** can react to form the anilide despite the steric hindrance at the angular position, because the reaction center is one bond more away from the carbonyl group.

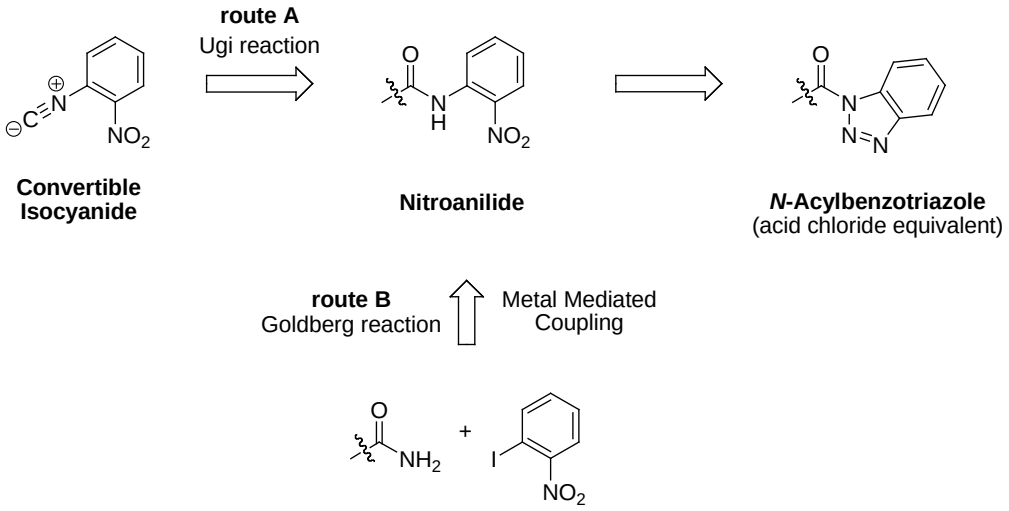

Scheme 2.8.2 Strategy for cleavage of sterically hindered amides via *N*-acylbenzotriazoles derived from *o*-nitroanilides

The conversion of a sterically hindered carboxamide to the corresponding methyl ester began with the hydration of aminonitrile **107** with hydrogen peroxide and K_2CO_3 to furnish carboxamide **116** in 91% yield (Scheme 2.8.3). We are pleased to find that the Goldberg reaction of carboxamide **116** with 2-iodonitrobenzene gave desired nitroanilide **117** in 91% yield.[23] Initial investigations into the Goldberg reaction showed that optimization was required for high yields of the product. Catalysts and solvents needed to be repurified and degassed prior to use. The K_3PO_4 base plays an essential role in that it required drying at 120°C under reduced pressure for 3 days and stored in a dry box. Sub-optimal reaction conditions gave an incomplete conversion. Tin-mediated chemoselective reduction of the nitro group of **117** gave anilide **118** without disturbing the allyl group and upon treatment of the crude mixture with isoamyl nitrite provided *N*-acylbenzotriazole **119**, which was detected by TLC and ^{1}H-NMR. Interestingly, the resulting isoamyl alcohol did not react with *N*-acylbenzotriazole to afford an isoamyl

ester. It is probably due to the steric hindrance of **119** and so-called Newman's rule of six regarding the alcohol.[24] Without purification, heating **119** at refluxing temperatures in MeOH gave the desired methyl ester **114** in 61% yield over three steps from **117**. The resulting benzotriazole by-product was conveniently removed simply by using 1N NaOH wash in the work-up procedures. Finally, the sterically hindered cyano group was successfully converted to the corresponding methyl ester via *N*-acylbenzotriazole in 5 steps in 51% overall yield.

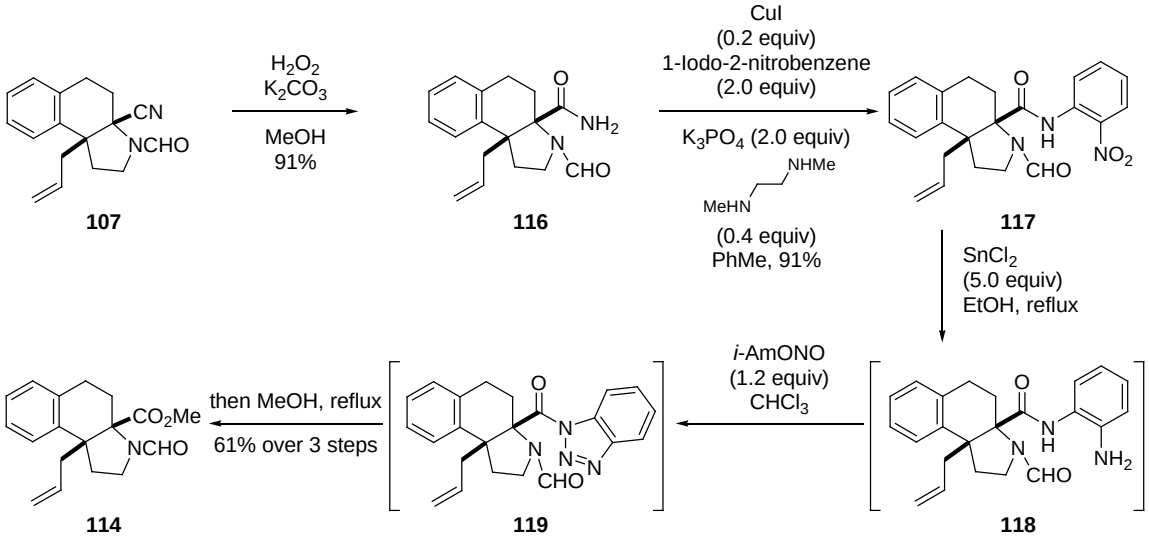

Scheme 2.8.3 Conversion of sterically hindered cyano group to the corresponding methyl ester via *N*-acylbenzotriazole

2.9 The Completion of Propellane Synthesis

The successful completion of the hasubanan skeleton was initiated with the regioselective hydroxy-carbonylation of the tethered olefin of methyl ester **114** with

$KMnO_4$ (Scheme 2.9.1). Methylation of alcohol **120** with silver oxide in MeI gave the methyl ether **115**. Our key Dieckmann cyclization was employed using NaHMDS as base. The resulting cyclic 1,3-dione (not shown) was detected by ^{1}H-NMR as a mixture of approximately 1:1 ratio of enol regioisomers, but decomposed to unidentified compounds upon purification. We decided to capture the resulting dione with TMS-diazomethane, but this gave us a 1:1 mixture of methyl enol ether isomers as previously reported, undesired **121** as the less polar product and desired **113** as the more polar product in 66% yield over two steps. The two isomers **113** and **121** were easily separable by SiO_2 column chromatography. Deformylation of **113** using HCl followed by *N*-methylation by treatment of the resulting amine **122** (not shown) with formaldehyde and formic acid allowed for the successful completion of the hasubanan propellane core **84**. Attempted conversion of the undesired methyl enol ether **121** to the 1,3-dione to recycle for the enol ether formation step was not successful as the compound decomposed under acidic conditions.

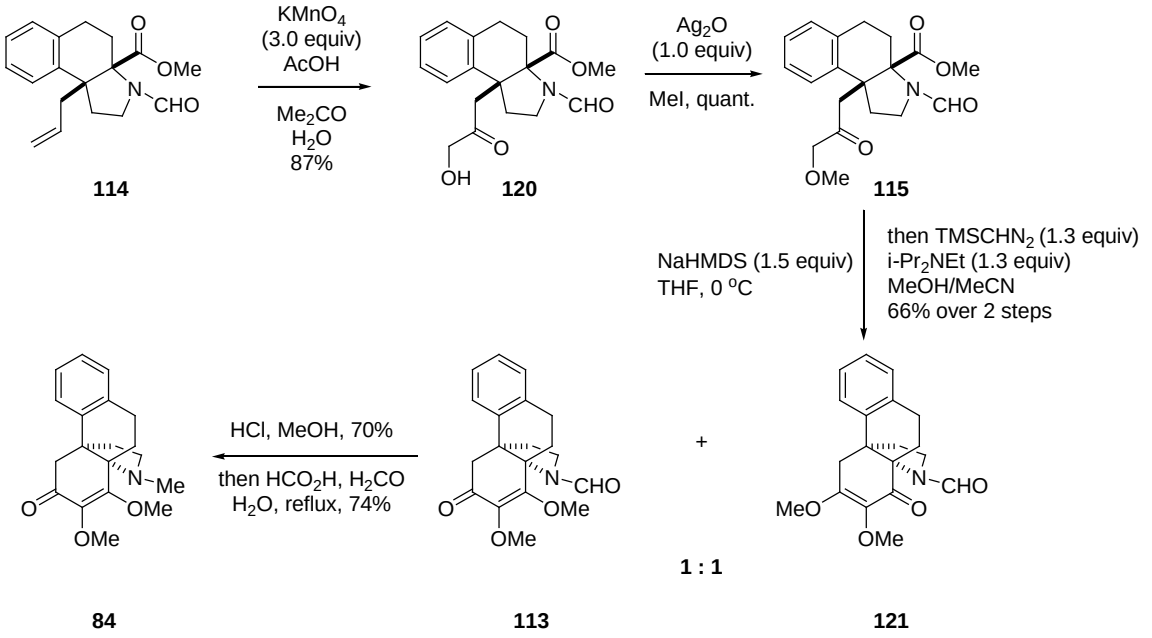

Scheme 2.9.1 Completion of the propellane core skeleton

We thought additional support is needed to confirm the structure of propellane **84** because it has never been fully characterized in the literature. Comparison of the propellane core structure **84** with the ^{13}C-NMR chemical shifts for cephatonine (**7**) showed a match with the reported values (Figure 2.9.1).[25] The ^{13}C-NMR signals for the aromatic rings are excluded in our comparison because the highly oxygenated phenyl group clearly affected the chemical shifts of the carbon signals. ^{13}C-NMR chemical shift of methylene carbon 6 of the benzylic position is affected by the difference of the aromatic ring ($\Delta\delta$ = 0.80 ppm). The average difference of ^{13}C-NMR chemical shifts between the propellane core **84** with cephatonine (**7**) was 0.29 ppm, and the maximum difference was 0.80 ppm on carbon 6 while the minimum difference was 0.04 ppm on carbon 1. This strongly supports the correct structure of **84** which we chose from two regioisomers after the enol ether formation, and also final propellane compound.

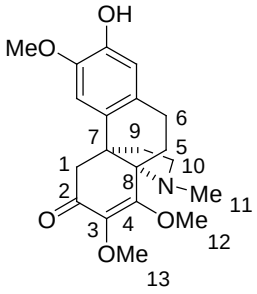

Cephatonine (**7**)

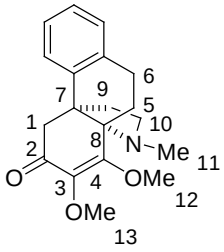

84

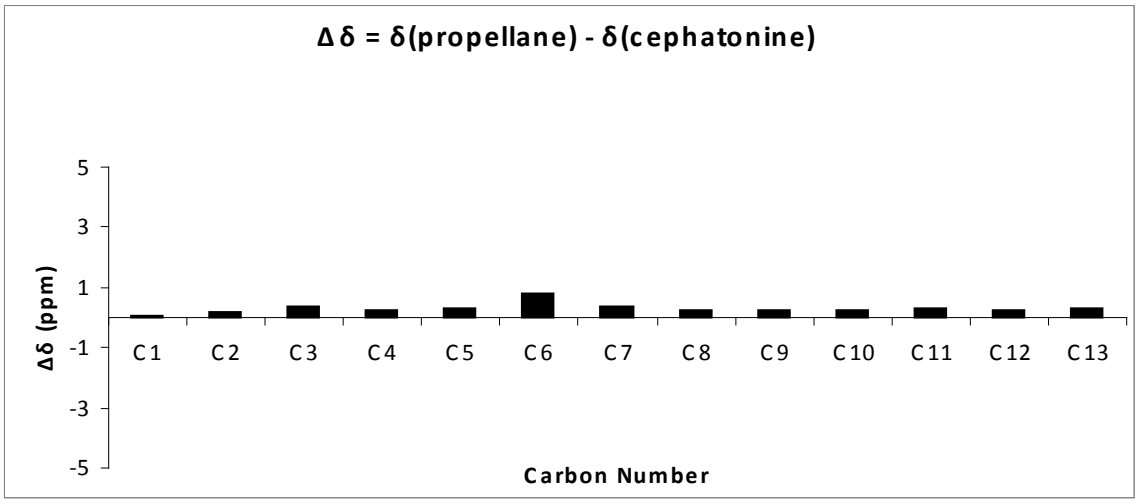

Figure 2.9.1 Difference in the ^{13}C-NMR chemical shift (ppm, in $CDCl_3$) of cephatonine (**7**) with those of propellane **84** prepared by us

2.10 The Synthesis of a Series of 2-Tetralone Derivatives

With these successes in hand, we then sought to explore the generality of the developed sequences in the synthesis of the hasubanan alkaloids. To obtain each hasubanan alkaloids **1-7**, we needed to start with the corresponding oxygenated 2-tetralone starting material. To demonstrate a rapid entry into the 2-tetralone starting materials, we pursued 6,7-dimethoxy-2-tetralone (**90**) from inexpensive, readily available

starting material (Scheme 2.10.1). Esterification of carboxylic acid **123** in ethanol with catalytic sulfuric acid gave ethyl ester **124** in 98% yield. Nucleophilic substitution of **124** with DMSO anion gave sulfoxide **125** in 43%. The resulting β-ketosulfoxide **125** was subjected to Pummerer rearrangement. After trifluoroacetylation of the sulfoxide, TFA was eliminated regioselectively to afford an electrophilic α-ketosulfonium ion. Regioselective Friedel-Crafts cyclization of the catechol moiety furnished methylthio-2-tetralone **126** in 70%. De-sulfuration with Raney Ni under a balloon of hydrogen gave 6,7-dimethoxy-2-tetralone (**90**) in 77% yield. By following the established route, the tetralone **90** will give runanine (**2**).

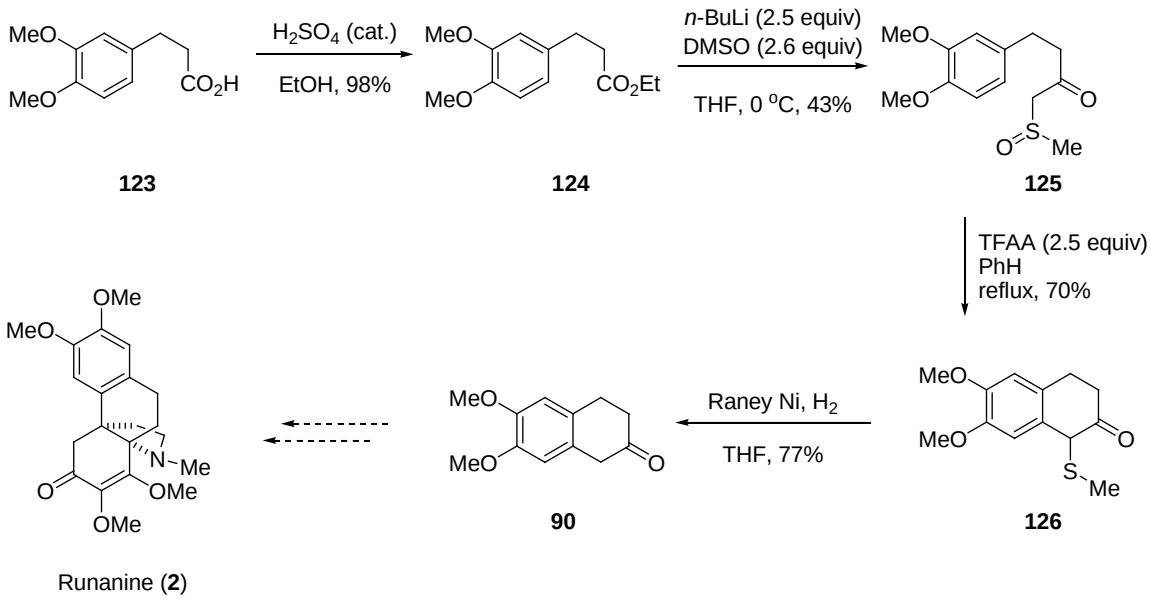

Scheme 2.10.1 Synthesis of 6,7-dimethoxy-2-tetralone (**90**)

2.11 Conclusions

We accomplished the synthesis of the common propellane core structure of the hasubanan alkaloids from 2-tetralone (**89**), which will be applicable to the total synthesis of acutumine (**38**). Several aspects of the investigations described in this account are noteworthy: (1) Synthesis of the heterobicycle **107** is accomplished with excellent diastereoselectivity. The *cis*-fused ring juncture is confirmed by X-ray crystal structure analysis. (2) Successful Thorpe cyclization towards nitrile moiety provided an amino analog of the hasubanan carbon skeleton. (3) Conversion of a sterically demanding nitrile functional group into the corresponding ester under mild conditions by way of an *N*-acylbenzotriazole. (4) A general strategy towards the common propellane core structure is accomplished. This strategy could be used towards the synthesis of various hasubanan alkaloids and acutumine.

Along with the successes the investigations, there are also remaining agenda that need to be addressed: (1) Asymmetric synthesis of 1,1-dialkylated tetralone **88**. The skeletal structure of the hasubanan alkaloids is different from morphinan alkaloids in forming a five membered pyrrolidine ring, and its absolute configuration is antipodal to that of morphinan. This has led Schultz to note that the unnatural enantiomer of these alkaloids may possess analgesic activities. To date there has been no reported analgesic activities of the unnatural enantiomer of the hasubanan alkaloids. Further investigations are required to access an enantio-controlled synthesis of tetralone **88**, thereby allowing an entry into the natural and unnatural enantiomer of the hasubanan alkaloids. (2) A regioselective methylation of the intermediate 1,3-dione to provide exclusively methyl enol ether **113**. Due to time constrains, we were not able to investigate heavily into the

penultimate intermediate. We are also interested in finding a route to recycle the undesired methyl enol ether **121** into the desired regioisomer **113**. In the next chapter, our synthetic approach toward acutumine (**38**) will be described.

2.12 Acknowledgements

Chapter 2, in part, is a reprint of the material as it appears in Nguyen, T. X.; Kobayashi, Y. "Synthesis of the Common Propellane Core Structure of the Hasubanan Alkaloids" *J. Org. Chem.* **2008**, *73*, 5536-5541. The dissertation author was the primary investigator and author of this paper.

2.13 Experimental

2.13.1 Materials and Methods

All reagents were commercially obtained (Aldrich, Fisher) at highest commercial quality and used without further purification except where noted. Organic solutions were concentrated by rotary evaporation below 40 °C at approximately 20 mmHg. Tetrahydrofuran (THF), methanol (MeOH), chloroform ($CHCl_3$), dichloromethane (DCM), ethyl acetate (EtOAc), acetonitrile (MeCN), *N*,*N*-dimethylformamide (DMF),

toluene (PhMe), ethanol (EtOH) and acetone were reagent grade and used without further purification. Yields refer to chromatographically and spectroscopically (^{1}H NMR, ^{13}C NMR) homogeneous materials, unless otherwise stated. Reactions were monitored by thin-layer chromatography (TLC) carried out on 0.25 mm E. Merck silica gel plates (60F-254) using UV light and cerium molybdate solution with heat as visualizing agents. E. Merck silica gel (60, particle size 0.040-0.063 mm) was used for flash chromatography. Preparative thin-layer chromatography separations were carried out on 0.50 mm E. Merck silica gel plates (60F-254). NMR spectra were recorded on Varian Mercury 300, 400 and/or Unity 500 MHz instruments and calibrated using the residual undeuterated solvent as an internal reference. Chemical shifts (δ) are reported in parts per million (ppm) and coupling constants (*J*) are reported in hertz (Hz). The following abbreviations were used to designate multiplicities: s= singlet, d= doublet, t= triplet, q= quartet, quint.= quintet, sp = septet, m= multiplet, br= broad. High resolution mass spectra (HRMS) were recorded on a Finnigan LCQDECA mass spectrometer under electrospray ionization (ESI) or atmospheric pressure chemical ionization (APCI) conditions, or on a Thermofinnigan Mat900XL mass spectrometer under electron impact (EI), chemical ionization (CI), or fast atom bombardment (FAB) conditions. X-ray data were recorded on a Bruker SMART APEX CCD X-ray diffractometer.

2.13.2 Preparative Procedures

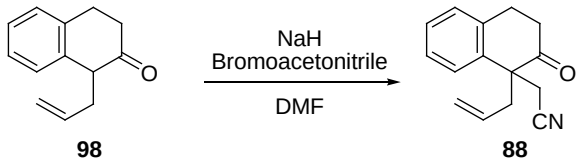

98 **88**

1,1-Alkylated 2-tetralone 88. To a solution of NaH (671 mg, 16.8 mmol, 1.5 equiv.) in DMF (30 mL) at 0 °C was added dropwise (±)-1-allyl-2-tetralone (**98**) (2.08 g, 11.2 mmol, 1.0 equiv.), then bromoacetonitrile (0.82 mL, 11.8 mmol, 1.05 equiv.). The solution was warmed to rt and stirred for 1 h, then quenched with sat aq NH_4Cl (300 mL) and extracted with EtOAc (3 x 200 mL). The combined organic layers were dried (Na_2SO_4), and the solvent was removed in vacuo. Flash chromatography (SiO_2, 10% EtOAc in hexanes elution) afforded **88** (2.04 g, 9.06 mmol, 81%) as a colorless oil. R_f (20% EtOAc in hexanes elution) = 0.35; HRMS (EI) *m* / *z* calcd for $C_{15}H_{15}NO$ (M^+) 225.1153, found 225.1148; ^{1}H NMR (500 MHz, $CDCl_3$) δ: 7.23 – 7.34 (m, 4H), 5.35 – 5.43 (m, 1H), 5.05 (d, *J* = 11.0 Hz, 1H), 5.04 (d, *J* = 17.0 Hz, 1H), 3.13 (t, *J* = 7.5 Hz, 2H), 3.04 (d, *J* = 16.5 Hz, 1H), 2.77 (d, *J* = 16.5 Hz, 1H), 2.74 (dd, *J* = 7.0, 15.0 Hz, 1H), 2.71 (dd, *J* = 8.0, 14.5 Hz, 1H), 2.62 (t, *J* = 7.5 Hz, 2H); ^{13}C NMR (100 MHz, $CDCl_3$) δ: 210.4, 136.6, 136.4, 131.3, 128.8, 127.8, 127.5, 126.3, 120.1, 117.3, 53.5, 44.0, 38.5, 27.9, 26.2; IR (film, cm^{-1}) 3078, 2976, 2910, 2357, 2339, 2248, 1716, 1640.

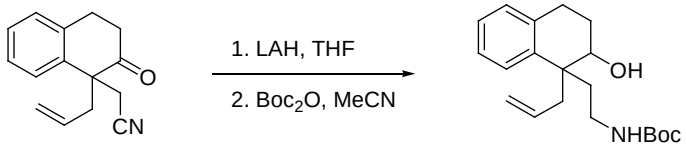

88 **101**

d.r. = 4:1

tert-Butyl 2-(1-allyl-1,2,3,4-tetrahydro-2-hydroxynaphthalen-1-yl)ethylcarbamate 101. To a solution of LAH (198 mg, 5.21 mmol, 3.0 equiv.) in THF (7 mL) was added **88** (391 mg, 1.74 mmol, 1.0 equiv.). The solution was stirred for 0.5 h then quenched with 0.20 mL H_2O, 0.20 mL NaOH (3M aqueous solution), then 0.60 mL H_2O, and extracted with EtOAc (3 x 50 mL). The combined organic layers were dried (Na_2SO_4), and the solvent was removed in vacuo. Crude ^{1}H-NMR spectrum is included in the supplemental section. To a solution of Boc_2O (0.37 mL, 1.74 mmol, 1.0 equiv.) in MeCN (10 mL) was added the amino alcohol in MeCN (1 mL). The solution was stirred for 15 min then quenched with H_2O (100 mL) and extracted with EtOAc (3 x 100 mL). The combined organic layers were dried (Na_2SO_4) and the solvent was removed in vacuo. Flash chromatography (SiO_2, 15% EtOAc in hexanes elution) afforded **101** (514 mg, 1.55 mmol, 89%) as a 4:1 mixture of diastereomers. R_f (20% EtOAc in hexanes elution) = 0.16; HRMS (EI) *m* / *z* calcd for $C_{20}H_{29}NO_3$ (M^+) 331.2147, found 331.2146; ^{1}H NMR (500 MHz, $CDCl_3$, major diastereomer) δ: 7.07 – 7.23 (m, 4H), 5.72 – 5.82 (m, 1H), 5.04 (d, *J* = 19.5 Hz, 1H), 5.03 (d, *J* = 9.0 Hz, 1H), 4.58 (s, 1H), 4.02 – 4.17 (m, 1H), 2.86 – 2.97 (m, 4H), 2.43 – 2.56 (m, 2H), 1.93 – 2.12 (m, 4H), 1.41 (s, 9H); ^{13}C NMR (100 MHz, $CDCl_3$, major diastereomer) δ: 156.1, 139.6, 135.9, 135.7, 129.2, 127.1, 126.0, 125.6, 117.4, 79.3, 70.9, 44.5, 41.3, 36.3, 35.4, 28.4, 27.6, 26.4; IR (film, cm^{-1}) 3388, 3071, 2934, 1722, 1688, 1638, 1258, 1175.

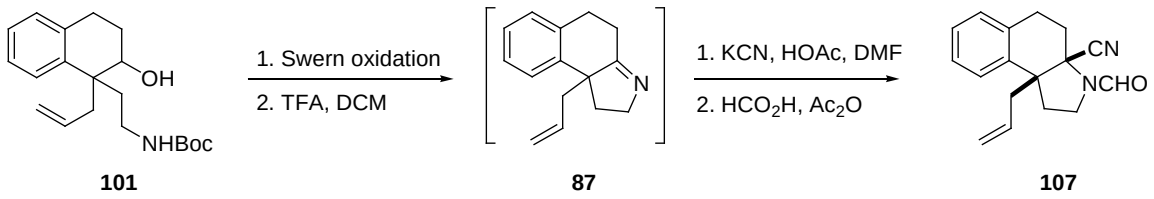

101 **87** **107**

9b-Allyl-3-formyl-2,3,3a,4,5,9b-hexahydro-1H-benzo[e]indole-3a-carbonitrile 107. To a solution of oxalyl chloride (0.44 mL, 5.02 mmol, 1.2 equiv.) in DCM (12 mL) at -78 °C was added dropwise dimethyl sulfoxide (0.65 mL, 9.19 mmol, 2.2 equiv.) in DCM (2 mL). Carbamate **101** (1.40 g, 4.10 mmol) in DCM (4 mL) was added dropwise and the solution was stirred for 5 min, then quenched with Et_3N (2.91 mL, 20.9 mmol, 5.0 equiv.). The cool bath was removed and the reaction mixture was diluted with H_2O (300 mL) and extracted with EtOAc (3 x 200 mL). The combined organic layers were dried (Na_2SO_4), and the solvent was removed in vacuo. The formation of aminoketone **102** was confirmed by ^{1}H-NMR of the crude mixture. Due to the instability, the crude mixture was subjected to the following cyclic imine formation. The resulting ketone was diluted in DCM (20 mL) and trifluoroacetic acid (6 mL) was added at rt. The solution was stirred for 30 min, then quenched with sat aq $NaHCO_3$ (200 mL) and extracted with DCM (3 x 200 mL). The combined organic layers were dried (K_2CO_3) and the solvent was removed in vacuo. The formation of cyclic imine **87** was confirmed by ^{1}H-NMR of the crude mixture. Due to the instability, the crude mixture was subjected to the following aminonitrile formation. The resulting imine **87** was diluted with DMF (6 mL) and acetic acid (1.19 mL). KCN (408 mg, 6.27 mmol, 1.5 equiv.) was added and the solution was allowed to stir at rt for 15 h. In a separate reaction mixture acetic anhydride (6.09 mL) was slowly added to formic acid (2.75 mL) at 0 °C. The resulting solution was

heated to 60 °C for 10 min, and then cooled to 0 °C. A solution of aminonitrile in DMF was then added to the mixed anhydride solution and allowed to stir at 0 °C for 30 min. The solution was quenched with water (500 mL) and extracted with EtOAc (3 x 200 mL). The combined organic layers were dried (Na_2SO_4), and the solvent was removed in vacuo. Flash chromatography (SiO_2, 30% EtOAc in hexanes elution) afforded **107** (950 mg, 3.57 mmol, 87%) as a yellow solid which was a single diastereomer. R_f (50% EtOAc in hexanes elution) = 0.45; Mp = 119 – 120 °C; HRMS (EI) *m* / *z* calcd for $C_{17}H_{18}N_2O$ (M^+) 266.1419, found 266.1411; ^{1}H NMR (500 MHz, $CDCl_3$, a mixture of rotamers in 1.8:1.0 ratio) δ: 8.53 (s, 0.64H), 8.32 (s, 0.36H), 7.35 (d, *J* = 7.5 Hz, 1H), 7.25 – 7.29 (m, 1H), 7.19 (t, *J* = 7.5 Hz, 1H), 7.09 (t, *J* = 7.0 Hz, 1H), 5.36 – 5.44 (m, 1H), 5.25 (d, *J* = 17.5 Hz, 0.5H), 5.24 (d, *J* = 17.0 Hz, 0.5H), 5.07 (d, *J* = 10.0 Hz, 0.5H), 5.05 (d, *J* = 10.5 Hz, 0.5H), 3.72 (dd, *J* = 8.0, 11.5 Hz, 0.5H), 3.63 (t, *J* = 7.5 Hz, 0.5H), 3.23 (td, *J* = 4.0, 13.5 Hz, 0.5H), 2.93 – 3.02 (m, 2H), 2.84 – 2.91 (m, 1.5H), 2.80 – 2.83 (m, 1H), 2.70 – 2.73 (m, 0.5H), 2.60 – 2.67 (m, 0.5H), 2.51 (td, *J* = 4.5, 14.5 Hz, 0.5H), 2.32 – 2.37 (m, 0.5H), 2.23 – 2.31 (m, 2H); ^{13}C NMR (100 MHz, $CDCl_3$) δ: 161.0, 160.0, 136.0, 135.6, 135.3, 134.3, 132.8, 132.7, 128.9 (2x), 127.4, 127.14, 127.10, 127.0, 126.72, 126.67, 119.6, 119.5, 119.3, 118.2, 62.8 (2x), 51.9, 51.8, 44.5, 44.3, 43.9, 42.3, 38.3, 37.5, 29.0, 26.1, 24.0, 23.3; IR (film, cm^{-1}) 3077, 2979, 2941, 2891, 2238, 2086, 1672.

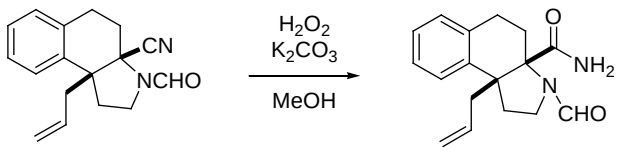

107 **116**

9b-Allyl-3-formyl-2,3,3a,4,5,9b-hexahydro-1H-benzo[e]indole-3a-carboxamide 116. To a solution of aminonitrile **107** (659 mg, 2.47 mmol) in MeOH (12 mL) was added K_2CO_3 (342 mg, 2.47 mmol) then hydrogen peroxide (35% aqueous solution, 7.32 mL, 74.2 mmol, 30 equiv.). The solution was stirred for 3 h, then quenched with sat aq Na_2SO_3 (200 mL) and extracted with EtOAc (3 x 100 mL). The combined organic layers were dried (Na_2SO_4), and the solvent was removed in vacuo. Flash chromatography (SiO_2, 7% MeOH in DCM elution) afforded **116** (637 mg, 2.25 mmol, 91%) as a white solid. R_f (5% MeOH in DCM elution) = 0.20; Mp = 220–221 °C; HRMS (EI) *m* / *z* calcd for $C_{17}H_{20}N_2O_2$ (M^+) 284.1525, found 284.1520; ^{1}H NMR (500 MHz, DMSO–d6, a mixture of rotamers in 1.2:1.0 ratio) δ: 7.39 (s, 0.55H), 7.33 (s, 0.45H), 6.71 (s, 0.51H), 6.61 (t, *J* = 8.5 Hz, 1H), 6.55 (s, 1H), 6.47 (s, 0.49H), 6.52 (dd, *J* = 7.0, 13.5 Hz, 1H), 6.29 (dd, *J* = 7.0, 14.0 Hz, 1H), 6.24 (t, *J* = 6.5 Hz, 1H), 4.83 – 4.91 (m, 1H), 3.95 – 4.01 (m, 2H), 2.94 (t, *J* = 9.0 Hz, 0.5H), 2.87 (t, *J* = 10.0 Hz, 0.5H), 1.87 – 1.94 (m, 2H), 1.57 – 1.73 (m, 3H), 1.33 – 1.48 (m, 2H), 1.11 – 1.29 (m, 2H); ^{13}C NMR (100 MHz, DMSO – d6) δ: 175.7, 174.5, 162.1, 162.0, 140.0, 139.7, 138.0, 136.7, 135.9, 135.6, 129.3, 129.1, 128.7 (2x), 127.4, 127.3, 126.9, 126.8, 118.6, 118.4, 71.5, 71.0, 53.1, 52.8, 45.4, 43.2, 43.1, 42.8, 38.3, 37.7, 27.6, 25.9, 25.5, 25.2; IR (film, cm^{-1}) 3416, 3234, 3066, 2922, 1678, 1656, 1640, 1608.

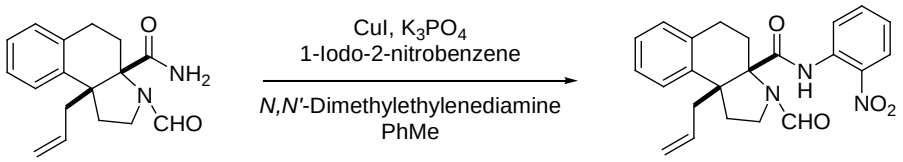

116 **117**

9b-Allyl-3-formyl-2,3,3a,4,5,9b-hexahydro-N-(2-nitrophenyl)-1H-benzo[e]indole-3a-carboxamide 117. A Schlenk tube was charged with CuI (21 mg, 0.11 mmol, 0.20 equiv.), 1-iodo-2-nitrobenzene (270 mg, 1.08 mmol, 2.0 equiv.), carboxamide **116** (154 mg, 0.54 mmol, 1.0 equiv.), K_3PO_4 (230 mg, 1.08 mmol, 2.0 equiv.), evacuated and backfilled with nitrogen. *N*,*N*'-Dimethylethylenediamine (23 uL, 0.22 mmol, 0.40 equiv.) and toluene (1 mL) were added under nitrogen. The reaction mixture was stirred at 80 °C for 15 h. The resulting yellow-brown suspension was filtered through a pad of silica gel eluting with ethyl acetate (50 mL). The filtrate was concentrated in vacuo and the residue was purified by flash chromatography (SiO_2, 50% EtOAc in hexanes elution) afforded **117** (195 mg, 0.49 mmol, 91%) as a yellow solid. R_f (50% EtOAc in hexanes elution) = 0.30; Mp = 175 °C; HRMS (EI) m / z calcd for $C_{23}H_{23}N_3O_4$ (M^+) 405.1689, found 405.1688; ^{1}H NMR (500 MHz, $CDCl_3$, a mixture of rotamers in 2.2:1.0 ratio) δ: 11.19 (s, 0.69H), 11.01 (s, 0.31H), 8.99 (d, *J* = 8.5 Hz, 0.69H), 8.91 (d, *J* = 9.0 Hz, 0.31H), 8.39 (s, 0.63H), 8.34 (s, 0.39H), 8.29 (d, *J* = 8.0 Hz, 0.38H), 8.25 (d, *J* = 8.0 Hz, 0.62H), 7.67 – 7.74 (m, 1H), 7.34 (d, *J* = 7.5 Hz, 1H), 7.21 – 7.29 (m, 2H), 7.16 – 7.20 (m, 1H), 7.08 – 7.13 (m, 1H), 5.52 – 5.64 (m, 1H), 4.77 – 4.90 (m, 2H), 4.00 (dd, *J* = 8.0 Hz, 11.5 Hz, 0.32H), 3.87 (t, *J* = 9.0 Hz, 0.68H), 2.99 – 3.16 (m, 2H), 2.71 – 2.90 (m, 3H), 2.54 – 2.60 (m, 1H), 2.47 – 2.51 (m, 1H), 2.33 – 2.43 (m, 1H), 2.28 (dd, *J* = 6.0, 12.5 Hz, 0.32H), 2.11 (dd, *J* = 5.5, 13.0 Hz, 0.68 H); ^{13}C NMR (100 MHz, $CDCl_3$) δ: 172.5, 171.7, 161.8, 161.2, 138.7, 138.1, 137.5, 136.9, 136.65, 136.61, 136.5, 135.8, 134.9, 134.3, 134.1, 133.8, 129.1, 129.0, 127.43, 127.40, 127.38, 127.2, 127.0, 126.9, 126.4, 126.2, 124.4, 123.8, 122.1, 121.9, 118.6, 118.2, 73.2, 72.7, 53.40, 53.37, 45.3,

43.2, 43.0, 42.7, 38.3, 37.5, 27.6, 25.7, 24.9, 24.8; IR (film, cm^{-1}) 2969, 2925, 2104, 1658, 1606.

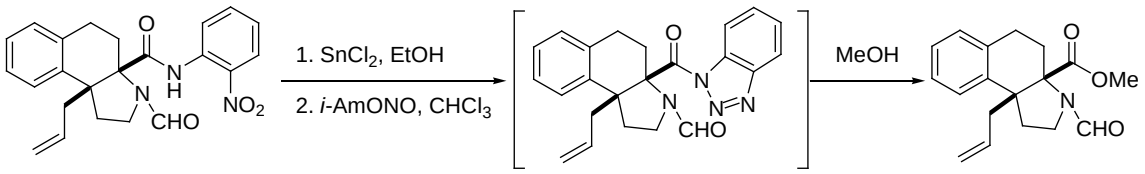

117 **119** **114**

Methyl-9b-allyl-3-formyl-2,3,3a,4,5,9b-hexahydro-1H-benzo[e]indole-3a-carboxylate 114. To a solution of **117** (1.89 g, 4.65 mmol, 1.0 equiv.) in EtOH (18 mL) was added $SnCl_2$ (4.41 g, 23.3 mmol, 5.0 equiv.). The solution was heated to reflux for 0.5 h, then quenched with H_2O (500 mL), and extracted with EtOAc (3 x 300 mL). The combined organic layers were dried (Na_2SO_4), and the solvent was removed in vacuo. Flash chromatography (SiO_2, 5% MeOH in DCM elution) afforded the anilide (1.62 g, 4.33 mmol, 93%). To a solution of the resulting anilide (464 mg, 1.24 mmol, 1.0 equiv.) in $CHCl_3$ (6 mL) was added *i*-AmONO (0.33 mL, 1.48 mmol, 1.2 equiv.). The reaction mixture was stirred for 15 h, then treated with MeOH (25 mL). The reaction mixture was heated to reflux for 15 h then quenched with 100 mL NaOH (1N aqueous solution) and extracted with EtOAc (3 x 200 mL). The resulting benzotriazole was cleanly removed by extraction with the aqueous basic solution. The combined organic layers were dried (Na_2SO_4), and the solvent was removed in vacuo. Flash chromatography (SiO_2, 30% EtOAc in hexanes elution) afforded **114** (261 mg, 0.88 mmol, 71%) as a colorless oil. R_f (50% EtOAc in hexanes elution) = 0.31; HRMS (EI) *m* / *z* calcd for $C_{18}H_{21}NO_3$ (M^+) 299.1521, found 299.1519; ^1H NMR (500 MHz, $CDCl_3$, a mixture of rotamers in 1.4:1.0

ratio) δ: 8.21 (s, 0.58H), 8.15 (s, 0.42H), 7.28 (t, *J* = 7.5 Hz, 1H), 7.17 – 7.20 (m, 1H), 7.10 (t, *J* = 7.0 Hz, 1H), 7.01 – 7.05 (m, 1H), 5.41 – 5.53 (m, 1H), 4.82 – 4.88 (m, 2H), 3.78 (s, 1.5H), 3.76 (s, 1.5H), 3.71 (dd, *J* = 9.5 Hz, 11.5 Hz, 0.5H), 3.63 (t, *J* = 9.0 Hz, 0.5H), 2.82 – 2.95 (m, 2H), 2.67 – 2.75 (m, 2H), 2.63 – 2.66 (m, 1H), 2.56 – 2.61 (m, 0.5H), 2.39 – 2.46 (m, 0.5H), 2.24 – 2.33 (m, 2H), 2.14 – 2.23 (m, 0.5H), 1.97 – 2.01 (m, 0.5H); ^{13}C NMR (100 MHz, $CDCl_3$) δ: 173.7, 172.9, 161.6, 160.6, 138.4, 138.0, 137.6, 135.8, 133.6, 133.4, 128.9, 128.8, 127.29, 127.27, 127.0, 126.8, 126.7, 126.6, 118.3, 118.0, 71.2, 70.7, 52.8, 52.6, 52.4 (2x), 45.1, 43.3, 42.8, 42.7, 37.9, 37.1, 26.7, 25.3, 24.9, 24.4; IR (film, cm^{-1}) 2951, 2925, 2882, 2244, 1728, 1658, 1379.

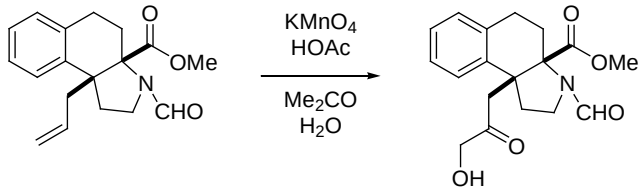

114 **120**

Methyl-3-formyl-2,3,3a,4,5,9b-hexahydro-9b-(3-hydroxy-2-oxopropyl)-1H-benzo[e]indole-3a-carboxylate 120. To a solution of **114** (241 mg, 0.81 mmol, 1.0 equiv.) in acetone (4.94 mL), water (1.08 mL) and acetic acid (300 µL) was added a solution of $KMnO_4$ (382 mg, 2.42 mmol, 3.0 equiv.) in acetone (6.51 mL) and water (1.45 mL). After 3 min a solution of H_2SO_4 (0.43 mL) in water (3 mL) was added, then $NaNO_2$ (181 mg, 2.62 mmol) was added whereupon the dark purple solution turned into a clear, colorless solution. The solution was diluted in water (100 mL) and extracted with EtOAc (3 x 100 mL). The combined organic layers were dried (Na_2SO_4), and the solvent was removed in vacuo. Flash chromatography (SiO_2, 70% EtOAc in hexanes elution)

afforded **120** (232 mg, 0.70 mmol, 87%) as a colorless oil. R_f (5% MeOH in DCM elution) = 0.23; HRMS (EI) *m* / *z* calcd for $C_{18}H_{21}NO_5$ (M^+) 331.1420, found 331.1410; ^{1}H NMR (500 MHz, $CDCl_3$, a mixture of rotamers in 1.3:1.0 ratio) δ: 8.25 (s, 0.57H), 8.22 (s, 0.43H), 7.09 – 7.13 (m, 1H), 7.15 – 7.20 (m, 3H), 4.01 (d, *J* = 19.0 Hz, 0.5H), 3.93 (d, *J* = 18.5 Hz, 0.5H), 3.81 – 3.90 (m, 1H), 3.79 (s, 1.5H), 3.76 (s, 1.5H), 3.71 (dd, *J* = 5.0, 13.5 Hz, 0.5H), 2.98 (d, *J* = 16.5 Hz, 1H), 2.75 – 2.91 (m, 5.5H), 2.59 – 2.73 (m, 1H), 2.42 – 2.52 (m, 1H), 2.22 – 2.36 (m, 1H); ^{13}C NMR (100 MHz, $CDCl_3$) δ: 207.1, 207.0, 173.8, 172.9, 161.7, 161.1, 137.9, 137.5, 137.1, 135.3, 129.53, 129.47, 127.4 (2x), 127.3, 127.2, 126.34, 126.29, 71.3, 70.7, 69.3, 69.2, 53.4, 53.0, 51.2, 51.1, 46.3, 45.8, 45.2, 42.7, 37.1, 36.3, 26.4, 25.4, 24.5, 24.4; IR (film, cm^{-1}) 3417, 2920, 2850, 1734, 1657.

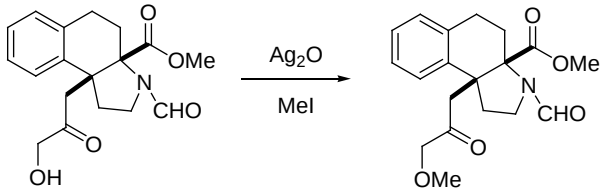

120 **115**

Methyl-3-formyl-2,3,3a,4,5,9b-hexahydro-9b-(3-methoxy-2-oxopropyl)-1H-benzo[e]indole-3a-carboxylate 115. To a solution of **120** (30 mg, 0.10 mmol, 1.0 equiv.) in MeI (4 mL) was added Ag_2O (31 mg, 0.14 mmol, 1.0 equiv.). The solution stirred for 15 h, then filtered through a pad of silica gel and concentrated in vacuo. Flash chromatography (SiO_2, 2% MeOH in DCM elution) afforded **115** (31 mg, 0.10 mmol, quant) as a colorless oil. R_f (5% MeOH in DCM elution) = 0.37; HRMS (EI) *m* / *z* calcd for $C_{19}H_{23}NO_5$ (M^+) 345.1576, found 345.1576; ^{1}H NMR (500 MHz, $CDCl_3$, a mixture

of rotamers in 1.3:1.0 ratio) δ: 8.24 (s, 0.57H), 8.21 (s, 0.43H), 7.18 – 7.23 (m, 1H), 7.07 – 7.18 (m, 3H), 3.79 (d, *J* = 17.0 Hz, 0.5H), 3.78 (s, 1.5H), 3.76 (s, 1.5H), 3.65 – 3.75 (s, 1.5H), 3.31 (s, 3H), 3.02 (d, *J* = 17.5 Hz, 1H), 2.77 – 2.99 (m, 4H), 2.45 – 2.74 (m, 3H), 2.19 – 2.32 (m, 2H); ^{13}C NMR (100 MHz, $CDCl_3$) δ: 205.3, 205.2, 173.7, 172.9, 161.4, 160.9, 138.3, 137.8, 137.0, 135.3, 129.2, 129.1, 127.1, 126.9, 126.86, 126.83, 126.3, 126.2, 78.34, 78.27, 71.2, 70.6, 59.3 (2x), 53.2, 52.8, 51.0, 50.8, 46.2, 45.7, 45.1, 42.6, 37.1, 36.3, 26.5, 25.4, 24.5, 24.4; IR (film, cm^{-1}) 2982, 2948, 2887, 1733, 1672.

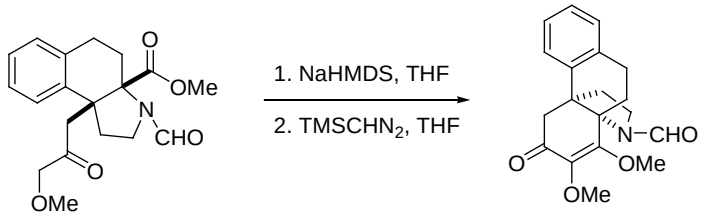

115 **113**

Enol ether 113. To a solution of NaHMDS (0.37 mL, 0.37 mmol, 1.0 M in THF, 1.5 equiv.) in THF (1 mL) at 0 °C was added **115** (86 mg, 0.25 mmol, 1.0 equiv.) in THF (1 mL). The solution was warmed to rt and stirred for 30 min, then quenched with 1N HCl (5 ml) and extracted with EtOAc (3 x 20 mL). The combined organic layers were dried (Na_2SO_4), and the solvent was removed in vacuo. To the resulting dione in MeOH (0.20 mL) and MeCN (1.80 mL) was added *i*Pr_2NEt (56 µL, 0.32 mmol, 1.3 equiv.) then $TMSCHN_2$ (0.16 mL, 0.32 mmol, 0.20 M in diethyl ether, 1.3 equiv.). The solution was stirred for 15 h, then quenched with 1N HCl (5 mL) and extracted with EtOAc (3 x 20 mL). The combined organic layers were dried (Na_2SO_4), and the solvent was removed in vacuo. Flash chromatography (SiO_2, 2% MeOH in DCM elution) afforded desired enol ether **113** (27 mg, 0.083 mmol, 33%) as a colorless oil and the regioisomer **121** (27 mg,

0.083 mg, 33%) as a colorless oil. R_f (5% MeOH in DCM elution) = 0.39; HRMS (ESI) *m*/*z* calcd for $C_{19}H_{21}NO_4$ (M^+) 327.1471, found 327.1462; ^{1}H NMR ($CDCl_3$, 500 MHz) δ: 8.43 (s, 1H), 7.26 (d, *J* = 8.5 Hz, 1H), 7.24 (t, *J* = 7.5 Hz, 1H), 7.17 (t, *J* = 8.0 Hz, 1H), 7.07 (d, *J* = 7.5 Hz, 1H), 4.15 (s, 3H), 3.70 (s, 3H), 3.53 – 3.57 (m, 1H), 3.00 – 3.05 (m, 1H), 3.00 (d, *J* = 17 Hz, 1H), 2.83 – 2.90 (m, 1H), 2.76 – 2.81 (m, 1H), 2.70 (d, *J* = 17 Hz, 1H), 2.56 – 2.61 (m, 1H), 2.27 – 2.30 (m, 2H), 2.16 – 2.22 (m, 1H); ^{13}C NMR ($CDCl_3$, 100 MHz) δ: 192.2, 162.6, 161.6, 138.6, 136.3, 134.3, 129.4, 127.6, 127.3, 127.0, 66.8, 61.9, 61.0, 48.9, 46.9, 42.5, 34.0, 26.7, 24.5; IR (film, cm^{-1}) 2927, 2850, 1655, 1612, 1457, 1370. Other methyl enol ether regioisomer **121**: R_f (5% MeOH in DCM elution) = 0.36; HRMS (ESI) *m*/*z* calcd for $C_{19}H_{21}NO_4$ (M^+) 327.1471, found 327.1468; ^{1}H NMR ($CDCl_3$, 400 MHz) δ: 8.49 (s, 1H), 7.28 (d, *J* = 7.6 Hz, 1H), 7.23 (t, *J* = 7.2 Hz, 1H), 7.16 (t, *J* = 7.6 Hz, 1H), 7.06 (d, *J* = 7.6 Hz, 1H), 4.00 (s, 3H), 3.66 (s, 3H), 3.47 – 3.52 (m, 1H), 2.98 (d, *J* = 19 Hz, 1H), 2.81 – 2.94 (m, 2H), 2.76 (d, *J* = 18 Hz, 1H), 2.71 – 2.77 (m, 1H), 2.20 – 2.27 (m, 2H), 2.05 – 2.15 (m, 1H), 1.81 – 1.86 (m, 1H); ^{13}C NMR ($CDCl_3$, 100 MHz) δ: 193.7, 162.4, 160.8, 138.8, 134.3, 133.9, 129.6, 127.41, 127.37, 126.0, 68.3, 60.9, 58.5, 47.2, 41.5, 36.6, 32.9, 25.8, 23.9; IR (film, cm^{-1}) 3056, 2990, 2948, 1668, 1614, 1425, 1377.

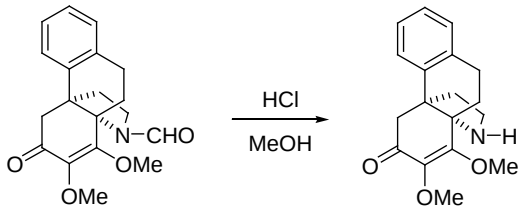

113 **122**

Amine 122. To a solution of **113** (12 mg, 0.035 mmol) in MeOH (2 mL) was added conc. HCl (30 µL) and heated to 65 °C for 15 h. The reaction mixture was quenched with 1N NaOH (5 mL) and extracted with EtOAc (3 x 10 mL). The combined organic layers were dried (Na_2SO_4), and the solvent was removed in vacuo. Flash chromatography (SiO_2, 4% MeOH in DCM elution) afforded **122** (7.4 mg, 0.025 mmol, 70%) as a yellow oil. R_f (5% MeOH in DCM elution) = 0.33; HRMS (EI) *m* / *z* calcd for $C_{18}H_{21}NO_3$ (M^+) 299.1521, found 299.1517; ^{1}H NMR (500 MHz, $CDCl_3$) δ: 7.23 (d, *J* = 8.0 Hz, 1H), 7.19 (t, *J* = 7.5 Hz, 1H), 7.10 (t, *J* = 7.0 Hz, 1H), 7.06 (d, *J* = 7.5 Hz, 1H), 4.14 (s, 3H), 3.68 (s, 3H), 3.08 – 3.15 (m, 1H), 2.97 (d, *J* = 17.0 Hz, 1H), 2.90 – 2.91 (m, 1H), 2.78 – 2.83 (m, 1H), 2.66 – 2.71 (m, 1H), 2.62 (d, *J* = 16.5 Hz, 1H), 2.39 (s, 1H), 2.21 – 2.31 (m, 2H), 2.16 – 2.20 (m, 1H), 1.84 – 1.90 (m, 1H); ^{13}C NMR (75 MHz, $CDCl_3$) δ: 193.8, 165.7, 142.6, 136.7, 134.7, 129.1, 127.9, 127.0, 126.3, 66.6, 61.6, 61.0, 48.2, 46.7, 42.4, 37.8, 26.9, 25.5; IR (film, cm^{-1}) 3350, 2922, 2854, 1716, 1670, 1609, 1449, 1328, 1243, 1061.

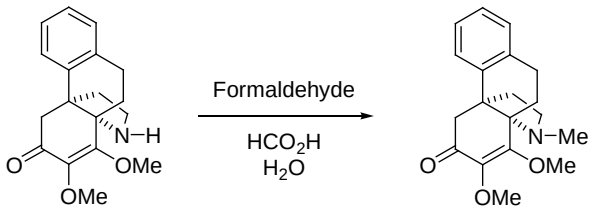

122 **84**

Bisdesmethoxyhasubanonine 84. To a solution of **122** (7.4 mg, 0.025 mmol) in water (1 mL) was added formaldehyde (0.04 mL, 0.53 mmol) then formic acid (0.04 mL, 0.93 mmol). The reaction mixture was heated to reflux for 15 h, then cooled to rt and diluted with $NaHCO_3$ (10 mL) and extracted with EtOAc (3 x 10 mL). The combined organic

layers were dried (Na_2SO_4), and the solvent was removed in vacuo. Flash chromatography (SiO_2, 5% MeOH in DCM elution) afforded **84** (5.7 mg, 0.022 mmol, 74%) as a white solid. R_f (5% MeOH in DCM elution) = 0.34; Mp = 106 °C; HRMS (EI) *m* / *z* calcd for $C_{15}H_{15}NO$ (M^+) 313.1678, found 313.1668; ^1H NMR (500 MHz, $CDCl_3$) δ: 7.22 (d, *J* = 7.5 Hz, 1H), 7.17 (t, *J* = 7.5 Hz, 1H), 7.08 (t, *J* = 8.0 Hz, 1H), 7.02 (d, *J* = 7.0 Hz, 1H), 4.09 (s, 3H), 3.63 (m, 3H), 3.02 (d, *J* = 16 Hz, 1H), 2.74 – 2.87 (m, 3H), 2.64 (d, *J* = 16 Hz, 1H), 2.60 – 2.65 (m, 1H), 2.53 (s, 3H), 2.20 – 2.24 (m, 1H), 2.13 – 2.18 (m, 1H), 2.05 – 2.11 (m, 1H), 1.97 – 2.03 (m, 1H); ^{13}C NMR (100 MHz, $CDCl_3$) δ: 194.1, 165.6, 143.0, 138.3, 135.1, 128.8, 128.0, 126.9, 126.1, 67.5, 61.0, 60.9, 51.6, 48.6, 48.4, 37.6, 36.5, 25.9, 23.0; IR (film, cm^{-1}) 2917, 2845, 2796, 1667, 1597, 1451, 1330, 1245, 1119, 1056.

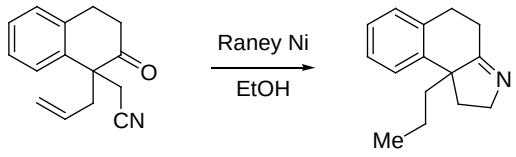

88 **99**

2,4,5,9b-Tetrahydro-9b-propyl-1H-benzo[e]indole (99). To a solution of 2-tetralone **88** (32 mg, 0.142 mmol, 1.0 equiv.) in EtOH (15 mL) was added approximately 0.25 mL solution of Raney Ni slush. The reaction mixture was stirred for 2 h, sparged under a nitrogen balloon, and filtered through a plug of silica gel. The solvent was removed and flash chromatography (SiO_2, 50% EtOAc in hexanes elution) afforded **99** (30 mg, 0.142

mmol, quant.) as a colorless oil. Crude ^{1}H-NMR spectrum is included in the supplemental section.

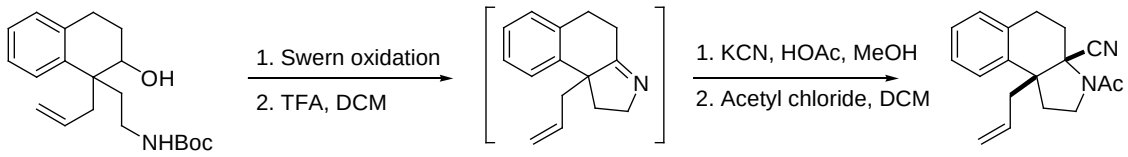

101 **87** **103**

3-Acetyl-9b-allyl-2,3,3a,4,5,9b-hexahydro-1H-benzo[e]indole-3a-carbonitrile 103. To a solution of oxalyl chloride (0.14 mL, 1.39 mmol, 1.2 equiv.) in DCM (2.90 mL) at -78 °C was added dropwise dimethyl sulfoxide (0.18 mL, 2.57 mmol, 2.2 equiv.) in DCM (0.58 mL). Carbamate **101** (353 mg, 1.07 mmol) in DCM (1.16 mL) was added dropwise and the solution was stirred for 5 min, then quenched with Et_3N (0.81 mL, 5.81 mmol, 5.0 equiv.). The cool bath was removed and the reaction mixture was diluted with H_2O (300 mL) and extracted with EtOAc (3 x 200 mL). The combined organic layers were dried (Na_2SO_4), and the solvent was removed in vacuo. The formation of aminoketone **102** was confirmed by ^{1}H-NMR of the crude mixture. Crude ^{1}H-NMR spectrum is included in the supplemental section. Due to the instability, the crude mixture was subjected to the following cyclic imine formation. The resulting ketone was diluted in DCM (20 mL) and trifluoroacetic acid (6 mL) was added at rt. The solution was stirred for 30 min, then quenched with sat aq $NaHCO_3$ (200 mL) and extracted with DCM (3 x 200 mL). The combined organic layers were dried (K_2CO_3) and the solvent was removed in vacuo. The formation of cyclic imine **87** was confirmed by ^{1}H-NMR of the crude mixture. Crude ^{1}H-NMR spectrum is included in the supplemental section. Due to

the instability, the crude mixture was subjected to the following aminonitrile formation. The resulting imine **87** was diluted with MeOH (12 mL) and acetic acid (0.61 mL, 10.7 mmol, 10 equiv.). KCN (642 mg, 9.86 mmol, 9.3 equiv.) was added and the solution was allowed to stir at rt for 15 h. Crude ^{1}H-NMR spectrum is included in the supplemental section. The reaction mixture was diluted with DCM (30 mL) and acetyl chloride (0.59 mL, 10.7 mmol, 10 equiv.) was added at 0 °C. TEA (0.15 mL, 1.07 mmol, 1.0 equiv.) was added dropwise and stirred for 15 h. The reaction mixture was quenched with water (100 mL) and extracted with EtOAc (3 x 100 mL). The combined organic layers were dried (Na_2SO_4), and the solvent was removed in vacuo. Flash chromatography (SiO_2, 30% EtOAc in hexanes elution) afforded **103** (167 mg, 0.596 mmol, 56%) as a yellow solid which was a single diastereomer. R_f (50% EtOAc in hexanes elution) = 0.30. Crude ^{1}H-NMR spectrum is included in the supplemental section.

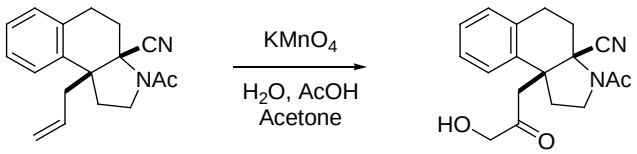

103 **106**

3-Acetyl-2,3,3a,4,5,9b-hexahydro-9b-(3-hydroxy-2-oxopropyl)-1H-benzo[e]indole-3a-carbonitrile 106. To a solution of **103** (78 mg, 0.280 mmol, 1.0 equiv.) in acetone (3.93 mL), water (0.78 mL) and acetic acid (190 µL) was added a solution of $KMnO_4$ (177 mg, 1.12 mmol, 4.0 equiv.) in acetone (1.49 mL) and water (0.49 mL). After 3 min a solution of H_2SO_4 (0.43 mL) in water (3 mL) was added, then $NaNO_2$ (145 mg, 2.10 mmol) was added whereupon the dark purple solution turned into a clear, colorless solution. The solution was diluted in water (100 mL) and extracted with EtOAc (3 x 100

mL). The combined organic layers were dried (Na_2SO_4), and the solvent was removed in vacuo. Flash chromatography (SiO_2, 70% EtOAc in hexanes elution) afforded **106** (40 mg, 0.129 mmol, 46%) as a colorless oil. R_f (5% MeOH in DCM elution) = 0.20. Crude ^{1}H-NMR spectrum is included in the supplemental section.

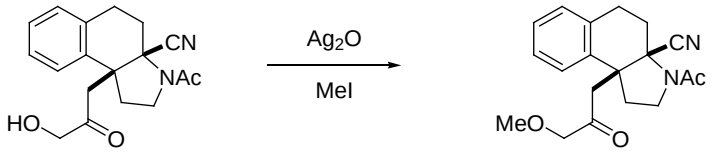

106 **104**

3-Acetyl-2,3,3a,4,5,9b-hexahydro-9b-(3-methoxy-2-oxopropyl)-1H-benzo[e]indole-3a-carbonitrile 104. To a solution of **106** (27 mg, 0.0877 mmol, 1.0 equiv.) in MeI (5 mL) was added Ag_2O (203 mg, 0.877 mmol, 10 equiv.). The solution stirred for 15 h, then filtered through a pad of silica gel and concentrated in vacuo. Flash chromatography (SiO_2, 2% MeOH in DCM elution) afforded **104** (15 mg, 0.0482 mmol, 55%) as a colorless oil. R_f (5% MeOH in DCM elution) = 0.30. Crude ^{1}H-NMR spectrum is included in the supplemental section.

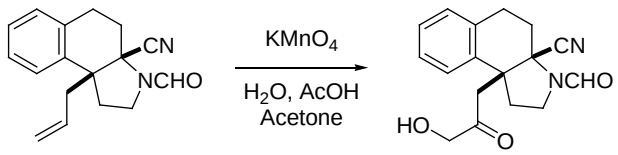

107 **108**

3-Formyl-2,3,3a,4,5,9b-hexahydro-9b-(3-hydroxy-2-oxopropyl)-1H-benzo[e]indole-3a-carbonitrile 108. To a solution of **107** (115 mg, 0.432 mmol, 1.0 equiv.) in acetone (6.06mL), water (1.40 mL) and acetic acid (260 µL) was added a solution of $KMnO_4$

(273 mg, 1.73 mmol, 4.0 equiv.) in acetone (2.37 mL) and water (0.80 mL). After 3 min a solution of H_2SO_4 (0.43 mL) in water (3 mL) was added, then $NaNO_2$ (123 mg, 1.79 mmol) was added whereupon the dark purple solution turned into a clear, colorless solution. The solution was diluted in water (100 mL) and extracted with EtOAc (3 x 100 mL). The combined organic layers were dried (Na_2SO_4), and the solvent was removed in vacuo. Flash chromatography (SiO_2, 3% MeOH in DCM elution) afforded **108** (75 mg, 0.251 mmol, 58%) as a colorless oil. R_f (5% MeOH in DCM elution) = 0.22. Crude ^{1}H-NMR spectrum is included in the supplemental section.

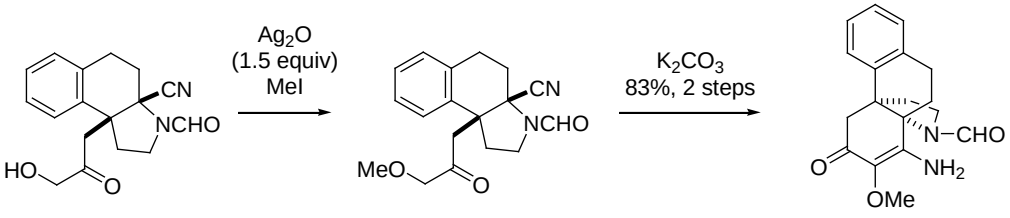

108 **109** **110**

Enamine 110. To a solution of alcohol **108** (196 mg, 0.657 mg, 1.0 equiv.) in MeI (4.0 mL) was added Ag_2O (304 mg, 1.31 mmol, 2.0 equiv.)**.** The solution was allowed to stir overnight at rt. TLC showed complete consumption of starting material. K_2CO_3 (200 mg) was added and stirred for 15 h. The solution was filtered through a plug of silica gel and concentrated. The combined organic solutions were dried (Na_2SO_4), and the solvent was removed in vacuo. Flash chromatography (SiO_2, 50% EtOAc in hexanes elution) afforded **110** (170 mg, 0.545 mmol, 83%) as a white solid. R_f (5% MeOH in DCM elution) = 0.20. Crude ^{1}H-NMR and ^{13}C-NMR spectrum are included in the supplemental section.

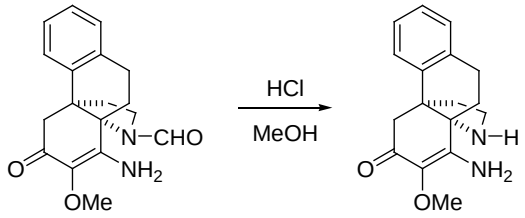

110 **111**

Amine 111. To a solution of enamine **110** (55 mg, 0.176 mmol, 1.0 equiv.) in MeOH (4.00 mL) was added HCl (0.13 mL). The solution was heated to reflux for 15 h. The solution was quenched with sat aq $NaHCO_3$ (20 mL) and extracted with EtOAc (3 x 20 mL). The combined organic layers were dried (Na_2SO_4), and the solvent was removed in vacuo. Flash chromatography (SiO_2, 5% MeOH in DCM elution) afforded **111** (21 mg, 0.0739 mmol, 42%) as a colorless oil. R_f (5% MeOH in DCM elution) = 0.20. Crude ^{1}H-NMR spectrum is included in the supplemental section.

2.14 Notes and References

(1) Bachmann, W. E.; Ross, A.; Dreiding, A. S.; Smith, P. A. *J. Org. Chem.* **1954**, *19*, 222-240.

(2) Eliel, E. L.; Pillar, C. *J. Am. Chem. Soc.* **1955**, *77*, 3600-3604.

(3) Bernd, P. *J. Org. Chem.* **2004**, *69*, 8287-8296.

(4) Bernd, P. *Tetrahedron: Asymmetry* **2005**, *16*, 3453-3459.

(5) Bernd, P. *J. Org. Chem.* **2005**, *9*, 1919-1929.

(6) Bernd, P. *J. Org. Chem.* **2003**, *68*, 7123-7125.

(7) Srinivasan, N. S. *Synthesis* **1979**, *7*, 520-521.

(8) Yu, Q.-s.; Luo, W.; Holloway, H. W.; Utsuki, T.; Perry, T.; Lahiri, D. K.; Greig, N. H.; Brossi, A. *Heterocycles* **2003**, *61*, 529-539.

(9) Nerinckx, W.; Vandewalle, M. *Tetrahedron* **1990**, *46*, 265-276.

(10) Pei, X.-F.; Yu, Q.-s.; Lu, B.-y.; Greig, N. H.; Brossi, A. *Heterocycles* **1996**, *42*, 229-236.

(11) Lee, T. B. K.; Wong, G. S. K. *J. Org. Chem.* **1991**, *56*, 872-875.

(12) Gorka, A.; Czuczai, B.; Szoleczky, P.; Hazai, L.; Szantay, C.; Hada, V. *Synth. Commun.* **2005**, *35*, 2371-2378.

(13) Silveira, C. C.; Braga, A. L.; Kaufman, T. S.; Lenardao, E. J. *Tetrahedron* **2004**, *60*, 8295-8328.

(14) Heathcock, C. H.; Norman, M. H.; Dickman, D. A. *J. Org. Chem.* **1990**, *55*, 798-811.

(15) Evans, D. A.; Scheerer, J. R. *Angew. Chem., Int. Ed.* **2005**, *44*, 6038-6042.

(16) Trost, B. M.; Van Vranken, D. L. *Chem. Rev.* **1996**, *96*, 395-422.

(17) Tsuji, J. *Tetrahedron* **1986**, *42*, 4361-4401.

(18) Basel, Y.; Hassner, A. *J. Org. Chem.* **2000**, *65*, 6368-6380.

(19) Vachal, P.; Jacobsen, E. N. *Org. Lett.* **2000**, *2*, 867-870.

(20) Gilley, C. B.; Kobayashi, Y. *J. Org. Chem.* **2008**, *73*, 4198-4204.

(21) Katritzky, A. R.; Lan, X.; Yang, J. Z.; Denisko, O. V. *Chem. Rev. (Washington, D. C.)* **1998**, *98*, 409-548.

(22) Katritzky, A. R.; Suzuki, K.; Wang, Z. *Synlett* **2005**, *11*, 1656-1665.

(23) Klapars, A.; Antilla, J. C.; Huang, X.; Buchwald, S. L. *J. Am. Chem. Soc.* **2001**, *123*, 7727-7729.

(24) Newman, M. S. *J. Am. Chem. Soc.* **1950**, *72*, 4783-4786.

(25) Zhang, H.; Yue, J.-M. *J. Nat. Prod.* **2005**, *68*, 1201-1207.

2.15 APPENDIX ONE: Spectra Relevant to Chapter Two

^{1}H-NMR of 1,1-disubstituted tetralone 88, 500 MHz, $CDCl_3$

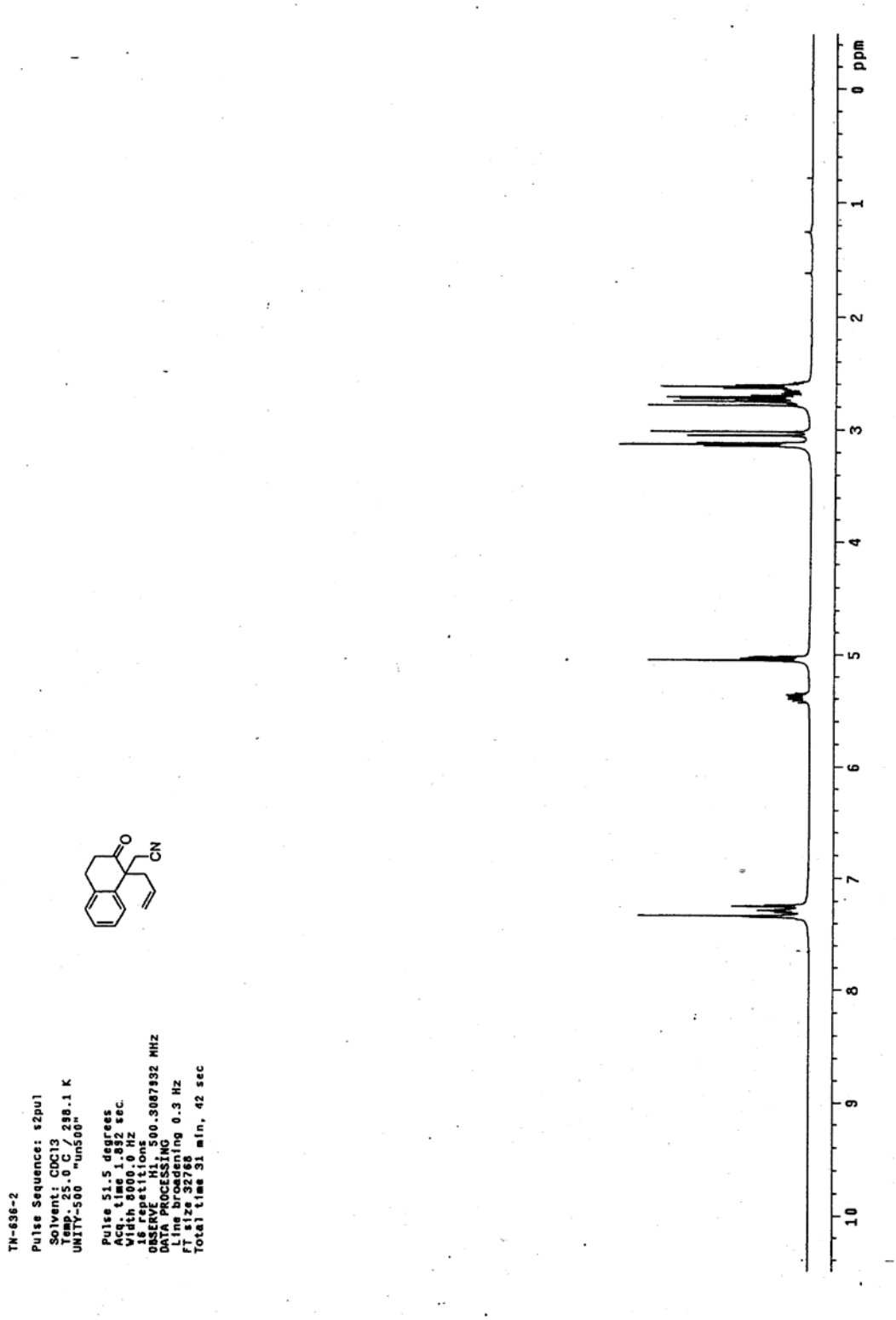

^{13}C-NMR of 1,1-disubstituted tetralone 88, 100 MHz, $CDCl_3$

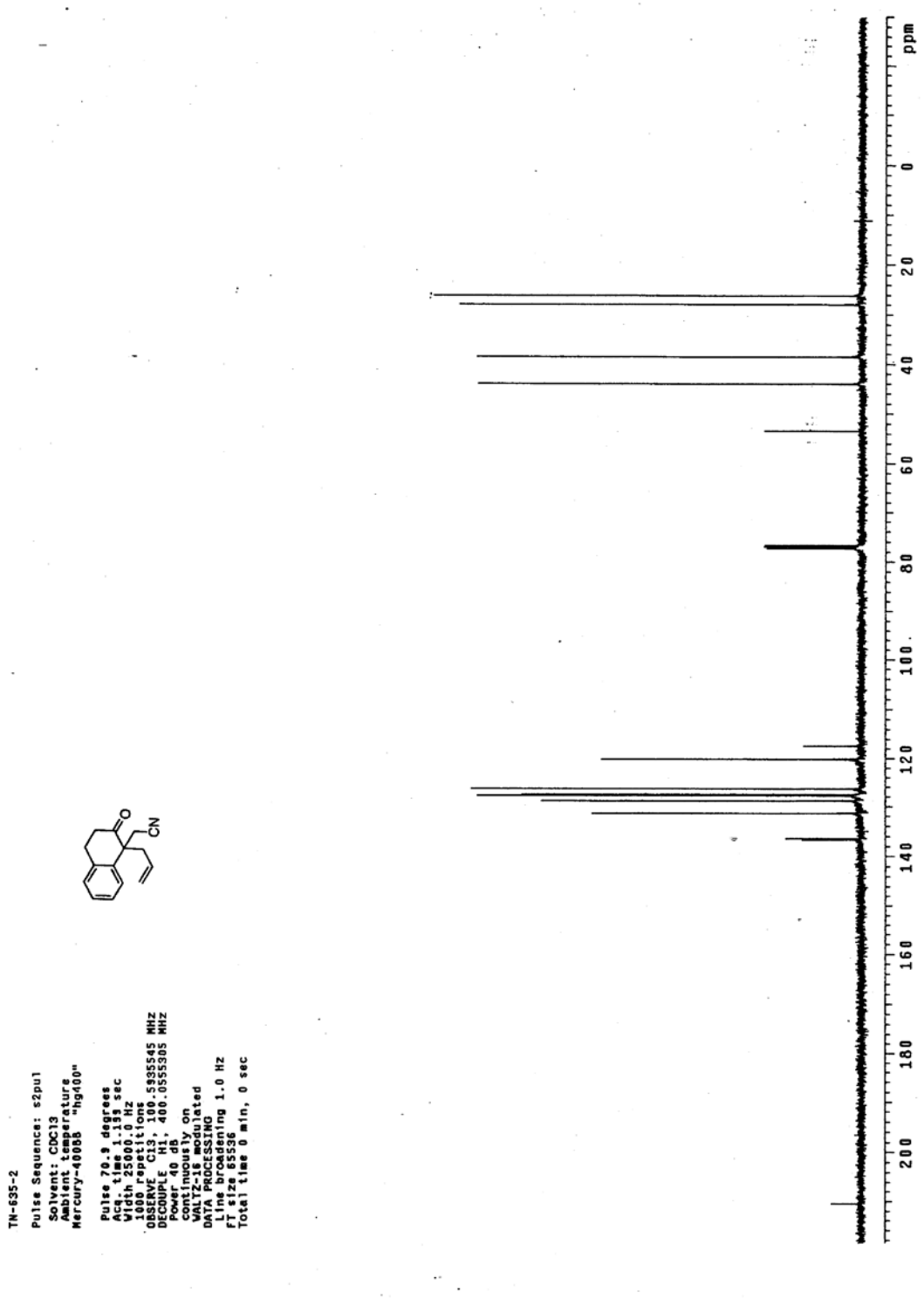

^{1}H-NMR of carbamate 101, 500 MHz, $CDCl_3$

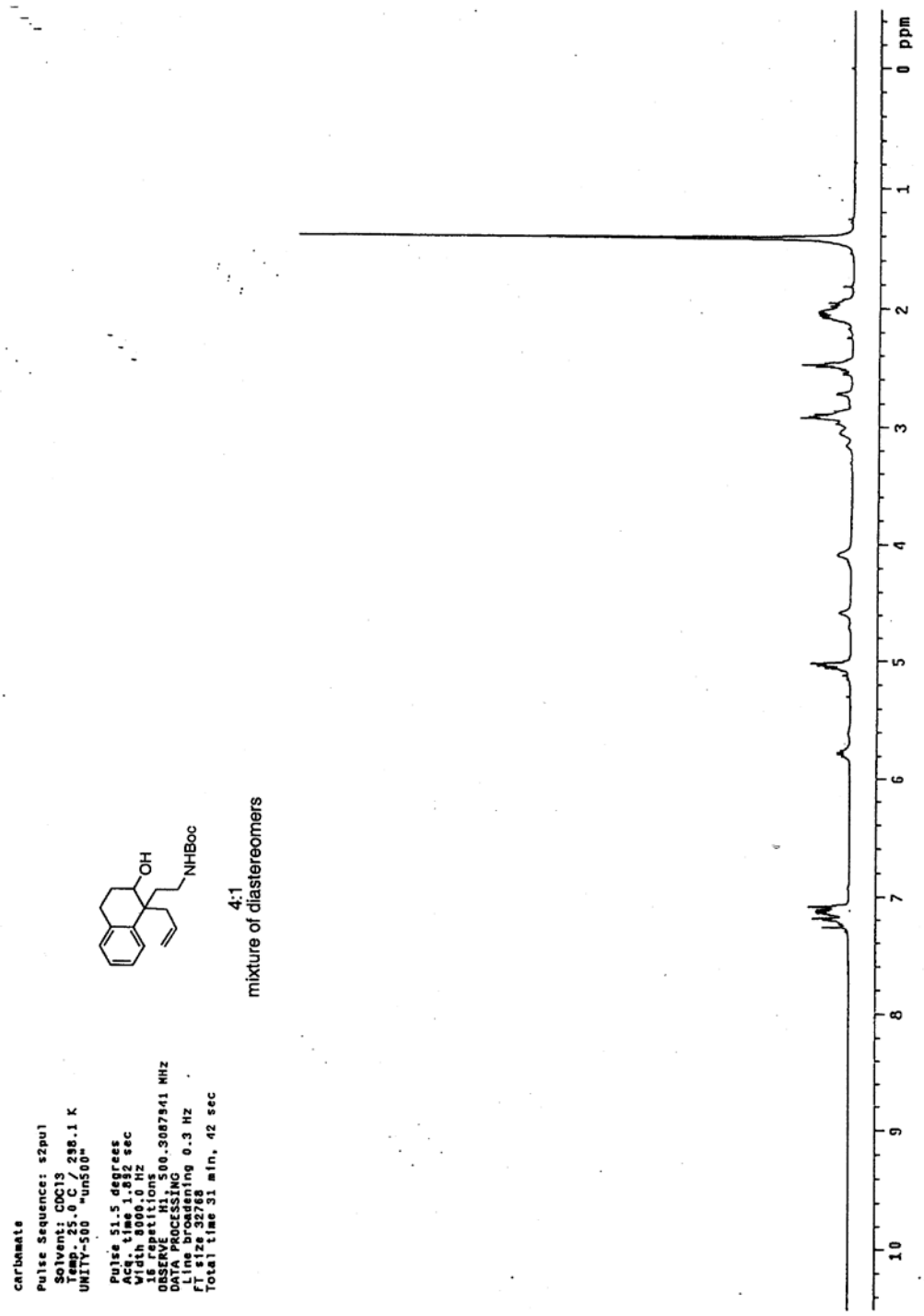

^{13}C-NMR of carbamate 101, 100 MHz, $CDCl_3$

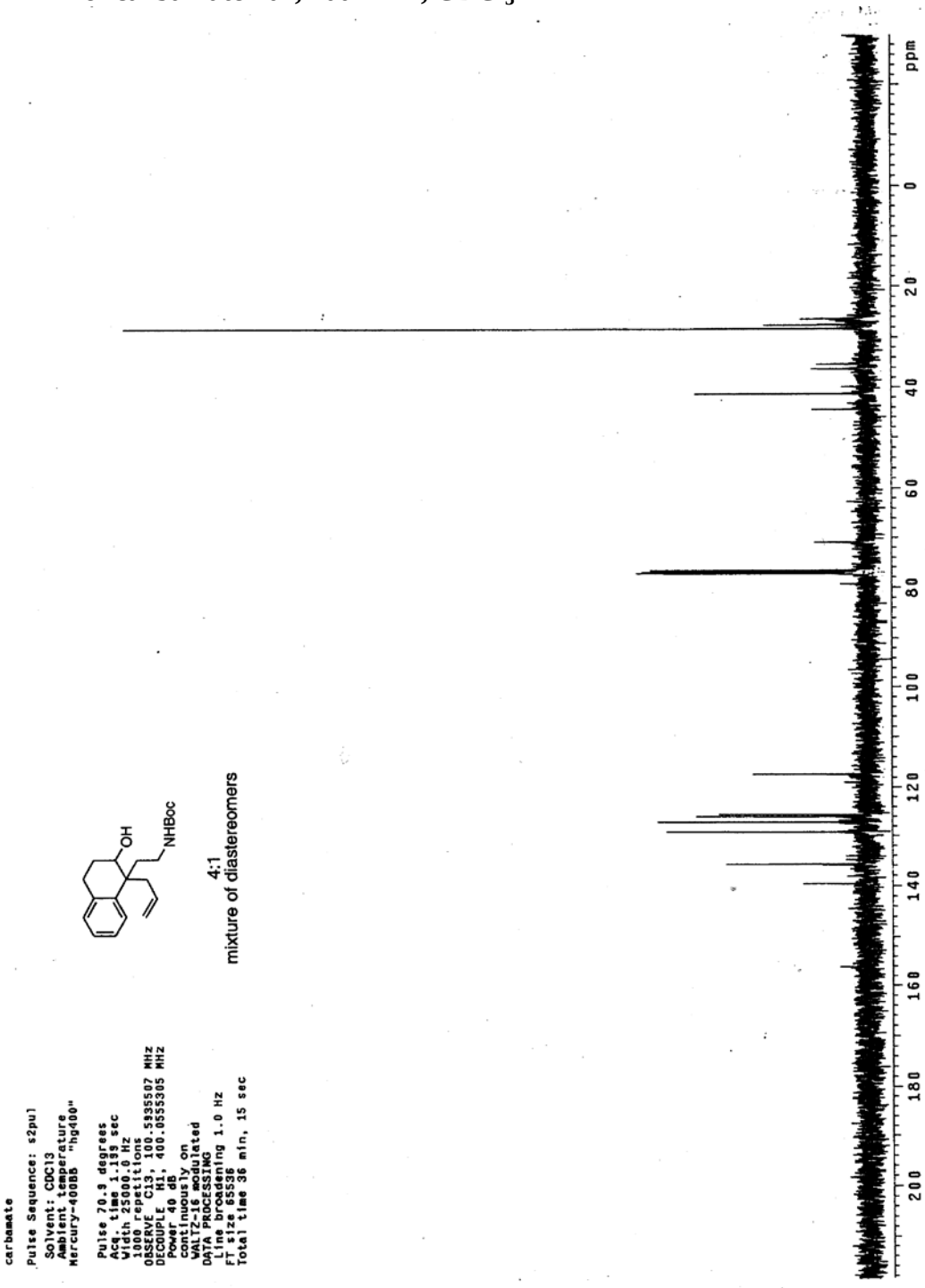

^{1}H-NMR of aminonitrile 107, 500 MHz, $CDCl_3$

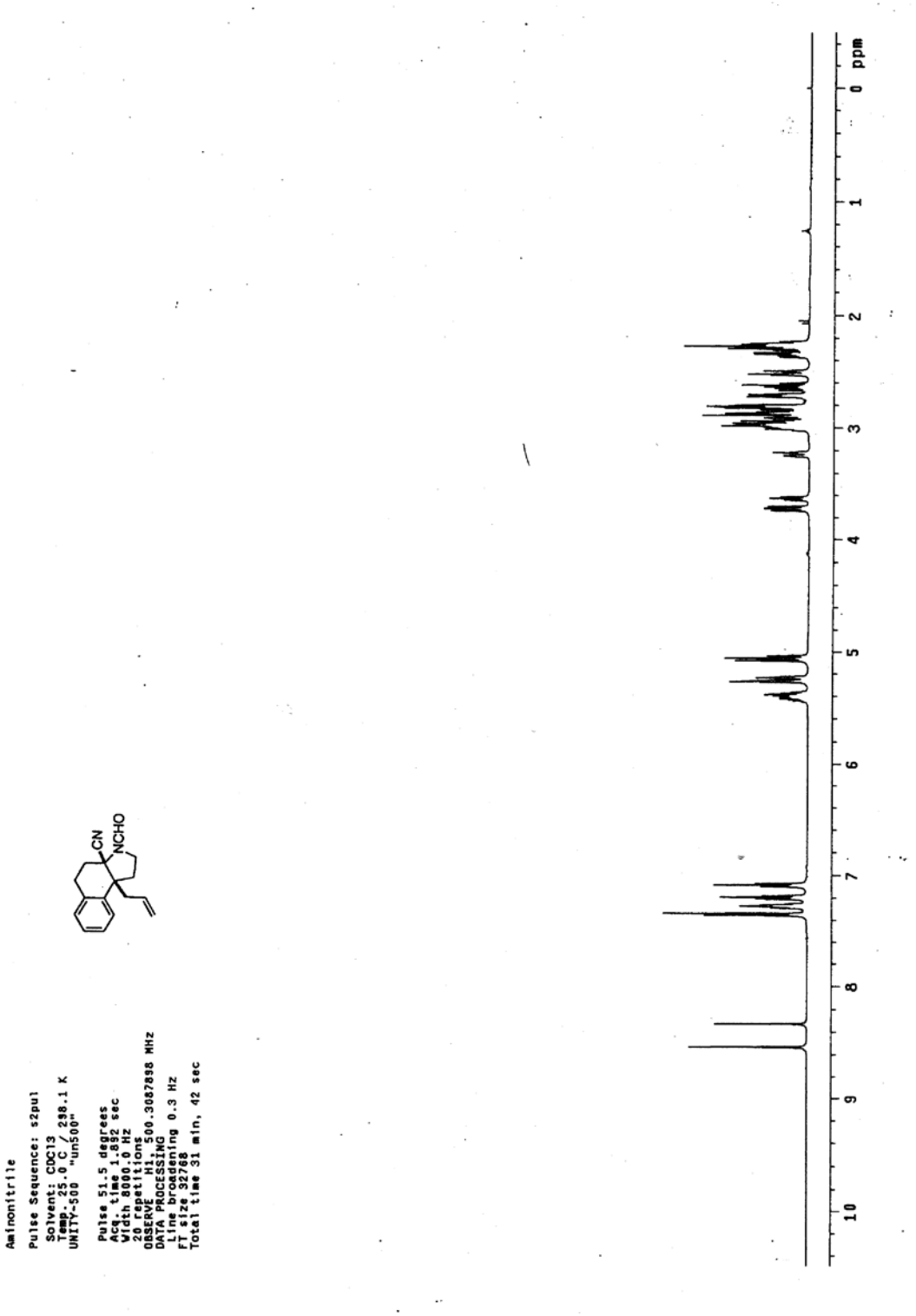

^{13}C-NMR of aminonitrile 107, 100 MHz, $CDCl_3$

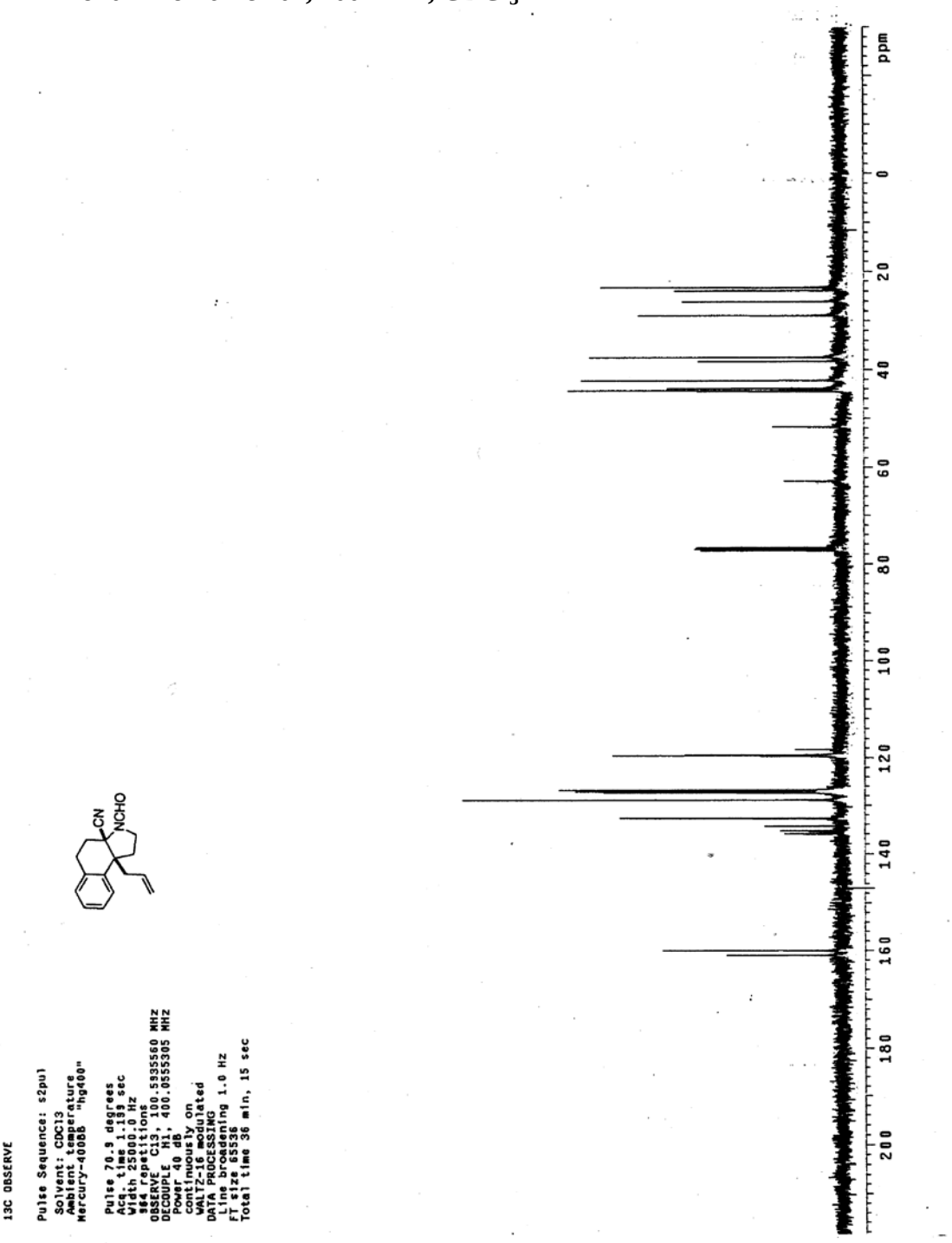

[1]H-NMR of carboxamide 116, 500 MHz, DMSO–d6

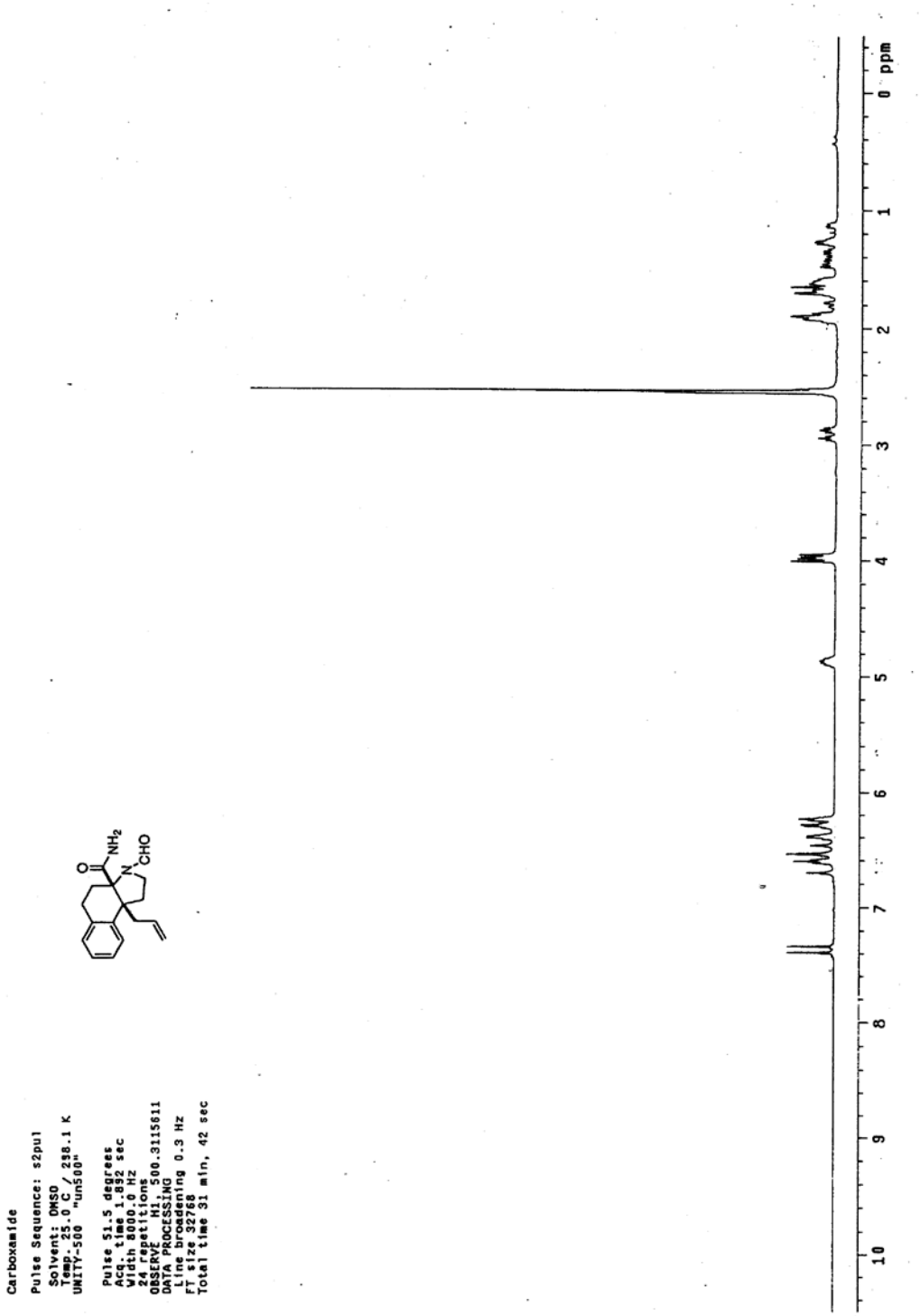

^{13}C-NMR of carboxamide 116, 100 MHz, DMSO – d6

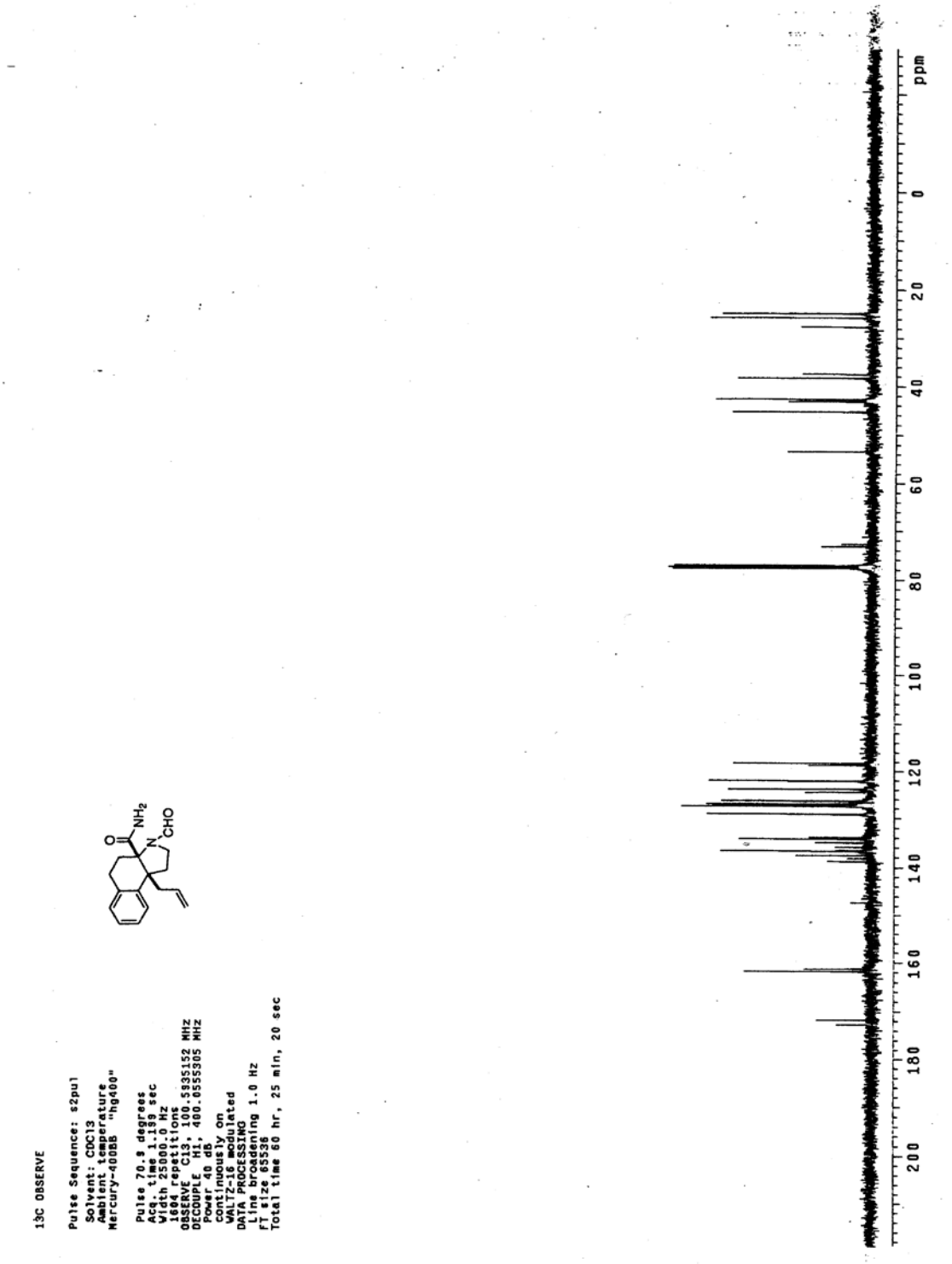

^{1}H-NMR of *ortho*-nitroaniline 117, 500 MHz, $CDCl_3$

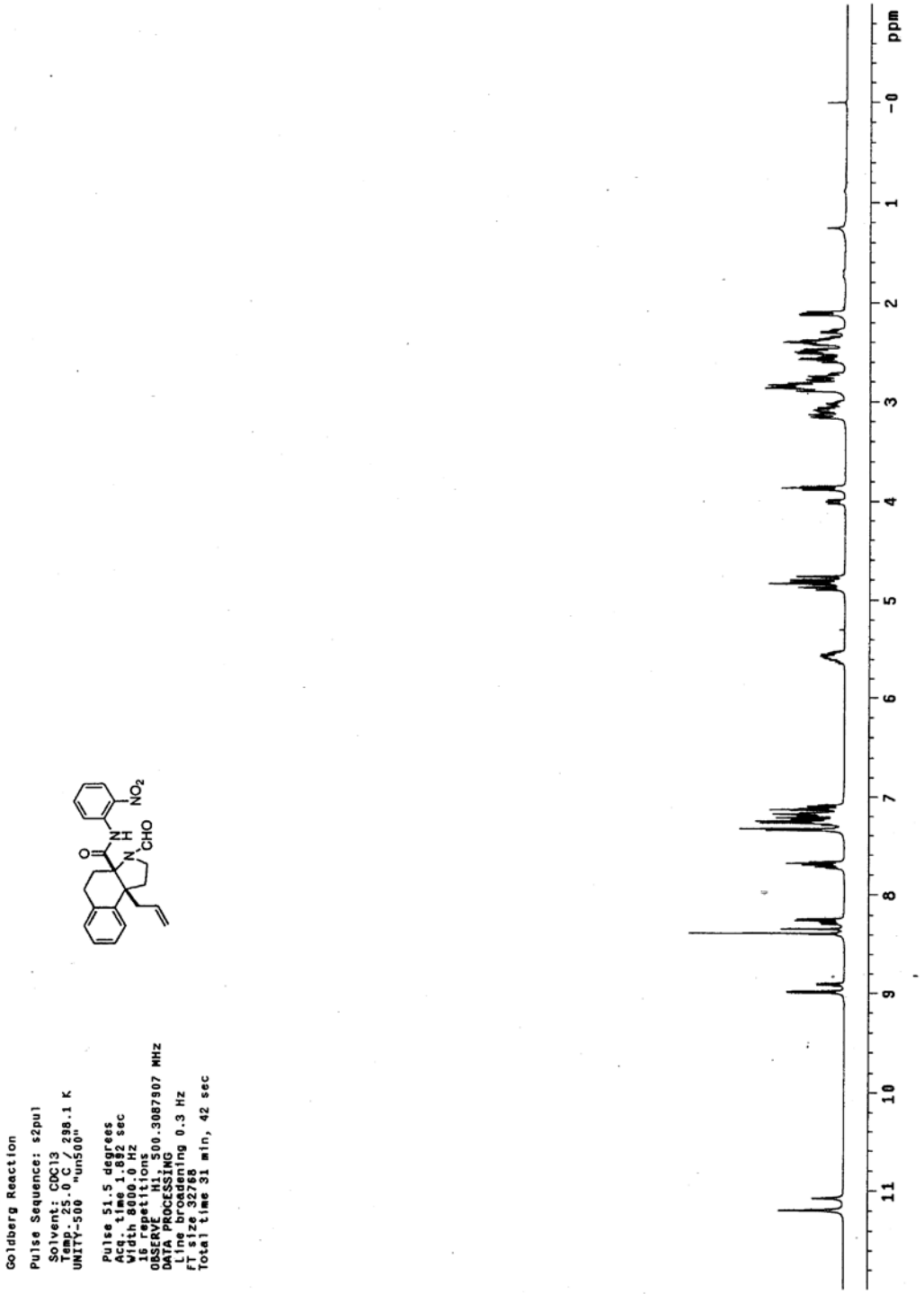

^{13}C-NMR of *ortho*-nitroaniline 117, 100 MHz, $CDCl_3$

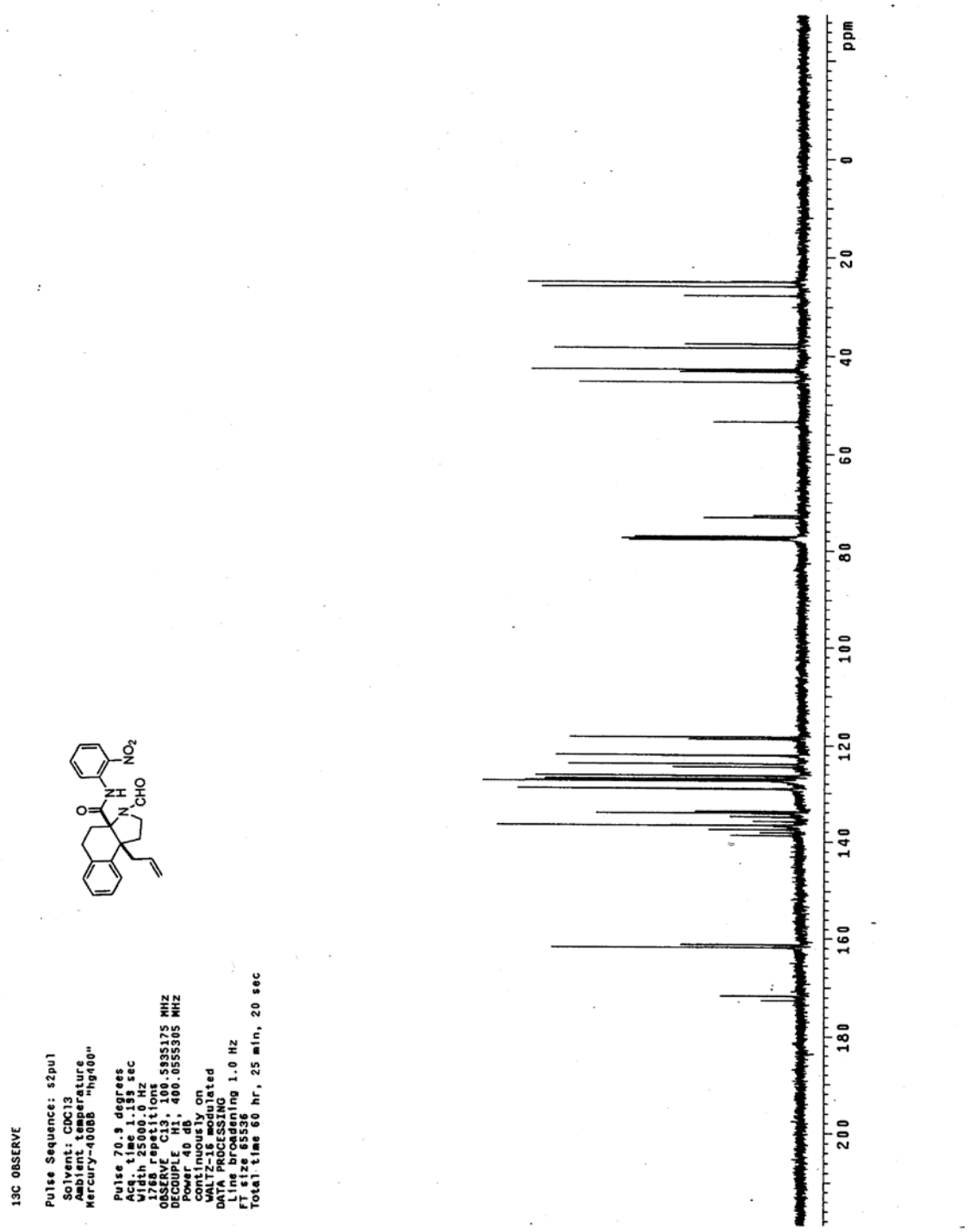

^{1}H-NMR of methyl ester 114, 500 MHz, $CDCl_3$

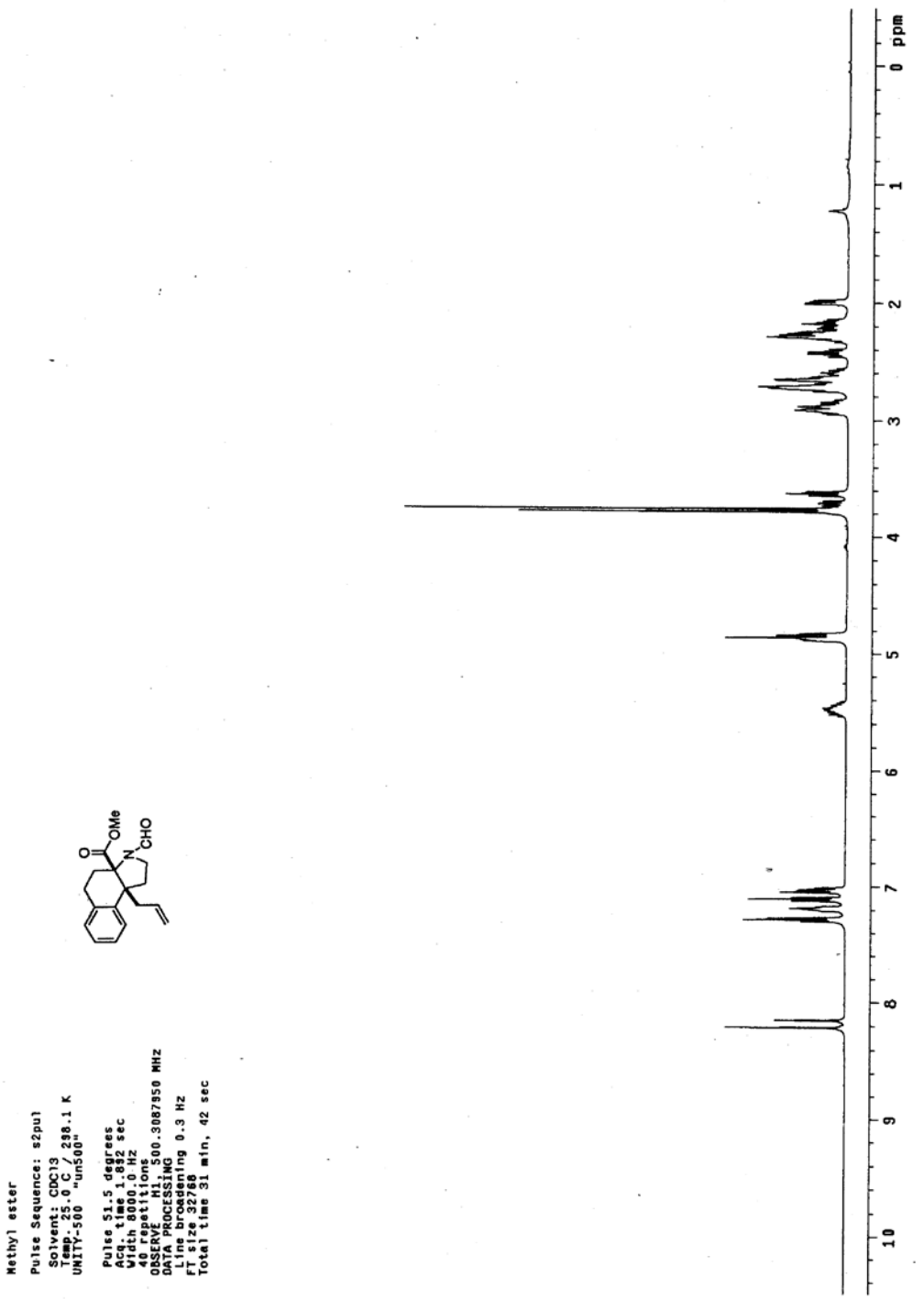

^{13}C-NMR of methyl ester 114, 100 MHz, $CDCl_3$

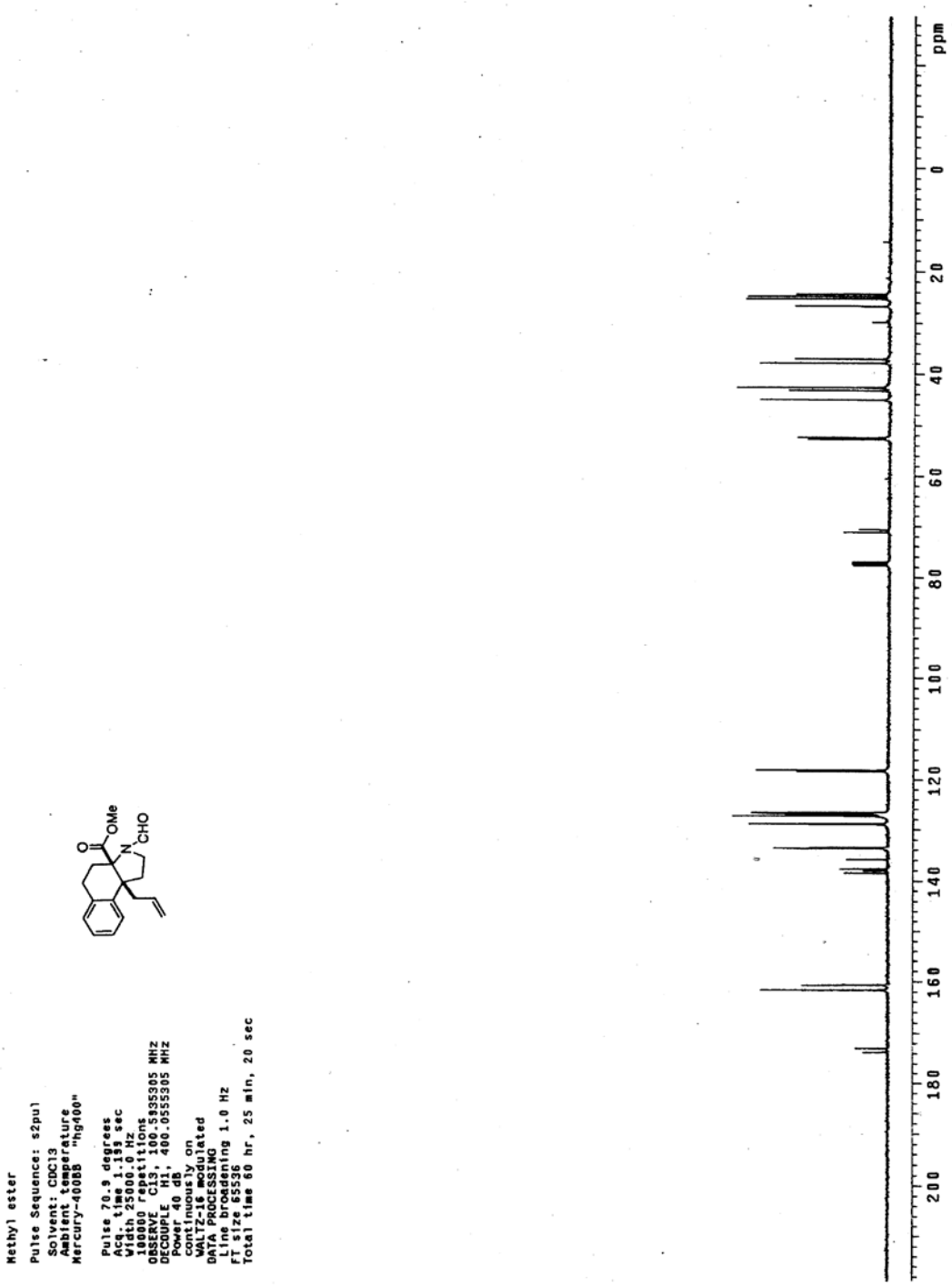

^{1}H-NMR of alcohol 120, 500 MHz, $CDCl_3$

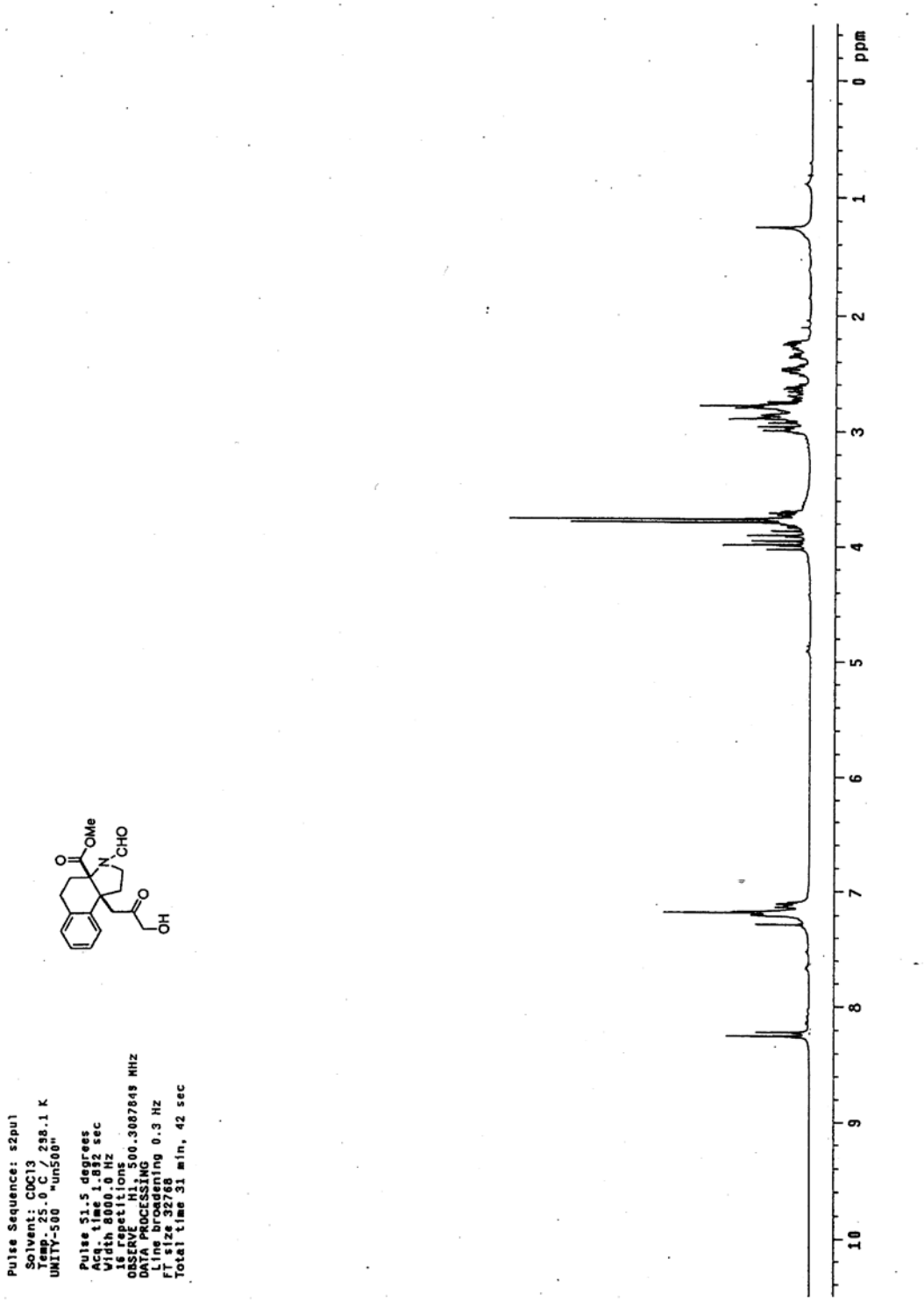

^{13}C-NMR of alcohol 120, 100 MHz, $CDCl_3$

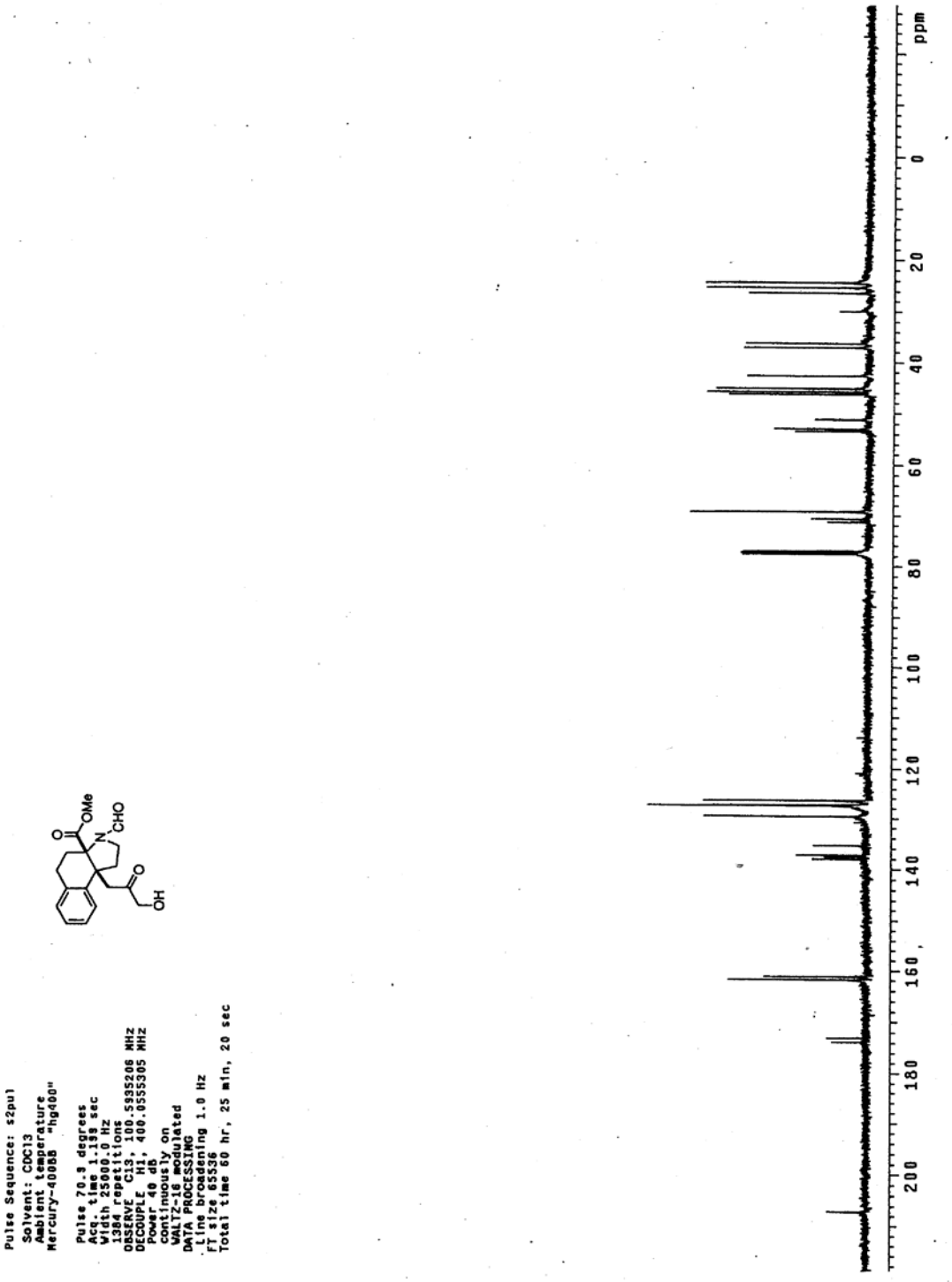

^{1}H-NMR of methyl ether 115, 500 MHz, $CDCl_3$

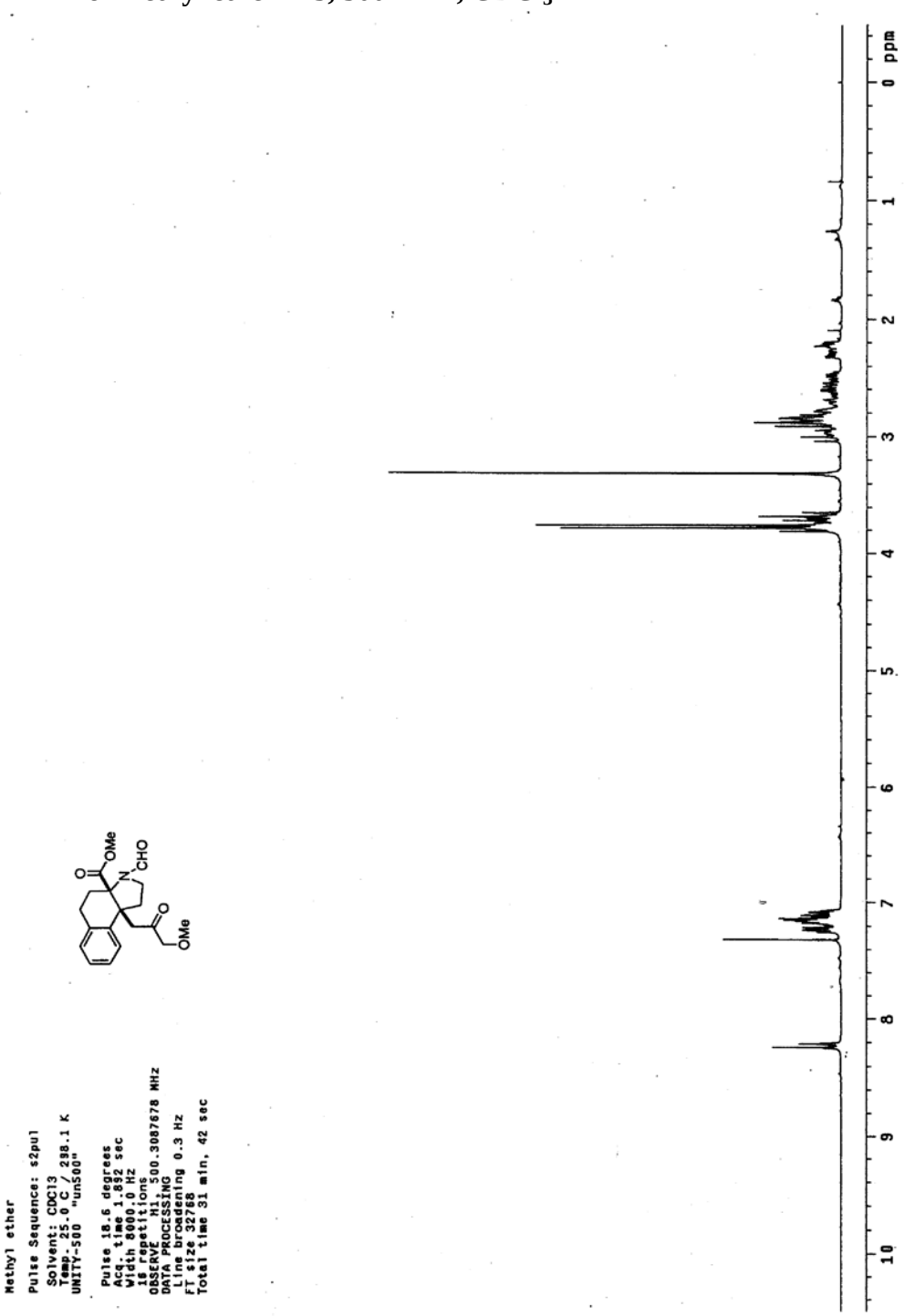

^{13}C-NMR of methyl ether 115, 100 MHz, $CDCl_3$

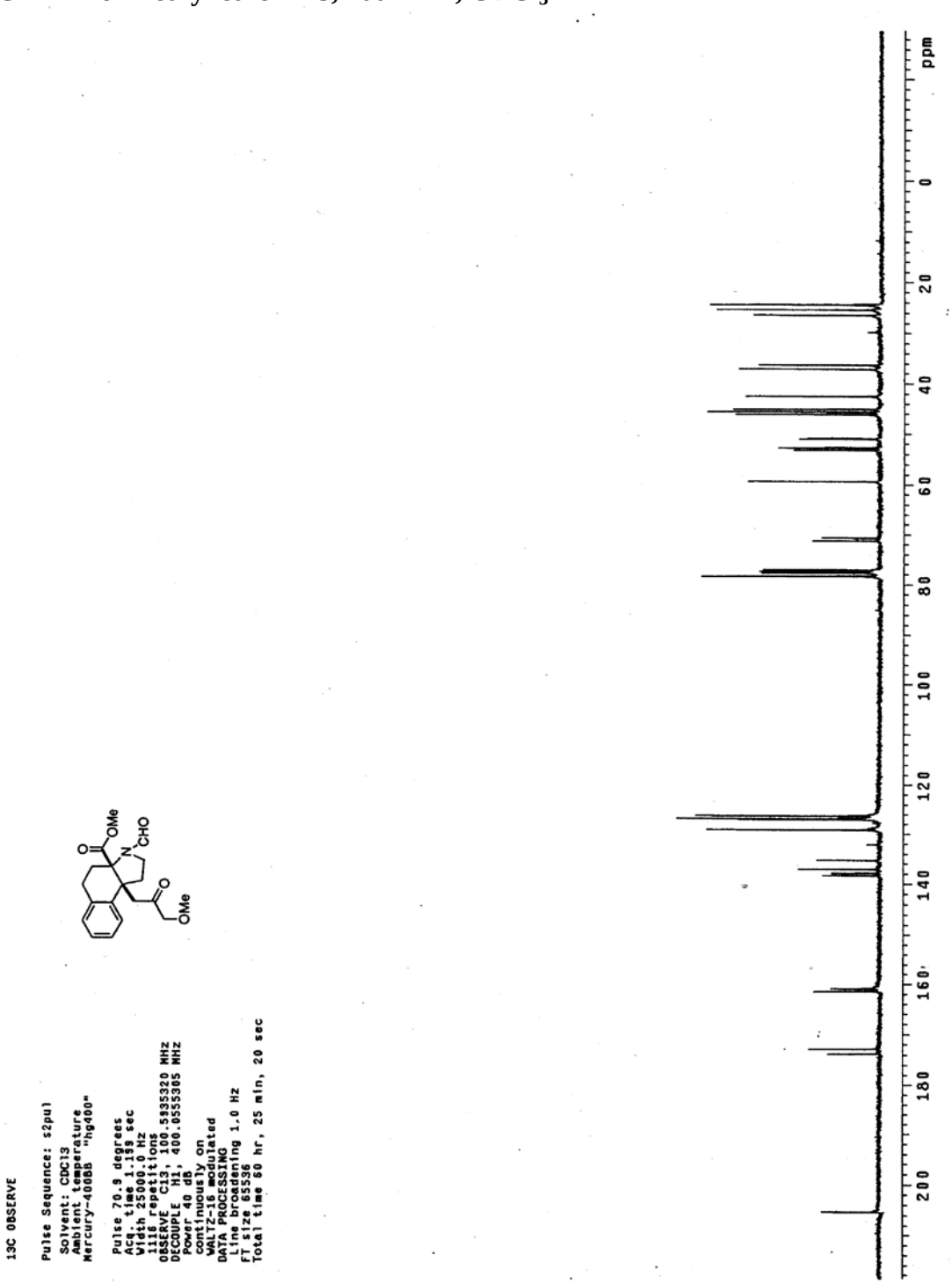

^{1}H-NMR of formamide 113, $CDCl_3$, 500 MHz

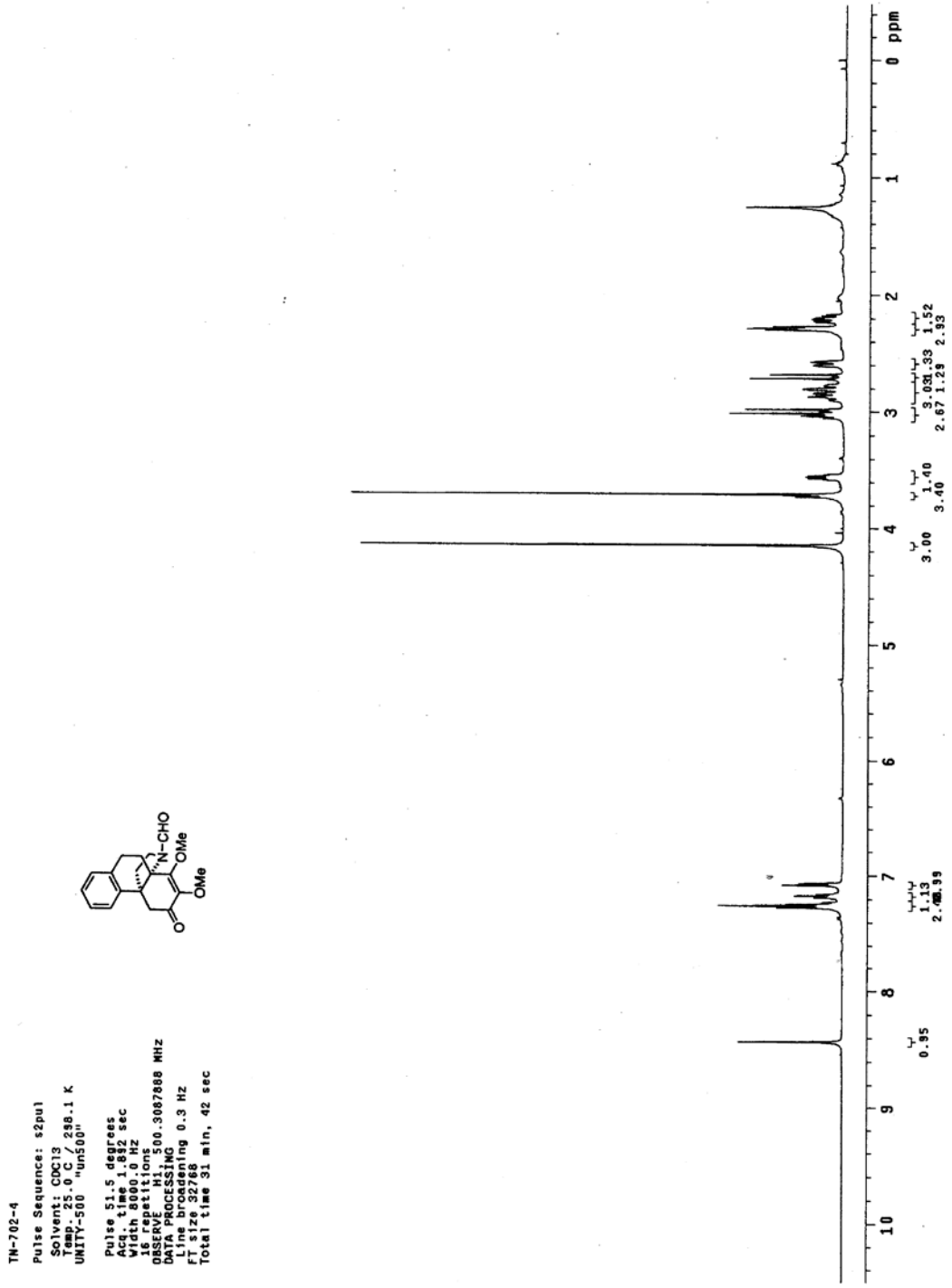

^{13}C-NMR of formamide 113, $CDCl_3$, 100 MHz

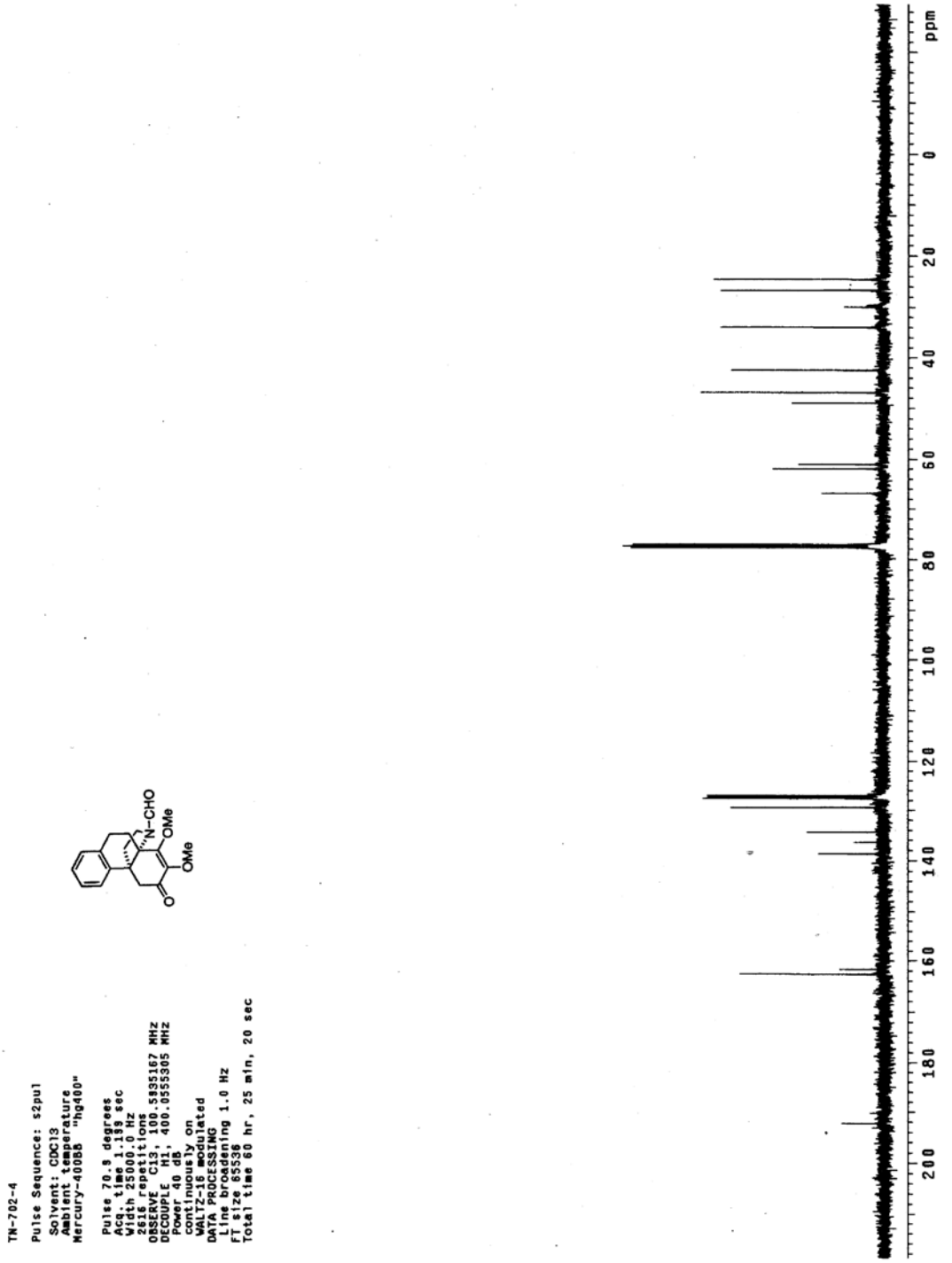

^{1}H-NMR of amine 122, 500 MHz, $CDCl_3$

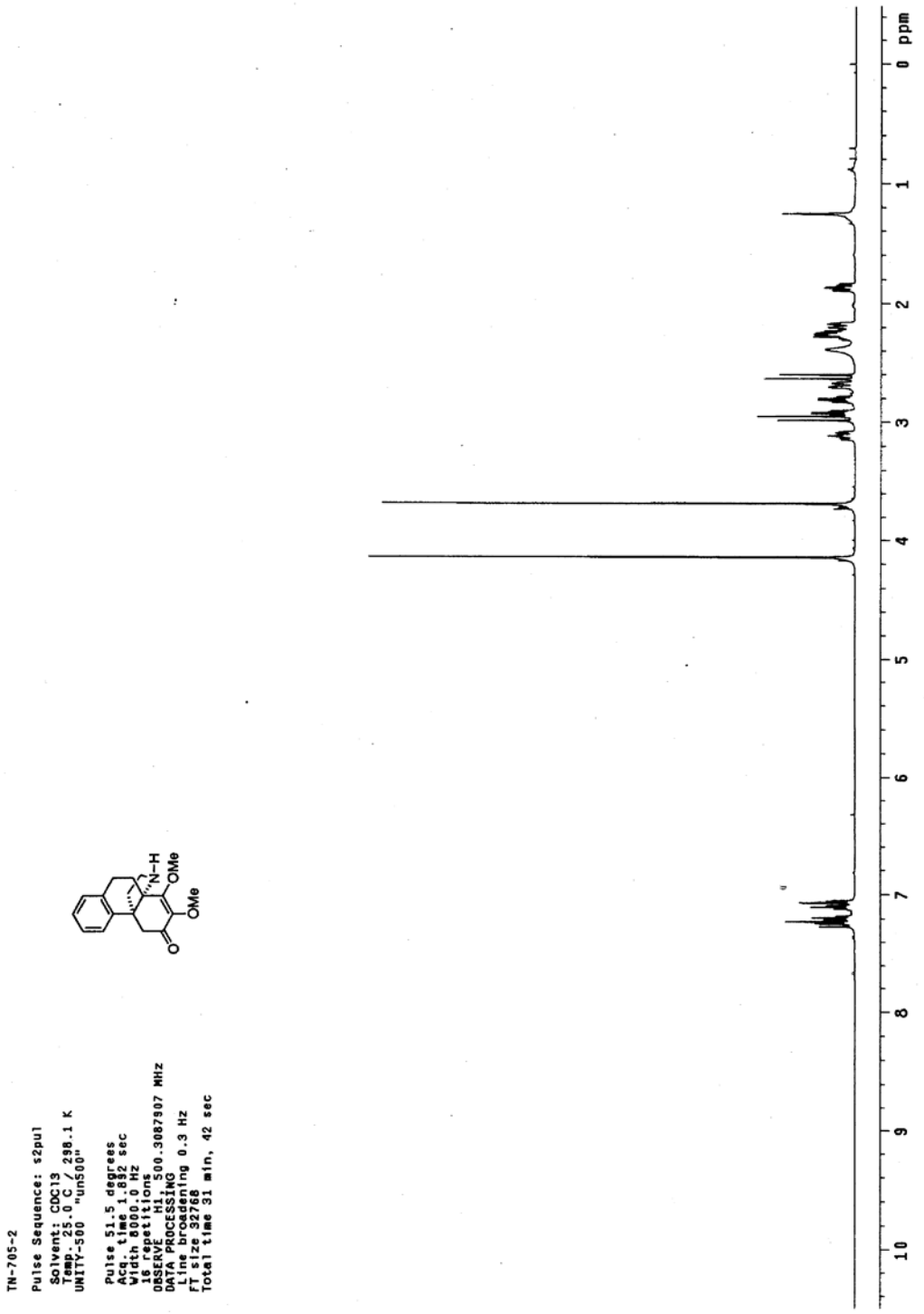

^{13}C-NMR of amine 122, 75 MHz, $CDCl_3$

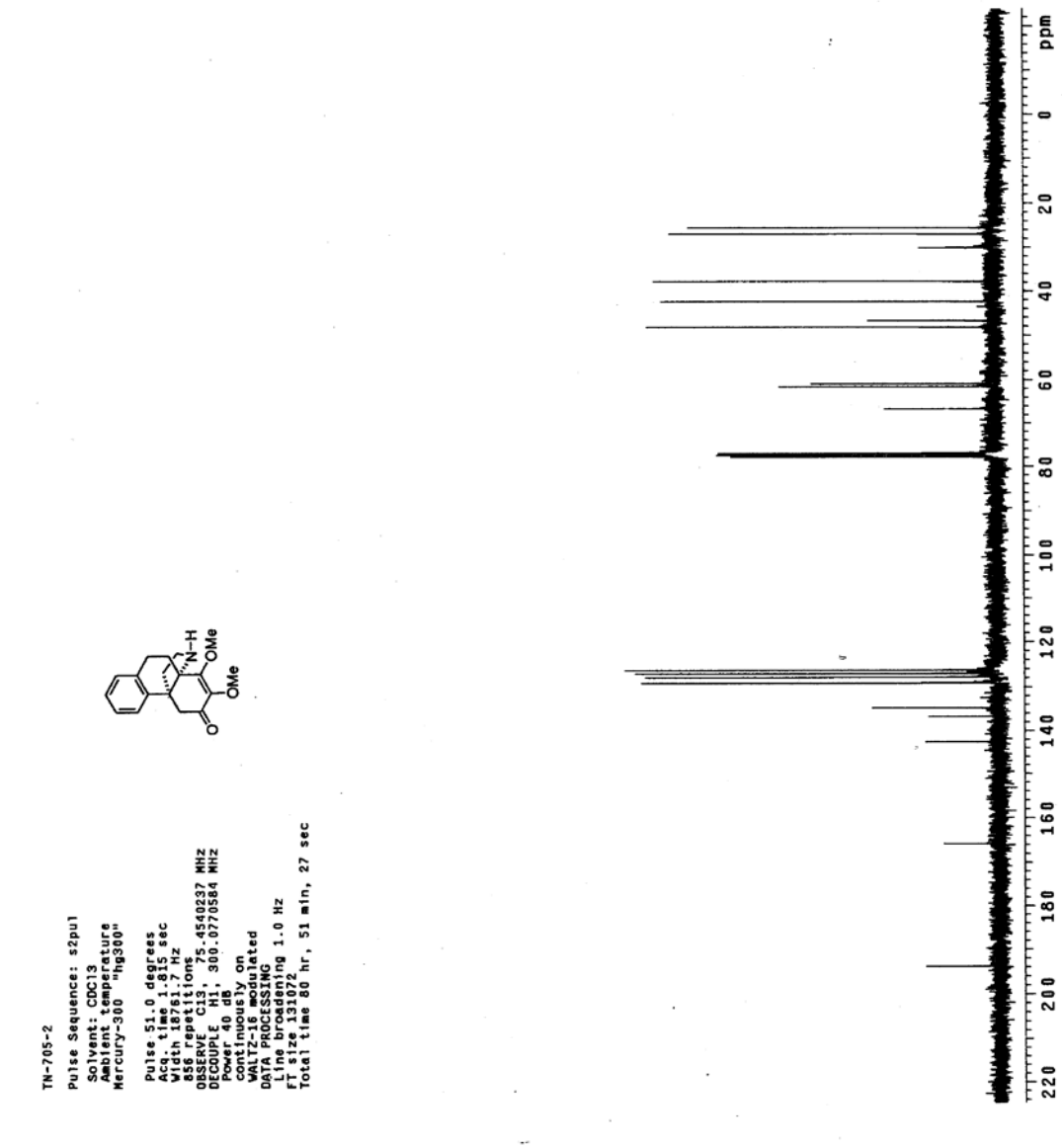

^{1}H-NMR of *N*-methylated amine 84, 500 MHz, $CDCl_3$

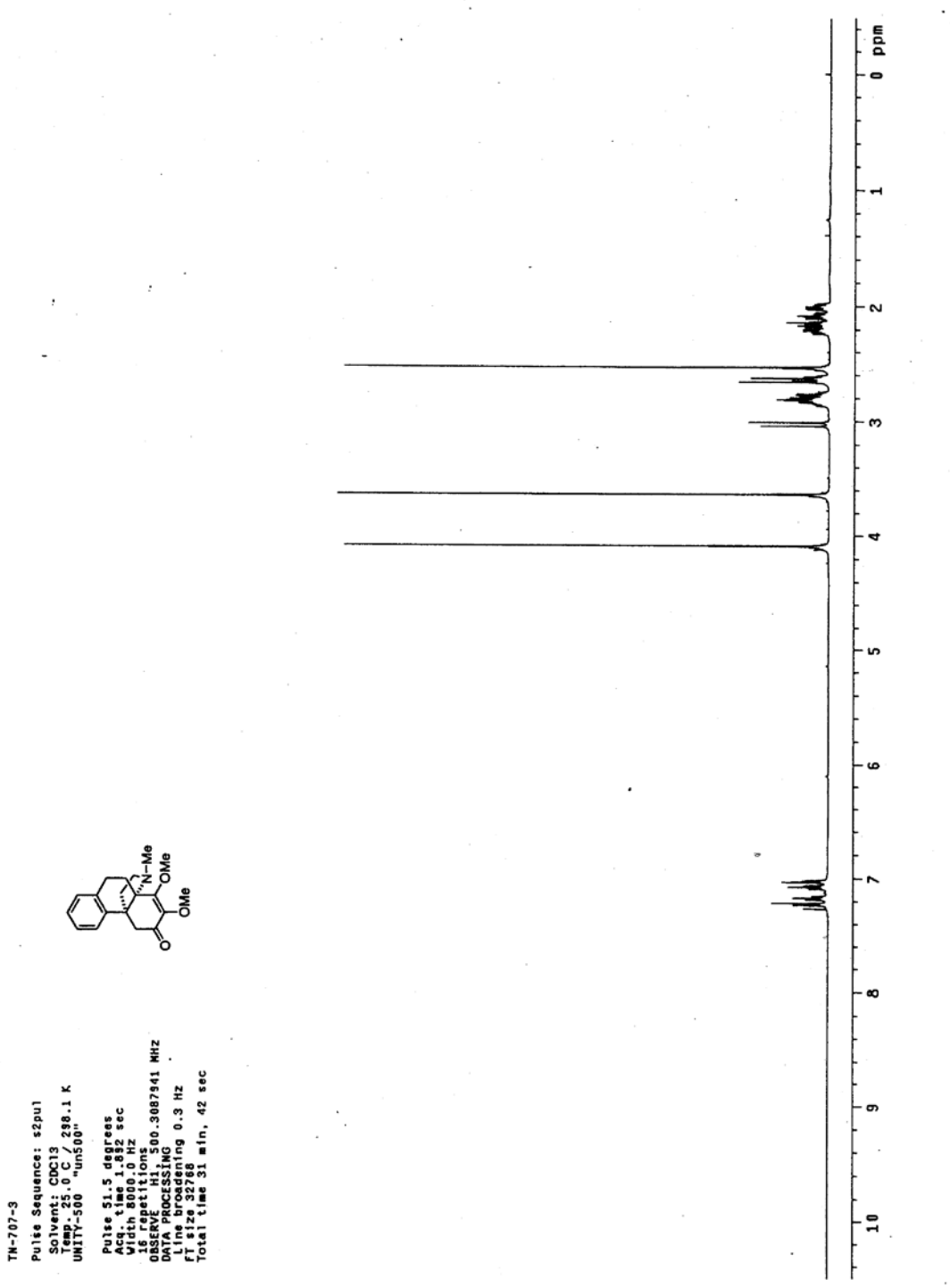

^{13}C-NMR of *N*-methylated amine 84, 100 MHz, $CDCl_3$

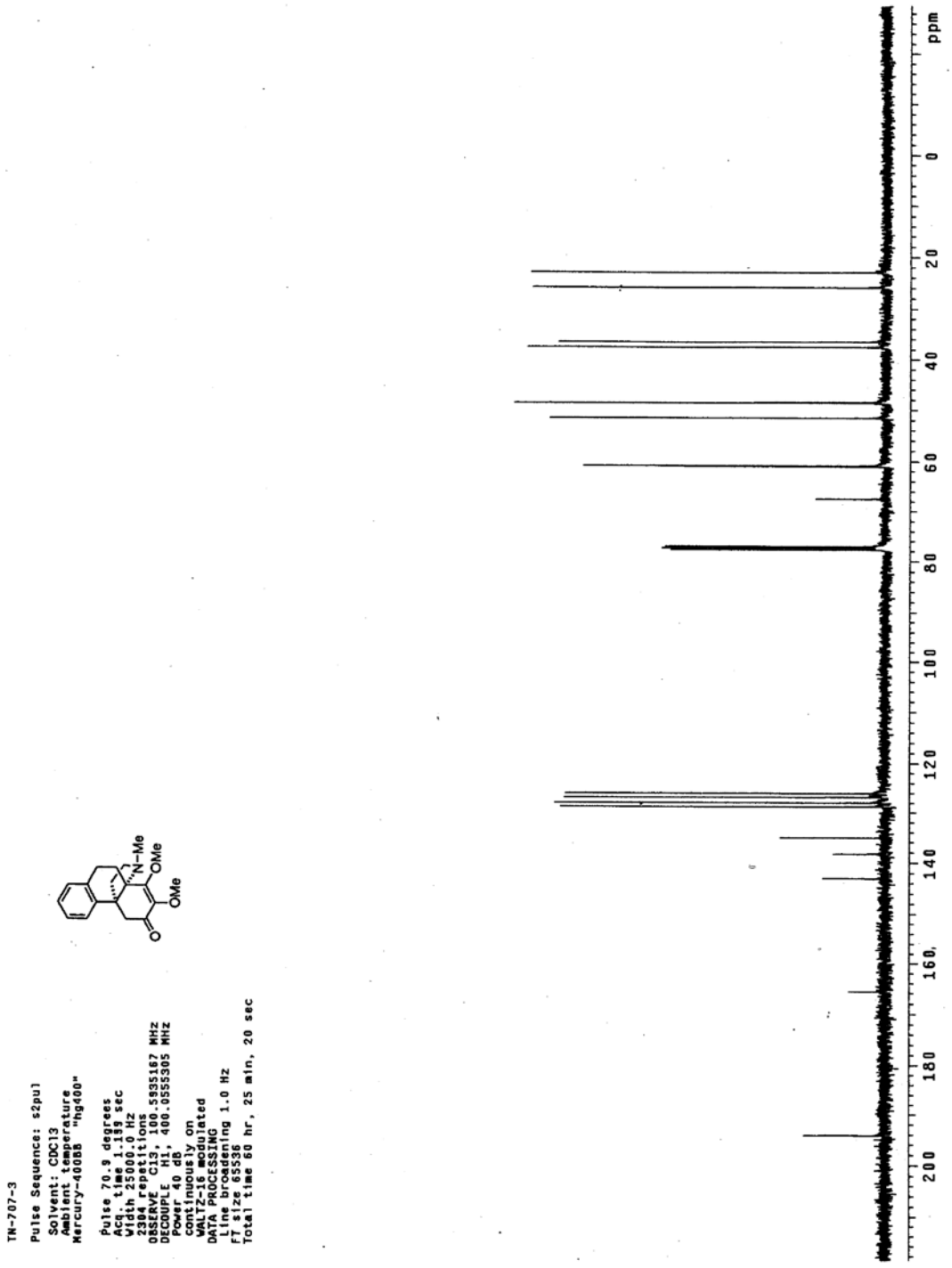

^{1}H-NMR of imine 99, 500 MHz, $CDCl_3$

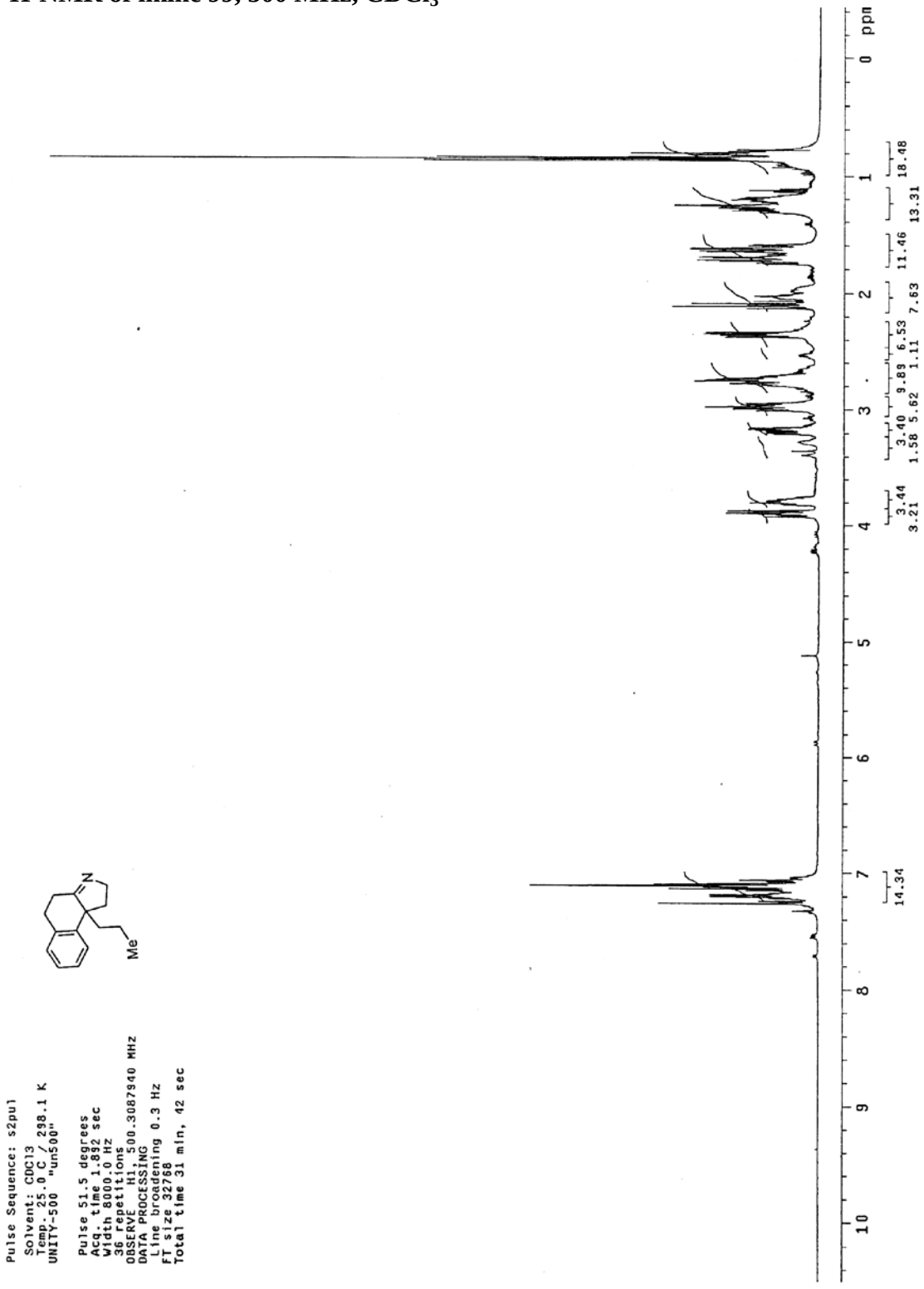

^{1}H-NMR of amino alcohol 100, 400 MHz, $CDCl_3$

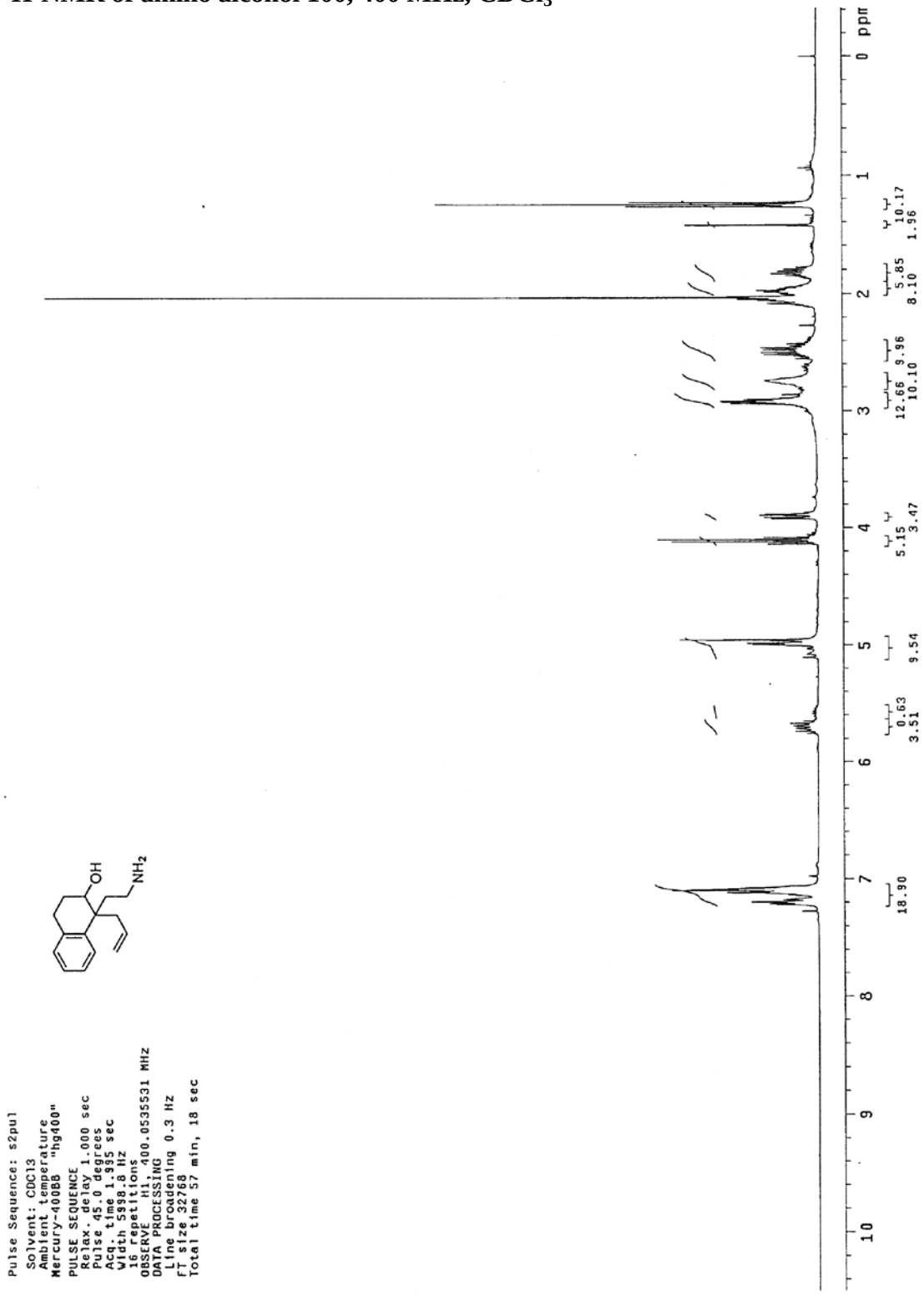

^{1}H-NMR of ketone 101, 400 MHz, $CDCl_3$

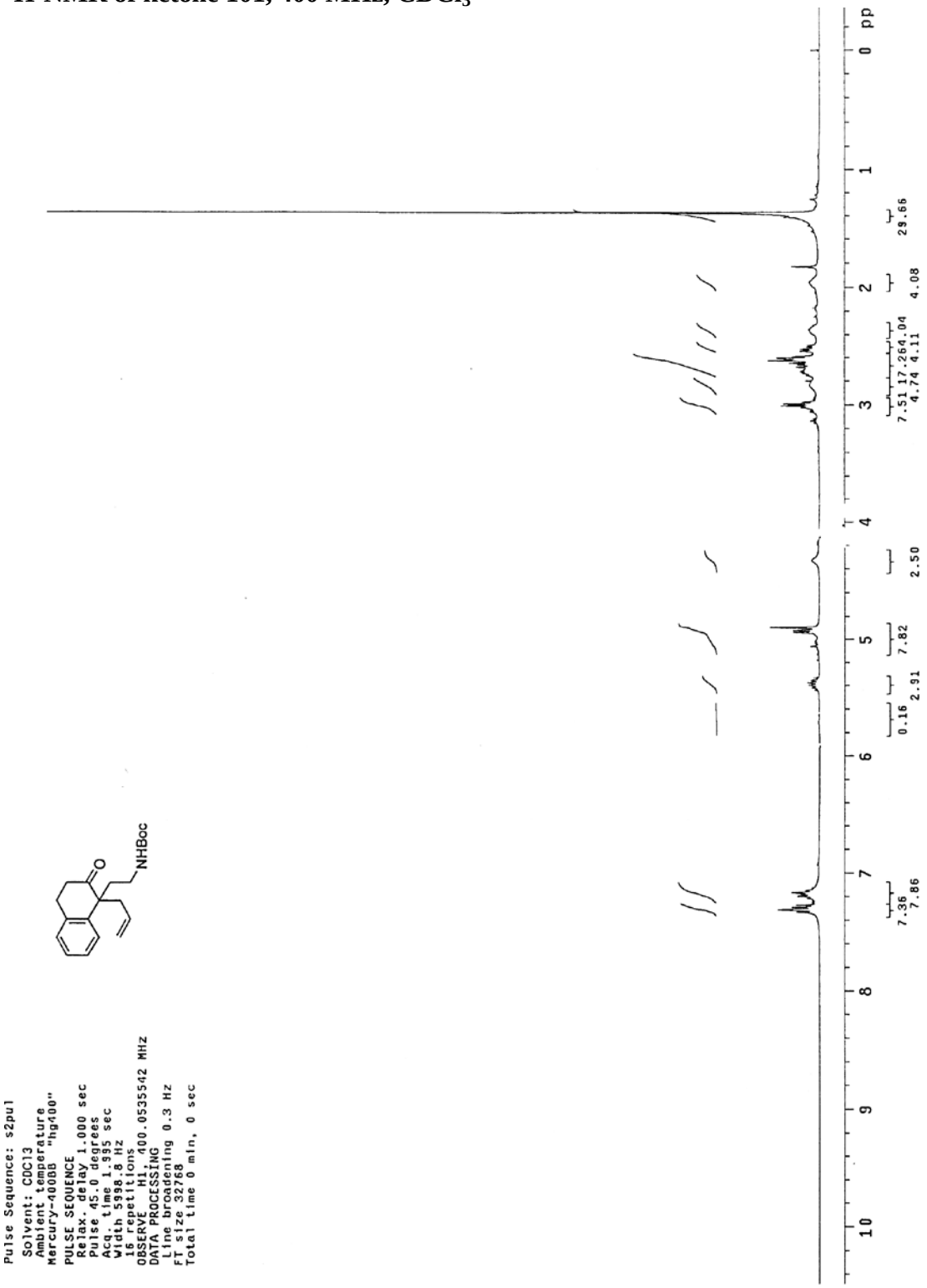

^{1}H-NMR of imine 87, 400 MHz, $CDCl_3$

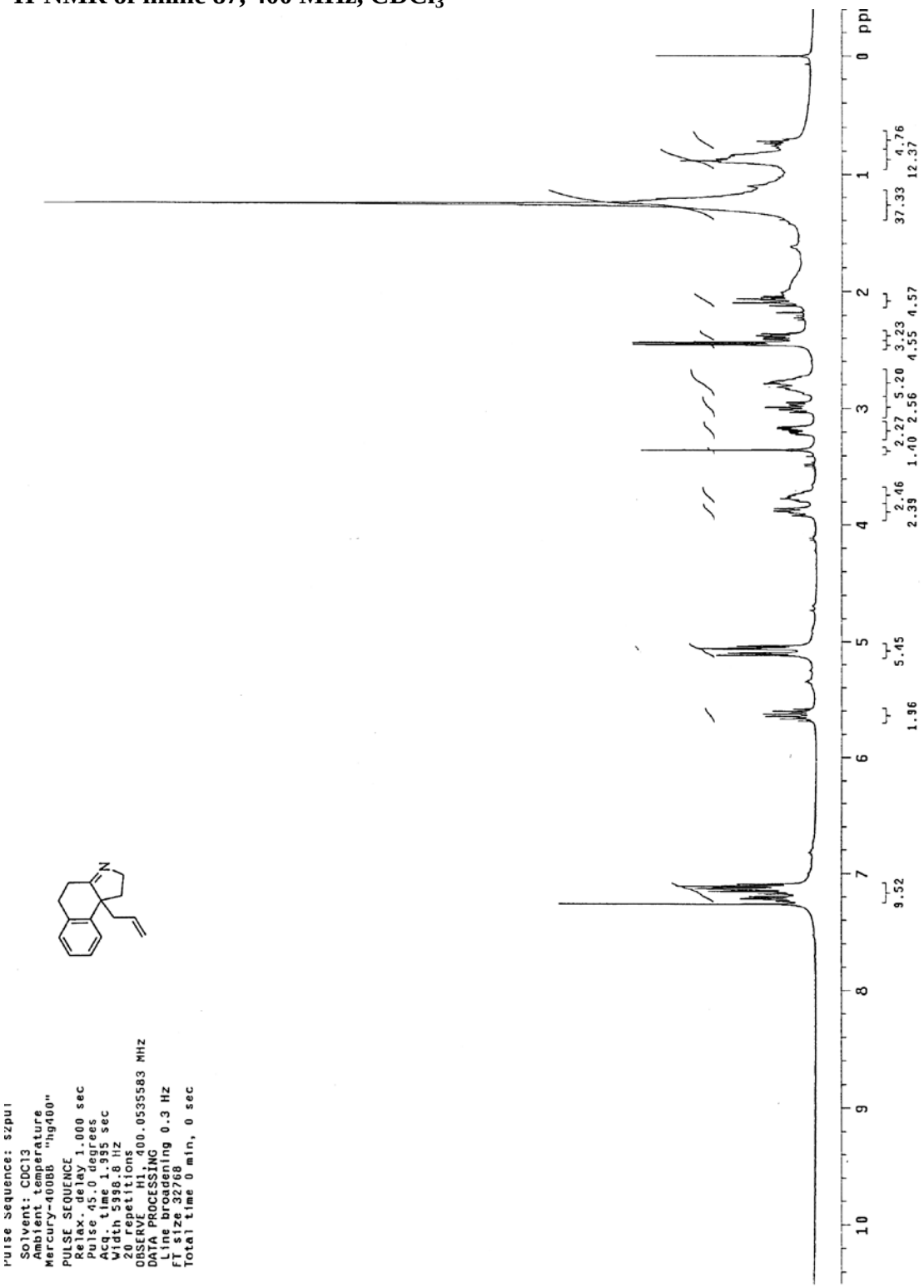

^{1}H-NMR of acetamide 103, 500 MHz, $CDCl_3$

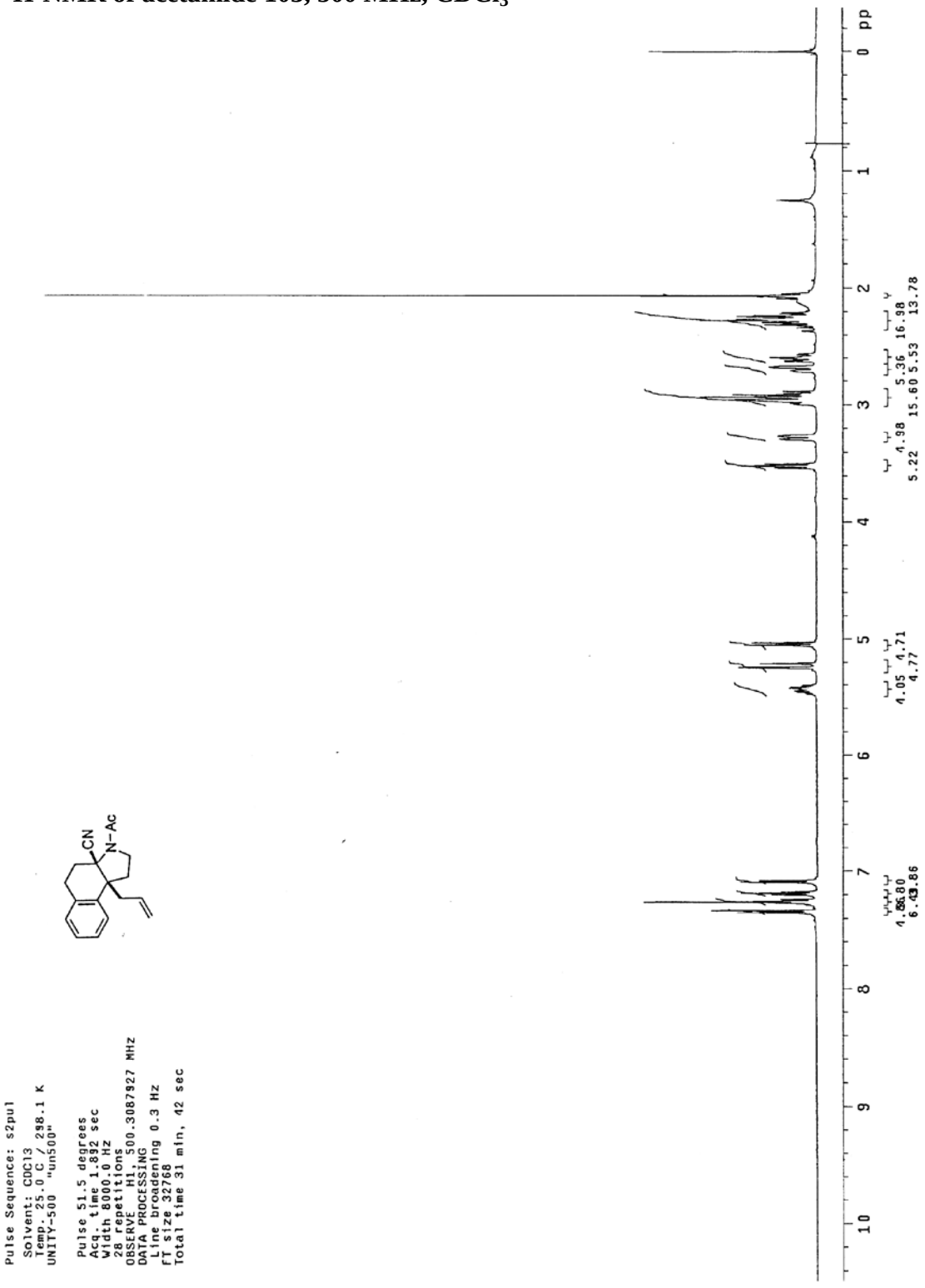

^{1}H-NMR of alcohol 106, 500 MHz, $CDCl_3$

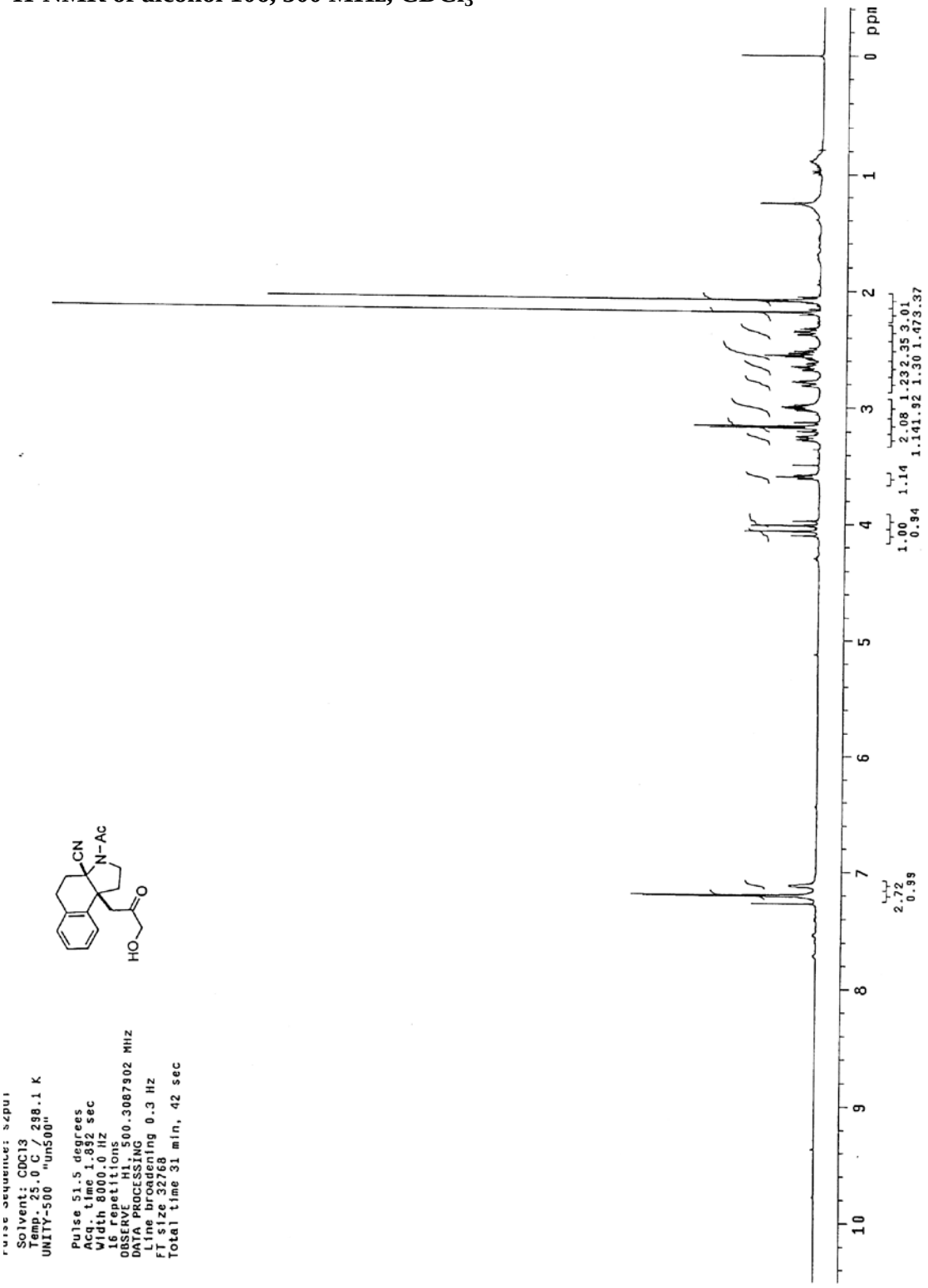

^{1}H-NMR of methyl ether 104, 500 MHz, $CDCl_3$

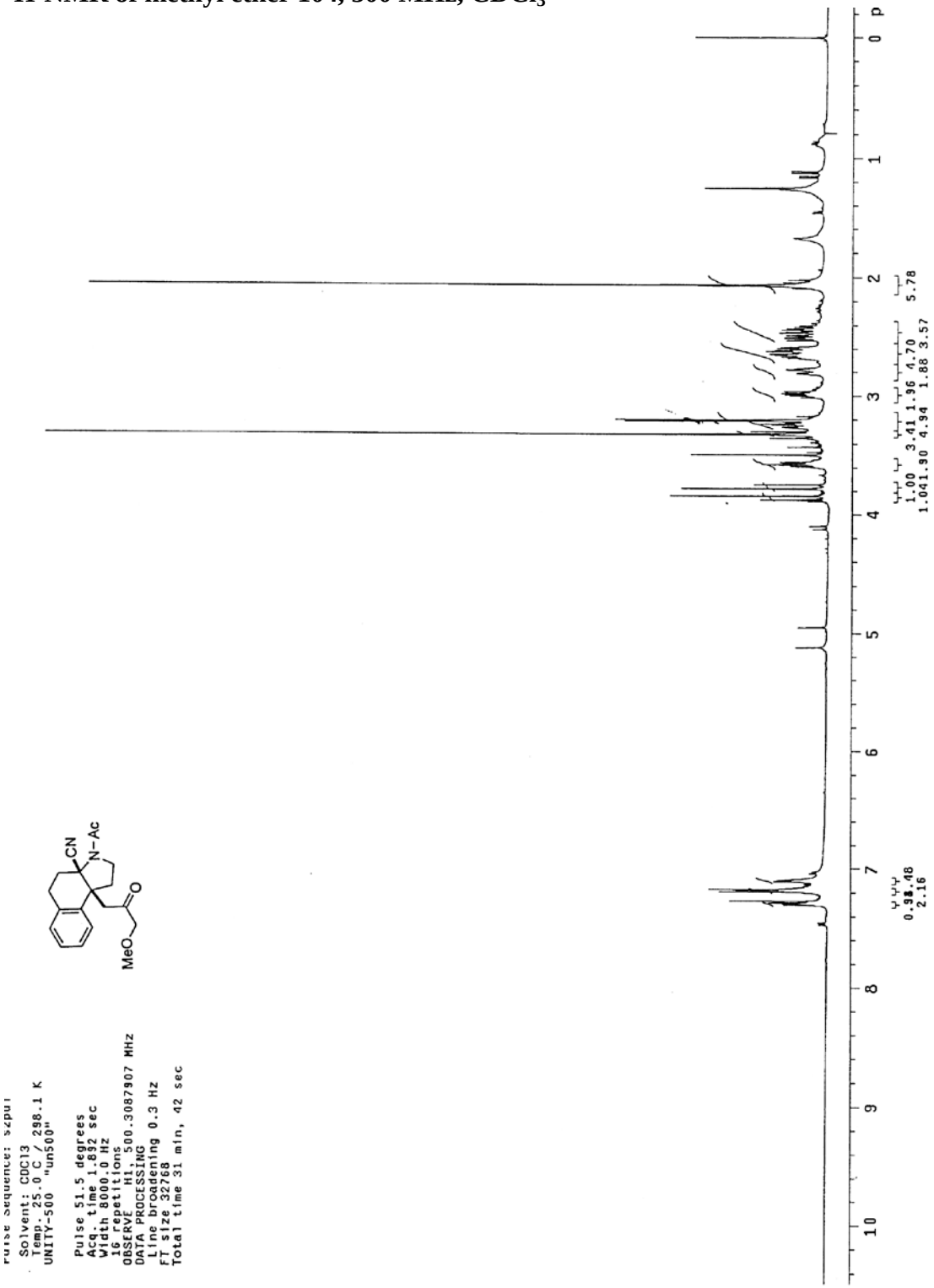

^{1}H-NMR of alcohol 108, 400 MHz, $CDCl_3$

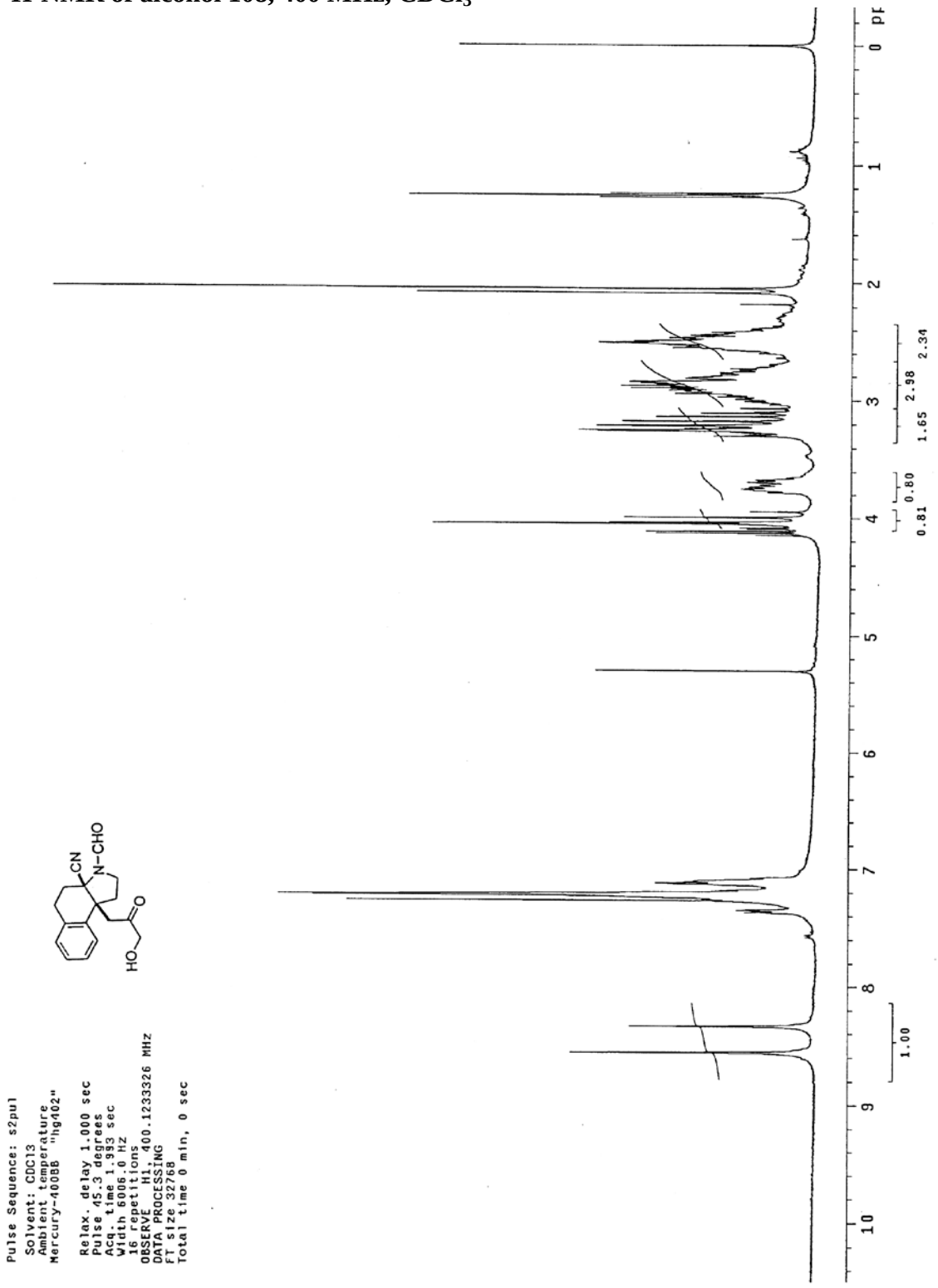

^{1}H-NMR of methyl ether 109, 500 MHz, $CDCl_3$

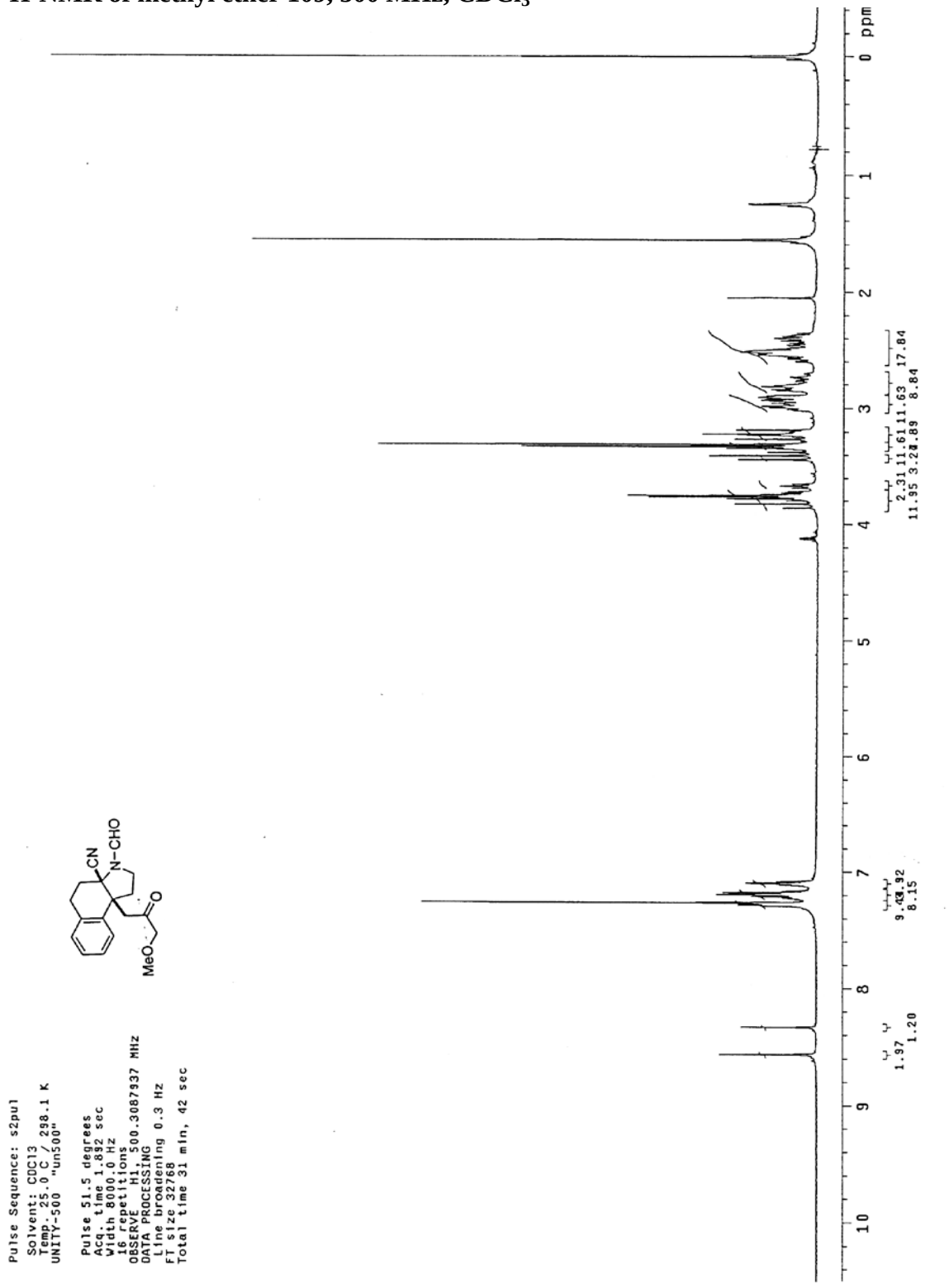

^{1}H-NMR of enamine 110, 500 MHz, $CDCl_3$

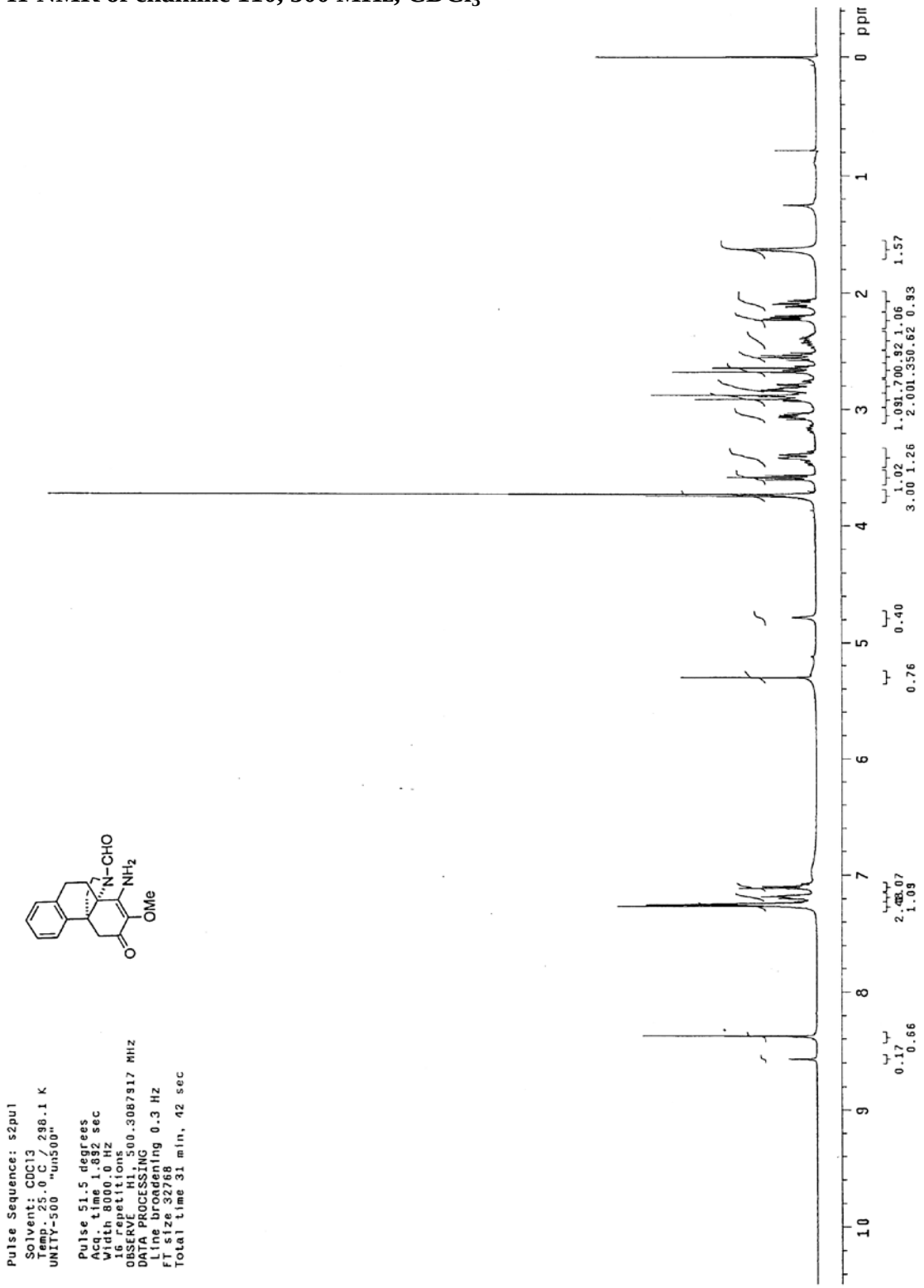

^{13}C-NMR of enamine 110, 100 MHz, $CDCl_3$

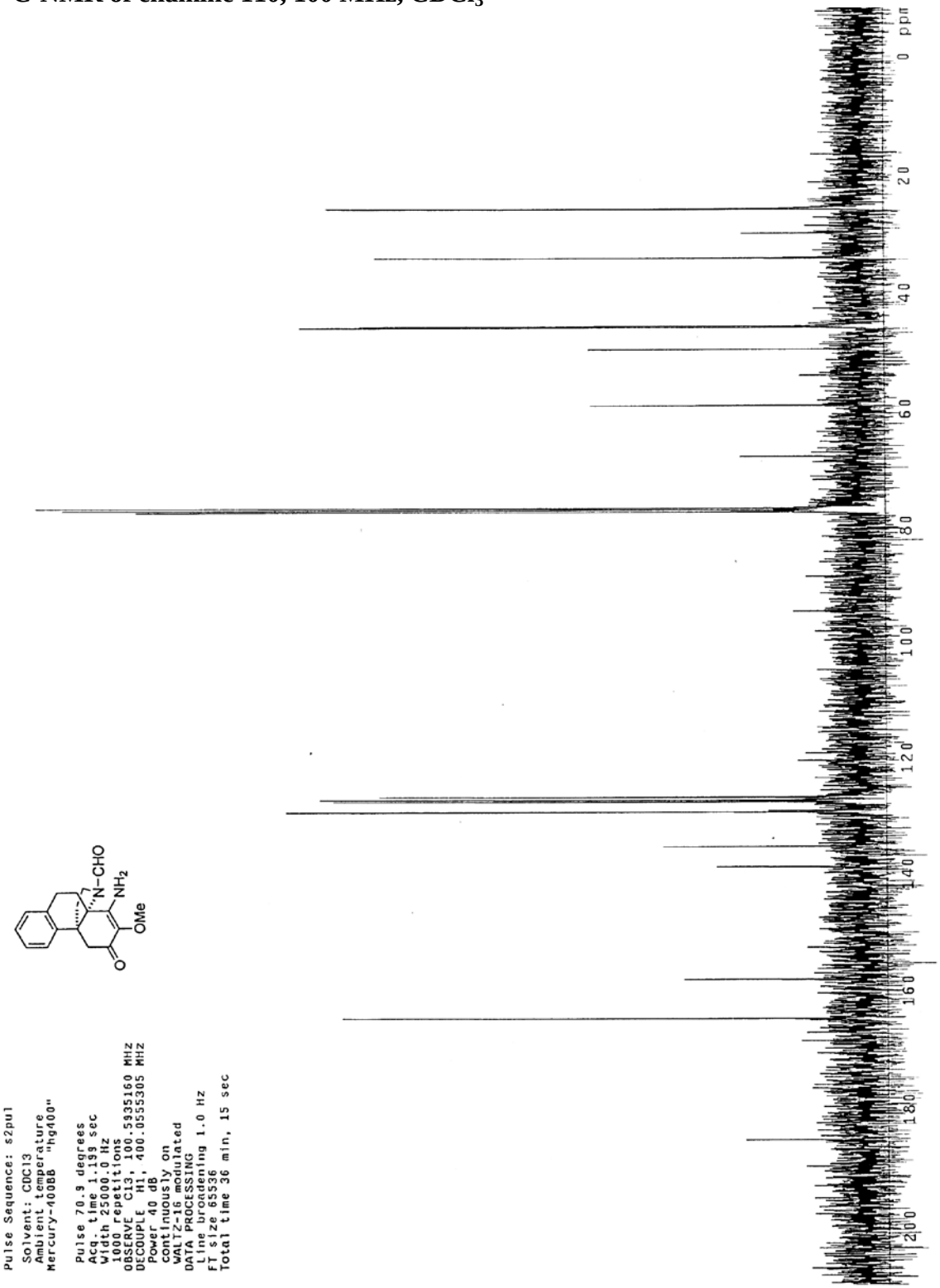

^{1}H-NMR of amine 111, 500 MHz, $CDCl_3$

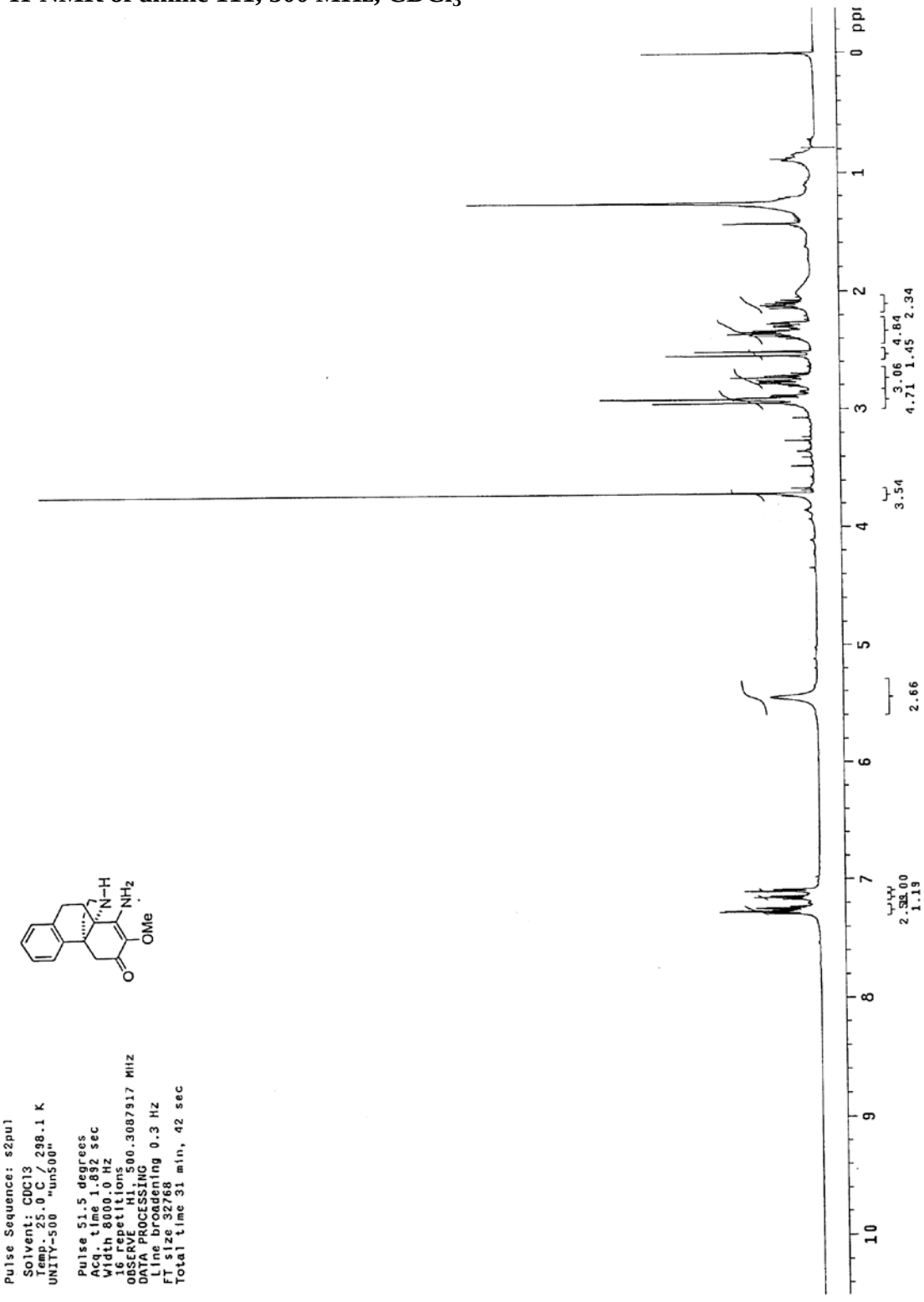

2.16 APPENDIX TWO: X-Ray Crystallography Reports Relevant to Chapter Two

X-ray Crystal Structure Report of Heterocycle **103**

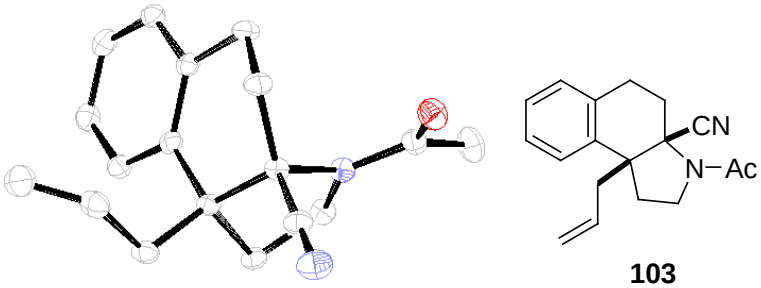

103

A colorless rod 0.40 x 0.40 x 0.37 mm in size was mounted on a Cryoloop with Paratone oil. Data were collected in a nitrogen gas stream at 100(2) K using phi and omega scans. Data collection was 100.0% complete to 25.00° in θ. A total of 16854 reflections were collected covering the indices, -11<=*h*<=11, -18<=*k*<=18, -12<=*l*<=12. 3471 reflections were found to be symmetry independent, with an R_{int} of 0.0467. Indexing and unit cell refinement indicated a primitive, orthorhombic lattice. The space group was found to Pna2(1). The data were integrated using the Bruker SAINT software program and scaled using the SADABS software program. Solution by direct methods (SIR-2004) produced a complete heavy-atom phasing model consistent with the proposed structure. All non-hydrogen atoms were refined anisotropically by full-matrix least-squares (SHELXL-97). All hydrogen atoms were placed using a riding model. Their positions were constrained relative to their parent atom using the appropriate HFIX command in SHELXL-97.

Table 2.16.1 Crystal data and structure refine for **103**.

X-ray ID	kob05a	
Sample/notebook ID	KOB05	
Empirical formula	C18 H20 N2 O	
Formula weight	280.36	
Temperature	100(2) K	
Wavelength	0.71073 Å	
Crystal system	Orthorhombic	
Space group	Pna2(1)	
Unit cell dimensions	a = 15.618(2) Å	α= 90°.
	b = 8.3232(13) Å	β= 90°.
	c = 11.3913(18) Å	γ = 90°.
Volume	1480.8(4) $Å^3$	
Z	4	
Density (calculated)	1.258 Mg/m^3	
Absorption coefficient	0.079 mm^{-1}	
F(000)	600	
Crystal size	0.40 x 0.40 x 0.37 mm^3	
Crystal color/habit	colorless rod	
Theta range for data collection	2.61 to 28.29°.	
Index ranges	-20<=h<=19, -10<=k<=10, -15<=l<=14	
Reflections collected	16854	
Independent reflections	3471 [R(int) = 0.0467]	
Completeness to theta = 25.00°	100.0%	
Absorption correction	none	
Max. and min. transmission	0.9715 and 0.9692	
Refinement method	Full-matrix least-squares on F^2	
Data / restraints / parameters	3471 / 1 / 199	
Goodness-of-fit on F^2	1.055	
Final R indices [I>2sigma(I)]	R1 = 0.0458, wR2 = 0.1058	
R indices (all data)	R1 = 0.0485, wR2 = 0.1079	
Absolute structure parameter	-0.9(13)	
Largest diff. peak and hole	0.378 and -0.179 $e.Å^{-3}$	

Table 2.16.2 Atomic coordinates (x 10^4) and equivalent isotropic displacement parameters ($Å^2$x 10^3) for **103**. U(eq) is defined as one third of the trace of the orthogonalized U^{ij} tensor.

	x	y	z	U(eq)
O(1)	4876(1)	3304(1)	6683(1)	26(1)
N(1)	3484(1)	3392(2)	7208(1)	18(1)
N(2)	3640(1)	616(2)	5011(1)	27(1)
C(1)	3165(1)	3349(2)	5985(1)	16(1)
C(2)	3512(1)	4737(2)	5230(1)	20(1)
C(3)	3327(1)	6332(2)	5819(2)	20(1)
C(4)	2393(1)	6501(2)	6138(1)	17(1)
C(5)	2056(1)	8045(2)	6308(1)	20(1)
C(6)	1211(1)	8283(2)	6616(2)	23(1)
C(7)	679(1)	6948(2)	6744(2)	23(1)
C(8)	1000(1)	5416(2)	6571(1)	21(1)
C(9)	1862(1)	5164(2)	6275(1)	17(1)
C(10)	2168(1)	3420(2)	6147(1)	16(1)
C(11)	2061(1)	2565(2)	7342(1)	18(1)
C(12)	2789(1)	3234(2)	8079(2)	19(1)
C(13)	1650(1)	2538(2)	5185(1)	19(1)
C(14)	1723(1)	3233(2)	3974(2)	24(1)
C(15)	1123(1)	4118(2)	3469(2)	30(1)
C(16)	4333(1)	3387(2)	7453(2)	21(1)
C(17)	4569(1)	3487(2)	8735(2)	31(1)
C(18)	3434(1)	1799(2)	5439(1)	20(1)

Table 2.16.3 Bond lengths and angles for **103**.

O(1)-C(16)	1.223(2)		
N(1)-C(16)	1.354(2)	C(5)-C(6)	1.381(2)
N(1)-C(12)	1.476(2)	C(6)-C(7)	1.394(2)
N(1)-C(1)	1.480(2)	C(7)-C(8)	1.384(2)
N(2)-C(18)	1.145(2)	C(8)-C(9)	1.403(2)
C(1)-C(18)	1.492(2)	C(9)-C(10)	1.5349(19)
C(1)-C(2)	1.539(2)	C(10)-C(11)	1.546(2)
C(1)-C(10)	1.570(2)	C(10)-C(13)	1.547(2)
C(2)-C(3)	1.515(2)	C(11)-C(12)	1.519(2)
C(3)-C(4)	1.509(2)	C(13)-C(14)	1.500(2)
C(4)-C(9)	1.398(2)	C(14)-C(15)	1.324(3)
C(4)-C(5)	1.402(2)	C(16)-C(17)	1.509(2)
C(16)-N(1)-C(12)	125.46(14)		
C(16)-N(1)-C(1)	121.54(13)	C(4)-C(9)-C(8)	118.53(13)
C(12)-N(1)-C(1)	112.56(12)	C(4)-C(9)-C(10)	123.89(13)
N(1)-C(1)-C(18)	108.57(12)	C(8)-C(9)-C(10)	117.57(12)
N(1)-C(1)-C(2)	112.90(12)	C(9)-C(10)-C(11)	108.56(12)
C(18)-C(1)-C(2)	108.52(13)	C(9)-C(10)-C(13)	110.68(12)
N(1)-C(1)-C(10)	102.83(12)	C(11)-C(10)-C(13)	110.44(12)
C(18)-C(1)-C(10)	111.14(11)	C(9)-C(10)-C(1)	110.85(11)
C(2)-C(1)-C(10)	112.76(11)	C(11)-C(10)-C(1)	101.12(11)
C(3)-C(2)-C(1)	110.05(12)	C(13)-C(10)-C(1)	114.68(12)
C(4)-C(3)-C(2)	111.89(12)	C(12)-C(11)-C(10)	103.75(12)
C(9)-C(4)-C(5)	119.43(13)	N(1)-C(12)-C(11)	102.19(13)
C(9)-C(4)-C(3)	121.77(13)	C(14)-C(13)-C(10)	115.34(12)
C(5)-C(4)-C(3)	118.80(13)	C(15)-C(14)-C(13)	124.08(18)
C(6)-C(5)-C(4)	121.70(14)	O(1)-C(16)-N(1)	122.12(16)
C(5)-C(6)-C(7)	118.80(14)	O(1)-C(16)-C(17)	121.84(15)
C(8)-C(7)-C(6)	120.27(15)	N(1)-C(16)-C(17)	116.04(15)
C(7)-C(8)-C(9)	121.25(14)	N(2)-C(18)-C(1)	179.38(17)

Table 2.16.4 Anisotropic displacement parameters ($Å^2 x\ 10^3$) for **103**. The anisotropic displacement factor exponent takes the form: $-2\pi^2[\ h^2 a^{*2} U^{11} + ... + 2\ h\ k\ a^*\ b^*\ U^{12}\ ]$.

U^{11}	U^{22}	U^{33}	U^{23}	U^{13}	U^{12}
O(1)21(1)	29(1)	28(1)	-3(1)	2(1)	1(1)
N(1)20(1)	19(1)	15(1)	-1(1)	1(1)	-1(1)
N(2)34(1)	21(1)	26(1)	-3(1)	5(1)	0(1)
C(1)18(1)	16(1)	14(1)	-2(1)	2(1)	-1(1)
C(2)20(1)	19(1)	19(1)	1(1)	5(1)	-2(1)
C(3)20(1)	16(1)	24(1)	1(1)	2(1)	-4(1)
C(4)21(1)	19(1)	13(1)	1(1)	0(1)	-2(1)
C(5)25(1)	18(1)	17(1)	1(1)	-2(1)	-1(1)
C(6)28(1)	20(1)	21(1)	0(1)	-2(1)	5(1)
C(7)20(1)	28(1)	22(1)	2(1)	2(1)	3(1)
C(8)21(1)	22(1)	19(1)	3(1)	0(1)	-2(1)
C(9)21(1)	17(1)	12(1)	1(1)	0(1)	0(1)
C(10)17(1)	17(1)	14(1)	0(1)	2(1)	-2(1)
C(11)22(1)	18(1)	15(1)	3(1)	3(1)	-2(1)
C(12)22(1)	22(1)	15(1)	-1(1)	2(1)	1(1)
C(13)22(1)	17(1)	19(1)	-2(1)	0(1)	-3(1)
C(14)28(1)	26(1)	17(1)	-4(1)	-1(1)	-8(1)
C(15)40(1)	29(1)	22(1)	0(1)	-7(1)	-5(1)
C(16)21(1)	17(1)	26(1)	-5(1)	-3(1)	1(1)
C(17)26(1)	40(1)	26(1)	-8(1)	-6(1)	1(1)
C(18)22(1)	19(1)	17(1)	3(1)	4(1)	-3(1)

Table 2.16.5 Hydrogen coordinates (x 10^4) and isotropic displacement parameters ($Å^2$x 10^3) for **103**.

	x	y	z	U(eq)
H(2A)	4138	4610	5123	23
H(2B)	3239	4712	4446	23
H(3A)	3679	6424	6539	24
H(3B)	3492	7217	5284	24
H(5A)	2419	8951	6209	24
H(6A)	995	9336	6739	28
H(7A)	95	7091	6949	28
H(8A)	630	4518	6655	25
H(11A)	1499	2819	7699	22
H(11B)	2113	1386	7254	22
H(12A)	2637	4288	8423	23
H(12B)	2950	2484	8717	23
H(13A)	1841	1405	5158	23
H(13B)	1038	2540	5415	23
H(14A)	2232	3025	3543	29
H(15A)	588(14)	4320(30)	3780(20)	32(5)
H(15B)	1198(15)	4570(30)	2720(30)	49(7)
H(17A)	5192	3582	8811	46
H(17B)	4374	2514	9140	46
H(17C)	4294	4430	9087	46

X-ray Crystal Structure Report of Enamine **110**

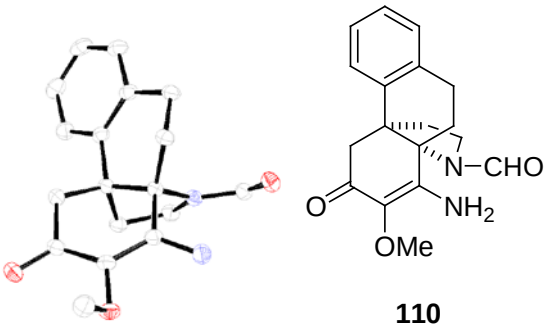

110

A colorless needle 0.25 x 0.25 x 0.25 mm in size was mounted on a Cryoloop with Paratone oil. Data were collected in a nitrogen gas stream at 100(2) K using phi and omega scans. Crystal-to-detector distance was 60 mm and exposure time was 5 seconds per frame using a scan width of 0.5°. Data collection was 98.8% complete to 67.00° in_θ. A total of 10598 reflections were collected covering the indices, -11<=*h*<=11, -18<=*k*<=18, -12<=*l*<=12. 2720 reflections were found to be symmetry independent, with an R_{int} of 0.0202. Indexing and unit cell refinement indicated a primitive, monoclinic lattice. The space group was found to be P2(1)/c (No. 14). The data were integrated using the Bruker SAINT software program and scaled using the SADABS software program. Solution by direct methods (SIR-2004) produced a complete heavy-atom phasing model consistent with the proposed structure. All non-hydrogen atoms were refined anisotropically by full-matrix least-squares (SHELXL-97). All hydrogen atoms were placed using a riding model. Their positions were constrained relative to their parent atom using the appropriate HFIX command in SHELXL-97.

Table 2.16.6 Crystal data and structure refinement for **110**.

X-ray ID	kob09	
Sample/notebook ID	TN-482	
Empirical formula	C18 H20 N2 O3	
Formula weight	312.36	
Temperature	100(2) K	
Wavelength	1.54178 Å	
Crystal system	Monoclinic	
Space group	P2(1)/c	
Unit cell dimensions	a = 9.8911(11) Å	α= 90°.
	b = 15.4488(18) Å	β= 98.796(4)°.
	c = 10.1578(11) Å	γ = 90°.
Volume	1533.9(3) $Å^3$	
Z	4	
Density (calculated)	1.353 Mg/m^3	
Absorption coefficient	0.753 mm^{-1}	
F(000)	664	
Crystal size	0.25 x 0.25 x 0.25 mm^3	
Crystal color/habit	colorless block	
Theta range for data collection	4.52 to 68.74°.	
Index ranges	-11<=h<=11, -18<=k<=18, -12<=l<=12	
Reflections collected	10598	
Independent reflections	2720 [R(int) = 0.0202]	
Completeness to theta = 67.00°	98.8 %	
Absorption correction	Semi-empirical from equivalents	
Max. and min. transmission	0.8340 and 0.8340	
Refinement method	Full-matrix least-squares on F^2	
Data / restraints / parameters	2720 / 0 / 209	
Goodness-of-fit on F^2	1.089	
Final R indices [I>2sigma(I)]	R1 = 0.0378, wR2 = 0.0968	
R indices (all data)	R1 = 0.0387, wR2 = 0.0975	
Largest diff. peak and hole	0.199 and -0.207 $e.Å^{-3}$	

Table 2.16.7 Atomic coordinates (x 10^4) and equivalent isotropic displacement parameters ($Å^2$x 10^3) for **110**. U(eq) is defined as one third of the trace of the orthogonalized U^{ij} tensor.

	x	y	z	U(eq)
C(1)	3049(1)	663(1)	2019(1)	19(1)
C(2)	3032(1)	1109(1)	671(1)	20(1)
C(3)	2487(1)	729(1)	-508(1)	20(1)
C(4)	1917(1)	-119(1)	-602(1)	21(1)
C(5)	1767(1)	-560(1)	691(1)	22(1)
C(6)	2857(1)	-330(1)	1873(1)	19(1)
C(7)	2423(1)	-743(1)	3115(1)	21(1)
C(8)	2376(2)	-1648(1)	3168(1)	26(1)
C(9)	1893(2)	-2074(1)	4199(2)	31(1)
C(10)	1466(2)	-1599(1)	5218(2)	31(1)
C(11)	1529(1)	-705(1)	5195(1)	27(1)
C(12)	1993(1)	-264(1)	4145(1)	22(1)
C(13)	2016(1)	711(1)	4140(1)	23(1)
C(14)	1961(1)	1078(1)	2746(1)	21(1)
C(15)	5190(1)	-118(1)	2787(1)	24(1)
C(16)	4304(1)	-632(1)	1716(1)	22(1)
C(17)	5002(1)	1387(1)	3496(1)	23(1)
C(18)	1278(2)	1493(1)	-2317(1)	26(1)
N(1)	4443(1)	711(1)	2802(1)	20(1)
N(2)	3562(1)	1906(1)	692(1)	26(1)
O(1)	2575(1)	1195(1)	-1664(1)	23(1)
O(2)	1487(1)	-480(1)	-1672(1)	28(1)
O(3)	4516(1)	2123(1)	3488(1)	26(1)

Table 2.16.8 Bond lengths [Å] and angles [°] for **110**.

C(1)-N(1)	1.4844(17)	C(11)-C(12)	1.4006(19)
C(1)-C(2)	1.5302(17)	C(11)-H(11)	0.9500
C(1)-C(14)	1.5353(17)	C(12)-C(13)	1.5061(19)
C(1)-C(6)	1.5508(17)	C(13)-C(14)	1.5184(18)
C(2)-N(2)	1.3372(18)	C(13)-H(13A)	0.9900
C(2)-C(3)	1.3683(19)	C(13)-H(13B)	0.9900
C(3)-O(1)	1.3911(15)	C(14)-H(14A)	0.9900
C(3)-C(4)	1.4246(19)	C(14)-H(14B)	0.9900
C(4)-O(2)	1.2365(16)	C(15)-N(1)	1.4788(16)
C(4)-C(5)	1.5065(17)	C(15)-C(16)	1.5136(19)
C(5)-C(6)	1.5278(18)	C(15)-H(15A)	0.9900
C(5)-H(5A)	0.9900	C(15)-H(15B)	0.9900
C(5)-H(5B)	0.9900	C(16)-H(16A)	0.9900
C(6)-C(7)	1.5331(17)	C(16)-H(16B)	0.9900
C(6)-C(16)	1.5361(18)	C(17)-O(3)	1.2347(17)
C(7)-C(12)	1.3996(19)	C(17)-N(1)	1.3317(17)
C(7)-C(8)	1.400(2)	C(17)-H(17)	0.9500
C(8)-C(9)	1.381(2)	C(18)-O(1)	1.4275(17)
C(8)-H(8)	0.9500	C(18)-H(18A)	0.9800
C(9)-C(10)	1.387(2)	C(18)-H(18B)	0.9800
C(9)-H(9)	0.9500	C(18)-H(18C)	0.9800
C(10)-C(11)	1.382(2)	N(2)-H(2A)	0.8800
C(10)-H(10)	0.9500	N(2)-H(2B)	0.8800

N(1)-C(1)-C(2)	109.84(10)	C(2)-C(3)-C(4)	123.54(12)
N(1)-C(1)-C(14)	112.58(10)	O(1)-C(3)-C(4)	119.61(11)
C(2)-C(1)-C(14)	109.29(10)	O(2)-C(4)-C(3)	123.56(12)
N(1)-C(1)-C(6)	100.96(10)	O(2)-C(4)-C(5)	119.74(12)
C(2)-C(1)-C(6)	112.00(10)	C(3)-C(4)-C(5)	116.59(11)
C(14)-C(1)-C(6)	112.00(10)	C(4)-C(5)-C(6)	115.38(11)
N(2)-C(2)-C(3)	120.63(12)	C(4)-C(5)-H(5A)	108.4
N(2)-C(2)-C(1)	116.72(11)	C(6)-C(5)-H(5A)	108.4
C(3)-C(2)-C(1)	122.64(12)	C(4)-C(5)-H(5B)	108.4
C(2)-C(3)-O(1)	116.76(11)	C(6)-C(5)-H(5B)	108.4

Table 2.16.8 (Continued)

H(5A)-C(5)-H(5B)	107.5	C(13)-C(14)-H(14A)	109.3
C(5)-C(6)-C(7)	107.29(10)	C(1)-C(14)-H(14A)	109.3
C(5)-C(6)-C(16)	113.87(11)	C(13)-C(14)-H(14B)	109.3
C(7)-C(6)-C(16)	109.97(10)	C(1)-C(14)-H(14B)	109.3
C(5)-C(6)-C(1)	111.51(10)	H(14A)-C(14)-H(14B)	108.0
C(7)-C(6)-C(1)	112.21(10)	N(1)-C(15)-C(16)	103.12(10)
C(16)-C(6)-C(1)	102.04(10)	N(1)-C(15)-H(15A)	111.1
C(12)-C(7)-C(8)	118.92(12)	C(16)-C(15)-H(15A)	111.1
C(12)-C(7)-C(6)	123.43(12)	N(1)-C(15)-H(15B)	111.1
C(8)-C(7)-C(6)	117.52(12)	C(16)-C(15)-H(15B)	111.1
C(9)-C(8)-C(7)	121.46(14)	H(15A)-C(15)-H(15B)	109.1
C(9)-C(8)-H(8)	119.3	C(15)-C(16)-C(6)	102.24(10)
C(7)-C(8)-H(8)	119.3	C(15)-C(16)-H(16A)	111.3
C(8)-C(9)-C(10)	119.61(14)	C(6)-C(16)-H(16A)	111.3
C(8)-C(9)-H(9)	120.2	C(15)-C(16)-H(16B)	111.3
C(10)-C(9)-H(9)	120.2	C(6)-C(16)-H(16B)	111.3
C(11)-C(10)-C(9)	119.71(13)	H(16A)-C(16)-H(16B)	109.2
C(11)-C(10)-H(10)	120.1	O(3)-C(17)-N(1)	126.09(13)
C(9)-C(10)-H(10)	120.1	O(3)-C(17)-H(17)	117.0
C(10)-C(11)-C(12)	121.35(14)	N(1)-C(17)-H(17)	117.0
C(10)-C(11)-H(11)	119.3	O(1)-C(18)-H(18A)	109.5
C(12)-C(11)-H(11)	119.3	O(1)-C(18)-H(18B)	109.5
C(7)-C(12)-C(11)	118.93(13)	H(18A)-C(18)-H(18B)	109.5
C(7)-C(12)-C(13)	121.32(12)	O(1)-C(18)-H(18C)	109.5
C(11)-C(12)-C(13)	119.75(12)	H(18A)-C(18)-H(18C)	109.5
C(12)-C(13)-C(14)	112.21(11)	H(18B)-C(18)-H(18C)	109.5
C(12)-C(13)-H(13A)	109.2	C(17)-N(1)-C(15)	121.09(11)
C(14)-C(13)-H(13A)	109.2	C(17)-N(1)-C(1)	126.78(11)
C(12)-C(13)-H(13B)	109.2	C(15)-N(1)-C(1)	112.09(10)
C(14)-C(13)-H(13B)	109.2	C(2)-N(2)-H(2A)	120.0
H(13A)-C(13)-H(13B)	107.9	C(2)-N(2)-H(2B)	120.0
C(13)-C(14)-C(1)	111.40(11)	H(2A)-N(2)-H(2B)	120.0
		C(3)-O(1)-C(18)	113.08(10)

Symmetry transformations used to generate equivalent atoms:

Table 2.16.9 Anisotropic displacement parameters ($Å^2 x\ 10^3$) for **110**. The anisotropic displacement factor exponent takes the form: $-2\pi^2[\ h^2 a^{*2} U^{11} + ... + 2\ h\ k\ a^*\ b^*\ U^{12}\ ]$.

U^{11}	U^{22}	U^{33}	U^{23}	U^{13}	U^{12}
C(1)20(1)	20(1)	17(1)	-1(1)	3(1)	-1(1)
C(2)20(1)	21(1)	21(1)	1(1)	7(1)	1(1)
C(3)21(1)	24(1)	16(1)	3(1)	6(1)	1(1)
C(4)21(1)	26(1)	18(1)	-1(1)	5(1)	1(1)
C(5)25(1)	21(1)	19(1)	-1(1)	5(1)	-4(1)
C(6)23(1)	19(1)	17(1)	-1(1)	5(1)	0(1)
C(7)19(1)	25(1)	19(1)	3(1)	3(1)	-1(1)
C(8)29(1)	26(1)	25(1)	2(1)	4(1)	-2(1)
C(9)29(1)	28(1)	34(1)	11(1)	1(1)	-4(1)
C(10)23(1)	42(1)	28(1)	15(1)	4(1)	-2(1)
C(11)20(1)	41(1)	20(1)	6(1)	4(1)	1(1)
C(12)17(1)	31(1)	19(1)	2(1)	2(1)	0(1)
C(13)22(1)	30(1)	19(1)	-2(1)	7(1)	1(1)
C(14)21(1)	23(1)	19(1)	-2(1)	5(1)	2(1)
C(15)22(1)	24(1)	26(1)	0(1)	5(1)	4(1)
C(16)24(1)	21(1)	23(1)	0(1)	8(1)	2(1)
C(17)22(1)	27(1)	21(1)	-2(1)	4(1)	-1(1)
C(18)27(1)	26(1)	23(1)	4(1)	2(1)	0(1)
N(1)19(1)	21(1)	19(1)	-2(1)	4(1)	1(1)
N(2)36(1)	24(1)	19(1)	1(1)	4(1)	-7(1)
O(1)23(1)	29(1)	17(1)	4(1)	5(1)	-1(1)
O(2)35(1)	30(1)	19(1)	-4(1)	4(1)	-5(1)
O(3)30(1)	23(1)	26(1)	-5(1)	5(1)	1(1)

Table 2.16.10 Hydrogen coordinates (x 10^4) and isotropic displacement parameters ($Å^2$x 10^3) for **110**.

	x	y	z	U(eq)
H(5A)	1785	-1194	552	26
H(5B)	859	-411	923	26
H(8)	2682	-1976	2480	32
H(9)	1855	-2688	4209	37
H(10)	1130	-1887	5929	37
H(11)	1253	-384	5905	32
H(13A)	2860	915	4705	28
H(13B)	1225	931	4531	28
H(14A)	2109	1711	2802	25
H(14B)	1042	973	2231	25
H(15A)	5270	-413	3661	28
H(15B)	6116	-26	2557	28
H(16A)	4414	-1263	1873	27
H(16B)	4519	-492	820	27
H(17)	5855	1294	4048	28
H(18A)	689	996	-2597	39
H(18B)	1407	1836	-3101	39
H(18C)	849	1854	-1703	39
H(2A)	3563	2191	-58	31
H(2B)	3911	2145	1455	31

CHAPTER THREE

Progress Towards the

Total Synthesis of (-)-Acutumine

3.1 Retrosynthetic Analysis

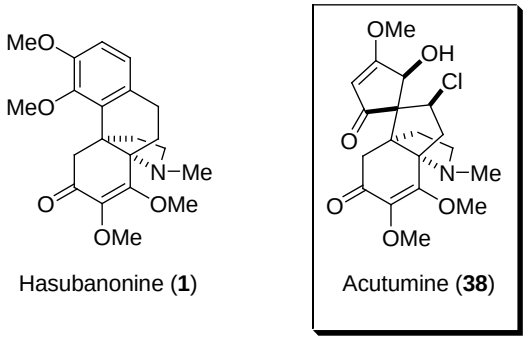

Figure 3.1.1 Structure of (-)-hasubanonine (**1**) and (-)-acutumine (**38**)

Given the close structural similarity between the hasubanan alkaloids and acutumine, the development of a unified strategy was central to our synthetic design. With the previously developed stereoselective strategy towards the southern [4.4.3.0] propellane core structure in hand, we turned our attention to the northern spirocyclic core structure of acutumine (**38**).[1] Our outline for the synthesis of acutumine (**38**) is shown in

Scheme 3.1.1. We chose to pursue the synthesis of acutumine (**38**) en route from dechloroacutumine (**62**). Dechloroacutumine (**62**) is particularly significant in allowing further investigations into the biological halogenation processes of higher plant species, from which acutumine was isolated. Dechloroacutumine (**62**) has been identified as a biosynthetic precursor of acutumine (**38**), and the availability is severely limited although acutumine is relatively available.[2-5] Chlorinated natural products are predominantly isolated from bacterial and fungi sources. Acutumine is characteristic in that it is a chlorinated natural product derived from higher plants.[6] An access to ample supplies of dechloroacutumine (**62**) would allow for further investigations into their biosynthetic pathways particularly in the chlorination step.

Following the previously developed scheme for the synthesis of the hasubanan alkaloids as described in Chapter 2, the southern [4.3.3.0] propellane core structure is envisaged to come from the Dieckmann cyclization of *cis*-fused bicycle **128** (Scheme 3.1.1). The bicycle **128** is predicted to derive from the spirocycle **129**. For our key transformation, we focused on the photo[2+2]cycloaddition reaction to assemble the requisite stereocenters. We have foreseen the difficulty in creating multiple contiguous stereocenters in a congested site; because it is a [2+2] reaction of two tethered unsaturated bonds, the stereochemical outcome depends only on the face selectivity of each π-bond in the transition state. The outcome of the relative stereochemistry is predicted from a transition state as depicted in Scheme 3.1.1. Spirocycle **130** is expected to derive from the retro-aldol reaction of the strained fused tetracycle **131**. The photocycloaddition precursor **133** is envisaged to come from an aldehyde coupling partner **135** and dioxinyloxysilane **134**.

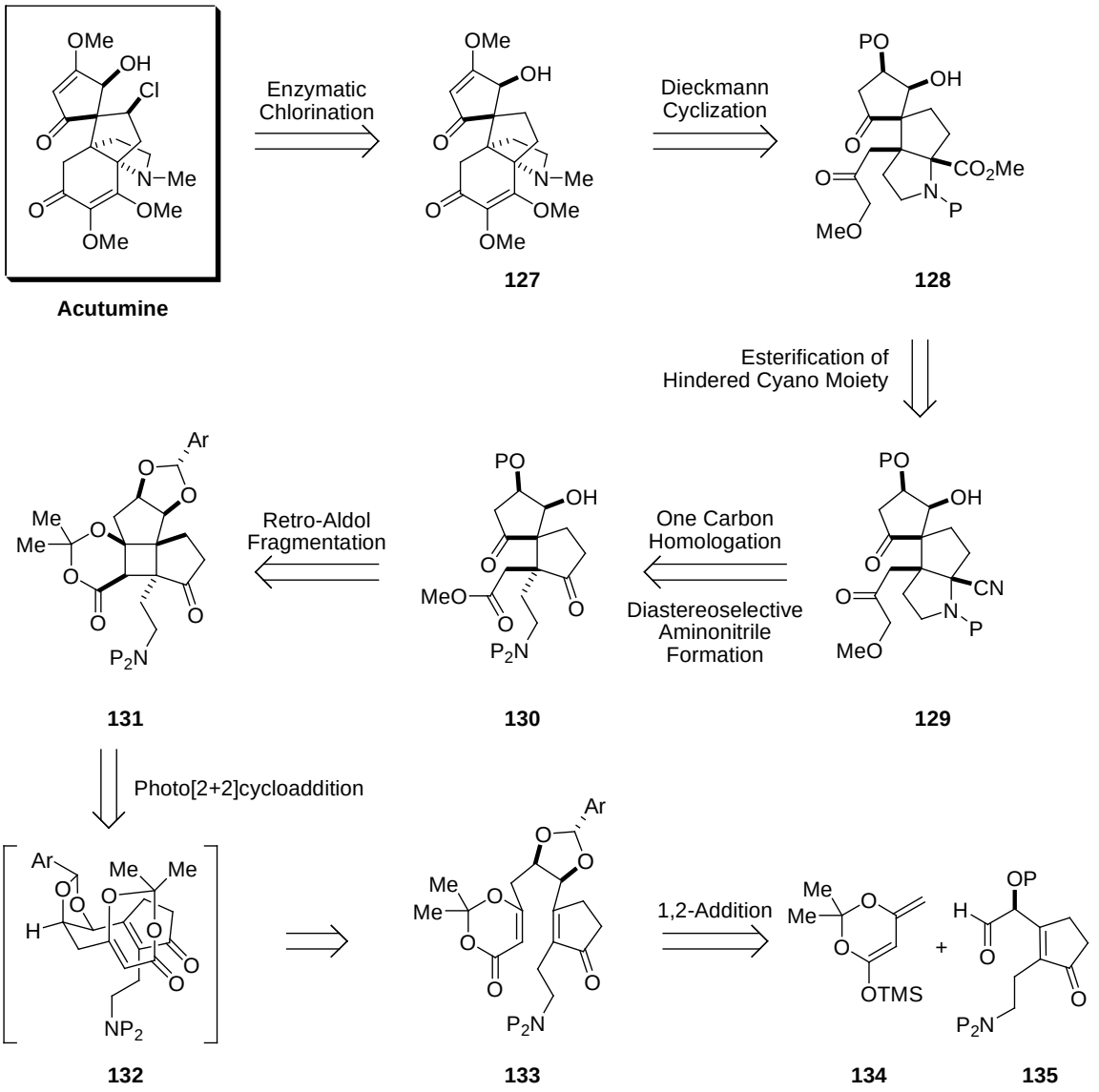

Scheme 3.1.1 Retrosynthetic analysis of acutumine (**38**)

In our preliminary studies, we were interested in investigating the feasibility of the photochemical cycloaddition reaction to generate the northern spirocyclic core structure of acutumine (**38**) (Scheme 3.1.2). We elected the advanced intermediate spirocycle **137** as our key model in the preliminary studies. Compared to the spirocycle

130 in the proposed synthesis of acutumine (**38**), the model spirocycle **137** contains tethered ethyl phenyl moiety in lieu of an ethyl amino moiety and lack one hydroxyl group. As a model study to investigate the feasibility of the photo[2+2]cycloaddition reaction, the amino group was not necessary. We chose the phenyl group because its high molecular weight made it less volatile and less polar. In addition, the phenyl group provided increased compatibility under various reaction conditions and can be easily seen under a UV lamp for TLC analysis. Preliminary studies on the biosynthesis of acutumine showed that dechloroacutumine (**62**) epimerizes at the hydroxyl position before its chlorination process (vide infra).[7] Therefore, a synthetic approach to both epimers of dechloroacutumine (**62**) at the hydroxyl position is of high interest. Further biological studies would allow for a more in-depth understanding of the halogenation processes.

The retrosynthetic analysis of spirocycle **137** is shown in Scheme 3.1.2. Selective methylation of 1,3-dione **138** followed with a one carbon homologation sequence would reveal **138**. Our key approach in the synthesis of the spirocyclic core is the retro-Aldol fragmentation of **139** from a photo[2+2]cycloaddition reaction. The cycloaddition precursor is envisioned to come from the coupling of the aldehyde partner **143** and the dioxinyloxysilane **134** (Route A).[8] Alternatively, the coupling partner can be derived from a selective deprotection of the tertiary alcohol and concomitant oxidation with allylic transposition to reveal the requisite 2,3-disubstituted cyclopentenone framework (Route B). The protected alcohol **141** is envisioned to come from the coupling of aldehyde **142** with the dioxinyloxysilane **134**. In our preliminary studies we discovered that handling of aldehyde **143** proved to be difficult due to low yields and it existed in its

conjugated enol tautomer; therefore, we chose the latter route to access the photocycloaddition precursor **141**.

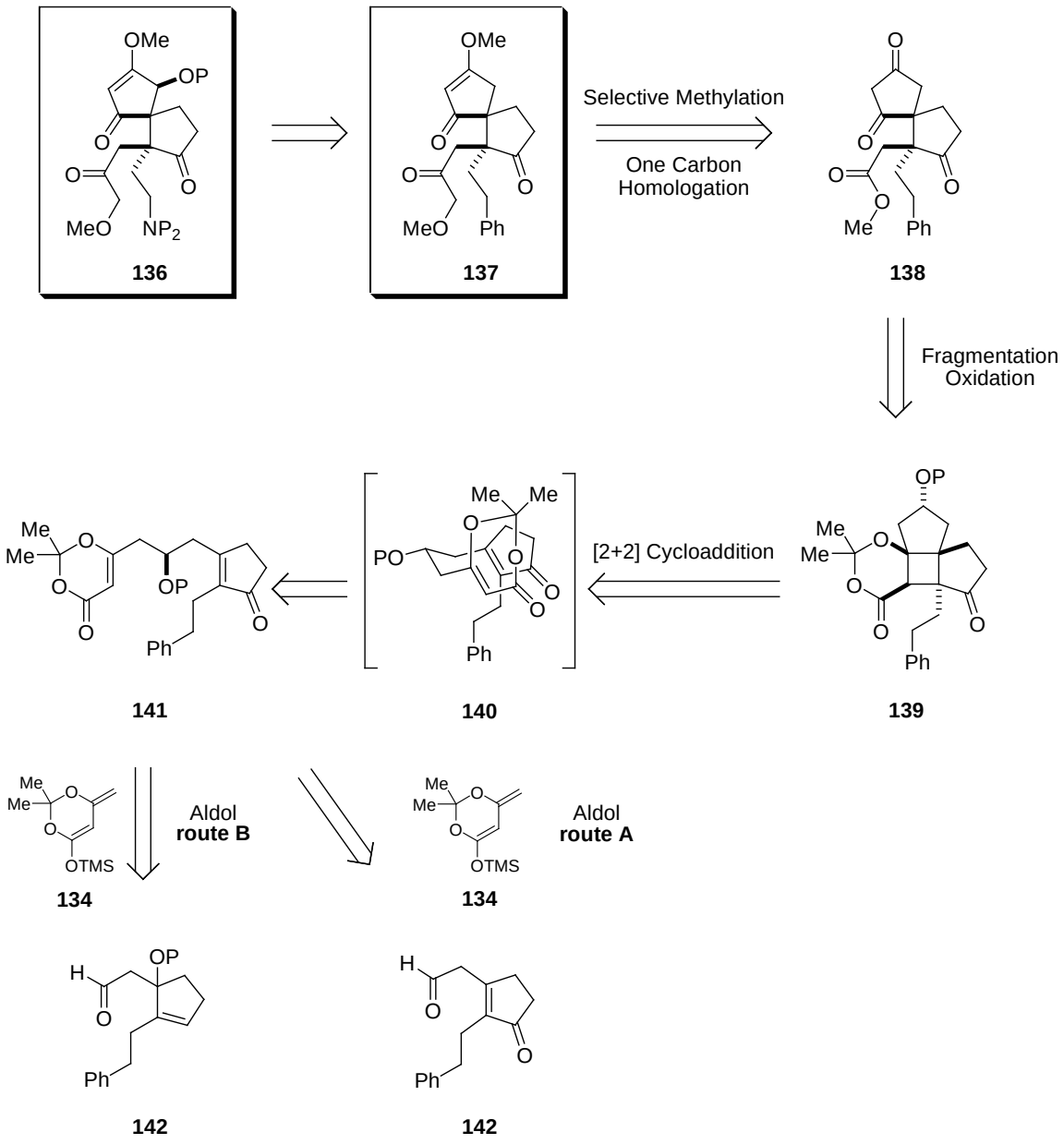

Scheme 3.1.2 Retrosynthetic analysis of the spirocycle **137**

Of the many possible variants of the photochemical reaction, we focused on two main precursors **144** and **147**. Each precursor provided distinct advantages for the proposed photocycloaddition reaction. We were interested in the cycloaddition of dioxinone **144** due to literature precedents of using the similar dioxinone foundation to synthesize the tetracyclic structure. It was reported that these reactions were regio- and stereoselective.[9] Fragmentation of the resulting dioxanone **145** would give the desired spirocyclic core. The dihydropyranone **147** is interesting in that the cyclic structure is envisioned to provide for a diastereocontrolled cycloaddition reaction to provide a rigid caged structure. Fragmentation of the resulting cyclobutane ring followed with methanolysis of the ester would provide the spirocyclic core.

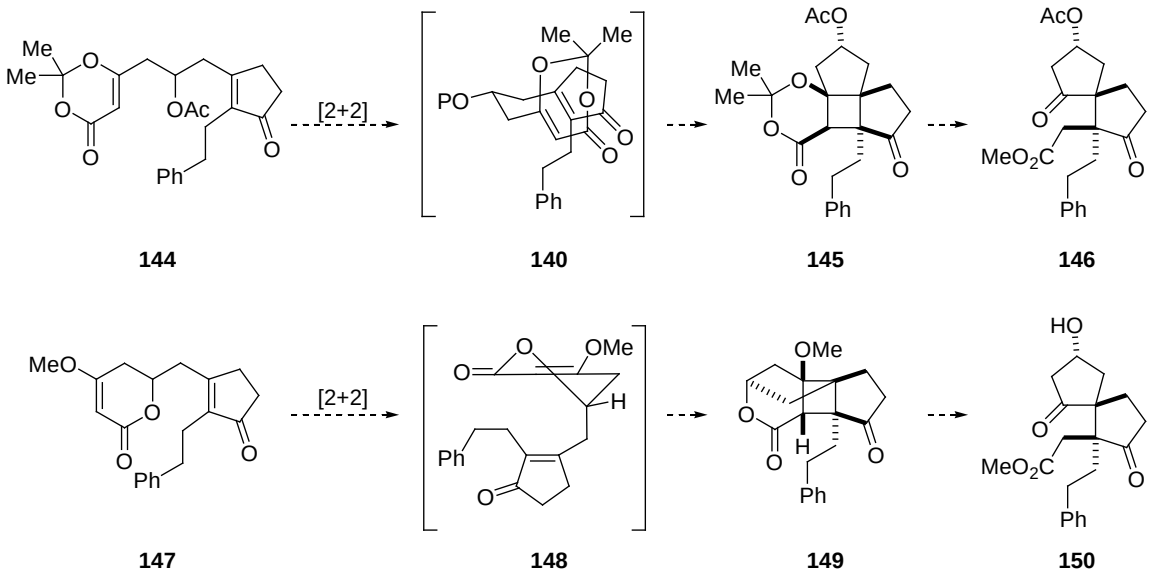

Scheme 3.1.3 Candidates for the photo[2+2]cycloaddition reaction

3.2 Synthesis of the 2,3-Disubstituted Cyclopentenone Foundation

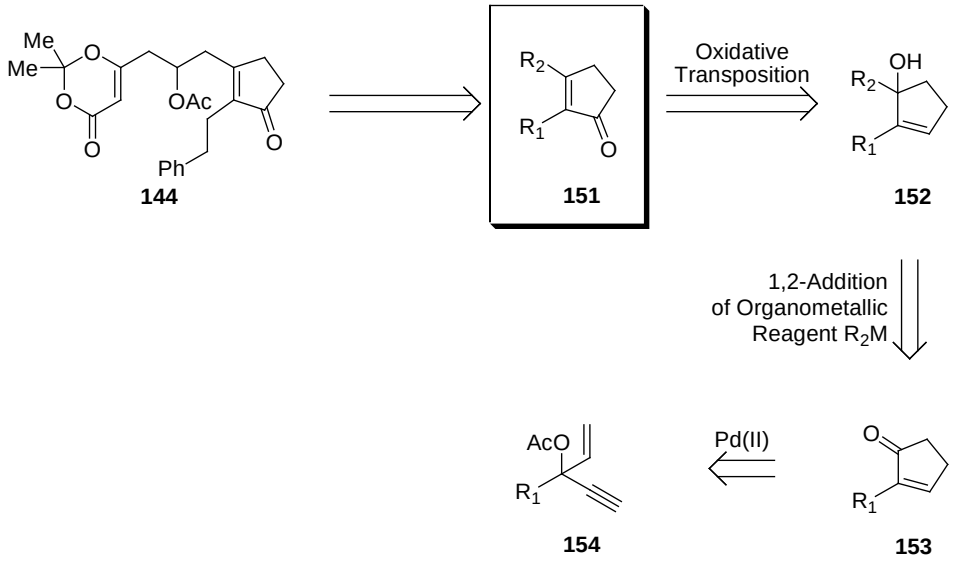

Scheme 3.2.1 Synthetic route to access 2,3-disubstituted cyclopentenones

In 1984, Rautenstrauch showed that Pd(II) salts catalyzed the cyclization of vinyl propargyl acetates to 2-substituted cyclopentenones.[10] Encouraged by this observation, we decided to make the cyclopentenone ring the foundational element of our synthesis. We envisioned that cyclopentenone **153** might be an effective precursor for the synthesis of 2,3-disubstituted cyclopentenone **151** after oxidation with allylic transposition of the 1,2-addition product **152** (Scheme 3.2.1).[11]

We began the synthesis of cyclopentenone **160** with the commercially available dihydrocinnamaldehyde **155** (Scheme 3.2.2). Lithiation of trimethylsilylacetylene with *n*-BuLi and subsequent addition to dihydrocinnamaldehyde **155** followed by treatment with K_2CO_3 in refluxing methanol to deprotect the TMS group at the terminal alkyne

position gave the propargyl alcohol **156** in 80% over 2 steps. IBX oxidation of the resulting alcohol gave ynone **157** in 81% yield.[12] Subsequent treatment with vinyl magnesium bromide gave the allyl propargyl alcohol **158** in high yields. The resulting alcohol was found to be unstable under silica gel chromatography. Presumably, residual acid promoted the formation of a stabilized carbocation that led to decomposition products. Therefore, the crude was subjected to the following reaction. The unstable intermediate was captured as the requisite acetate **159**. The key Pd(II) catalyzed cyclization proved to be reliable in forming the desired cyclopentenone **160**. This five step sequence could be conducted on multi-gram quantities thus allowing us a reliable method to access ample quantities of the 2-substituted cyclopentenone core.

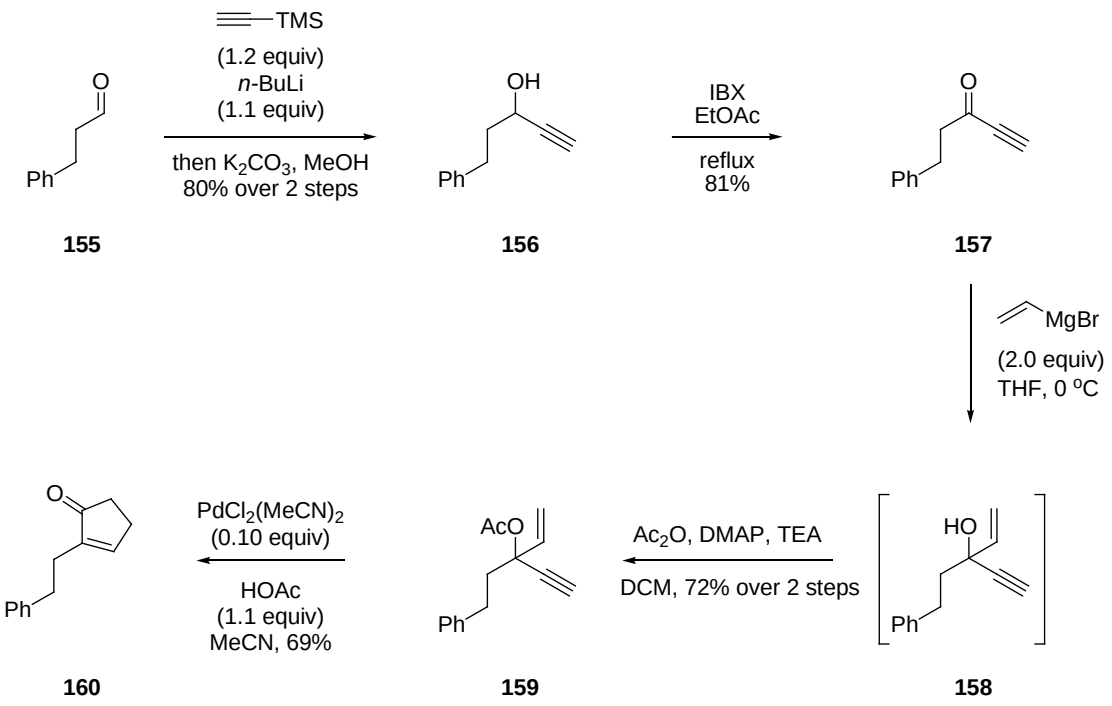

Scheme 3.2.2 Synthesis of 2-substituted cyclopentenone **160**

Although the mechanism of the reaction is not fully understood, Rautenstrauch proposed the following (Scheme 3.2.3).[10] The mechanism is presumed to start with the chelation to the Pd catalyst to give **162**. Oxidative cyclization followed with acetate migration gave **165**. Reductive elimination of palladacycle **165** gave the acetyl enol ether **166**. Hydrolysis of the resulting acetate provided cyclopentenone **167**.

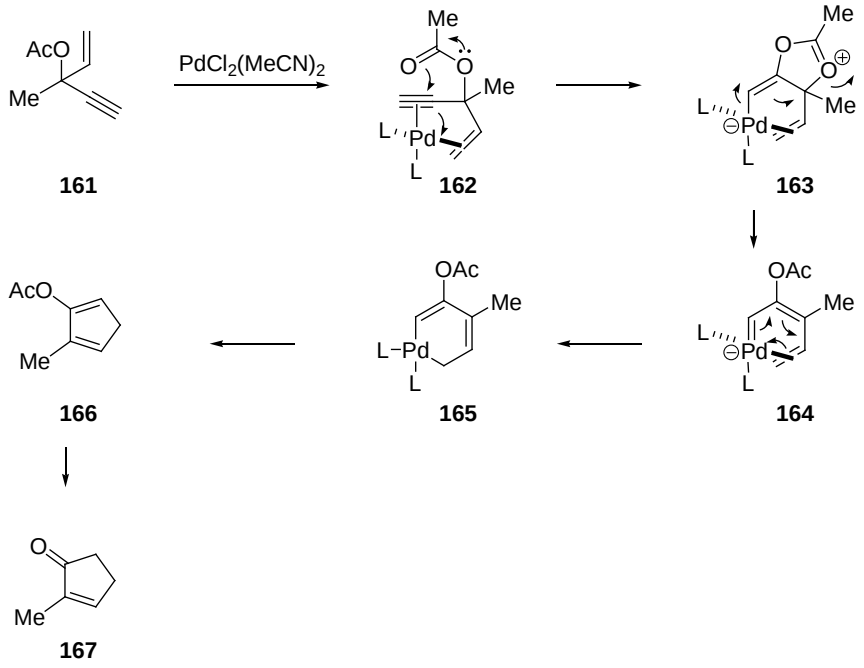

Scheme 3.2.3 Proposed mechanism for the synthesis of cyclopentenone **167**

3.3 Initial Attempt to Access Aldehyde Coupling Partner

Having secured a viable route to ample quantities of 2-substituted cyclopentenone **160**, we next focused on the construction of the aldehyde coupling partner 2,3-

disubstituted cyclopentenone **143**. As the α-hydroxylaldehyde equivalent, vinyl magnesium bromide was chosen to install as the second substituent on the cyclopentenone. 1,2-Addition with vinyl magnesium bromide to cyclopentenone **160** gave the allyl alcohol **168** (Scheme 3.3.1). We took the opportunity to explore the allylic oxidative transposition reaction as a key reaction to construct the 2,3-disubstituted cyclopentenone system. Gratifyingly, treatment of the tertiary allylic alcohol **168** with IBX in refluxing EtOAc gave cyclopentenone **169** in 79% yield.[13] The oxidation reaction with allylic transposition with the competing tethered vinyl moiety was not detected.

With the 2,3-disubstituted cyclopentenone **169** in hand, efforts were next directed to the synthesis of aldehyde **143**. In our previous studies towards the synthesis of the hasubanan alkaloids it was discovered that $KMnO_4$ allowed for a regioselective hydroxy-carbonylation of a terminal olefin to give α-hydroxylketone.[14] Unfortunately, such an expeditious transformation is not available to construct the β-hydroxyl aldehyde moiety directly from a terminal olefin moiety. Therefore, we decided to choose a stepwise approach via 1,2-diol. Chemoselective dihydroxylation of the pendant olefin was employed with OsO_4 to give the diol **170** in 76% yield.[15] The resulting primary alcohol was selectively protected as the pivaloyl acetate followed by methylation of the remaining secondary alcohol to give methyl ether **171** in 70% and 71% yield, respectively. In an attempt to remove the pivaloyl protecting group, treatment of **171** with NaOH led to the elimination of the pivaloate to form conjugate dienone **173**. The acidity at the γ position of the cyclopentenone proved to be detrimental in our synthetic route. As an alternative route, we investigated into the selective deprotection and concomitant oxidation of di-silylated ether **174** under the reported Swern oxidation. To

this end, the 1,2-diol **170** was di-silylated as the di-TES ether **174**. Unfortunately, Swern oxidation gave a complex mixture of products.[16] The desired α-silyloxyaldehyde **175** was not detected.

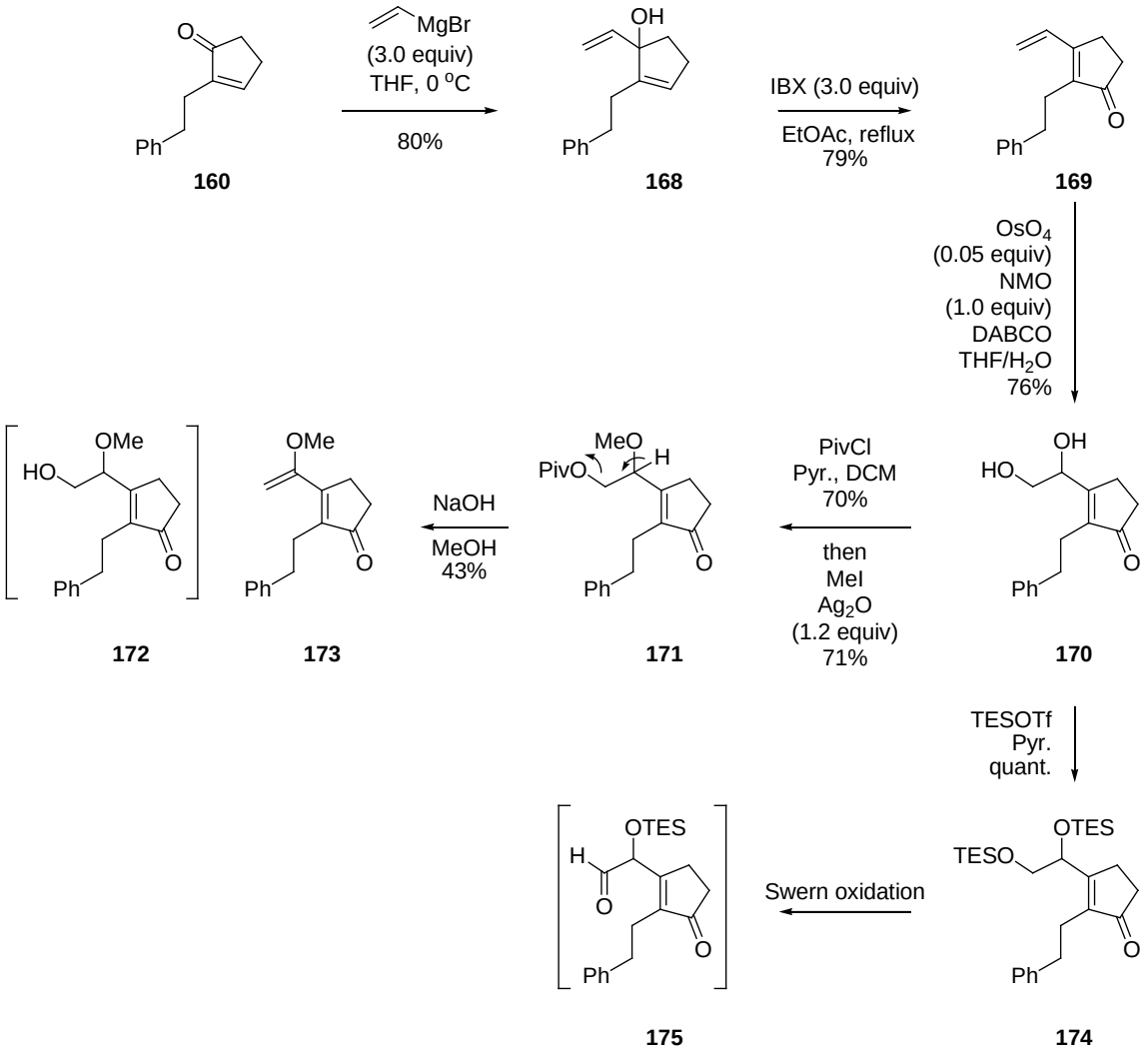

Scheme 3.3.1 Synthesis of 2,3-disubstituted cyclopentenone **173**

In the experiments leading to the β-hydroxyl aldehyde it was discovered that the acidity of the cyclopentenone at the γ position allowed for the elimination of the pivaloate

moiety to form conjugated dienone. We decided to attenuate the acidity at the γ position by reducing the enone to the allylic alcohol **176** (Scheme 3.3.2). Although the reaction increased a number of stereocenter, reinstallation of the carbonyl group will be possible after the [2+2] photocycloaddition reaction. The reduction was smoothly accomplished by using $NaBH_4$ in MeOH to give the allylic alcohol **176** in near quantitative yields as a 1:1 mixture of diastereomers. Methylation was employed using Ag_2O in iodomethane. Gratifyingly, reduction of the enone moiety did allow for a successful removal of the pivaloyl protecting group in 70% yield. Unfortunately, oxidation of the resulting alcohol **178** with DMP gave low yields of the aldehyde as handling of the intermediate proved to be difficult as the aldehyde existed in its more stable enol tautomer.[17]

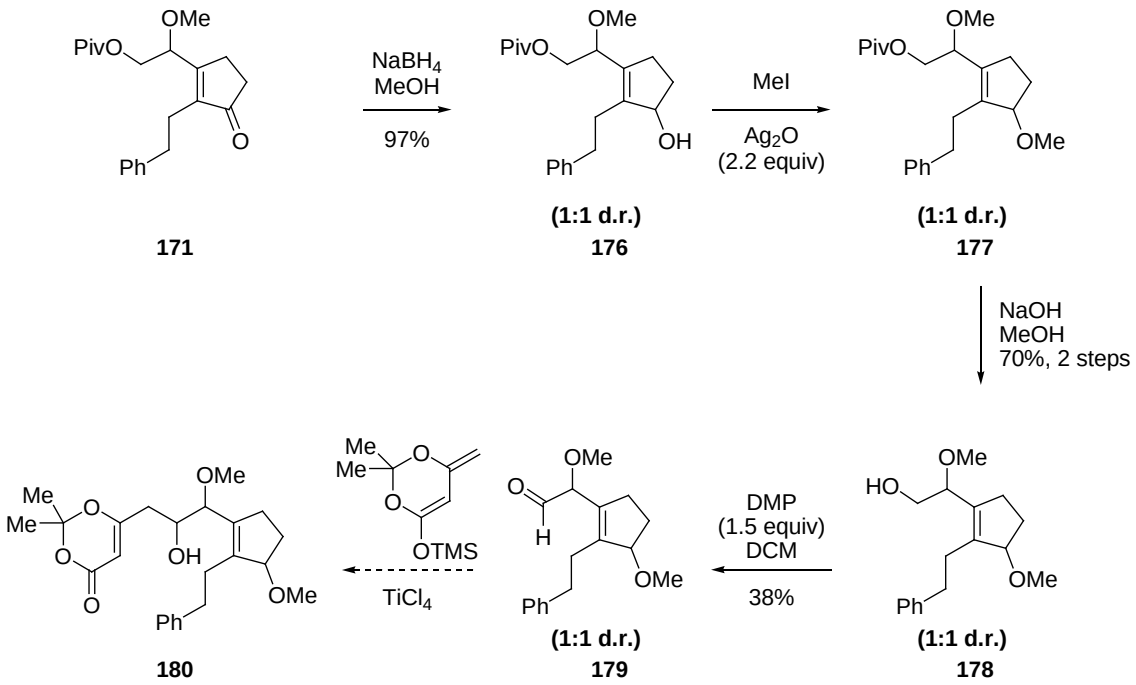

Scheme 3.3.2 Synthesis of aldehyde **179**

3.4 Synthesis of the Photocycloaddition Precursor 144

Given the difficulty in the synthesis and handling of the aldehyde coupling partner **179**, we came to the conclusion that efforts toward the aldehyde were unlikely to be fruitful. Of the many conceivable variants of our postulated synthesis of the cycloaddition precursor, we decided to reverse the sequence of two series of chemical transformations. Namely, we opted to form a more stable aldehyde variant **142**, form the western fragment of the photocycloaddition partner, and then finally oxidize the protected tertiary allylic alcohol to provide the desired precursor (Scheme 3.4.1).

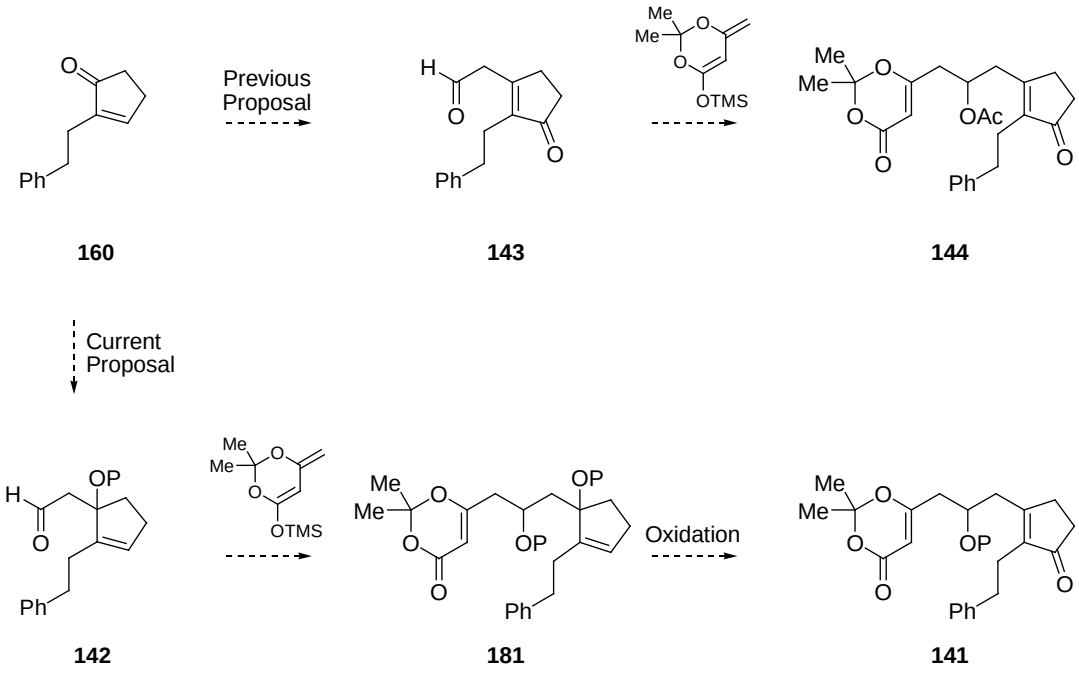

Scheme 3.4.1 Revised synthetic sequence to generate photocycloaddition precursors

Without much hesitation, we thus decided to explore the photochemical reaction of dioxinone **144**. There were two motivating factors that led us to pursue this synthetic route: (1) The cycloaddition precursor was in a linear, open form allowing access to a fused ring juncture as opposed to a caged structure in our proposed photocycloaddition product **149**. We anticipated the possibility of forming mixtures of acetate epimers in **145**. (2) Previous studies by the Winkler group demonstrated that similar dioxinone **182** participated in the photocycloaddition reaction to provide the desired fused ring structure (Scheme 3.4.2).[18] In addition, Haddad also showed the photo[2+2]cycloaddition reaction of dioxinone **187** with a tethered terminal olefin (Scheme 3.4.3).[19]

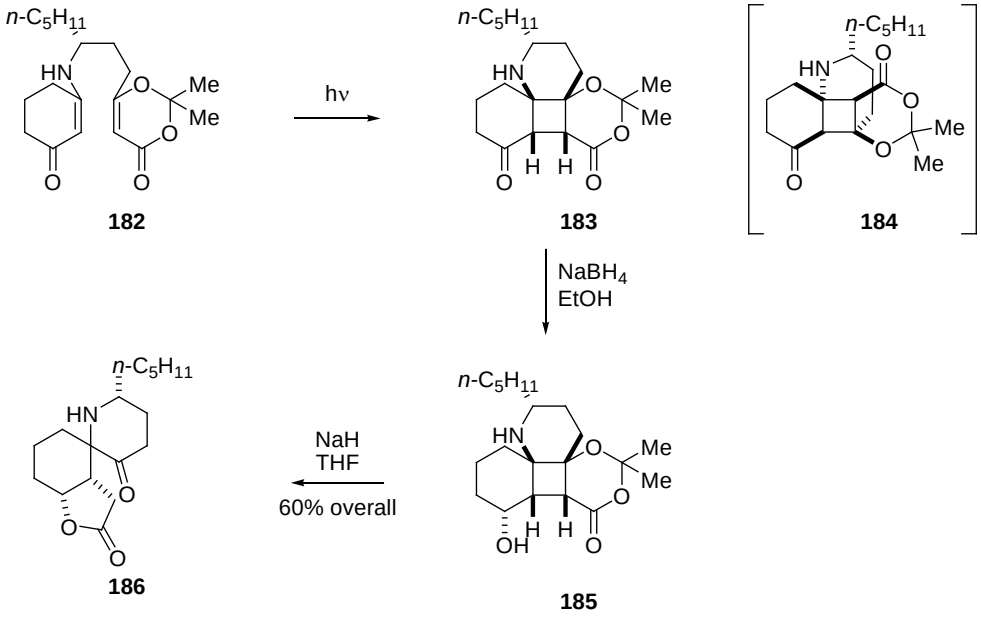

Scheme 3.4.2 Winkler's stereoselective synthesis of (-)-perhydrohistrionicotoxin

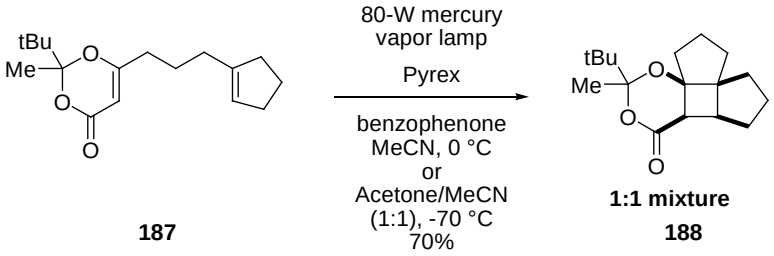

Scheme 3.4.3 Photo[2+2]cycloaddition reaction between dioxinone **187** and tethered olefin by the Haddad group

This conjecture was tested by preparing the dioxinone **144** (Scheme 3.4.4). Toward this goal, 1,2-addition of the ethyl thioacetate anion to cyclopentenone **160** gave the tertiary allylic alcohol **189** in near quantitative yields. We chose ethyl thioacetate as our aldehyde equivalent because the Fukuyama reduction (Et_3SiH and Pd/C in acetone) allows the convenient reduction of thioesters to aldehydes.[20] Unfortunately, initial investigations into this mild protocol did not give the desired aldehyde. We resorted to reducing the thioester moiety under harsher reaction conditions using DIBAL-H. The resulting tertiary allylic alcohol **189** was protected as the silyl ether **190** in 98% yield. From the thioester **190**, reduction using DIBAL-H gave the aldehyde **191**. During our investigations it was discovered that the tertiary allylic alcohol **189** needed to be protected for the reduction of the thioester moiety to proceed. Without the protecting group, reduction gave recovered starting material. We chose the trimethylsilyl ether as the preferred protecting group due to its chemical lability. Isolation of the resulting aldehyde **191** is possible; however, its stability proved to be a challenge. After ^{1}H-NMR confirmation of the crude aldehyde **191**, coupling with dioxinyloxysilane **134** gave 23% of the alcohol **192** over 2 steps.[21] The reaction was accompanied by 46% of the di-silylated product. The overall transformation proved to be effective in giving a total of

69% of the coupling product over 2 steps. The resulting alcohol was protected as its acetate **194**. Fortunately, under the identical acetylation conditions, the di-silylated product **193** was selectively deprotected at the less bulky secondary silyl ether position, and acetylated to provide **194** in 71% yield. Jones oxidation of tertiary allylic silyl ether **194** gave the desilylated product with concomitant oxidation with allylic transposition to provide the 2,3-disubstituted cyclopentenone **144**.[11]

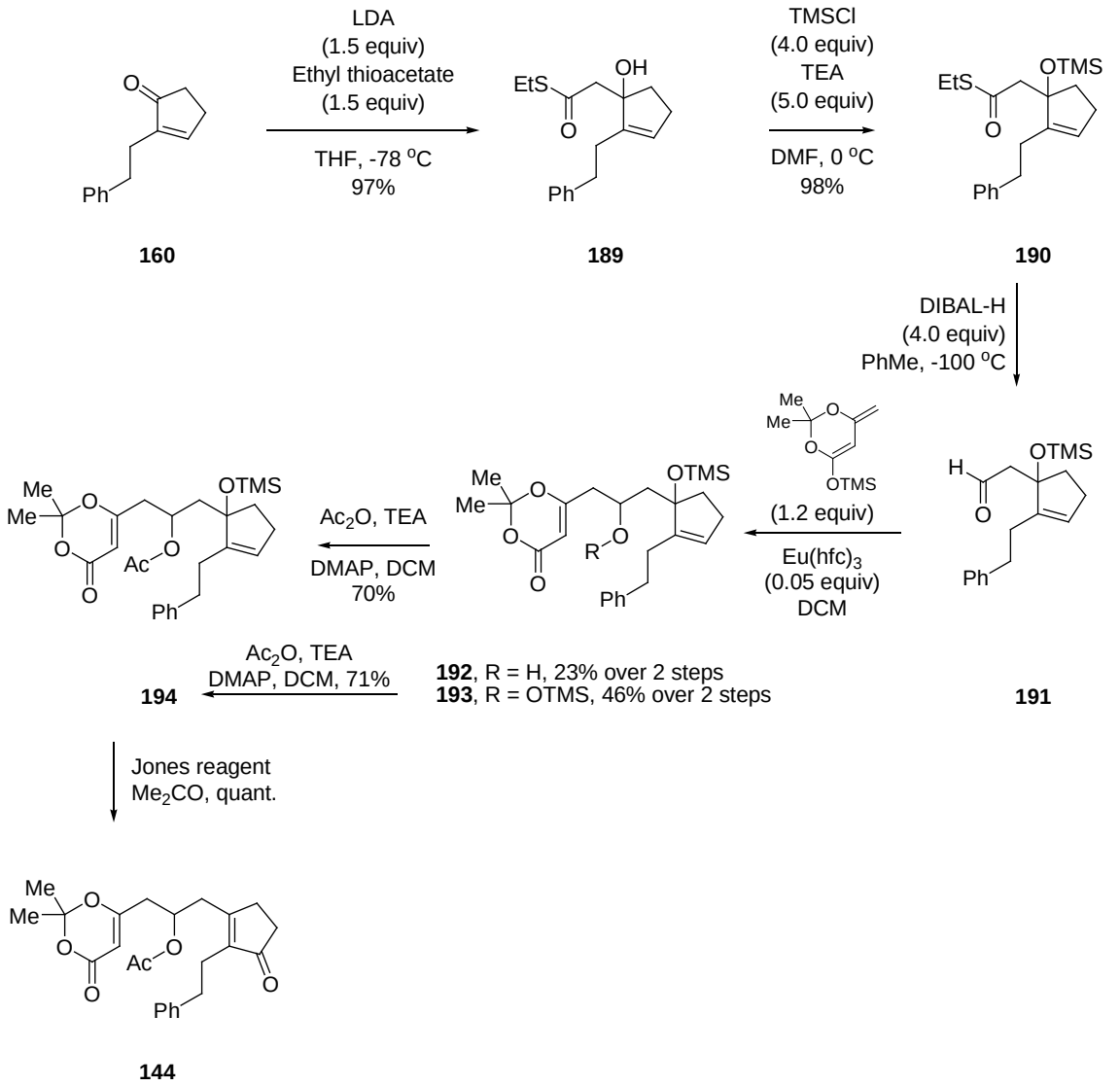

Scheme 3.4.4 Synthesis of dioxinone **194**

3.5 Photocycloaddition Reaction of Dioxinone 144

With the photo[2+2]cycloaddition precursor in hand, we attempted the proposed cyclization. Analysis by UV-Vis spectroscopy showed the enone chromophore absorbed

at 254 nm which corresponded to the $\pi \rightarrow \pi^*$ transition. At such a low absorption, this precluded the use of Pyrex glassware, which filtered light wavelengths below 290 nm. We resorted to using Quartz glassware, and ran the reaction in degassed solvent as the presence of oxygen might quench the biradical intermediate.[9] In addition, the reaction mixture was typically run at a much diluted 0.01 M solution as to prevent dimerization via an intermolecular cycloaddition. After overnight irradiation of **144** with a 500 watt Ace-Hanovia photochemical lamp at room temperature, analysis by TLC and ^{1}H-NMR showed only recovered starting material.

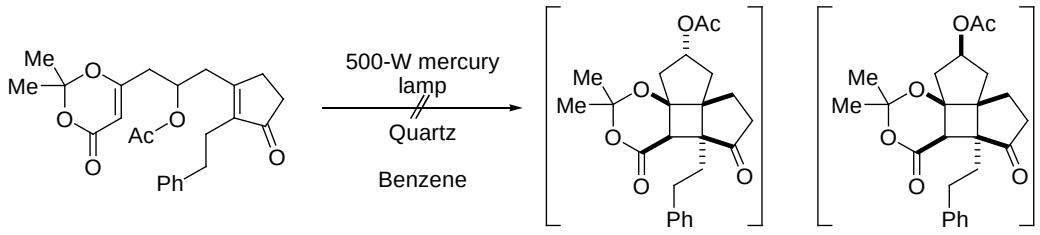

144 **145** **145b**

Scheme 3.5.1 Photocycloaddition reaction of dioxinone **144**

3.6 Synthesis of Photocycloaddition Precursor 202

We originally envisioned that the key spirocycle in acutumine (**38**) might be assembled from the fragmentation of cyclobutanes **145** and **149**. Although the proposed photo[2+2]cycloaddition reaction to access the cyclobutane core was attractive, this approach could be problematic since it involves forming four contiguous stereocenters in

a congested site, two of which are quaternary carbon stereocenters. Initial investigations into the photo[2+2]cycloaddition reaction of dioxinone **144** gave recovered starting material. Alternatively, we thought the cycloaddition reaction might be more feasible if the pendant ethyl phenyl moiety was removed completely.

In accord with our previous synthetic sequence, cyclopent-2-enone (**195**) was coupled to the anion of methyl thioacetate to provide the allylic tertiary alcohol **196** in quantitative yields. The resulting tertiary allylic alcohol **196** was protected as the silyl ether **197** in 80% yield. From the thioester **197**, reduction using DIBAL-H gave the aldehyde **198** cleanly, as indicated by ^{1}H-NMR. Coupling with dioxinyloxysilane **134** gave 21% of the alcohol **199** over 2 steps. The reaction was accompanied by 33% of the di-silylated product. The overall transformation gave a total of 54% of the coupling product over 2 steps. The resulting alcohol was protected as its acetate **201** in 76% yield. Fortunately, under the acetylation conditions, the di-silylated product **200** was selectively deprotected at the less bulky secondary silyl ether position, and acetylated to provide **201** in 70% yield. Jones oxidation of tertiary allylic silyl ether **201** gave the desilylated product with concomitant oxidation with allylic transposition to provide the 3-substituted cyclopentenone **202**.

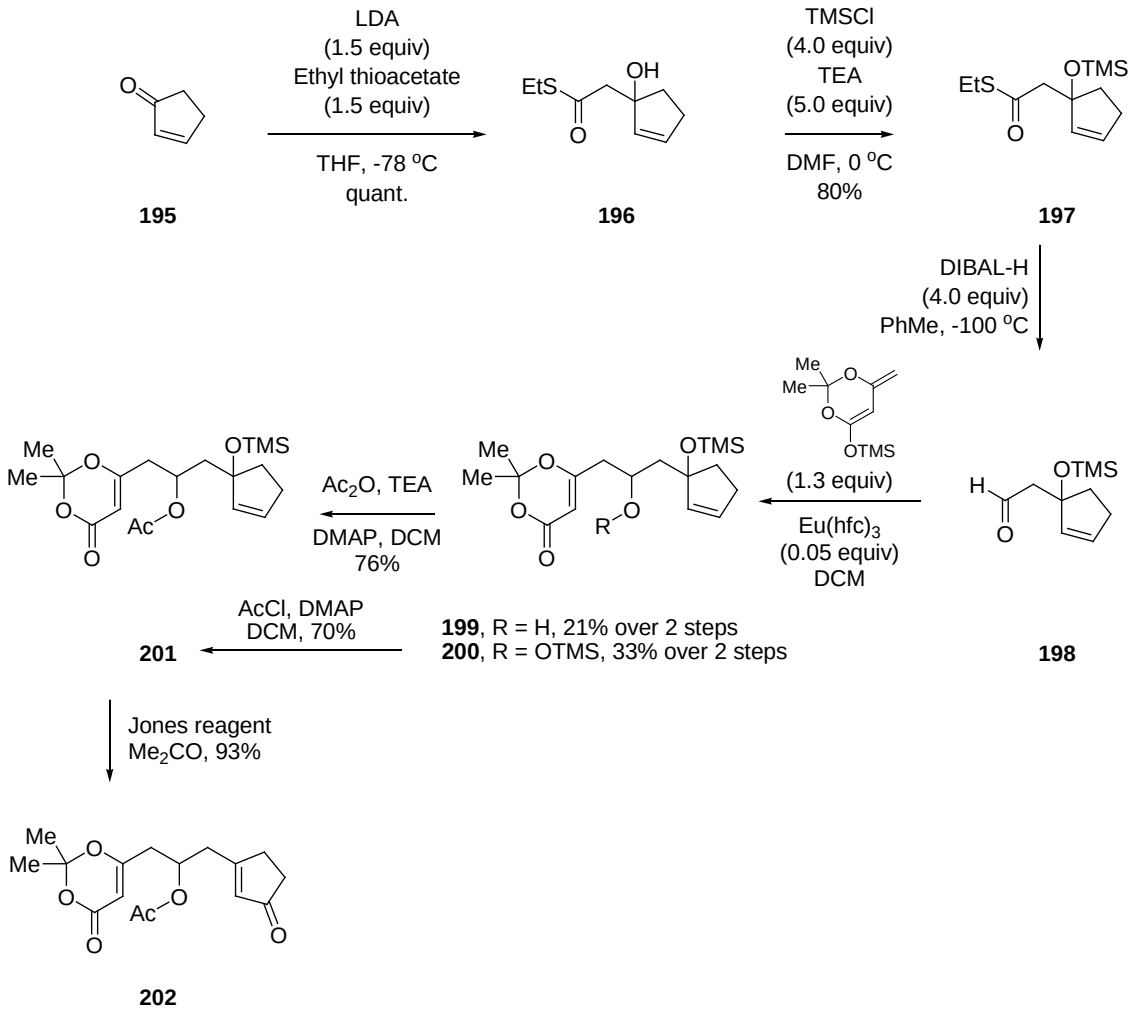

Scheme 3.6.1 Synthesis of cyclopentenone **202**

3.7 Photocycloaddition Reaction of Cyclopentenone 202

With the 3-substituted cyclopentenone **202** in hand, we attempted to test our hypothesis that the 2,3-disubstituted cyclopentenone **144** is too demanding a substrate to undergo the requisite photo[2+2]cycloaddition. Due to the small size of the ring fusion,

we expected *cis*-fused bicycles to control the relative stereochemistry about the cyclobutane ring. We also anticipated the possibility of forming a mixture of diastereomers at the acetate position. Indeed, photolysis of cyclopentenone **202** for 3 days cleanly gave 57% (brsm) of the desired cyclobutane as a 1.5:1.0 mixture of diastereomers at the acetate position. Failure to obtain a stereoselective cycloaddition reaction did not prove to be detrimental to our synthetic sequence as the epimeric stereocenter will be oxidized in subsequent steps. Literature precedent indicated that dioxinone **202** is capable of undergoing a regioselective photo[2+2]cycloaddition reaction to provide fused ring juncture in **203** as opposed to the caged ring juncture in **204**.[18,19] Comparison of the predicted ^{13}C-NMR chemical shifts with the isolated product of the reaction also supports the desired regioisomer as the isolated product.

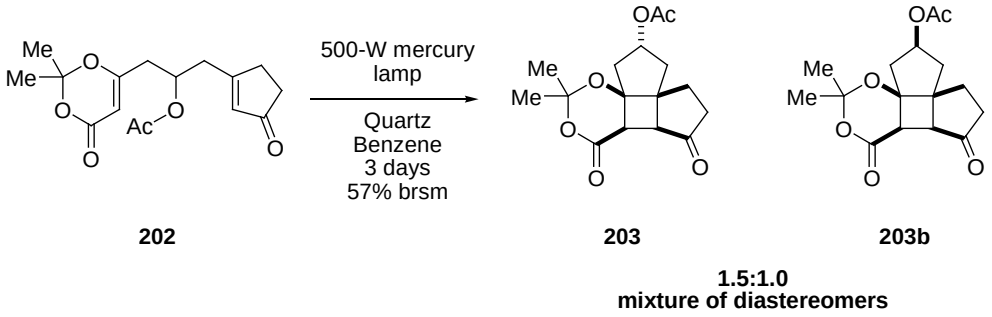

Scheme 3.7.1 Photocycloaddition reaction of cyclopentenone **202**

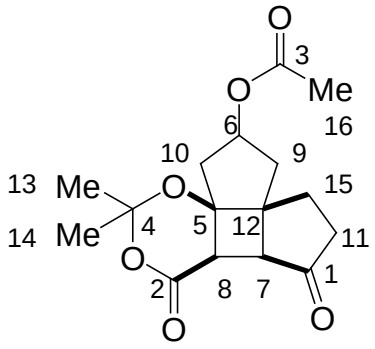

203

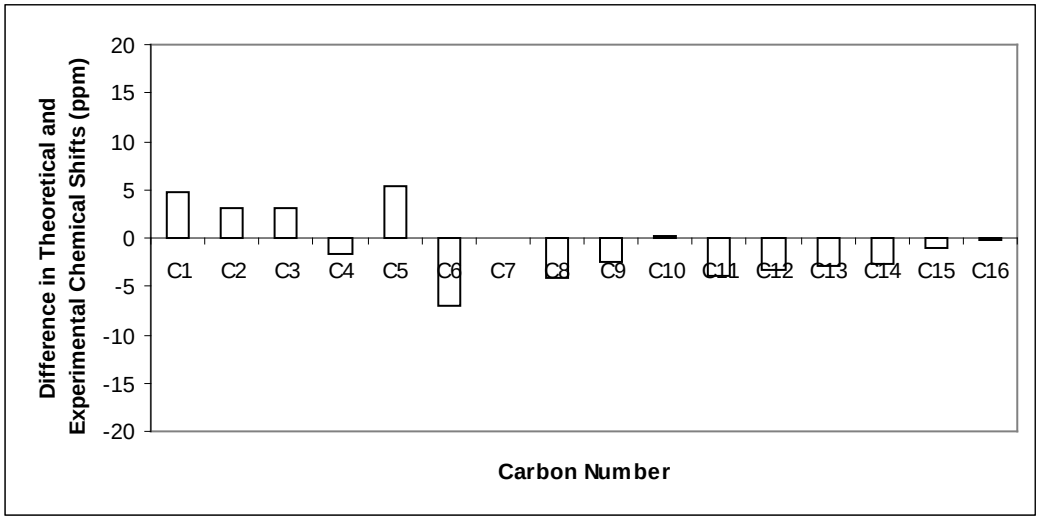

Figure 3.7.1 Difference between calculated and experimental ^{13}C-NMR shifts for cycloadduct **203** ($\Delta\delta = \delta$(calculated) – δ(observed) in ppm)

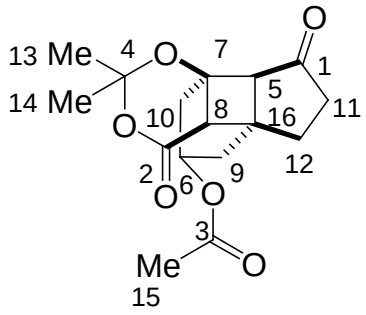

204

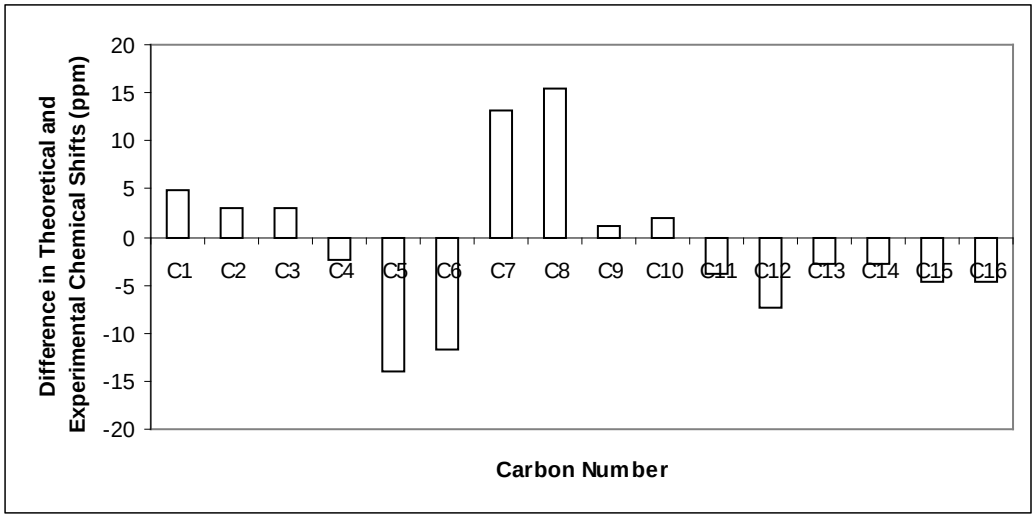

Figure 3.7.2 Difference between calculated and experimental ^{13}C-NMR shifts for cycloadduct **204** ($\Delta\delta = \delta$(calculated) – δ(observed) in ppm)

3.8 Synthesis of the Photocycloaddition Precursor 147

From all the possible strategies, we decided to pursue the one involving a formal hetero Diels-Alder reaction of diene **205** with aldehyde **191** to give the desired dihydropyranone **206**.[8] We chose the cyclic form of the photocycloaddition partner due to its potential of undergoing a diastereoselective reaction. Based on molecular modeling

we anticipated a diastereoselective reaction; however, the issue of regiochemistry of the [2+2] reaction was of high concern.

From the previously synthesized silyl ether **190**, reduction of the thioester moiety with DIBAL-H gave the desired aldehyde **191**. The intermediate aldehyde was used in its crude form after ^{1}H-NMR indicated a clean conversion. Formal hetero Diels-Alder reaction of aldehyde **191** with diene **205** in the presence of a lanthanide shift base, Eu(hfc)$_3$ gave the desired dihydropyranone **206** as a 1:1 mixture of diastereomers in 59% over 2 steps. To our delight treatment of the resulting dihydropyranone **206** with Jones reagent gave the silyl deprotected tertiary allylic alcohol and concomitant oxidation with allylic transposition in 92% yield. The methyl enol ether moiety proved to be stable under the sulfuric acid conditions in Jones reagent.

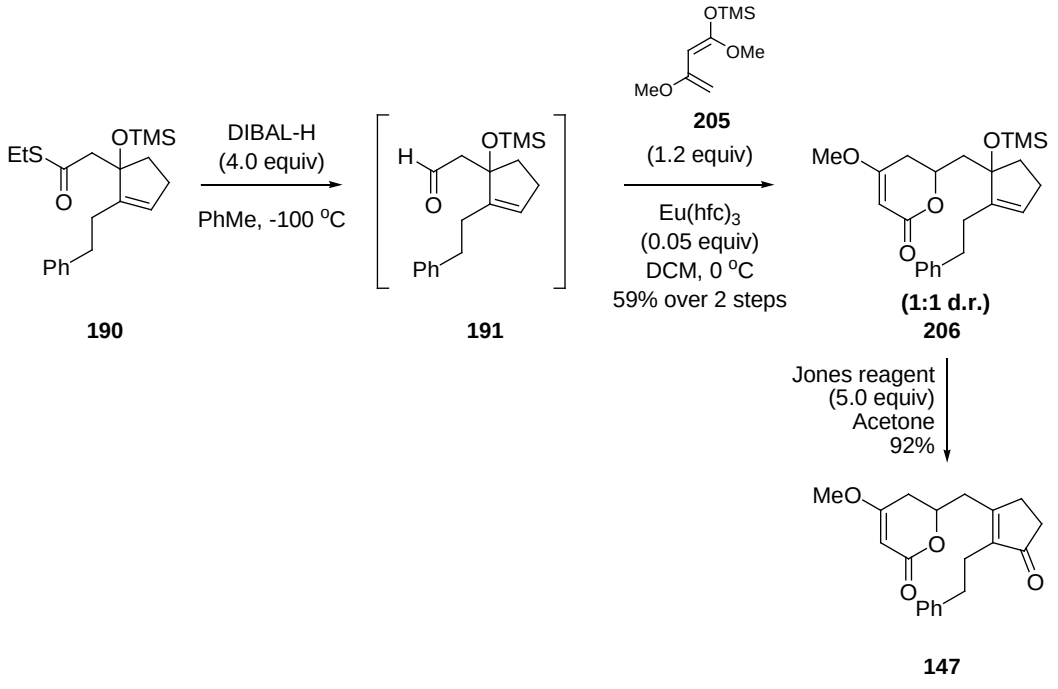

Scheme 3.8.1 Synthesis of methyl enol ether **147**

3.9 Photocycloaddition Reaction of Cyclopentenone 147

With all the required building block in hand, we proceeded to assemble them toward the targeted photochemical adduct (Scheme 3.9.1). Photolysis of cyclopentenone **147** in deoxygenated benzene gave 28% of what was assigned the undesired regioisomer, cyclobutane **207**. Comparisons of the two cyclobutane regioisomers **149** and **207** reveal a simple way to distinguish between the two compounds. The ^{13}C-NMR signal of **149** and **207** should show six downfield shifts (≥125 ppm) and twelve upfield shifts (≤100 ppm). However, for cyclobutane **149**, the ^{13}C-NMR signal for the fully substituted ether oxygen C7 is predicted to around 96.3 ppm whereas the signal for regioisomeric cyclobutane **207** C7 is predicted to be around 79.5 ppm. The difference in 16.8 ppm gave us confidence in using ^{13}C-NMR data for structure assignment. Indeed, the ^{13}C-NMR spectrum was devoid of signals near 96.3 ppm. The signal that corresponded to C7 came off at 78.3 ppm, which is only a 1.2 ppm shift from the predicted value.

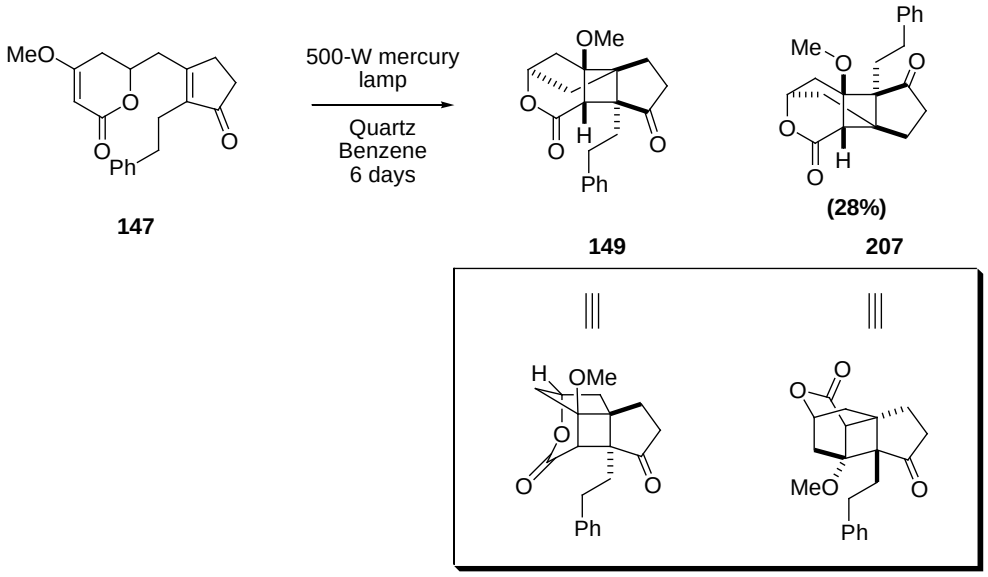

Scheme 3.9.1 Photocycloaddition reaction of cyclopentenone **147**

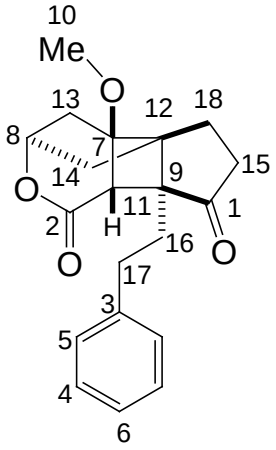

149

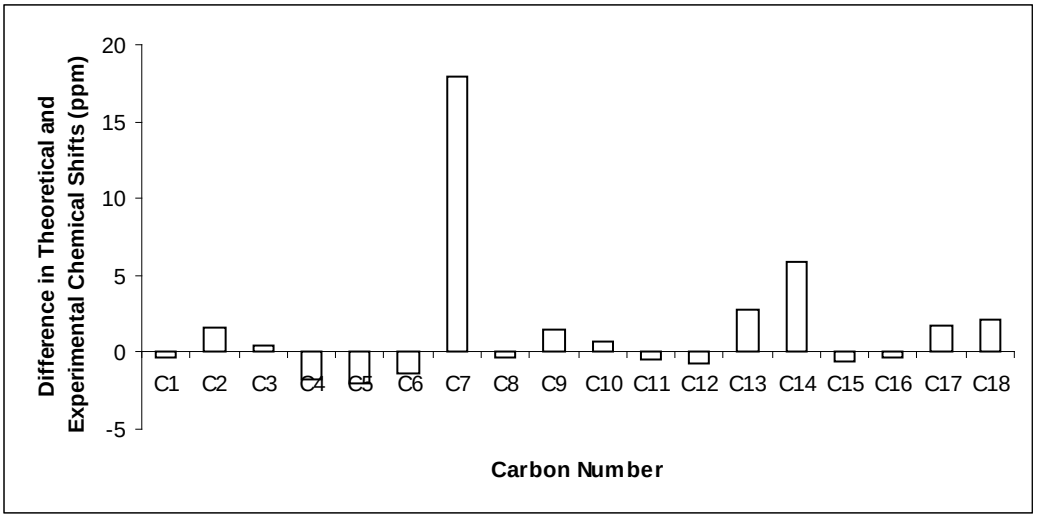

Figure 3.9.1 Difference between calculated and experimental ^{13}C-NMR shifts for cycloadduct **149** ($\Delta\delta = \delta$(calculated) – δ(observed) in ppm)

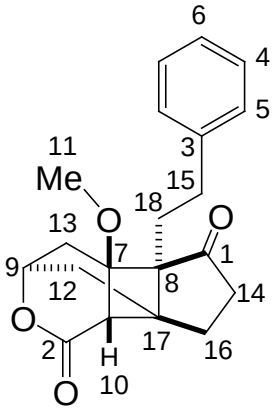

207

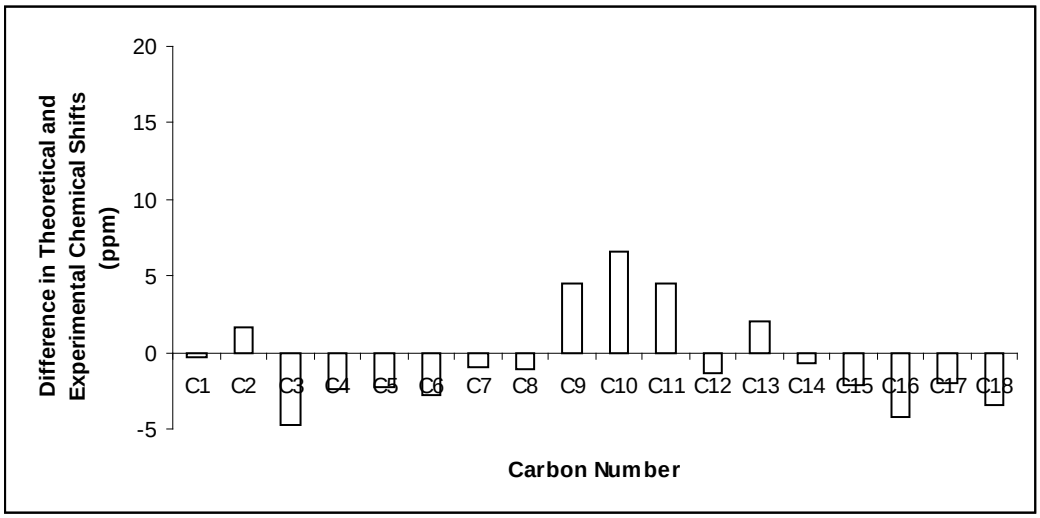

Figure 3.9.2 Difference between calculated and experimental ^{13}C-NMR shifts for cycloadduct **207** ($\Delta\delta = \delta$(calculated) – δ(observed) in ppm)

Attempts to characterize **207** by X-ray crystal structure analysis proved to be difficult as we only obtained poor quality crystals. Fortunately, complexation of the phenyl group to a cationic ruthenium complex allowed for quality crystals to be analyzed.[22] Indeed, the regio- and relative stereochemistry of the photo[2+2]cycloaddition reaction was in good agreement with cyclobutane **208** (Figure 3.9.2). In addition to the characterized cyclobutane product, we also obtained 20% of

isomeric photocycloaddition adducts; however, their assignment and chemical manipulations proved to be difficult. Although the investigations were promising in revealing that the cyclobutane core motifs could be accessed, the main issue was identifying an appropriate coupling partner to provide the cycloadduct with the correct desired regio- and stereochemistry. Given our inability to access the photocycloaddition adduct with the correct regiochemistry, we wondered whether the architectural complexity of the caged cyclobutane **149** rendered the photochemical ineffective.

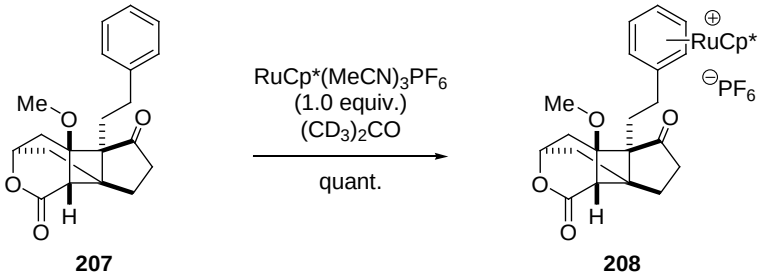

Scheme 3.9.2 Formation of ruthenium complex **208**

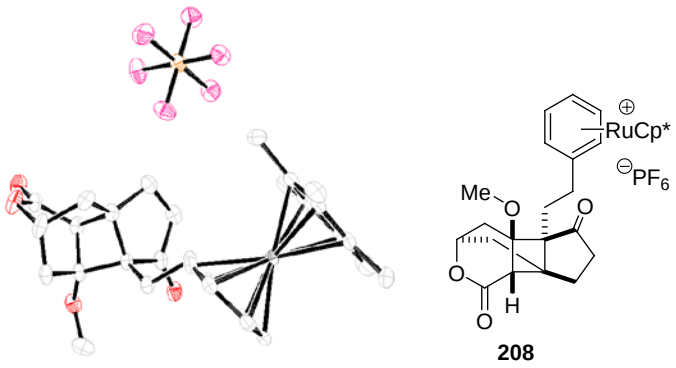

Figure 3.9.3 ORTEP figure of cyclobutane **208**

3.10 Conclusion

With a general strategy to access the southern propellane core of acutumine (**38**) from our investigations into 3,4-bisdesmethoxyhasubanone **84**, we turned our attention to the northern spirocycle fragment. Our proposed photo[2+2]cycloaddition reaction was extensively pursued with the photolysis of three precursors **144**, **147** and **202**. Photolysis of cyclopentenone **144** proved to be difficult as we were only able to recover starting materials. We then synthesized cyclopentenone **202**, a similar substrate to **144** differing only in the absence of the pendant ethyl phenyl moiety. This allowed for a more accessible cyclobutane and provided the desired products. A variant of the possible cycloaddition precursors, we also synthesized dioxinone **147**. We only managed to obtain the undesired regioisomer of the cycloaddition reaction. Initial investigations showed the feasibility of obtaining the requisite cyclobutane fragment via a photo[2+2]cycloaddition reaction. Further investigations are needed to find a suitable substrate that would allow for an efficient and diastereoselective reaction.

3.11 Acknowledgements

I would like to acknowledge Professor Arnold Rheingold and the UCSD X-Ray Crystallography Facilities and David Hitt for his preparation of the cationic ruthenium complex.

3.12 Experimental

3.12.1 Materials and Methods

All reagents were commercially obtained (Aldrich, Fisher) at highest commercial quality and used without further purification except where noted. Organic solutions were concentrated by rotary evaporation below 40 °C at approximately 20 mmHg. Tetrahydrofuran (THF), methanol (MeOH), chloroform ($CHCl_3$), dichloromethane (DCM), ethyl acetate (EtOAc), acetonitrile (MeCN), *N*,*N*-dimethylformamide (DMF), toluene (PhMe), ethanol (EtOH) and acetone were reagent grade and used without further purification. Yields refer to chromatographically and spectroscopically (^{1}H NMR, ^{13}C NMR) homogeneous materials, unless otherwise stated. Reactions were monitored by thin-layer chromatography (TLC) carried out on 0.25 mm E. Merck silica gel plates (60F-254) using UV light and cerium molybdate solution with heat as visualizing agents. E. Merck silica gel (60, particle size 0.040-0.063 mm) was used for flash chromatography. Preparative thin-layer chromatography separations were carried out on 0.50 mm E. Merck silica gel plates (60F-254). NMR spectra were recorded on Varian Mercury 300, 400 and/or Unity 500 MHz instruments and calibrated using the residual undeuterated solvent as an internal reference. Chemical shifts (δ) are reported in parts per million (ppm) and coupling constants (*J*) are reported in hertz (Hz). The following abbreviations

were used to designate multiplicities: s= singlet, d= doublet, t= triplet, q= quartet, quint.= quintet, sp = septet, m= multiplet, br= broad. High resolution mass spectra (HRMS) were recorded on a Finnigan LCQDECA mass spectrometer under electrospray ionization (ESI) or atmospheric pressure chemical ionization (APCI) conditions, or on a Thermofinnigan Mat900XL mass spectrometer under electron impact (EI), chemical ionization (CI), or fast atom bombardment (FAB) conditions. X-ray data were recorded on a Bruker SMART APEX CCD X-ray diffractometer.

3.12.2 Preparative Procedures

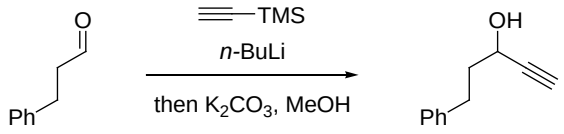

155 **156**

5-Phenylpent-1-yn-3-ol (156). To a solution of trimethylsilylacetylene (23.2 mL, 1.64 mol, 1.2 equiv.) in THF (250 mL) at -78 °C was added *n*-BuLi (60.2 mL, 1.50 mol, 1.1 equiv.). The solution was stirred for 30 min, then **155** (20.0 mL, 1.37 mol, 1.0 equiv.) was added dropwise. The solution was warmed to 0 °C for 2 h then quenched with sat aq NH_4Cl (300 mL) and extracted with EtOAc (3 x 500 mL). The combined organic layers were dried (Na_2SO_4), and the solvent was removed in vacuo. The resulting mixture was diluted with MeOH (125 mL) and K_2CO_3 (18.9 g, 1.37 mol, 1.0 equiv.) was added and heated to reflux for 15 h. The solution was filtered and extracted with EtOAc (3 x 300

mL). The combined organic layers were dried (Na_2SO_4), and the solvent was removed in vacuo. Flash chromatography (SiO_2, 5% EtOAc in hexanes elution) afforded **156** (17.5 g, 1.09 mol, 80% over 2 steps) as a colorless oil. R_f (20% EtOAc in hexanes elution) = 0.40; HRMS (EI) *m* / *z* calcd for $C_{11}H_{12}O$ (M^+) 160.0883, found 160.0883; ^{1}H NMR (400 MHz, $CDCl_3$) δ: 7.27 – 7.31 (m, 2H), 7.18 – 7.25 (m, 3H), 4.36 – 4.37 (m, 1H), 2.81 (t, *J* = 7.8 Hz, 2H), 2.51 (d, *J* = 2.4 Hz, 1H), 2.01 – 2.09 (m, 2H), 1.96 (s, 1H); ^{13}C NMR (100 MHz, $CDCl_3$) δ: 141.1, 128.82, 128.79, 126.4, 84.9, 73.7, 61.9, 39.4, 31.6; IR (film, cm^{-1}) 3389, 2943, 1636, 1378, 1030.

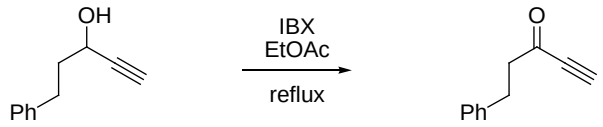

156 **157**

5-Phenylpent-1-yn-3-one (157). To a solution of **156** (13.3 g, 83.1 mmol, 1.0 equiv.) in EtOAc (125 mL) was added 2-iodoxybenzoic acid (34.5 g, 1.23 mol, 1.5 equiv.) and heated to reflux for 15 h. The solution was filtered and diluted with water (500 mL) and extracted with EtOAc (3 x 500 mL). The combined organic layers were dried (Na_2SO_4), and the solvent was removed in vacuo. Flash chromatography (SiO_2, 5% EtOAc in hexanes elution) afforded **157** (10.7 g, 67.3 mmol, 81%) as a colorless oil. R_f (20% EtOAc in hexanes elution) = 0.50; HRMS (EI) *m* / *z* calcd for $C_{11}H_{10}O$ (M^+) 158.0726, found 158.0723; ^{1}H NMR (400 MHz, $CDCl_3$) δ: 7.27 – 7.31 (m, 2H), 7.18 – 7.24 (m, 3H), 3.23 (s, 1H), 3.00 (t, *J* = 6.8 Hz, 2H), 2.92 (t, *J* = 6.4 Hz, 2H); ^{13}C NMR (100 MHz, $CDCl_3$) δ: 186.6, 140.2, 128.9, 128.6, 126.7, 81.6, 79.2, 47.2, 29.8; IR (film, cm^{-1}) 3034, 2921, 2084, 1668, 1450, 1095.

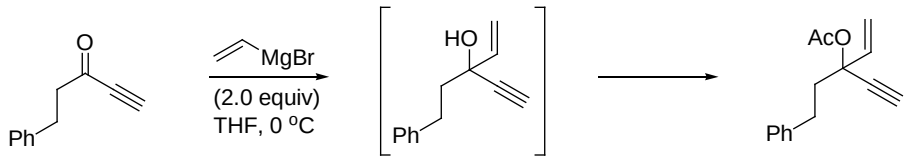

157 **158** **159**

3-Phenethylpent-4-en-1-yn-3-yl acetate (159). To a solution of vinylmagnesium bromide (98 mL, 68.8 mmol, 0.7 M in THF, 2.0 equiv.) at 0 °C was added **157** (5.44 g, 34.4 mmol, 1.0 equiv.). The solution was stirred for 1 h, then quenched with sat aq NH_4Cl (100 mL) and extracted with EtOAc (3 x 300 mL). The combined organic layers were dried (Na_2SO_4), and the solvent was removed in vacuo. The resulting mixture was diluted with DCM (125 mL) and cooled to 0 °C. DMAP (1.68 g, 13.7 mmol, 0.4 equiv.), Ac_2O (13.1 mL, 1.38 mol, 4.0 equiv.) and TEA (33.1, 1.38 mol, 4.0 equiv.) was added and stirred for 15 h. The reaction mixture was quenched with sat aq $NaHCO_3$ (200 mL) and extracted with EtOAc (3 x 300 mL). The combined organic layers were dried (Na_2SO_4), and the solvent was removed in vacuo. Flash chromatography (SiO_2, 5% EtOAc in hexanes elution) afforded **159** (5.66 g, 24.8 mmol, 72% over 2 steps) as a colorless oil R_f (30% EtOAc in hexanes elution) = 0.39; HRMS (ESI) *m*/*z* calcd for $C_{15}H_{16}O_2Na$ ($M+Na^+$) 251.1043, found 251.1042; ^{1}H NMR (400 MHz, $CDCl_3$) δ: 7.26 – 7.31 (m, 2H), 7.20 – 7.21 (m, 3H), 5.93 (dd, *J* = 9.6, 16.8 Hz, 1H), 5.64 (d, *J* = 17.6 Hz, 1H), 5.43 (d, *J* = 10.4 Hz, 1H), 2.75 – 2.85 (m, 2H), 2.77 (s, 1H), 2.26 – 2.34 (m, 1H), 2.06 – 2.13 (m, 1H), 2.05 (s, 3H); ^{13}C NMR (100 MHz, $CDCl_3$) δ: 169.3, 141.5, 137.6, 128.8 (2x), 126.3, 117.4, 81.0, 77.5, 76.6, 42.9, 30.6, 22.0; IR (film, cm^{-1}) 2973, 2091, 1729, 1360, 1223.

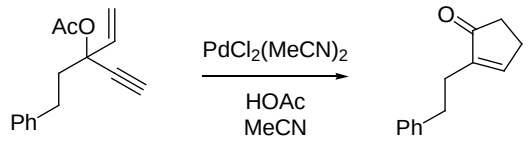

159 **160**

2-phenethylcyclopent-2-enone (160). To a solution of **159** (4.03 g, 17.7 mmol, 1.0 equiv.) in MeCN (24 mL) was added $PdCl_2(MeCN)_2$ (456 mg, 1.76 mmol, 0.1 equiv.) and HOAc (1.05 mL, 18.3 mmol, 1.0 equiv.). The reaction mixture was heated to 80 °C for 4 h then filtered through silica gel. The solvent was removed in vacuo. Flash chromatography (SiO_2, 10% EtOAc in hexanes elution) afforded **160** (2.27 g, 12.2 mmol, 69%) as a colorless oil R_f (30% EtOAc in hexanes elution) = 0.50; HRMS (ESI) *m*/*z* calcd for $C_{13}H_{14}O$ (M^+) 187.1117, found 187.1119; ^{1}H NMR (400 MHz, $CDCl_3$) δ: 7.24 – 7.29 (m, 3H), 7.17 – 7.20 (m, 3H), 2.80 (t, *J* = 7.6 Hz, 2H), 2.49 – 2.55 (m, 4H), 2.40 (t, *J* = 4.4 Hz, 2H); ^{13}C NMR (100 MHz, $CDCl_3$) δ: 210.2, 158.6, 145.5, 141.6, 128.6, 128.5, 126.2, 64.4, 34.9, 34.0, 26.7; IR (film, cm^{-1}) 2913, 1699, 1623, 1457, 1261.

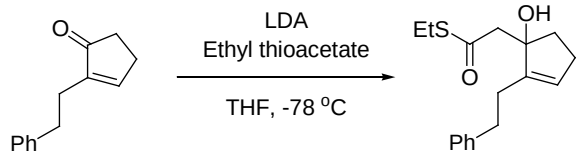

160 **189**

S-Ethyl 2-(1-hydroxy-2-phenethylcyclopent-2-enyl)ethanethioate (189). To a solution of diisopropyl amine (0.11 mL, 0.805 mmol, 1.5 equiv.) in THF (2.00 mL) at 0 °C was added *n*-BuLi (0.32 mL, 0.805 mmol, 2.5 M in hexanes, 1.5 equiv.). The solution was stirred for 5 min then cooled to -78 °C. Ethyl thioacetate (86 µL, 0.805 mmol, 1.5 equiv.)

was added, followed by **160** (100 mg, 0.537 mmol, 1.0 equiv.). The reaction mixture was stirred for 1 h then quenched by pouring into ice-cold 2% HCl (20 mL) and extracted with EtOAc (3 x 50 mL). The combined organic layers were dried (Na_2SO_4), and the solvent was removed in vacuo. Flash chromatography (SiO_2, 10% EtOAc in hexanes elution) afforded **189** (142 mg, 0.521 mmol, 97%) as a colorless oil R_f (10% EtOAc in hexanes elution) = 0.10; HRMS (ESI) *m*/*z* calcd for $C_{17}H_{22}O_2SNa$ ($M+Na^+$) 313.1233, found 313.1231; ^1H NMR (400 MHz, $CDCl_3$) δ: 7.26 – 7.30 (m, 2H), 7.17 – 7.22 (m, 3H), 5.61 (m, 1H), 3.48 (s, 1H), 2.76 – 2.92 (m, 4H), 2.91 (d, *J* = 14.8 Hz, 1H), 2.67 (d, *J* = 15.2 Hz, 1H), 2.37 – 2.48 (m, 2H), 2.15 – 2.29 (m, 3H), 1.93 – 2.01 (m, 1H), 1.26 (t, *J* = 7.6 Hz, 3H); ^{13}C NMR (100 MHz, $CDCl_3$) δ: 200.7, 146.6, 142.5, 128.66, 128.65, 127.5, 126.2, 85.2, 51.5, 38.7, 34.5, 29.3, 28.4, 23.9, 14.9; IR (film, cm^{-1}) 3299, 2928, 1646, 1277.

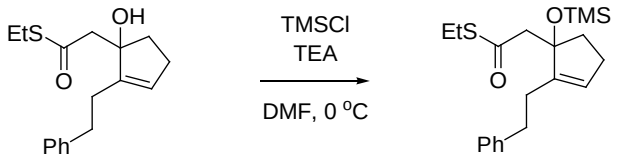

189 **190**

S-Ethyl 2-(1-trimethylsiloxy-2-phenethylcyclopent-2-enyl)ethanethioate (190). To a solution of **189** (408 mg, 1.40 mmol, 1.0 equiv.) in DMF (1.00 mL) at 0 °C was added TEA (0.98 mL, 7.02 mmol, 5.0 equiv.) and TMSCl (0.71 mL, 5.62 mmol, 4.0 equiv.). The reaction mixture was allowed to slowly warm up to room temperature and stirred for 15 h. The reaction was quenched with sat aq $NaHCO_3$ (50 mL) and extracted with EtOAc (3 x 50 mL). The combined organic layers were dried (Na_2SO_4), and the solvent

was removed in vacuo. Flash chromatography (SiO_2, 2% EtOAc in hexanes elution) afforded **190** (500 mg, 1.38 mmol, 98%) as a colorless oil R_f (10% EtOAc in hexanes elution) = 0.50; HRMS (ESI) *m*/*z* calcd for $C_{20}H_{20}O_2SSi$ (M^+) 362.1730, found 362.1718; ^{1}H NMR (400 MHz, $CDCl_3$) δ: 7.27 – 7.32 (m, 2H), 7.20 – 7.27 (m, 3H), 5.53 – 5.54 (m, 1H), 2.90 (d, *J* = 13.2 Hz, 1H), 2.84 (q, *J* = 7.6 Hz, 2H), 2.64 (d, *J* = 13.2 Hz, 1H), 2.47 – 2.53 (m, 1H), 2.30 – 2.37 (m, 3H), 2.17 – 2.24 (m, 2H), 1.98 – 2.05 (m, 2H), 1.22 (t, *J* = 7.6 Hz, 3H), 0.09 (s, 9H); ^{13}C NMR (100 MHz, $CDCl_3$) δ: 197.1, 147.6, 142.8, 128.70, 128.67, 126.2, 126.1, 87.6, 54.1, 37.4, 34.4, 29.7, 28.5, 23.8, 15.1, 2.2; IR (film, cm^{-1}) 2928, 1684, 1654, 1450, 1034.

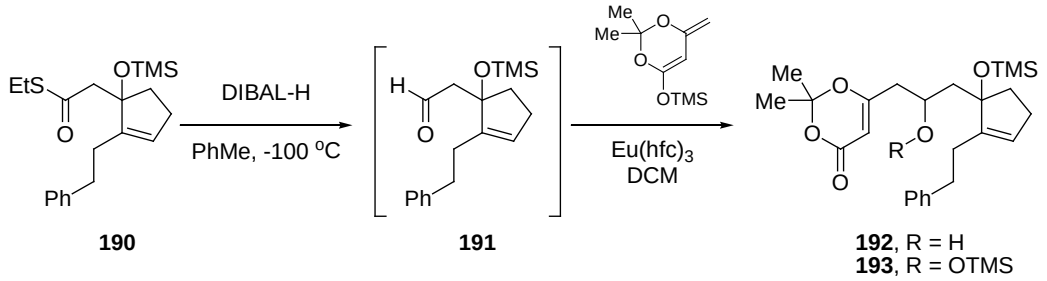

190 **191** **192**, R = H **193**, R = OTMS

Alcohol 192. To a solution of **190** (120 mg, 0.331 mmol, 1.0 equiv.) in PhMe (30 mL) at -100 °C was added DIBAL-H (1.32 mL, 1.32 mmol, 1.0 M solution in PhMe, 4.0 equiv.). The solution was stirred for 30 min, then quenched by dropwise addition of 3:1 MeOH:H_2O buffered at pH 7.0 (1.00 mL) then sat aq Rochelle's salt (50 mL). The reaction mixture was stirred vigorously for 1 h then extracted with EtOAc (3 x 100 mL). The combined organic layers were dried (Na_2SO_4), and the solvent was removed in vacuo. The resulting solution was diluted with DCM (2.00 mL) and cooled to 0 °C and stirred for 5 min. 2,2-Dimethyl-6-methylene-6H-1,3-dioxin-4-yloxy-trimethylsilane **134**

(106 mg, 0.496 mmol, 1.5 equiv.) was added and stirred for 15 h. The solvent was removed in vacuo. Flash chromatography (SiO_2, 10% EtOAc in hexanes elution) afforded **192** (34 mg, 0.0761 mmol, 23% over 2 steps) as a single diastereomer and the corresponding di-silylated product **193** (79 mg, 0.152 mmol, 46% over 2 steps) as a single diastereomer. R_f (20% EtOAc in hexanes elution) = 0.15; HRMS (ESI) *m*/*z* calcd for $C_{22}H_{26}O_5Na$ ($M+Na^+$) 393.1678, found 393.1676; ^1H NMR (400 MHz, $CDCl_3$) δ: 7.26 – 7.38 (m, 2H), 7.20 – 7.25 (m, 3H), 5.59 – 5.61 (m, 1H), 5.37 (s, 1H), 4.18 – 4.23 (m, 1H), 3.70 – 3.80 (s, 1H), 2.76 – 2.87 (m, 2H), 2.22 – 2.47 (m, 6H), 2.10 – 2.16 (m, 2H), 2.19 – 2.00 (m, 2H), 1.71 (s, 3H), 1.70 (s, 3H), 0.12 (s, 9H); ^{13}C NMR (100 MHz, $CDCl_3$) δ: 169.5, 148.9, 142.4, 128.8, 128.6, 126.3, 126.2, 106.8, 95.4, 89.5, 67.1, 47.3, 42.7, 40.9, 34.8, 29.5, 29.2, 25.7, 25.2, 25.0, 2.2; IR (film, cm^{-1}) 2948, 2358, 1720, 1430. Di-silylated product **193**: R_f (20% EtOAc in hexanes elution) = 0.51; HRMS (ESI) *m*/*z* calcd for $C_{28}H_{44}O_5Si_2Na$ ($M+Na^+$) 539.2625, found 539.2627; ^1H NMR (400 MHz, $CDCl_3$) δ: 7.26 – 7.32 (m, 2H), 7.19 – 7.25 (m, 3H), 5.52 (m, 1H), 5.28 (s, 1H), 4.19 – 4.25 (m, 1H), 2.76 – 2.830 (m, 2H), 2.69 (dd, *J* = 4.4, 14.0 Hz, 1H), 2.38 – 2.41 (m, 1H), 2.22 – 2.33 (m, 5H), 1.88 – 1.99 (m, 2H), 1.69 (s, 3H), 1.67 (s, 3H), 1.43 (dd, *J* = 4.4, 13.6 Hz, 1H), 0.12 (s, 9H), 0.07 (s, 9H); ^{13}C NMR (100 MHz, $CDCl_3$) δ: 170.3, 148.8, 142.6, 128.8, 128.6, 126.2, 125.5, 106.6, 95.3, 87.9, 67.9, 47.4, 44.0, 37.2, 34.5, 29.6, 28.6, 26.0, 24.9 (2x), 2.1, 0.8; IR (film, cm^{-1}) 2948, 2845, 2357, 1728, 1638, 1433, 1375, 1249.

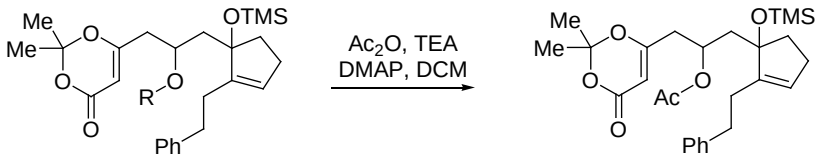

192, R = H
193, R = OTMS

194

Acetate 194. To a solution of **192** (34 mg, 0.0765 mmol, 1.0 equiv.) in DCM (3.00 mL) at to 0˚C was added DMAP (cat.), TEA (53 µL, 0.383 mmol, 5.0 equiv.) then acetic anhydride (29 µL, 0.306 mmol, 4.0 equiv.). The solution was stirred for 15 h then diluted with DCM (30 mL) and extracted with $NaHCO_3$ (3 x 50 mL). The combined organic layers were dried (Na_2SO_4), and the solvent was removed in vacuo. Flash chromatography (SiO_2, 30% EtOAc in hexanes elution) afforded **194** (26 mg, 0.536 mmol, 70%) as a colorless oil. The acetate **194** was accessed from the di-silylated **193** using the following procedure: To a solution of **193** (74 mg, 0.143 mmol, 1.0 equiv) in DCM (3.00 mL) at 0˚C was added DMAP (cat.), TEA (0.24 mL) and Ac_2O (0.16 mL). The solution was heated to reflux for 15 h then quenched with sat aq $NaHCO_3$ (50 mL) and extracted with DCM (3 x 50 mL). The combined organic layers were dried (Na_2SO_4), and the solvent was removed in vacuo. Flash chromatography (SiO_2, 30% EtOAc in hexanes elution) afforded **194** (49 mg, 0.101 mmol, 70%) as a colorless oil. R_f (20% EtOAc in hexanes elution) = 0.20; HRMS (ESI) *m*/*z* calcd for $C_{27}H_{38}O_6Na$ ($M+Na^+$) 509.2335, found 509.2333; ^1H NMR (400 MHz, $CDCl_3$) δ: 7.26 – 7.31 (m, 2H), 7.18 – 7.22 (m, 3H), 5.55 – 5.56 (m, 1H), 5.23 (s, 1H), 5.10 – 5.21 (m, 1H), 2.82 (t, *J* = 8.0 Hz, 2H), 2.56 (dd, *J* = 4.8, 11.2 Hz, 1H), 2.25 – 2.47 (m, 4H), 2.12 – 2.23 (m, 3H), 2.01 – 2.09 (m, 2H), 2.01 (s, 3H), 1.63 (s, 3H), 1.61 (s, 3H), 0.09 (s, 9H); ^{13}C NMR (100 MHz, $CDCl_3$) δ: 170.2, 168.3, 161.3, 148.0, 142.6, 128.8, 128.6, 126.3, 126.2,

107.0, 95.6, 88.0, 68.6, 44.4, 39.9, 38.3, 34.5, 29.6, 28.7, 25.9, 24.6, 21.6, 2.3; IR (film, cm^{-1}) 2942, 2845, 1728, 1626, 1389, 1241.

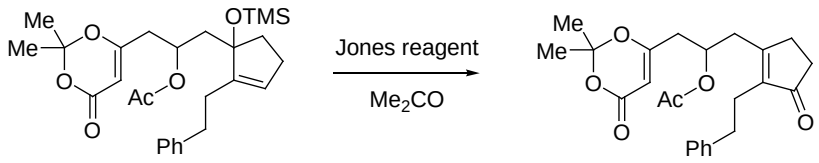

194 **144**

Cyclopentenone 144. To a solution of **194** (26 mg, 0.0535 mmol, 1.0 equiv.) in acetone (5.0 mL) at 0˚C was added Jones reagent (0.10 mL, 0.267 mmol, 2.67 M in water, 5.0 equiv.). The solution was stirred for 5 min, then quenched with $NaHCO_3$ and extracted with EtOAc (3 x 20 mL). The combined organic layers were dried (Na_2SO_4), and the solvent was removed in vacuo. Flash chromatography (SiO_2, 30% EtOAc in hexanes elution) afforded **144** (22 mg, 0.0535 mmol, quant.) as a colorless oil. R_f (50% EtOAc in hexanes elution) = 0.22; HRMS (ESI) *m/z* calcd for $C_{24}H_{28}O_6Na$ ($M+Na^+$) 435.1784, found 435.1783; ^1H NMR (400 MHz, $CDCl_3$) δ: 7.25 – 7.29 (m, 2H), 7.12 – 7.21 (m, 3H), 5.24 (s, 1H), 5.22 – 5.28 (m, 1H), 2.71 – 2.79 (m, 1H), 2.58 – 2.69 (m, 2H), 2.44 – 2.56 (m, 3H), 2.31 – 2.44 (m, 5H), 2.21 – 2.27 (m, 1H), 1.98 (s, 3H), 1.67 (s, 3H), 1.63 (s, 3H); ^{13}C NMR (100 MHz, $CDCl_3$) δ: 209.5, 170.1, 167.8, 167.0, 160.9, 142.2, 141.7, 128.9, 128.7, 126.5, 107.2, 96.0, 68.1, 38.8, 35.9, 34.7, 34.5, 29.7, 26.0, 25.9, 24.7, 21.2; IR (film, cm^{-1}) 2928, 2846, 1722, 1594, 1268, 1145.

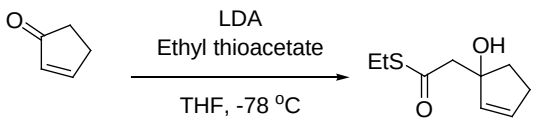

195 **196**

Ethyl 2-(1-hydroxycyclopent-2-enyl)ethanethioate (196). To a solution of diisopropyl amine (1.26 mL, 8.95 mmol, 1.5 equiv.) in THF (15 mL) at 0 °C was added *n*-BuLi (3.58 mL, 8.95 mmol, 2.5 M in hexanes, 1.5 equiv.). The solution was stirred for 5 min then cooled to -78 °C. Ethyl thioacetate (0.95 mL, 8.95 mmol, 1.5 equiv.) was added, followed by **195** (0.50 mL, 5.97 mmol, 1.0 equiv.). The reaction mixture was stirred for 1 h then quenched by pouring into ice-cold 2% HCl (20 mL) and extracted with EtOAc (3 x 50 mL). The combined organic layers were dried (Na_2SO_4), and the solvent was removed in vacuo. Flash chromatography (SiO_2, 10% EtOAc in hexanes elution) afforded **196** (1.11 g, 5.97 mmol, quant.) as a colorless oil R_f (20% EtOAc in hexanes elution) = 0.32; HRMS (ESI) *m*/*z* calcd for $C_9H_{14}O_2SNa$ ($M+Na^+$) 209.0612, found 209.0614; ^1H NMR (400 MHz, $CDCl_3$) δ: 5.91 – 5.94 (m, 1H), 5.72 – 5.75 (m, 1H), 3.42 (s, 1H), 2.92 (q, *J* = 7.2 Hz, 2H), 2.90 (d, *J* = 12.8 Hz, 1H), 2.89 (d, *J* = 12.8 Hz, 1H), 2.48 – 2.68 (m, 1H), 2.18 – 2.36 (m, 1H), 1.86 – 2.06 (m, 2H), 1.27 (t, *J* = 7.2 Hz, 3H); ^{13}C NMR (100 MHz, $CDCl_3$) δ: 199.9, 135.0, 134.4, 84.3, 53.5, 37.8, 31.1, 23.6, 14.9; IR (film, cm^{-1}) 3300, 2920, 1640.

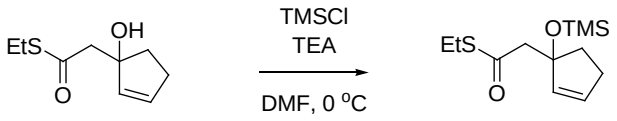

196 **197**

Ethyl 2-(1-trimethylsilyloxycyclopent-2-enyl)ethanethioate (197). To a solution of **196** (500 mg, 2.68 mmol, 1.0 equiv.) in DMF (3.00 mL) at 0 °C was added TEA (1.49 mL, 10.7 mmol, 4.0 equiv.) and TMSCl (1.02 mL, 8.05 mmol, 3.0 equiv.). The reaction mixture was allowed to slowly warm up to room temperature and stirred for 15 h. The reaction was quenched with sat aq $NaHCO_3$ (50 mL) and extracted with EtOAc (3 x 50 mL). The combined organic layers were dried (Na_2SO_4), and the solvent was removed in vacuo. Flash chromatography (SiO_2, 5% EtOAc in hexanes elution) afforded **197** (1.23 g, 2.15 mmol, 80%) as a colorless oil R_f (20% EtOAc in hexanes elution) = 0.67; HRMS (ESI) *m*/*z* calcd for $C_{12}H_{22}O_2SSi$ (M^+) 258.1110, found 258.1115; ^{1}H NMR (400 MHz, $CDCl_3$) δ: 5.88 (m, 2H), 2.87 (d, *J* = 13.2 Hz, 1H), 2.85 (q, *J* = 7.6 Hz, 2H), 2.77 (d, *J* = 13.2 Hz, 1H), 2.41 – 2.54 (m, 1H), 2.17 – 2.31 (m, 2H), 1.92 – 1.98 (m, 1H), 1.24 (t, *J* = 7.6 Hz, 3H), 0.08 (s, 9H); ^{13}C NMR (100 MHz, $CDCl_3$) δ: 197.1, 136.0, 134.0, 86.6, 56.1, 38.7, 31.0, 23.7, 15.0, 2.2; IR (film, cm^{-1}) 2930, 1680, 1652.

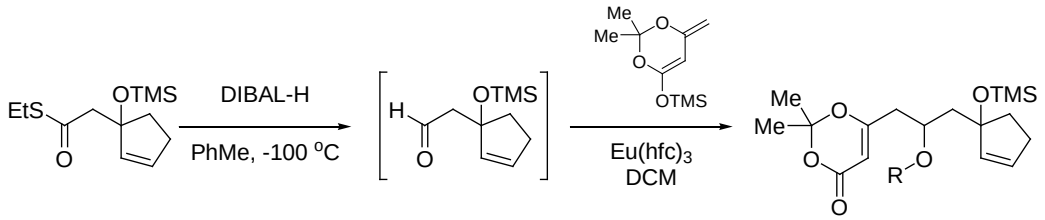

197 **198** **199**, R = H **200**, R = OTMS

Alcohol 199. To a solution of **197** (583 mg, 2.26 mmol, 1.0 equiv.) in PhMe (40 mL) at -100 °C was added DIBAL-H (6.02 mL, 9.02 mmol, 1.5 M solution in PhMe, 4.0 equiv.). The solution was stirred for 30 min, then quenched by dropwise addition of 3:1 MeOH:H_2O buffered at pH 7.0 (1.00 mL) then sat aq Rochelle's salt (50 mL). The

reaction mixture was stirred vigorously for 1 h then extracted with EtOAc (3 x 100 mL). The combined organic layers were dried (Na_2SO_4), and the solvent was removed in vacuo. The resulting solution was diluted with DCM (3.00 mL) and cooled to 0 °C and stirred for 5 min. 2,2-Dimethyl-6-methylene-6H-1,3-dioxin-4-yloxy-trimethylsilane **134** (629 mg, 2.93 mmol, 1.3 equiv.) was added and stirred for 15 h. The solvent was removed in vacuo. Flash chromatography (SiO_2, 10% EtOAc in hexanes elution) afforded **199** (165 mg, 0. 474 mmol, 21% over 2 steps) as a 1.5:1.0 mixture of diastereomers and the corresponding di-silylated product **200** (309 mg, 0.744 mmol, 33% over 2 steps) as a 1.5:1.0 mixture of diastereomers. R_f (20% EtOAc in hexanes elution) = 0.10; HRMS (ESI) *m/z* calcd for $C_{17}H_{28}O_5SiNa$ ($M+Na^+$) 363.1604, found 363.1606; ^1H NMR (400 MHz, $CDCl_3$) δ: 5.88 – 5.94 (m, 1H), 5.68 – 5.71 (m, 1H), 5.41, 5.39 (s, 1H), 4.79, 4.77 (s, 1H), 4.19 – 4.29, 4.37 – 4.42 (m, 1H), 2.42 – 2.57 (m, 2H), 2.24 – 2.35 (m, 2H), 1.87 – 2.17 (m, 4H), 1.72 (s, 3H), 1.70 (s, 3H), 0.11, 0.09 (s, 9H); ^{13}C NMR (100 MHz, $CDCl_3$) δ: 169.6 (2x), 161.7 (2x), 136.7, 135.5, 134.5, 134.1, 106.9 (2x), 95.5, 95.4, 90.2 (2x), 67.2 (2x), 48.7, 47.2, 42.5, 39.8, 36.7 (2x), 31.2, 31.0, 25.7 (2x), 25.2 (2x), 2.21 (2x); IR (film, cm^{-1}) 2948, 2350, 1725. Di-silylated product **200**: R_f (20% EtOAc in hexanes elution) = 0.40; HRMS (ESI) *m/z* calcd for $C_{20}H_{36}O_5Si_2Na$ ($M+Na^+$) 435.1999, found 435.1997; ^1H NMR (400 MHz, $CDCl_3$) δ: 5.82 – 5.86, 5.63 – 5.65 (m, 2H), 5.30, 5.29 (s, 1H), 4.13 – 4.19, 4.24 – 4.30 (m, 1H), 2.55 – 2.75 (m, 2H), 2.39 – 2.48 (m, 1H), 2.22 – 2.35 (m, 2H), 2.10 – 2.17 (m, 1H), 1.79 – 1.97 (m, 2H), 1.70 (s, 3H), 1.69 (s, 3H), 0.11, 0.09, 0.07, 0.05 (s, 18H); ^{13}C NMR (100 MHz, $CDCl_3$) δ: 170.22, 170.17, 161.2 (2x), 137.6, 136.6, 133.4, 133.2, 106.6 (2x), 95.4, 95.3, 87.2, 86.9, 67.7, 67.4, 50.6,

49.6, 43.7, 43.5, 40.0, 38.0, 31.3, 30.9, 25.94, 25.86, 25.0, 24.9, 2.4, 2.3, 0.70, 0.67; IR (film, cm^{-1}) 2940, 2840, 1730, 1633.

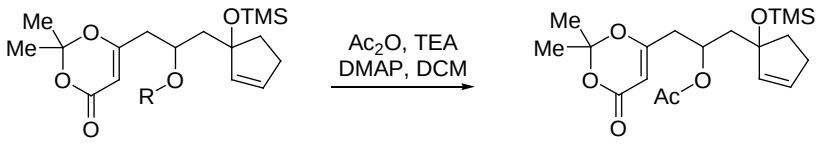

199, R = H
200, R = OTMS

201

Acetate 201. To a solution of **199** (165 mg, 0.485 mmol, 1.0 equiv.) in DCM (3.00 mL) at to 0˚C was added DMAP (cat.), TEA (0.41 mL, 2.91 mmol, 6.0 equiv.) then acetic anhydride (0.18 mL, 1.94 mmol, 4.0 equiv.). The solution was stirred for 15 h then diluted with DCM (30 mL) and extracted with $NaHCO_3$ (3 x 50 mL). The combined organic layers were dried (Na_2SO_4), and the solvent was removed in vacuo. Flash chromatography (SiO_2, 20% EtOAc in hexanes elution) afforded **201** (140 mg, 0.366 mmol, 76%) as a colorless oil. The acetate **201** was accessed from the di-silylated **200** using the following procedure: To a solution of **200** (309 mg, 0.749 mmol, 1.0 equiv) in DCM (4.00 mL) at 0 ˚C was added DMAP (cat.), and AcCl (0.10 mL). The solution was stirred for 15 h then quenched with sat aq $NaHCO_3$ (50 mL) and extracted with DCM (3 x 50 mL). The combined organic layers were dried (Na_2SO_4), and the solvent was removed in vacuo. Flash chromatography (SiO_2, 20% EtOAc in hexanes elution) afforded **201** (200 mg, 0.523 mmol, 70%) as a colorless oil. R_f (20% EtOAc in hexanes elution) = 0.29; HRMS (ESI) *m/z* calcd for $C_{19}H_{30}O_6SiNa$ ($M+Na^+$) 405.1709, found 405.1706; ^1H NMR (400 MHz, $CDCl_3$) δ: 5.75 – 5.84, 5.60 – 5.62 (m, 2H), 5.22 – 5.27 (m, 1H), 5.21 (s, 1H), 2.63 – 2.71 (m, 1H), 2.36 – 2.49 (m, 2H), 2.09 – 2.27 (m, 1H), 1.97 (s, 3H), 1.74 – 1.96 (m, 4H), 1.64 (s, 3H), 1.61 (s, 3H), 0.03, 0.02 (s, 9H) ; ^{13}C NMR

(100 MHz, $CDCl_3$) δ: 170.2 (2x), 168.5 (2x), 161.3 (2x), 136.9, 135.9, 133.7 (2x), 106.8 (2x), 95.4, 95.3, 86.9, 87.0, 68.8 (2x), 46.9, 46.2, 39.8, 39.7 (2x), 37.2, 31.3, 30.8, 21.5 (2x), 25.8 (2x), 24.7 (2x), 2.2 (2x); IR (film, cm^{-1}) 2940, 2847, 1726, 1620.

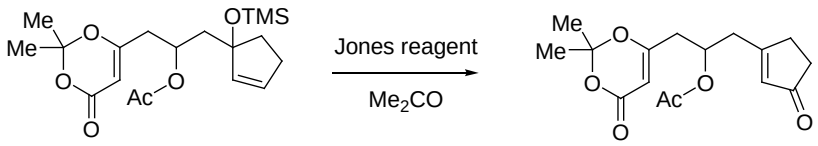

201 **202**

Cyclopentenone 202. To a solution of **201** (70 mg, 0.183 mmol, 1.0 equiv.) in acetone (3.0 mL) at 0˚C was added Jones reagent (0. 27 mL, 0.732 mmol, 2.67 M in water, 4.0 equiv.). The solution was stirred for 5 min, then quenched with $NaHCO_3$ and extracted with EtOAc (3 x 20 mL). The combined organic layers were dried (Na_2SO_4), and the solvent was removed in vacuo. Flash chromatography (SiO_2, 50% EtOAc in hexanes elution) afforded **202** (52 mg, 0.170 mmol, 93%) as a colorless oil. R_f (50% EtOAc in hexanes elution) = 0.10; HRMS (ESI) *m/z* calcd for $C_{16}H_{20}O_6Na$ ($M+Na^+$) 331.1158, found 331.1156; ^1H NMR (400 MHz, $CDCl_3$) δ: 5.97 (s, 1H), 5.30 – 5.37 (m, 1H), 5.25 (s, 1H), 2.75 – 2.81 (m, 1H), 2.60 – 2.70 (m, 2H), 2.50 – 2.56 (m, 3H), 2.37 – 2.40 (m, 2H), 1.99 (s, 3H), 1.66 (s, 3H), 1.62 (s, 3H); ^{13}C NMR (100 MHz, $CDCl_3$) δ: 209.6, 176.1, 170.2, 166.9, 160.8, 132.3, 107.1, 95.9, 67.9, 38.6, 38.1, 35.5, 32.0, 25.8, 24.7, 21.1; IR (film, cm^{-1}) 2925, 2835, 1720, 1600.

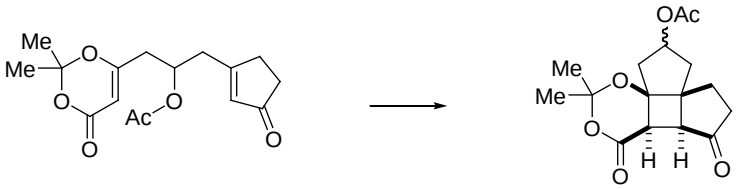

202 **203**

Cyclobutane 203. A dry, oxygen free benzene (17 mL) solution containing **202** (52 mg, 0.169 mmol, 0.01 M) in a quartz round bottom was subjected to photolysis at room temperature with a 500 watt Ace-Hanovia photochemical lamp for 3 d whereupon the solvent was removed in vacuo. Flash chromatography (SiO_2, 50% EtOAc in hexanes elution) afforded **203** (24 mg, 0.0775 mmol, 46% and 57% based on recovered starting material) as a colorless oil. R_f (50% EtOAc in hexanes elution) = 0.32; HRMS (ESI) *m*/*z* calcd for $C_{16}H_{20}O_6Na$ ($M+Na^+$) 331.1152, found 331.1156; ^1H NMR (400 MHz, $CDCl_3$) δ: 5.38 – 5.40, 5.12 – 5.20 (m, 1H), 3.48, 3.30 (d, *J* = 11.2 Hz, 1H), 2.97, 2.78 (dd, *J* = 1.6, 10.8 Hz, 1H), 2.52 – 2.71 (m, 1H), 2.28 – 2.46 (m, 3H), 2.18 – 2.28 (m, 2H), 2.09, 2.04 (s, 3H), 1.67 – 1.83 (m, 2H), 1.60 (s, 3H), 1.55 (s, 3H); ^{13}C NMR (100 MHz, $CDCl_3$) δ: 214.8, 213.7, 171.0, 170.5, 167.3, 166.6, 106.3, 106.1, 82.1, 79.7, 76.2, 76.1, 52.6, 51.5, 49.7, 48.4, 47.2, 45.2, 42.2, 40.5, 39.8, 39.7, 38.2, 38.1, 28.8 (2x), 28.6, 28.5, 25.9, 25.6, 21.7, 21.3; IR (film, cm^{-1}) 3012, 2850, 1732, 1590.

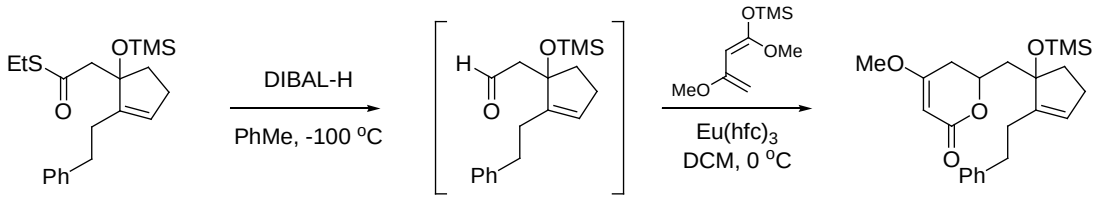

190 **191** **206**

5,6-Dihydro-6-((1-trimethylsiloxy-2-phenethylcyclopent-2-enyl)methyl)-4-methoxypyran-2-one (206). To a solution of **190** (785 mg, 2.17 mmol, 1.0 equiv.) in PhMe (40 mL) at -100 °C was added DIBAL-H (5.77 mL, 8.66 mmol, 1.5 M solution in PhMe, 4.0 equiv.). The solution was stirred for 30 min, then quenched by dropwise addition of 3:1 MeOH:H_2O buffered at pH 7.0 (1.00 mL) then sat aq Rochelle's salt (25 mL). The reaction mixture was stirred vigorously for 1 h then extracted with EtOAc (3 x 100 mL). The combined organic layers were dried (Na_2SO_4), and the solvent was removed in vacuo. The resulting solution was diluted with DCM (3.00 mL) and cooled to 0 °C whereupon $Eu(hfc)_3$ (129 mg, 0.108 mmol, 0.05 equiv) was added and stirred for 5 min. (*E*)-1,3-Dimethoxy-1-trimethylsiloxy-1,3-butadiene (468 mg, 3.25 mmol, 1.5 equiv.) was added and stirred for 15 h. The solvent was removed in vacuo. Flash chromatography (SiO_2, 20% EtOAc in hexanes elution) afforded **206** (512 mg, 1.28 mmol, 59% over 2 steps) as a mixture of diastereomers. R_f (20% EtOAc in hexanes elution) = 0.15; HRMS (ESI) *m*/*z* calcd for $C_{23}H_{32}O_4SiNa$ ($M+Na^+$) 423.1962, found 423.1960; ^{1}H NMR (400 MHz, $CDCl_3$) δ: 7.26 – 7.32 (m, 2H), 7.18 – 7.23 (m, 3H), 5.56, 5.62 (m, 1H), 5.10, 5.13 (s, 1H), 4.21 – 4.27, 4.62 – 4.68 (m, 1H), 3.72, 3.73 (s, 3H), 2.76 – 2.87 (m, 2H), 2.47 – 2.54 (m, 2H), 2.14 – 2.43 (m, 6H), 1.95 – 1.98 (m, 1H), 1.75 – 1.86 (m, 1H); ^{13}C NMR (100 MHz, $CDCl_3$) δ: 173.6, 173.2, 167.8, 167.6, 148.2, 147.1, 142.71, 142.65, 128.73, 128.71, 128.66, 128.62, 127.14 (2x), 126.23, 126.17, 90.56, 90.57, 87.9, 87.5, 74.3, 74.0, 56.3 (2x), 45.5, 45.2, 36.9, 37.0, 34.9, 34.51, 34.47, 34.4, 29.8, 29.6, 28.64, 28.61, 2.4, 2.1; IR (film, cm^{-1}) 2952, 1707, 1624, 1254, 1027.

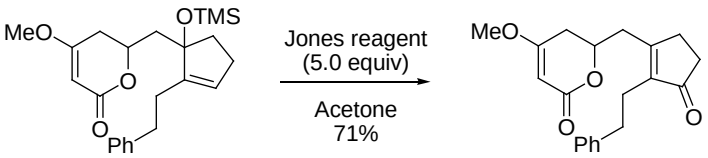

207 **147**

5,6-Dihydro-4-methoxy-6-((3-oxo-2-phenethylcyclopent-1-enyl)methyl)pyran-2-one (147). To a solution of **207** (200 mg, 0.499 mmol, 1.0 equiv.) in acetone (5 mL) at 0 °C was added Jones reagent (0.75 mL, 2.00 mmol, 2.67 M solution in water, 4.0 equiv.). The reaction mixture was stirred for 5 min then quenched with sat aq $NaHCO_3$ (20 mL) and extracted with EtOAc (3 x 50 mL). The combined organic layers were dried (Na_2SO_4), and the solvent was removed in vacuo. Flash chromatography (SiO_2, 30% EtOAc in hexanes elution) afforded **147** (150 mg, 0.460 mmol, 92%) as a colorless oil. R_f (50% EtOAc in hexanes elution) = 0.30; HRMS (ESI) *m*/*z* calcd for $C_{20}H_{22}O_4Na$ ($M+Na^+$) 349.1410, found 349.1411; ^1H NMR (400 MHz, $CDCl_3$) δ: 7.23 – 7.27 (m, 2H), 7.10 – 7.17 (m, 3H), 5.11 (s, 1H), 4.06 – 4.13 (m, 1H), 3.74 (s, 3H), 2.69 – 2.83 (m, 2H), 2.50 – 2.60 (m, 4H), 2.29 – 2.46 (m, 5H), 2.12 (dd, *J* = 4.0, 16.8 Hz, 1H); ^{13}C NMR (100 MHz, $CDCl_3$) δ: 209.7, 172.5, 168.3, 166.7, 141.9, 141.7, 129.0, 128.7, 126.4, 90.6, 73.9, 56.4, 36.0, 34.6, 34.2, 33.2, 30.4, 26.2; IR (film, cm^{-1}) 2952, 1691, 1624, 1223.

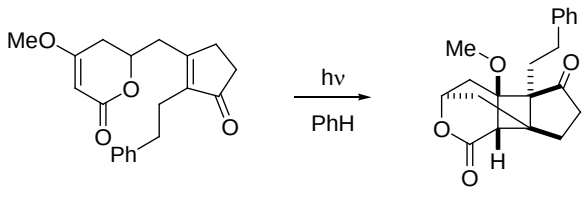

147 **207**

Cyclobutane 207. A dry, oxygen free PhH solution containing **147** (17 mg, 0.0521 mmol, 1.0 equiv.) was subjected to photolysis at 25 with a 500 watt Ace -Hanovia

photochemical lamp for 6 days to generate **207** (5 mg, 0.0153 mmol, 29%) as a white solid. R_f (50% EtOAc in hexanes elution) = 0.25; HRMS (ESI) *m*/*z* calcd for $C_{20}H_{22}O_4$ (M^+) 326.1513, found 326.1514; ^{1}H NMR (400 MHz, $CDCl_3$) δ: 7.21 – 7.31 (m, 3H), 7.09 – 7.18 (m, 2H), 4.83 (m, 1H), 3.24 (s, 3H), 2.81 (s, 1H), 2.40 – 2.72 (m, 3H), 2.01 – 2.27 (m, 3H), 1.57 – 1.99 (m, 6H); ^{13}C NMR (100 MHz, $CDCl_3$) δ: 218.2, 170.2, 141.3, 128.9, 128.3, 126.7, 78.3, 73.6, 60.6, 52.4, 48.3, 45.8, 38.0, 32.2, 32.0, 30.7, 28.6, 27.5; IR (film, cm^{-1}) 3011, 2984, 1697, 1630, 1250.

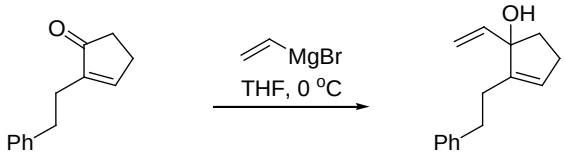

160 **168**

2-Phenethyl-1-vinylcyclopent-2-enol 168. To vinyl magnesium bromide (4.83 mL, 4.83 mmol, 1.00 M solution in THF, 3.0 equiv.) in THF (3.00 mL) at 0 °C was added cyclopentenone **160** (300 mg, 1.61 mmol, 1.0 equiv.). After 1 h, the reaction was quenched with sat aq NH_4Cl and extracted with EtOAc (3 x 100 mL). The combined organic layers were dried (Na_2SO_4), and the solvent was removed in vacuo. Flash chromatography (SiO_2, 10% EtOAc in hexanes elution) afforded **168** (276 mg, 1.29 mmol, 80%) as a colorless oil. R_f (20% EtOAc in hexanes elution) = 0.42. Crude ^{1}H-NMR spectrum is included in the supplemental section.

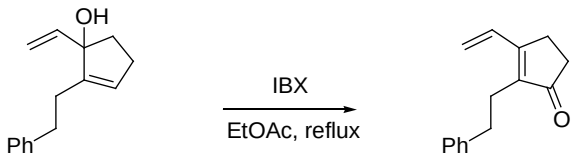

168 **169**

2-Phenethyl-3-vinylcyclopent-2-enone 169. To alcohol **168** (40 mg, 0.187 mmol, 1.0 equiv.) in EtOAc was added IBX (105 mg, 0.374 mmol, 2.0 equiv.). The reaction was heated to reflux for 1 h. The mixture was filtered through silica gel. The combined organic layers were dried (Na_2SO_4), and the solvent was removed in vacuo. Flash chromatography (SiO_2, 10% EtOAc in hexanes elution) afforded **169** (31 mg, 0.148 mmol, 79%) as a colorless oil. R_f (20% EtOAc in hexanes elution) = 0.40. Crude ^{1}H-NMR spectrum is included in the supplemental section.

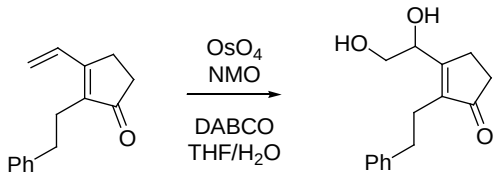

169 **170**

3-(1,2-Dihydroxyethyl)-2-phenethylcyclopent-2-enone 170. To a solution of olefin **169** (229 mg, 1.08 mmol, 1.0 equiv.) in THF/H_2O (5.00 mL, 10:1 v/v) was added OsO_4 (0.34 mL, 0.0539 mmol, 4% solution in water, 0.05 equiv.), NMO (126 mg, 1.08 mmol, 1.0 equiv.) and DABCO (cat.). The solution was stirred for 15 h and quenched with sat aq Na_2SO_3 (20 mL) and extracted with EtOAc (3 x 50 mL). The combined organic layers were dried (Na_2SO_4), and the solvent was removed in vacuo. Flash chromatography (SiO_2, 50% EtOAc in hexanes elution) afforded **170** (185 mg, 0.820

mmol, 76%) as a colorless oil. R_f (EtOAc) = 0.20. Crude ^{1}H-NMR spectrum is included in the supplemental section.

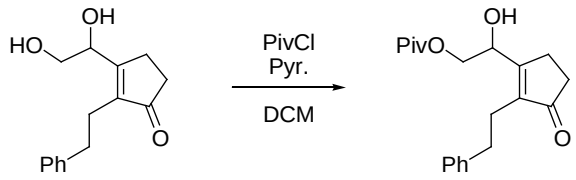

170 **209**

Pivaloate 209. To a solution of 1,2-diol **170** (85 mg, 0.345 mmol, 1.0 equiv.) in DCM (5.00 mL) was added Pyr. (0.03 mL) and PivCl (1.00 mL). The solution was stirred at rt for 15 h then quenched with sat aq $NaHCO_3$ (20 mL) and extracted with DCM (3 x 20 mL). The combined organic layers were dried (Na_2SO_4), and the solvent was removed in vacuo. Flash chromatography (SiO_2, 20% EtOAc in hexanes elution) afforded **209** (80 mg, 0.242 mmol, 70%) as a colorless oil. R_f (20% EtOAc in hexanes dilution) = 0.15. Crude ^{1}H-NMR spectrum is included in the supplemental section.

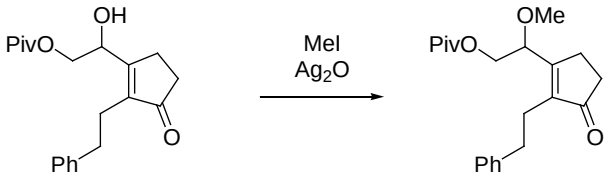

210 **171**

Methyl ether 171. To a solution of alcohol **210** (80 mg, 0.242 mmol, 1.0 equiv.) in MeI (3.00 mL) was added Ag_2O (66 mg, 0.285 mmol, 1.2 equiv.). The solution mixture was stirred at rt for 15 h then filtered through a plug of silica gel. The combined organic layers were dried (Na_2SO_4), and the solvent was removed in vacuo. Flash

chromatography (SiO_2, 10% EtOAc in hexanes elution) afforded **171** (59 mg, 0.172 mmol, 71%) as a colorless oil. R_f (20% EtOAc in hexanes dilution) = 0.25. Crude ^{1}H-NMR spectrum is included in the supplemental section.

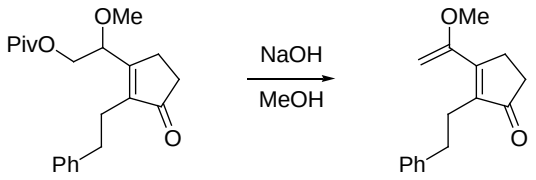

171 **173**

Dienone 173. To a solution of pivaloate **171** (10 mg, 0.0290 mmol, 1.0 equiv.) in MeOH (2.00 mL) was added NaOH (cat.). After 1 h, the reaction mixture was diluted in water (20 mL) and extracted with EtOAc (3 x 20 mL). The combined organic layers were dried (Na_2SO_4), and the solvent was removed in vacuo. Flash chromatography (SiO_2, 20% EtOAc in hexanes elution) afforded **173** (3 mg, 0.0125 mmol, 43%) as a colorless oil. R_f (20% EtOAc in hexanes dilution) = 0.30. Crude ^{1}H-NMR spectrum is included in the supplemental section.

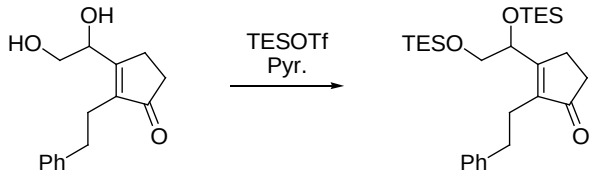

170 **174**

Silyl ether 174. To a solution of 1,2-diol **170** (15 mg, 0.0597 mmol, 1.0 equiv.) in Pyr. (1.00 mL) was added TESOTf (0.13 mL, 0.597 mmol, 10 equiv.) and DMAP (cat.). The reaction mixture was heated to 60°C for 3 h and quenched with sat aq $NaHCO_3$ and

extracted with EtOAc (3 x 10 mL). The combined organic layers were dried (Na_2SO_4), and the solvent was removed in vacuo. Flash chromatography (SiO_2, 20% EtOAc in hexanes elution) afforded **174** (28 mg, 0.0597 mmol, quant.) as a colorless oil. R_f (EtOAc) = 0.92. Crude ^{1}H-NMR spectrum is included in the supplemental section.

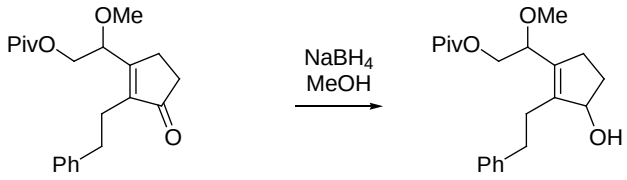

171 **(1:1 d.r.) 176**

Allylic alcohol 176. To a solution of enone **171** (36 mg, 0.105 mmol, 1.0 equiv.) in MeOH (3.00 mL) was added $NaBH_4$. The solution mixture was stirred at rt for 10 min then quenched with sat aq NH_4Cl (20 mL) and extracted with EtOAc (3 x 20 mL). The combined organic layers were dried (Na_2SO_4), and the solvent was removed in vacuo. Flash chromatography (SiO_2, 20% EtOAc in hexanes elution) afforded **176** (16 mg, 0.0470 mmol, 45%) as a colorless oil and the corresponding diastereomer **176b** (13 mg, 0.0387 mmol, 37%) as the more polar product and 5 mg of mixed diastereomers (0.0157 mmol, 15%). R_f of **176** (50% EtOAc in hexanes dilution) = 0.42. R_f of **176b** (50% EtOAc in hexanes dilution) = 0.27. Crude ^{1}H-NMR spectrum is included in the supplemental section for both **176** and **176b**.

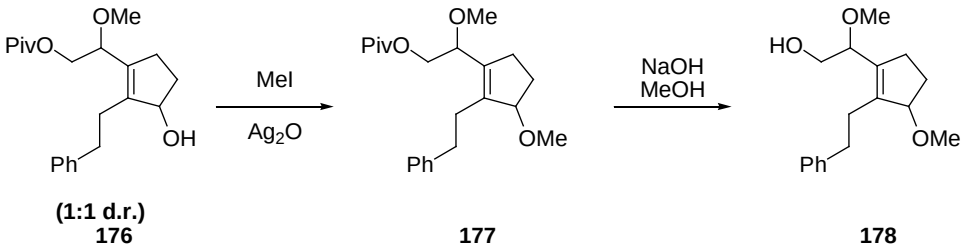

(1:1 d.r.)
176 **177** **178**

Alcohol 178. To a solution of **176** (16 mg, 0.0462 mmol, 1.0 equiv.) in MeI (3.00 mL) was added Ag_2O (24 mg, 0.104 mmol, 2.2 equiv.). The solution mixture was stirred at rt for 15 h then filtered through a plug of silica gel. The solvent was removed in vacuo and diluted with MeOH (3.00 mL). NaOH (small pellet) was added and the solution was stirred at rt for 3 h. The solution mixture was diluted with water (20 mL) and extracted with Et_2O (20 mL). The combined organic layers were dried (Na_2SO_4), and the solvent was removed in vacuo. Flash chromatography (SiO_2, 50% EtOAc in hexanes elution) afforded **178** (9 mg, 0.0323 mmol, 70% over 2 steps) as a colorless oil. R_f of **178** (50% EtOAc in hexanes dilution) = 0.27. Crude ^{1}H-NMR spectrum is included in the supplemental section.

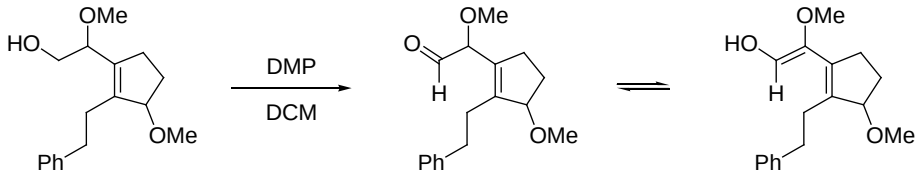

178 **179**

Aldehyde 179. To a solution of alcohol **178** (8 mg, 0.0297 mmol, 1.0 equiv.) in DCM (1.50 mL) at 0 ˚C was added DMP (19 mg, 0.0445 mmol, 1.5 equiv.). The solution was warmed up to rt slowly over the course of 15 h then filtered through a pad of silica gel. The combined organic layers were dried (Na_2SO_4), and the solvent was removed in

vacuo. Flash chromatography (SiO_2, 20% EtOAc in hexanes elution) afforded **179** (3 mg, 0.0113 mmol, 38%) as a colorless oil. R_f (50% EtOAc in hexanes elution) = 0.30. Crude ^{1}H-NMR spectrum is included in the supplemental section.

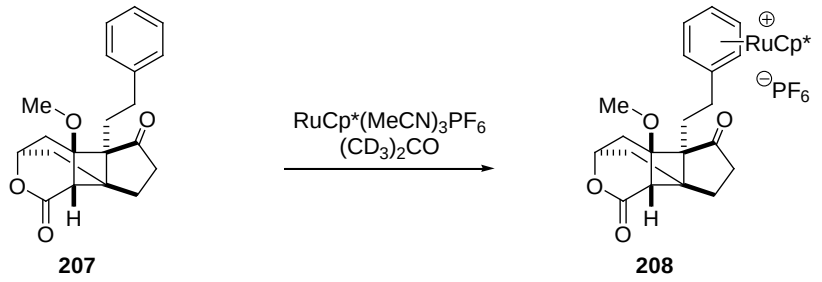

207 **208**

Cyclobutane 208. To cyclobutane **207** (7 mg, 0.0214 mmol, 1.0 equiv.) in $(CD_3)_2CO$ (1.0 mL) under an atmosphere of nitrogen was added $RuCp^*(MeCN)_3PF_6$ (10 mg, 0.0214 mmol, 1.0 equiv.). The reaction was allowed to stir for 15 h at room temperature. The solution was filtered and concentrated in vacuo. Flash chromatography (SiO_2, acetone elution) afforded **208** (15 mg, 0.0214 mmol, quant.). A ^{1}H-NMR spectra is included in the supplemental section.

3.13 Notes and References

(1) Nguyen, T. X.; Kobayashi, Y. *J. Org. Chem.* **2008**, *73*, 5536-5541.

(2) Sugimoto, Y.; Inanaga, S.; Kato, M.; Shimizu, T.; Hakoshima, T.; Isogai, A. *Phytochemistry* **1998**, *49*, 1293-1297.

(3) Babiker, H. A. A.; Sugimoto, Y.; Saisho, T.; Inanaga, S. *Phytochemistry* **1999**, *50*, 775-779.

(4) Babiker, H. A. A.; Sugimoto, Y.; Saisho, T.; Inanaga, S.; Hashimoto, M.; Isogai, A. *Biosci., Biotechnol., Biochem.* **1999**, *63*, 515-518.

(5) Sugimoto, Y.; Matsui, M.; Babiker, H. A. A. *Phytochemistry (Elsevier)* **2007**, *68*, 493-498.

(6) Goto, K.; Sudzuki, H. *Bull. Chem. Soc. Jpn.* **1929**, *4*, 220-224.

(7) Sugimoto, Y.; Babiker, H. A. A.; Saisho, T.; Furumoto, T.; Inanaga, S.; Kato, M. *J. Org. Chem.* **2001**, *66*, 3299-3302.

(8) Bednarski, M.; Danishefsky, S. *J. Am. Chem. Soc.* **1983**, *105*, 3716-3717.

(9) Winkler, J. D.; Bowen, C. M.; Liotta, F. *Chem. Rev.* **2003**, *95*, 2003-2020.

(10) Rautenstrauch, V. *J. Org. Chem.* **1984**, *49*, 950-952.

(11) Bowden, K.; Heilbron, I. M.; Jones, E. R. H.; Weedon, B. C. L. *J. Chem. Soc.* **1946**, 39.

(12) Frigerio, M.; Santagostino, M.; Sputore, S. *J. Org. Chem.* **1999**, *64*, 4537-4538.

(13) Shibuya, M.; Ito, S.; Takahashi, M.; Iwabuchi, Y. *Org. Lett.* **2004**, *6*, 4303-4306.

(14) Srinivasan, N. S. *Synthesis* **1979**, *7*, 520-521.

(15) VanRheenen, V.; Kelly, R. C.; Cha, D. Y. *Tetrahedron Lett.* **1976**, 1973-1976.

(16) Rodriguez, A.; Nomen, M.; Spur, B. W.; Godfroid, J. J.; Lee, T. H. *Tetrahedron* **2001**, *57*, 25-37.

(17) Dess, D. B.; Martin, J. C. *J. Org. Chem.* **1983**, *48*, 4155-4156.

(18) Winkler, J. D.; Hershberg, P. M. *J. Am. Chem. Soc.* **1989**, *111*, 4852-4856.

(19) Haddad, N.; Rukhman, I.; Abramovich, Z. *J. Org. Chem.* **1997**, *62*, 7629-7636.

(20) Fukuyama, T.; Lin, S.-C.; Li, L. *J. Am. Chem. Soc.* **1990**, *112*, 7050-7051.

(21) Takai, K.; Heathcock, C. H. *J. Org. Chem.* **1985**, *50*, 3247-3251.

(22) Steinmetz, B.; Schenk, W. A. *Organometallics* **1999**, *18*, 943-946.

3.14 APPENDIX ONE: Spectra Relevant to Chapter Three

^{1}H-NMR of 5-phenylpent-1-yn-3-ol 156, 400 MHz, $CDCl_3$

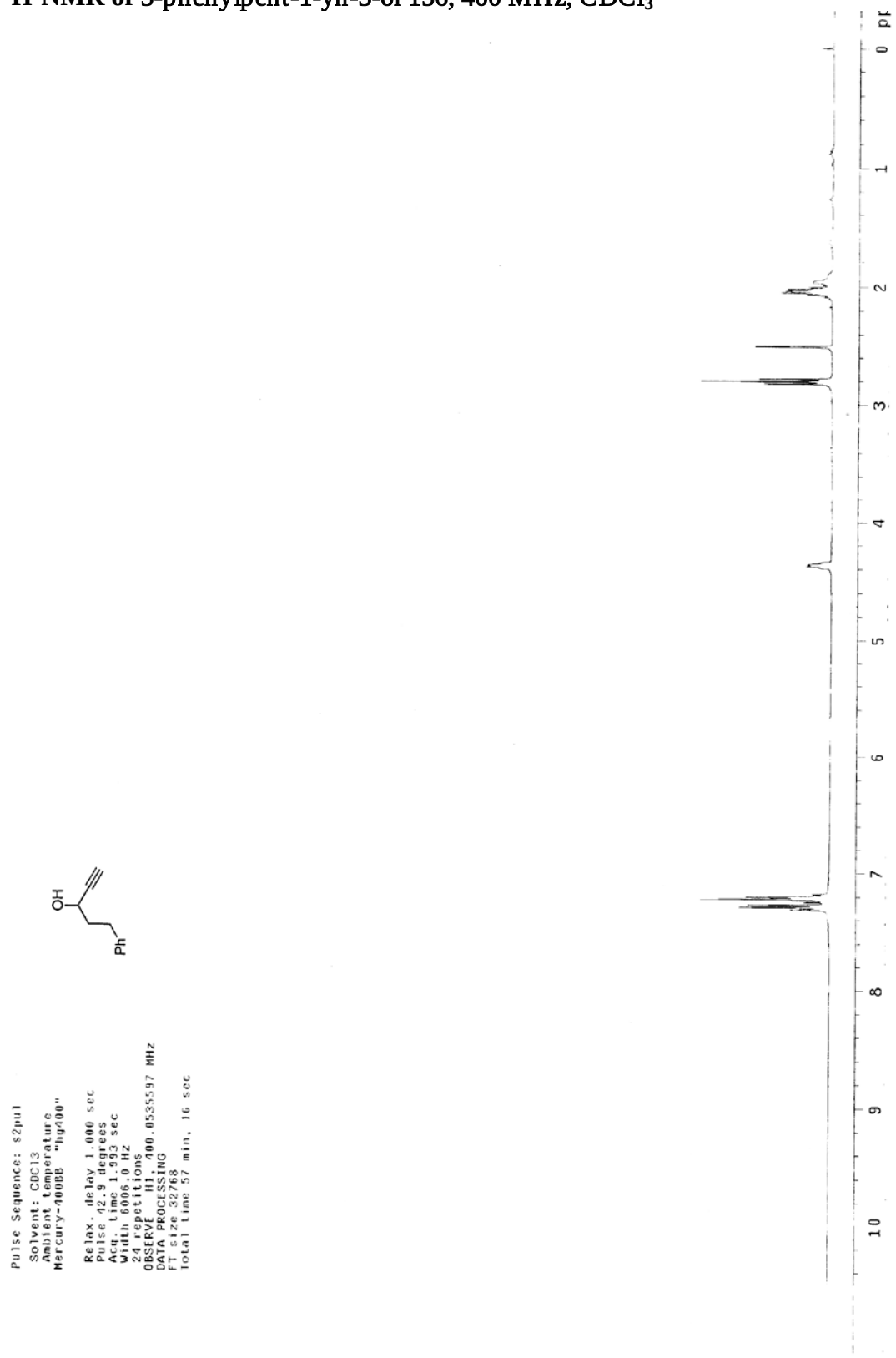

^{13}C-NMR of 5-phenylpent-1-yn-3-ol 156, 100 MHz, $CDCl_3$

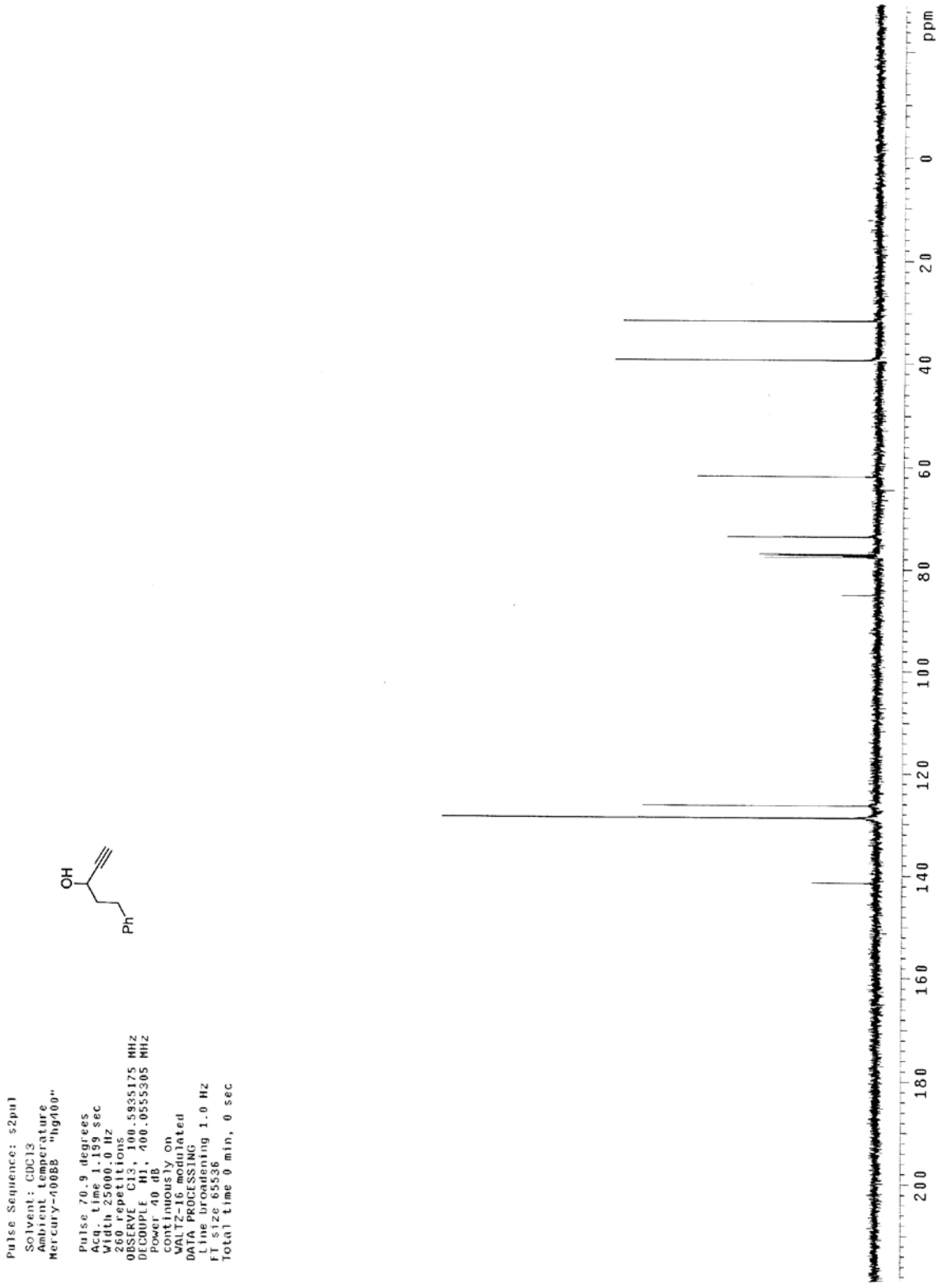

^{1}H-NMR of 5-phenylpent-1-yn-3-one 157, 400 MHz, $CDCl_3$

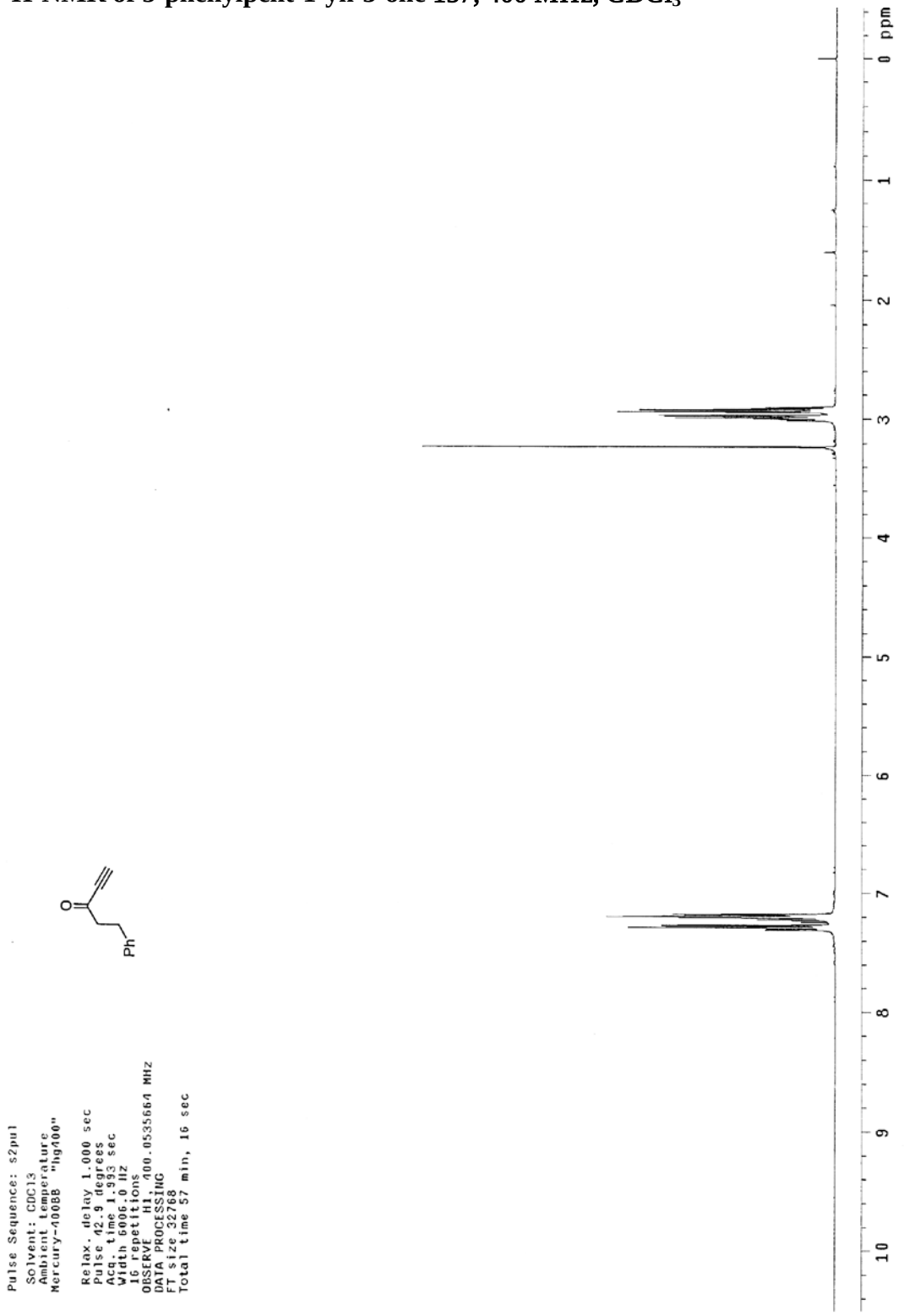

^{13}C-NMR of 5-phenylpent-1-yn-3-one 157, 100 MHz, $CDCl_3$

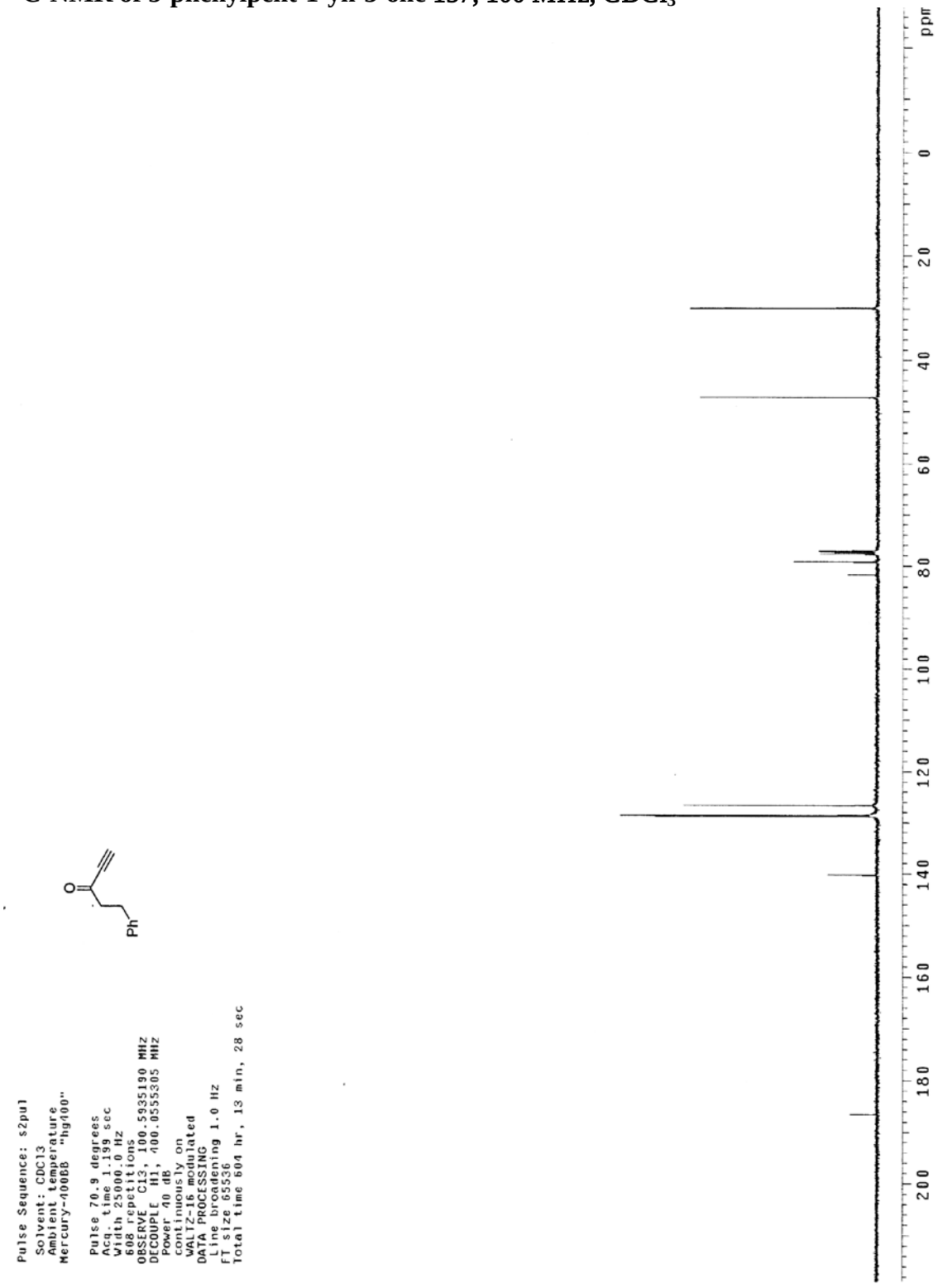

^{1}H-NMR of acetate 159, 400 MHz, $CDCl_3$

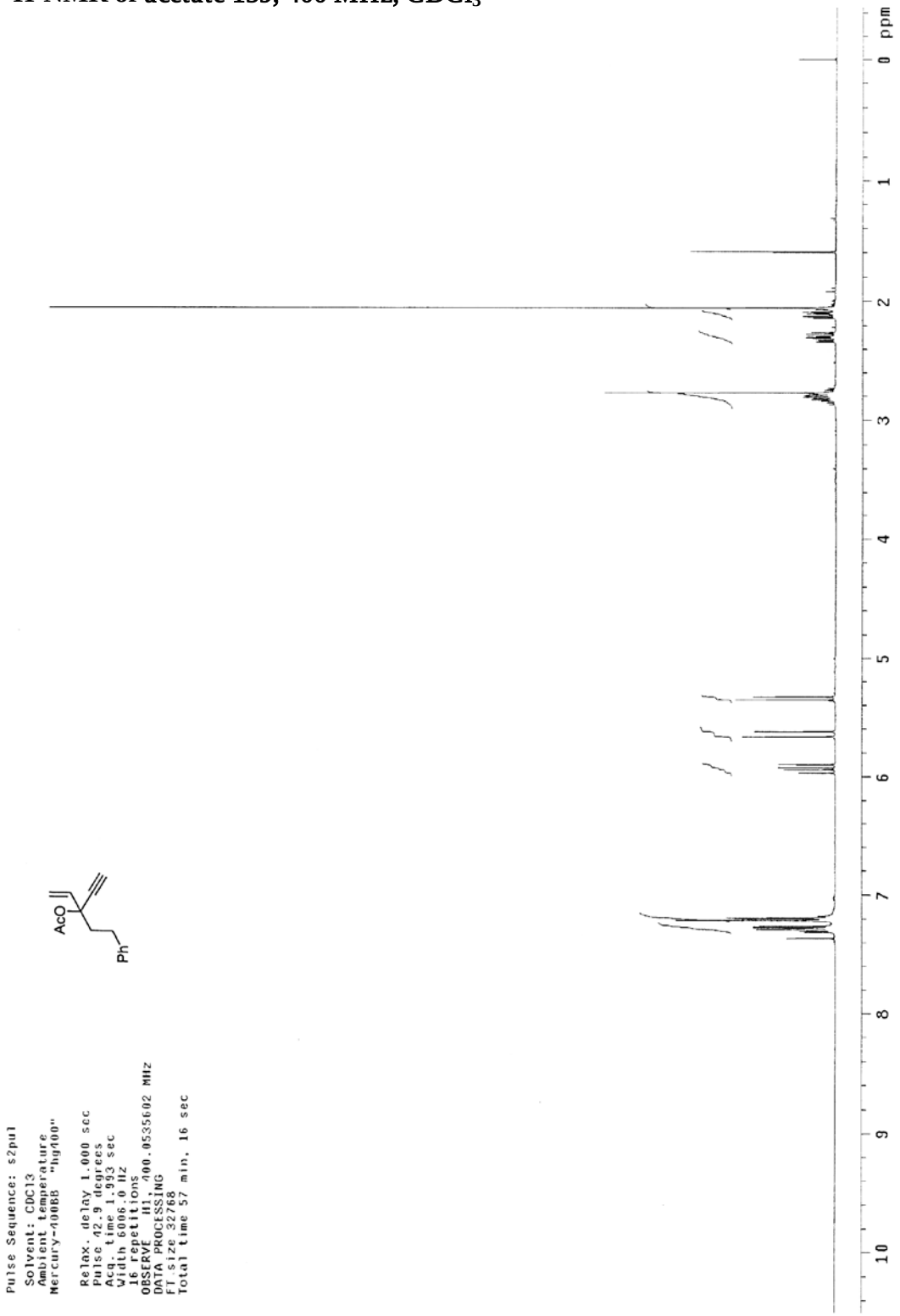

^{13}C-NMR of acetate 159, 100 MHz, $CDCl_3$

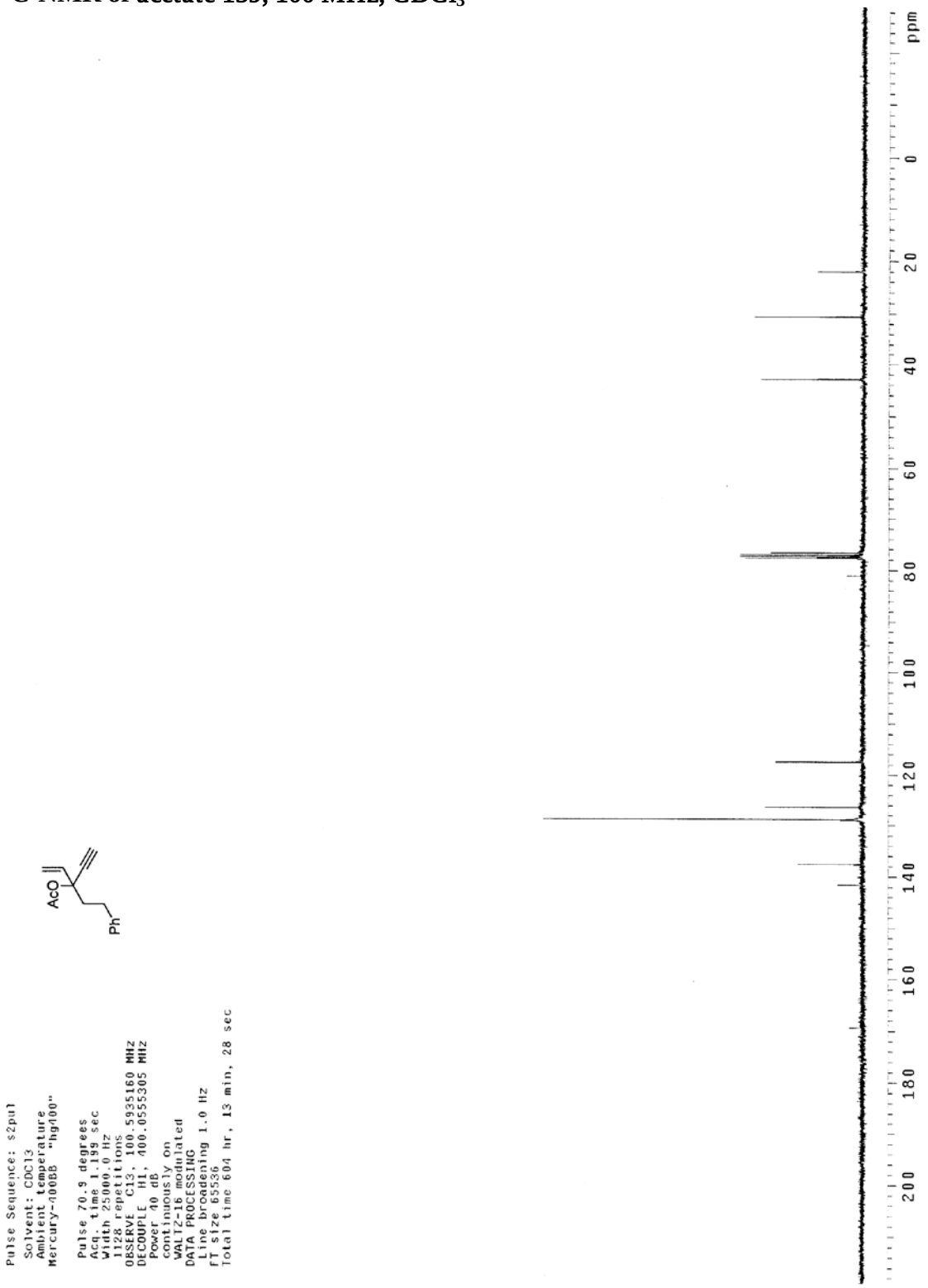

^{1}H-NMR of 2-phenethylcyclopent-2-enone 160, 400 MHz, $CDCl_3$

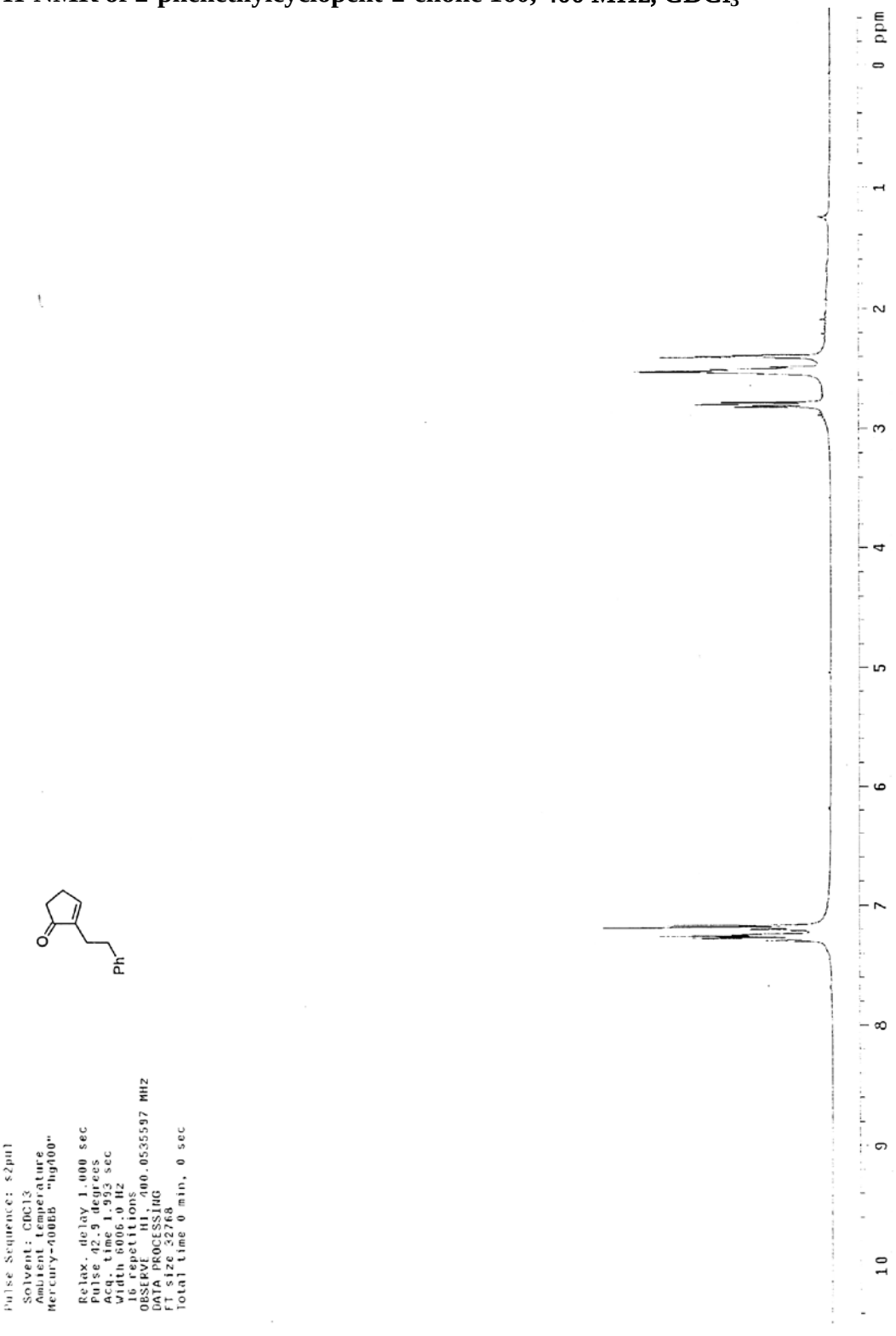

^{13}C-NMR of 2-phenethylcyclopent-2-enone 160, 100 MHz, $CDCl_3$

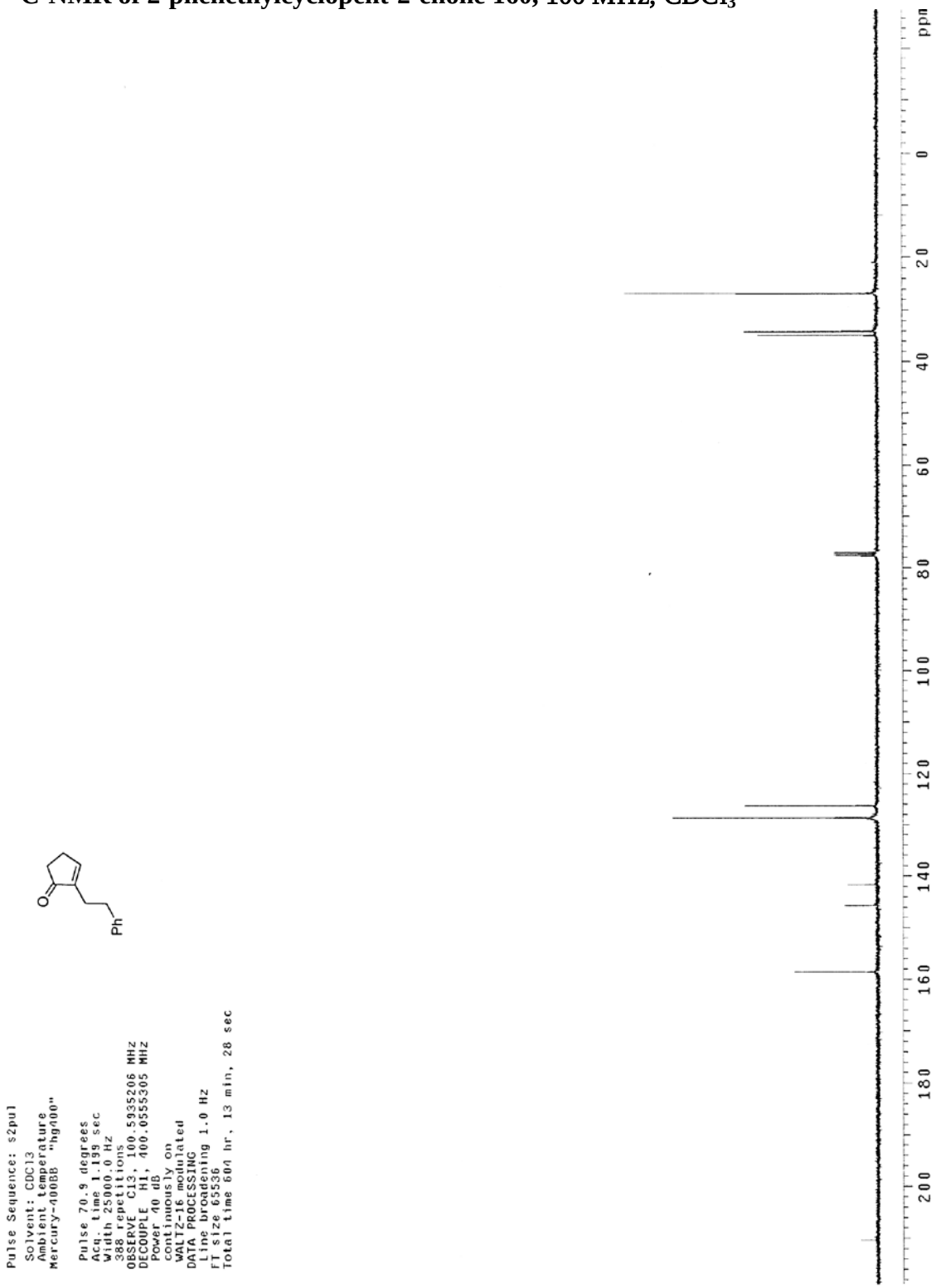

^{1}H-NMR of thioester 189, 400 MHz, $CDCl_3$

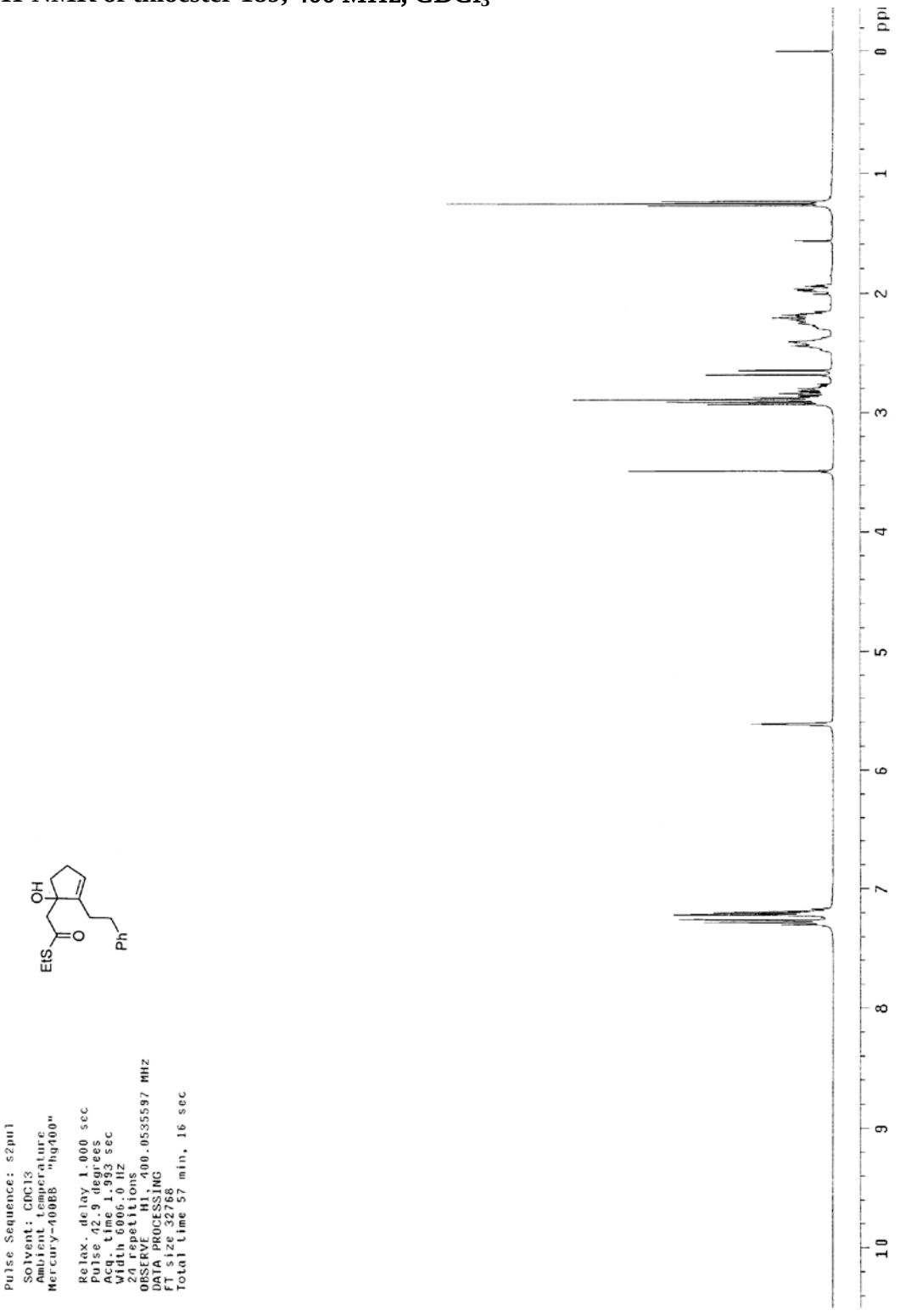

^{13}C-NMR of thioester 189, 100 MHz, $CDCl_3$

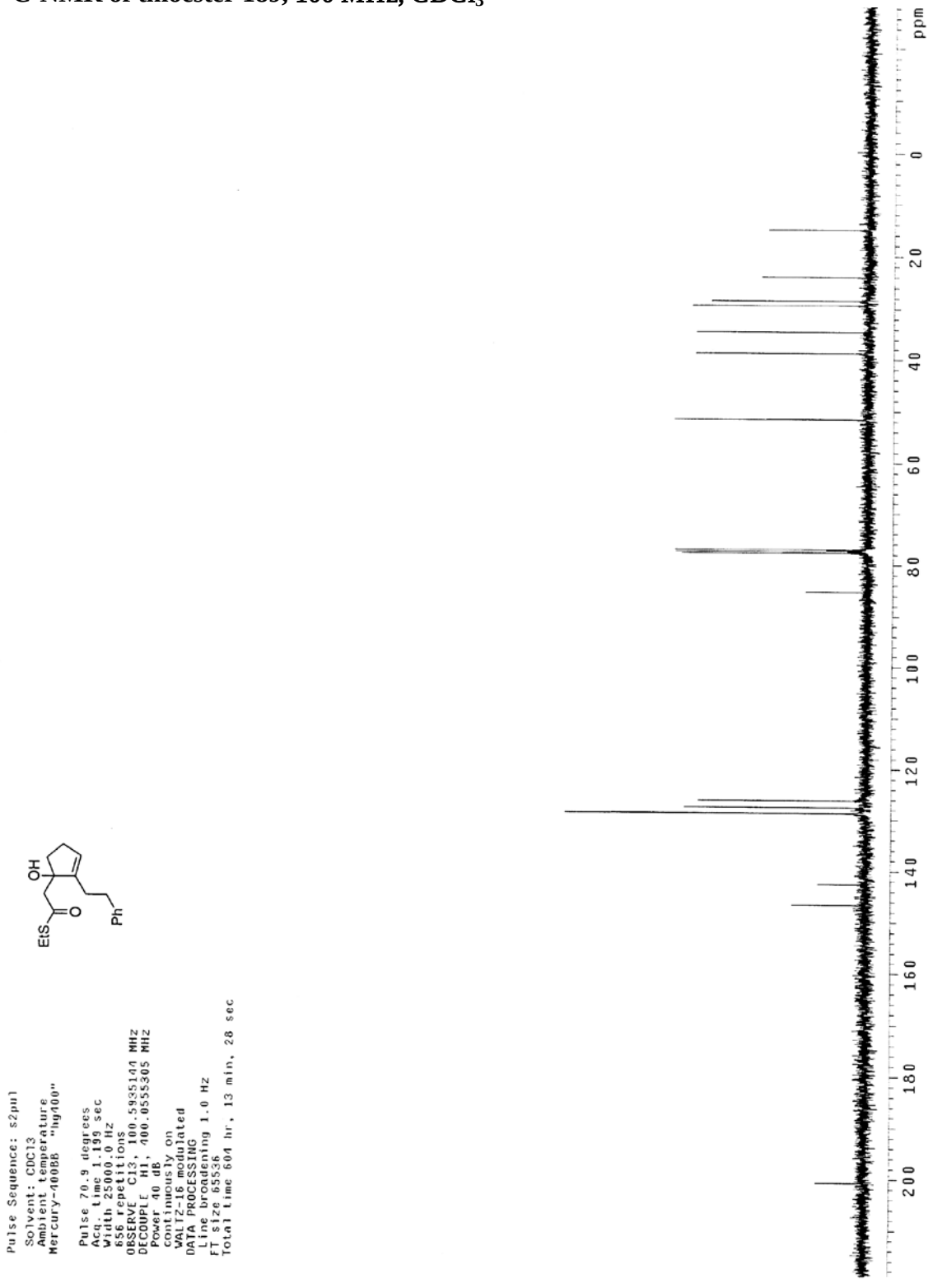

^{1}H-NMR of silyl ether 190, 400 MHz, $CDCl_3$

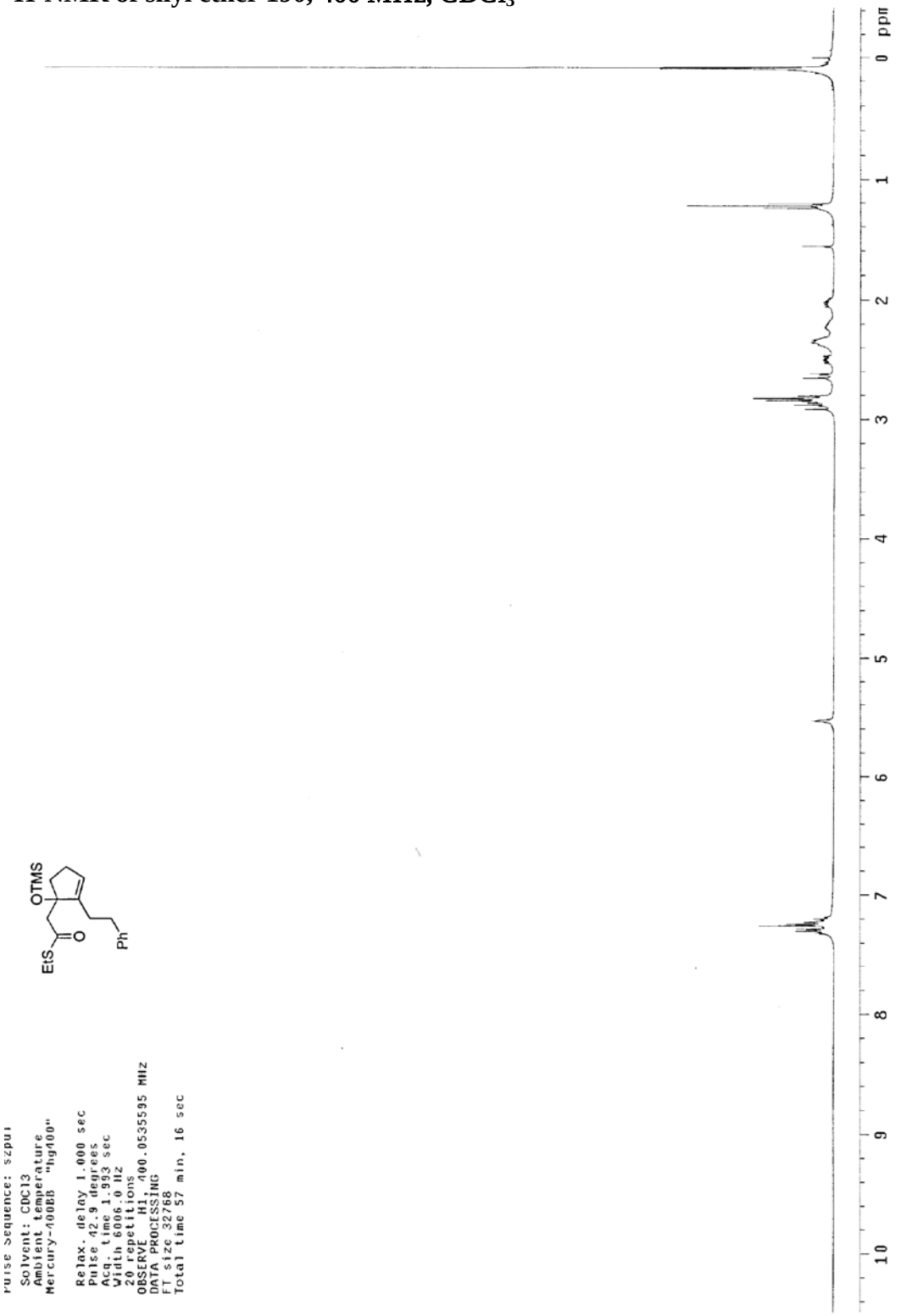

^{13}C-NMR of silyl ether 190, 100 MHz, $CDCl_3$

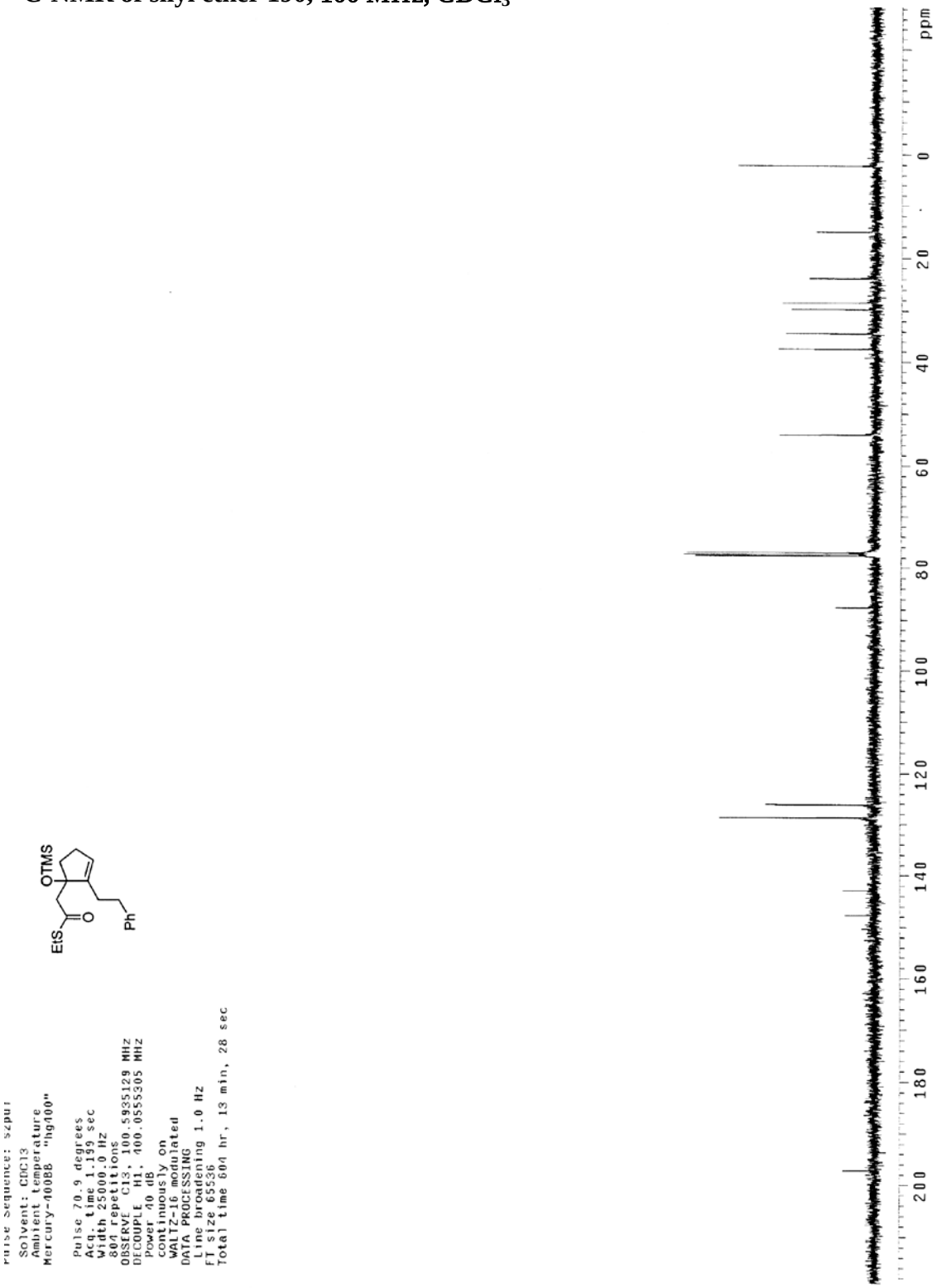


```
Pulse Sequence: szpul
Solvent: CDCl3
Ambient temperature
Mercury-400BB "hg400"

Pulse 70.9 degrees
Acq. time 1.199 sec
Width 25000.0 Hz
804 repetitions
OBSERVE C13, 100.5935129 MHz
DECOUPLE H1, 400.0555305 MHz
Power 40 dB
continuously on
WALTZ-16 modulated
DATA PROCESSING
Line broadening 1.0 Hz
FT size 65536
Total time 604 hr, 13 min, 28 sec
```

^{1}H-NMR of alcohol 192, 400 MHz, $CDCl_3$

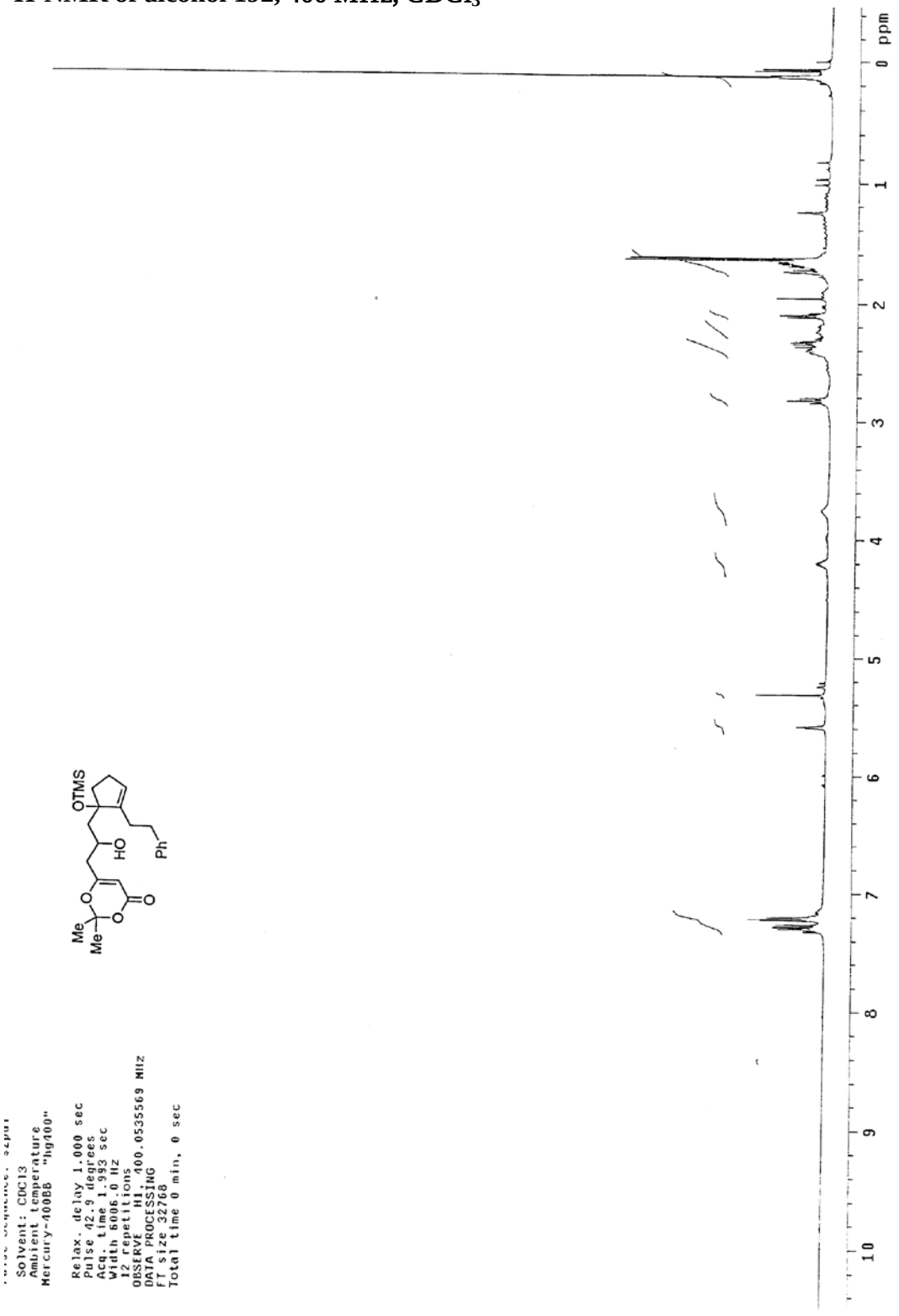

^{13}C-NMR of alcohol 192, 100 MHz, $CDCl_3$

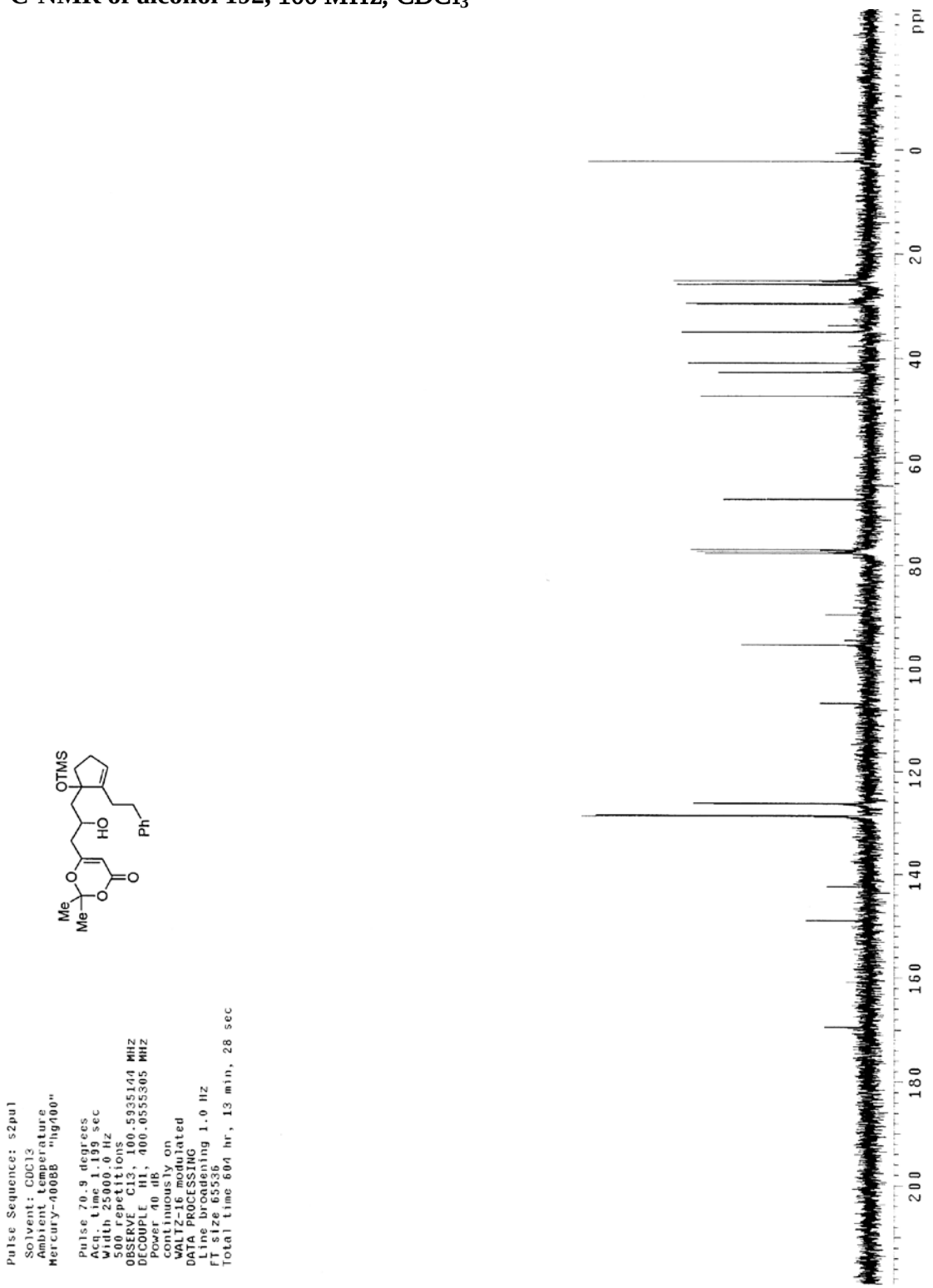

^{1}H-NMR of silyl ether 193, 400 MHz, $CDCl_3$

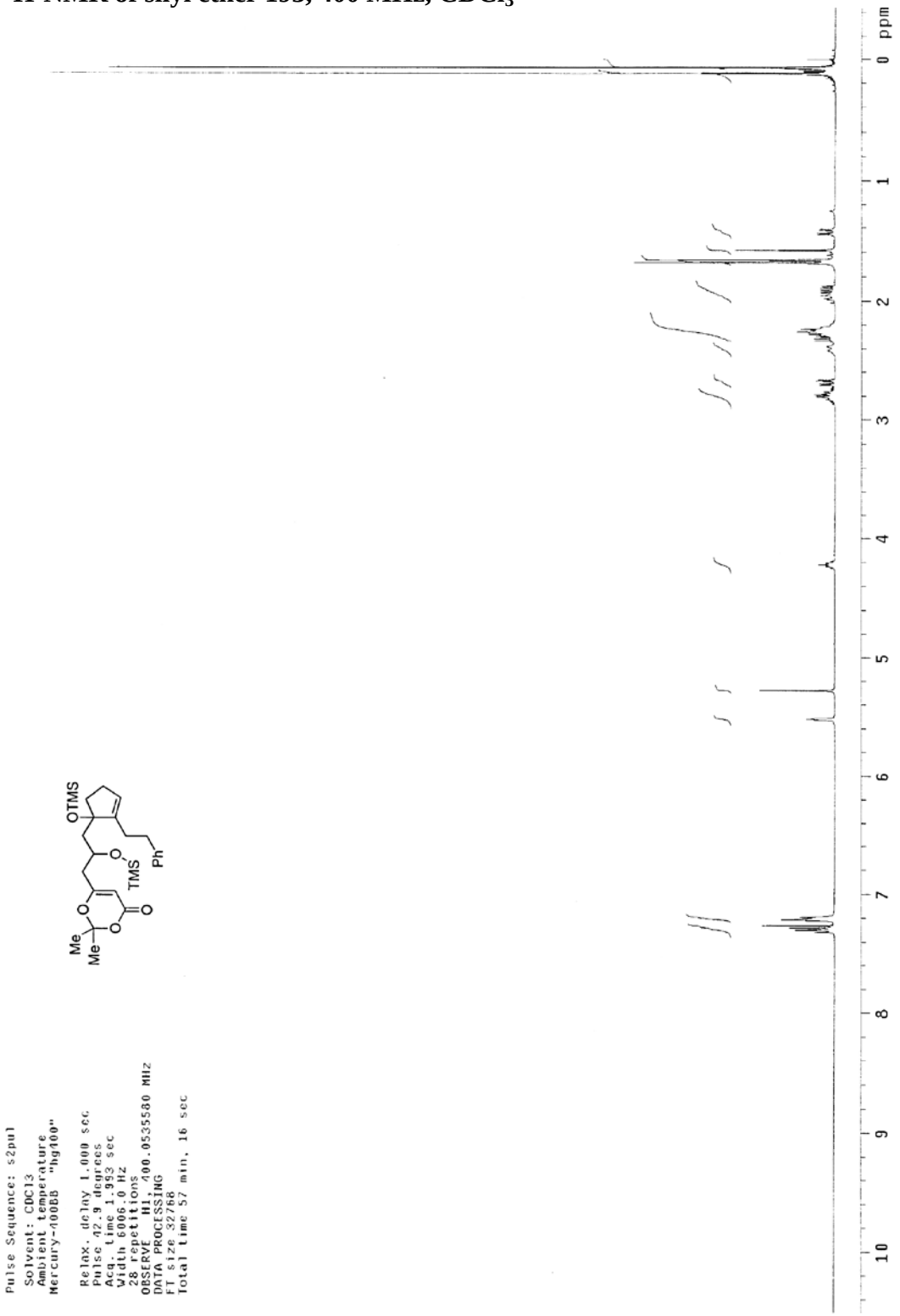

^{13}C-NMR of silyl ether 193, 100 MHz, $CDCl_3$

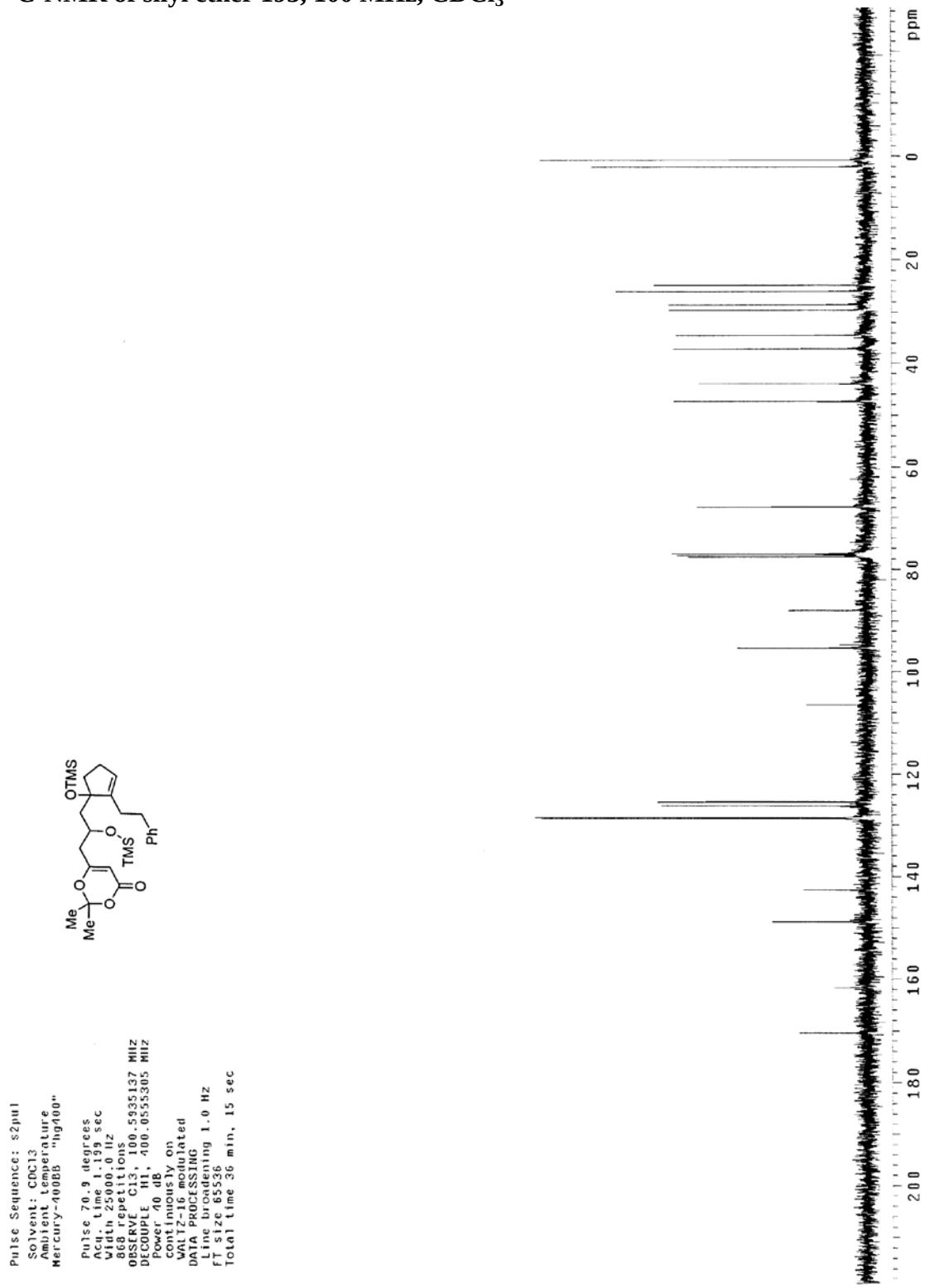

^{1}H-NMR of acetate 194, 400 MHz, $CDCl_3$

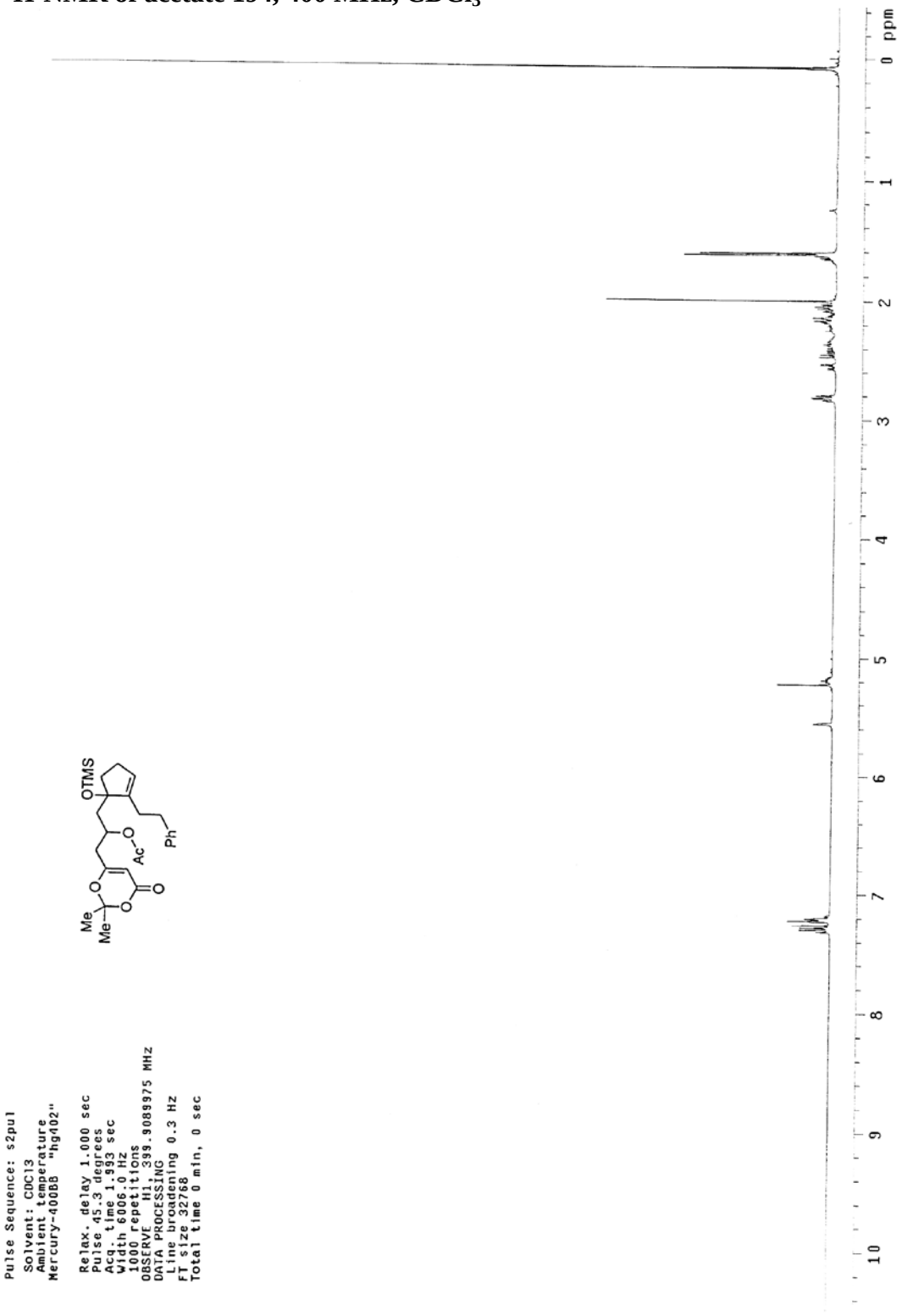

^{13}C-NMR of acetate 194, 100 MHz, $CDCl_3$

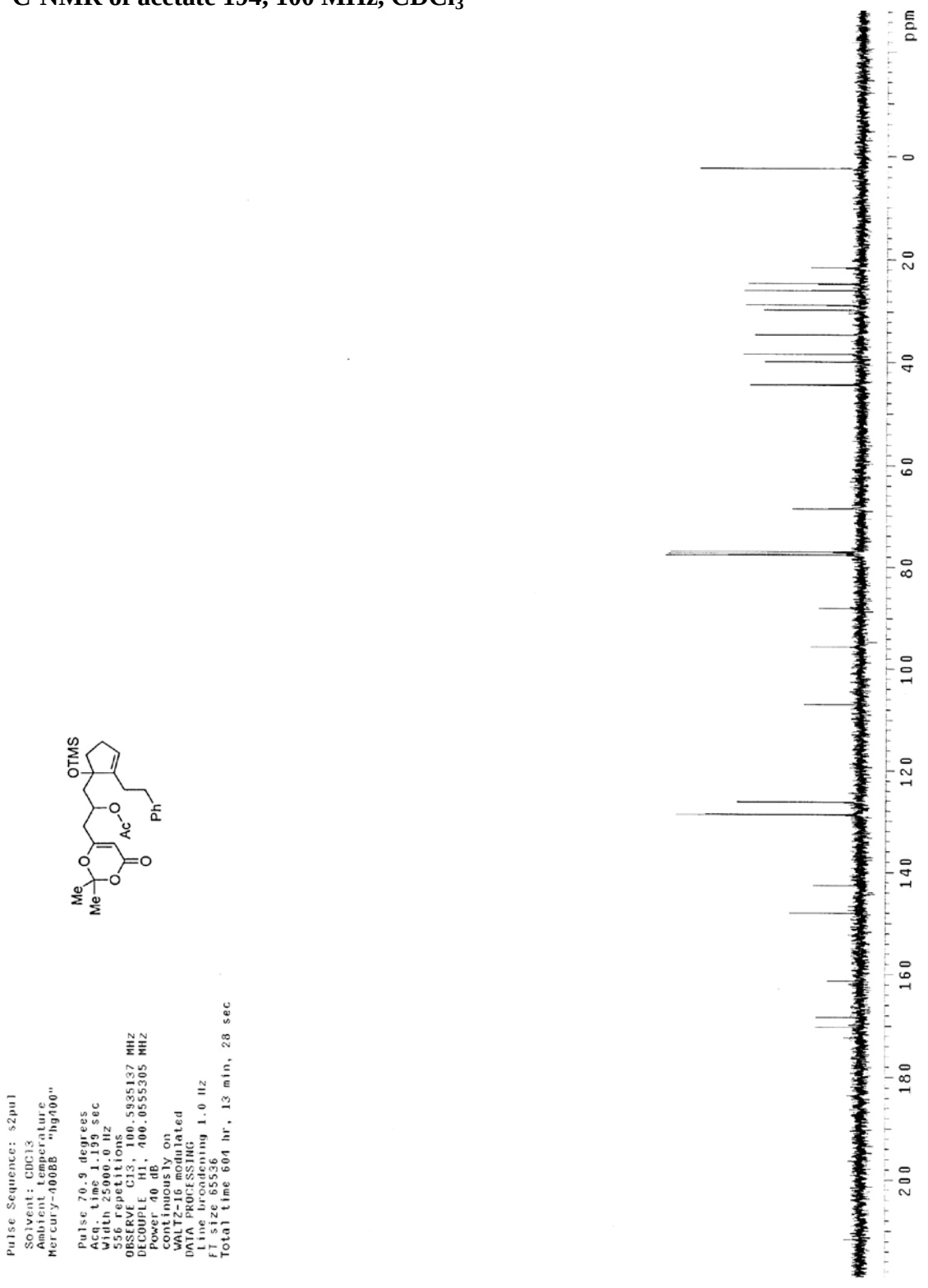

^{1}H-NMR of cyclopentenone 144, 400 MHz, $CDCl_3$

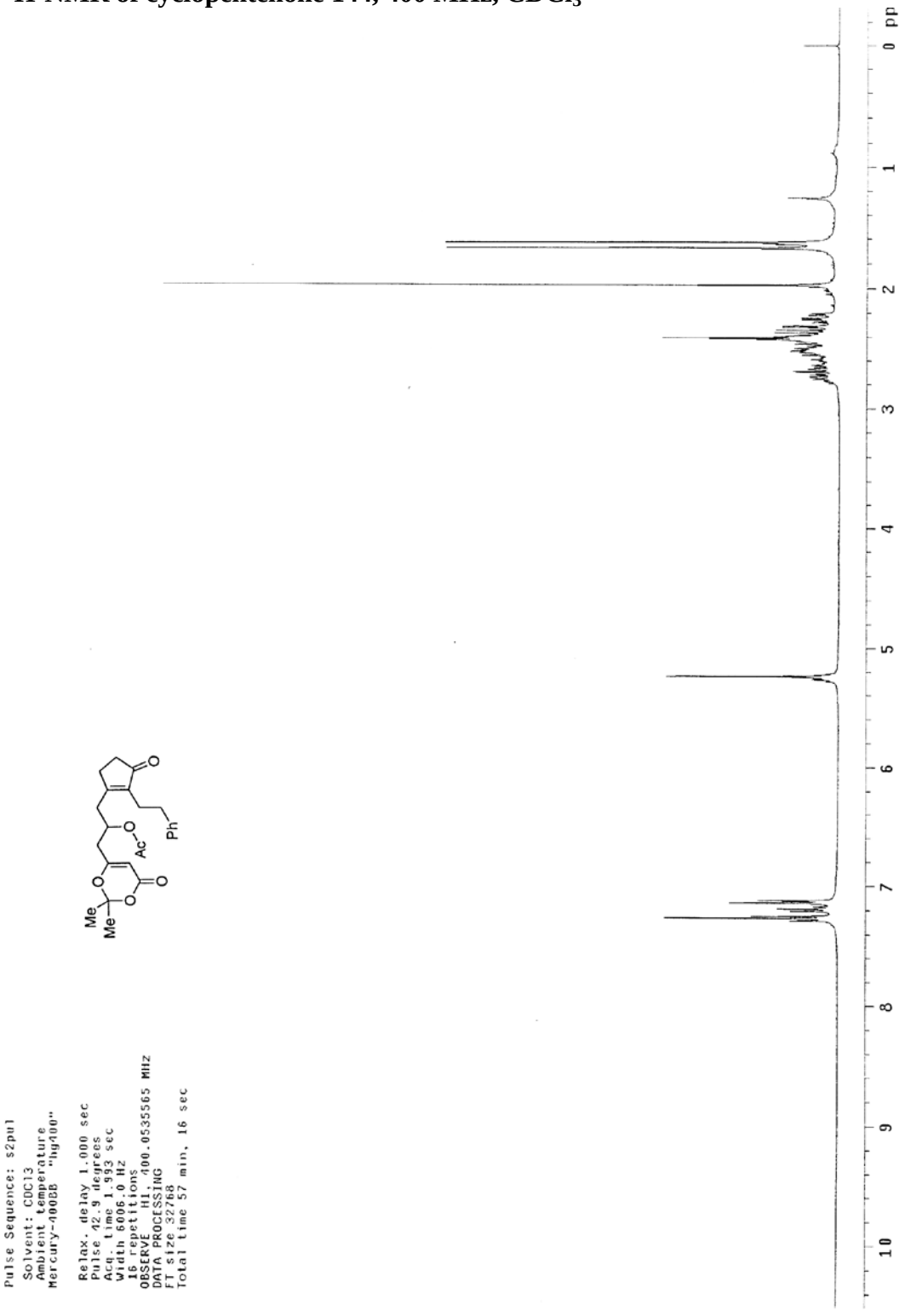

^{13}C-NMR of cyclopentenone 144, 100 MHz, $CDCl_3$

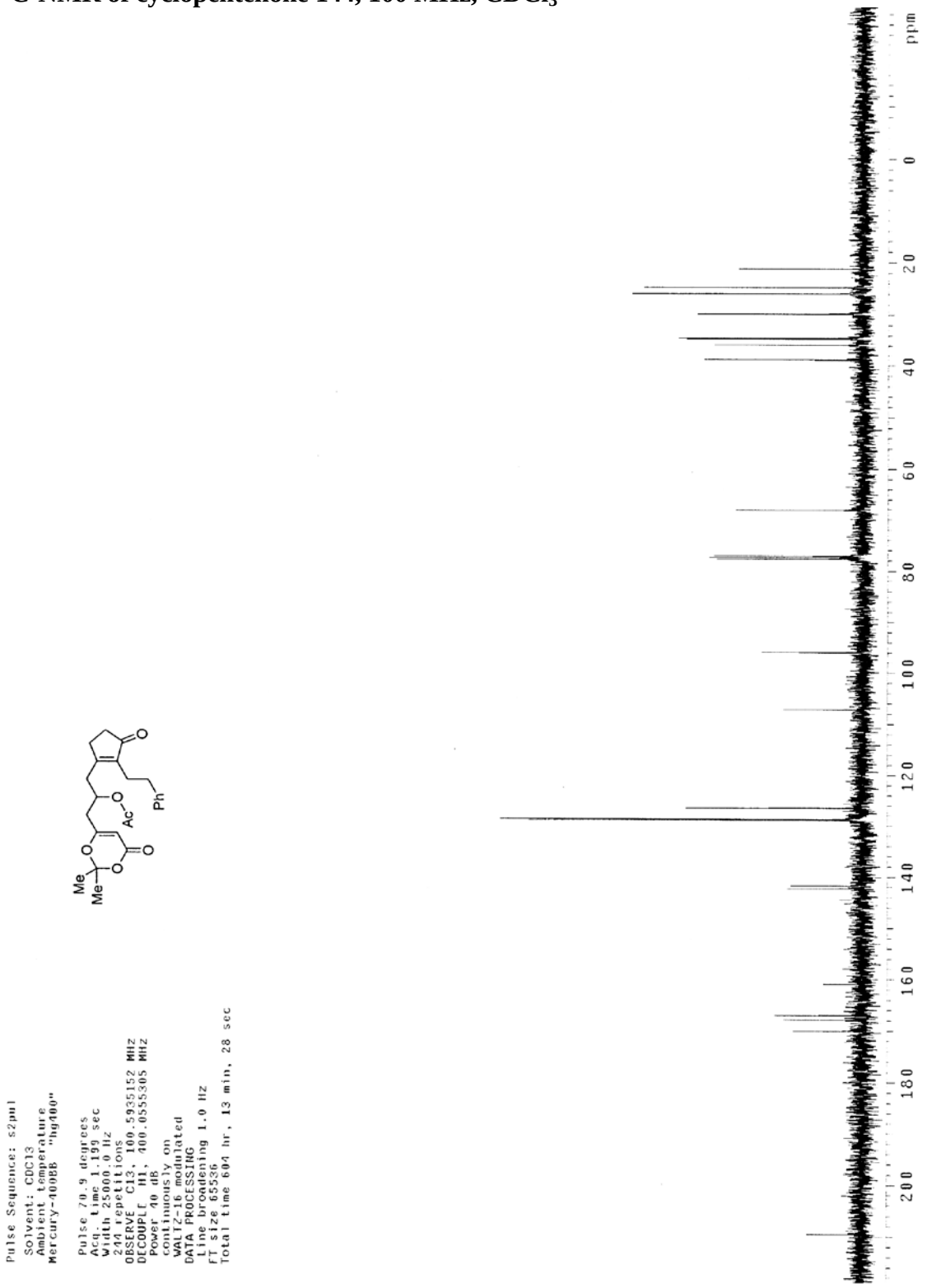

^{1}H-NMR of ethyl 2-(1-hydroxycyclopent-2-enyl)ethanethioate 196, 400 MHz, $CDCl_3$

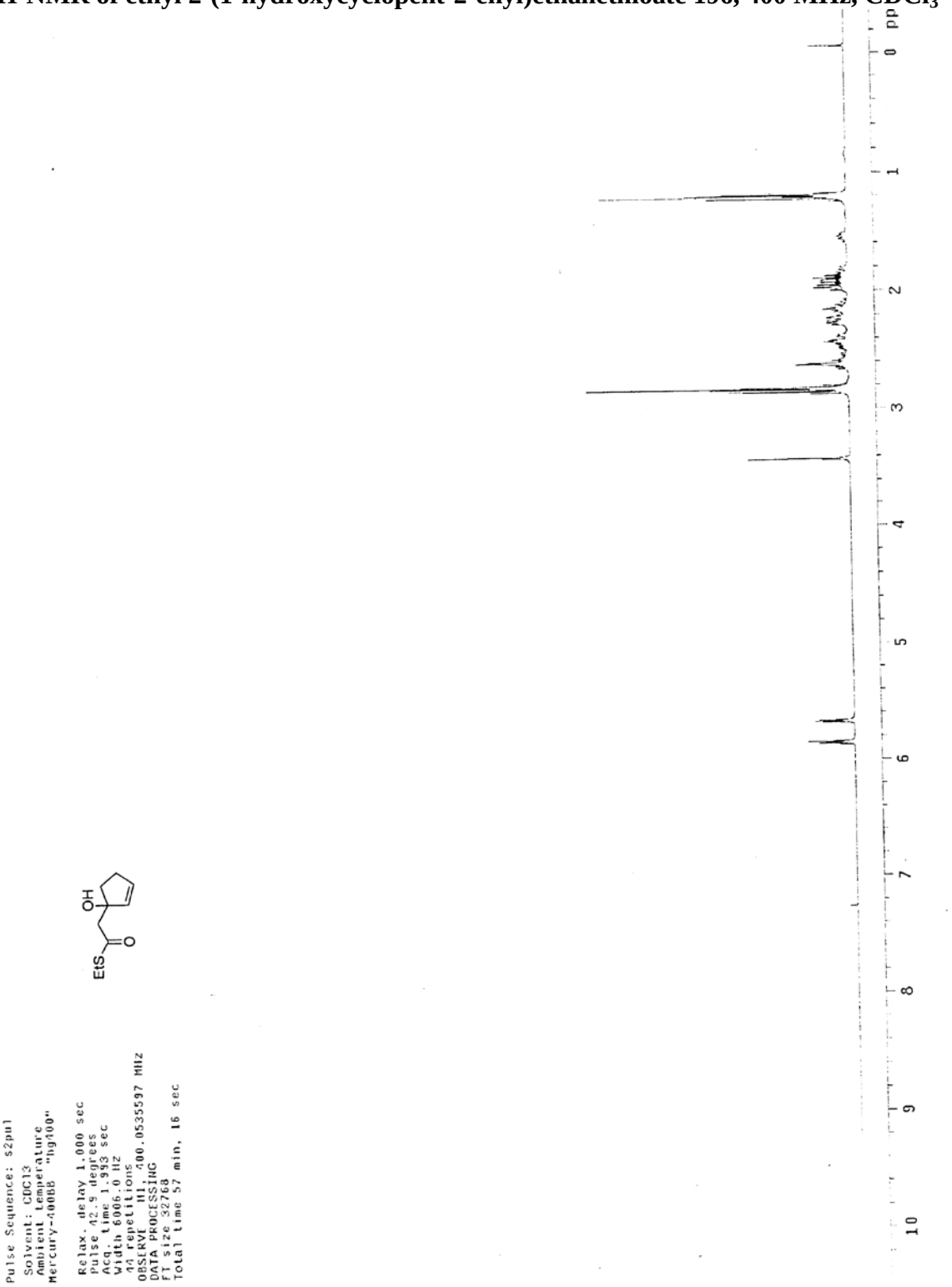

^{13}C-NMR of ethyl 2-(1-hydroxycyclopent-2-enyl)ethanethioate 196, 100 MHz, $CDCl_3$

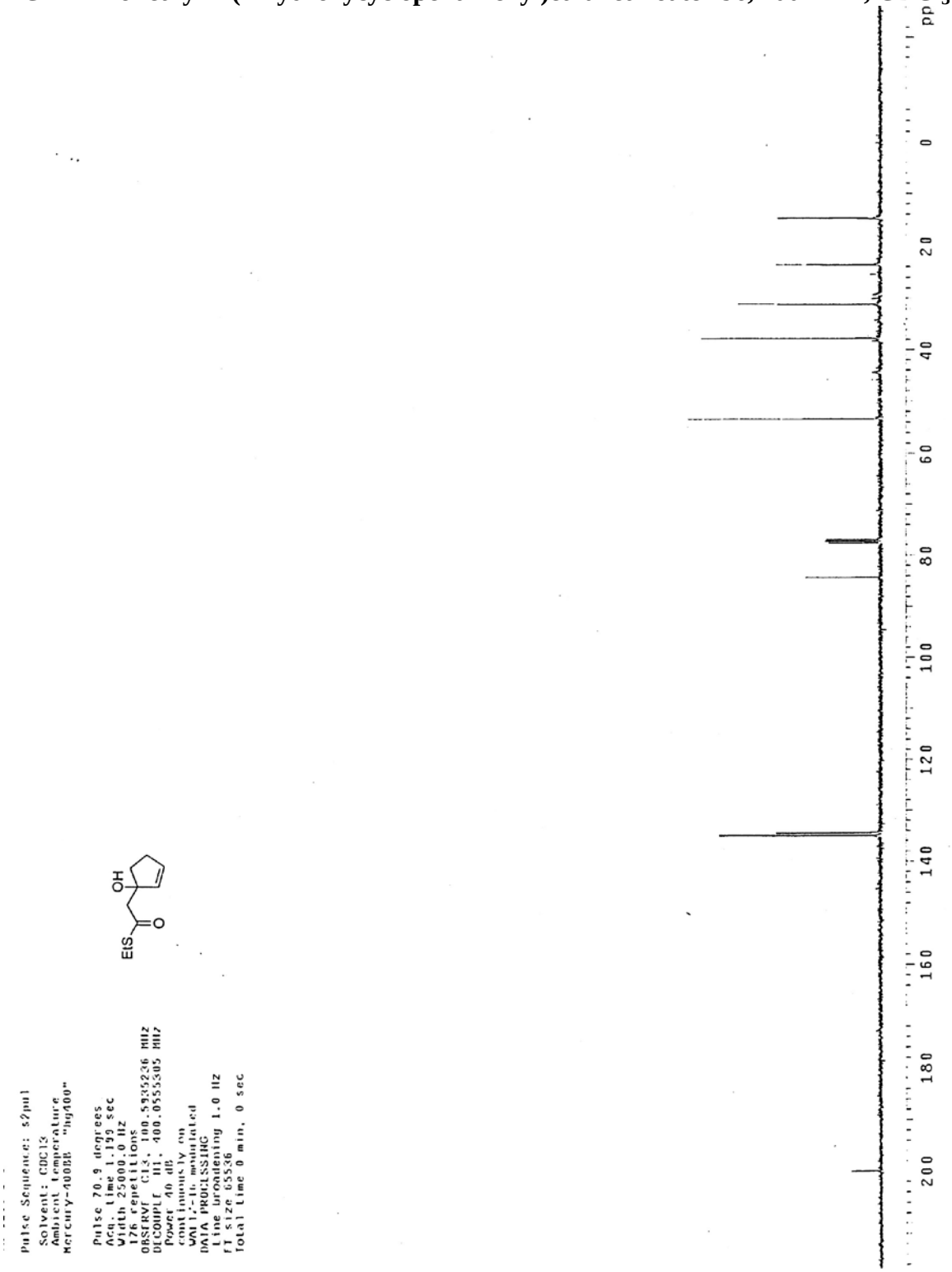

2-(1-trimethylsilyloxycyclopent-2-enyl)ethanethioate 197, 400 MHz, $CDCl_3$

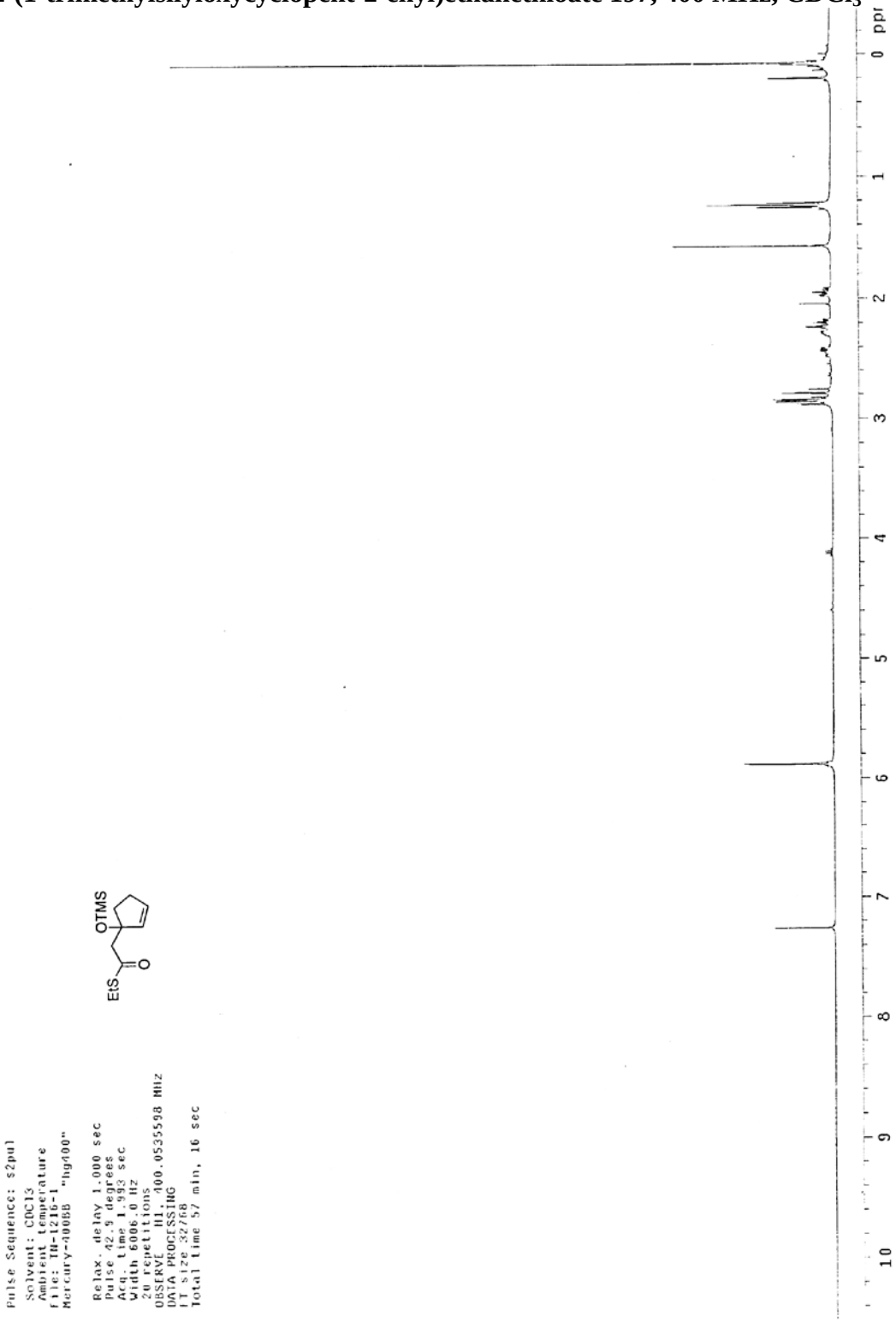

2-(1-trimethylsilyloxycyclopent-2-enyl)ethanethioate 197, 100 MHz, $CDCl_3$

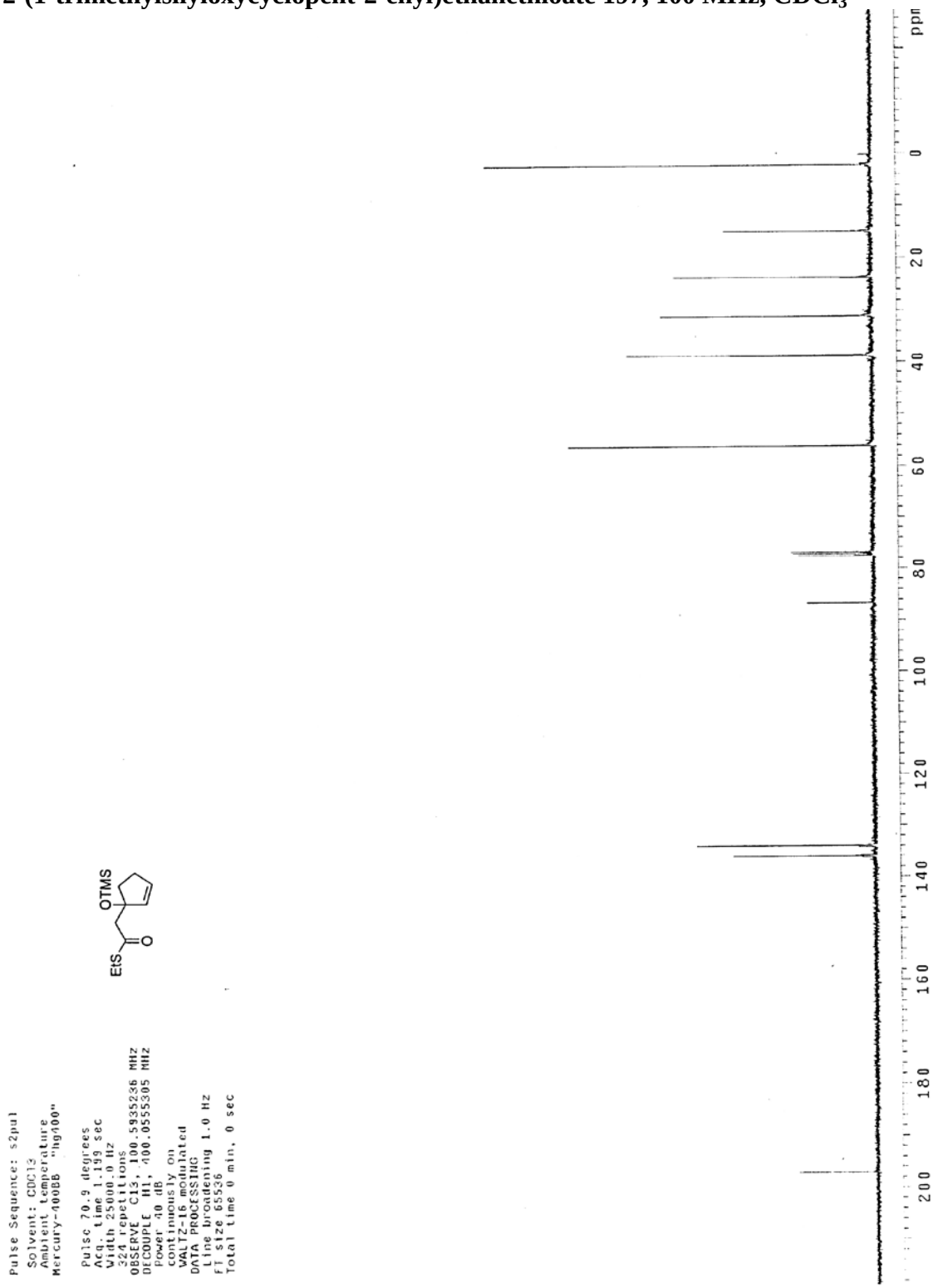

^{1}H-NMR of alcohol 199, 400 MHz, $CDCl_3$

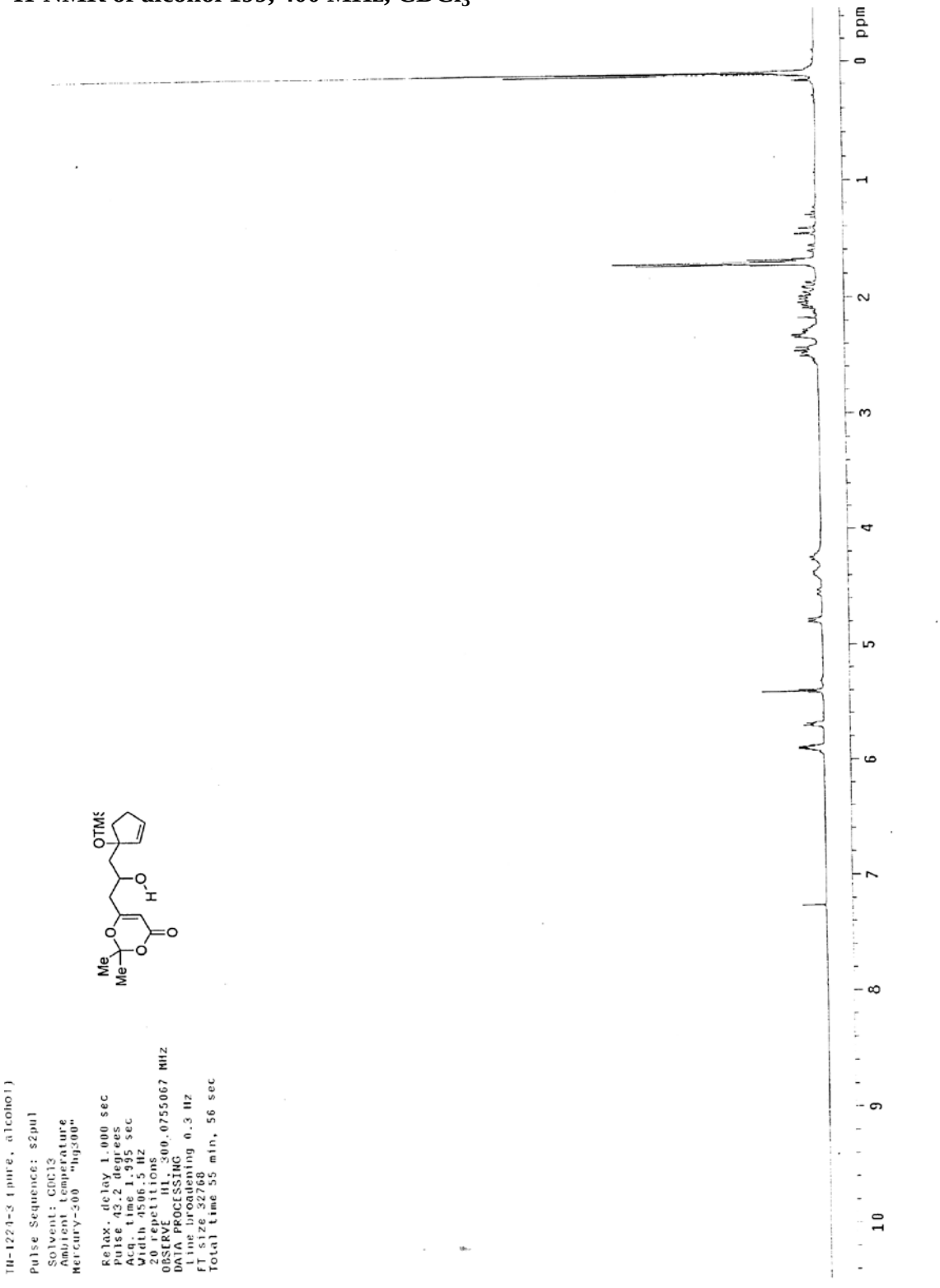

^{13}C-NMR of alcohol 199, 100 MHz, $CDCl_3$

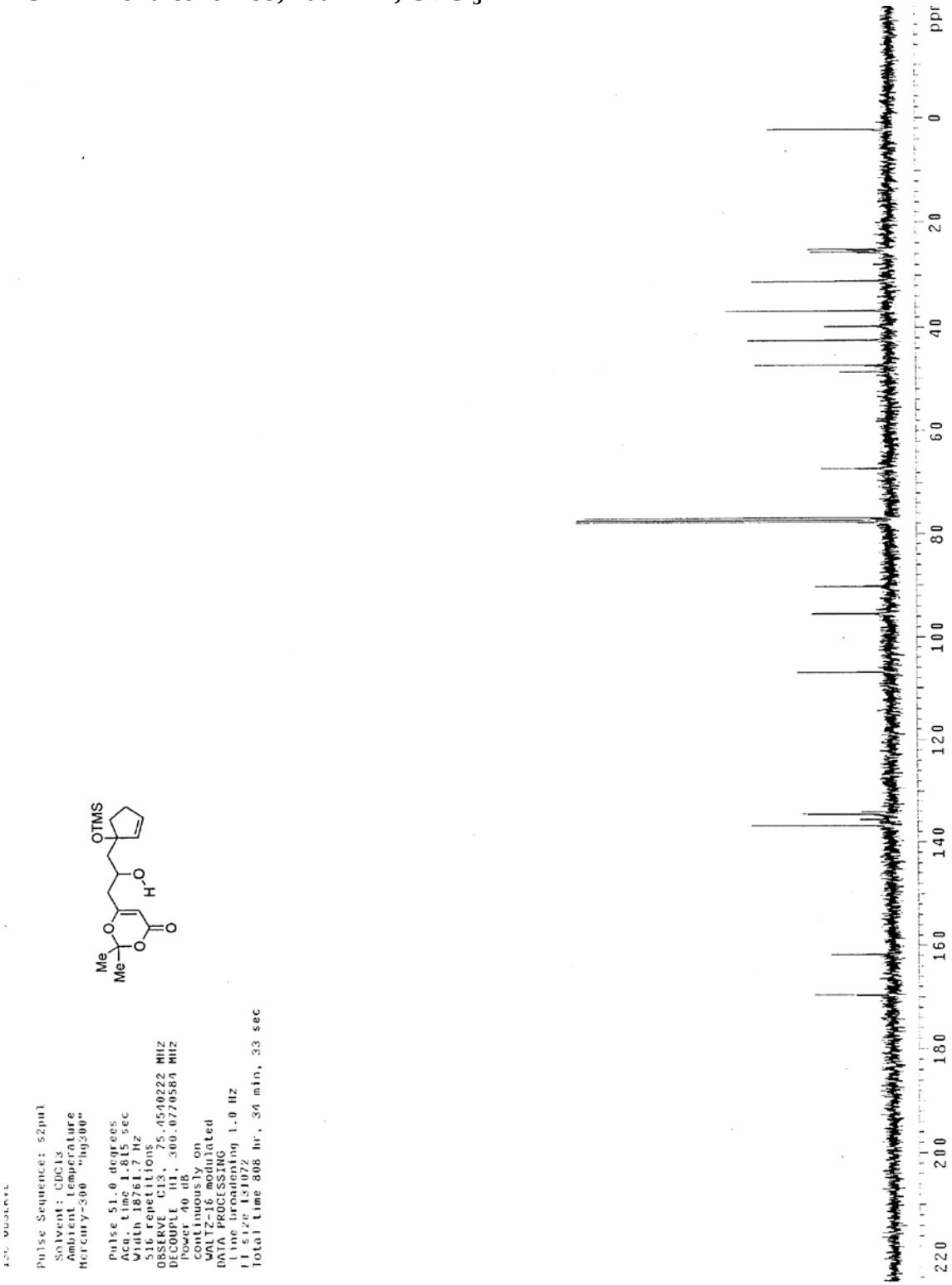

^{1}H-NMR of silyl ether 200, 400 MHz, $CDCl_3$

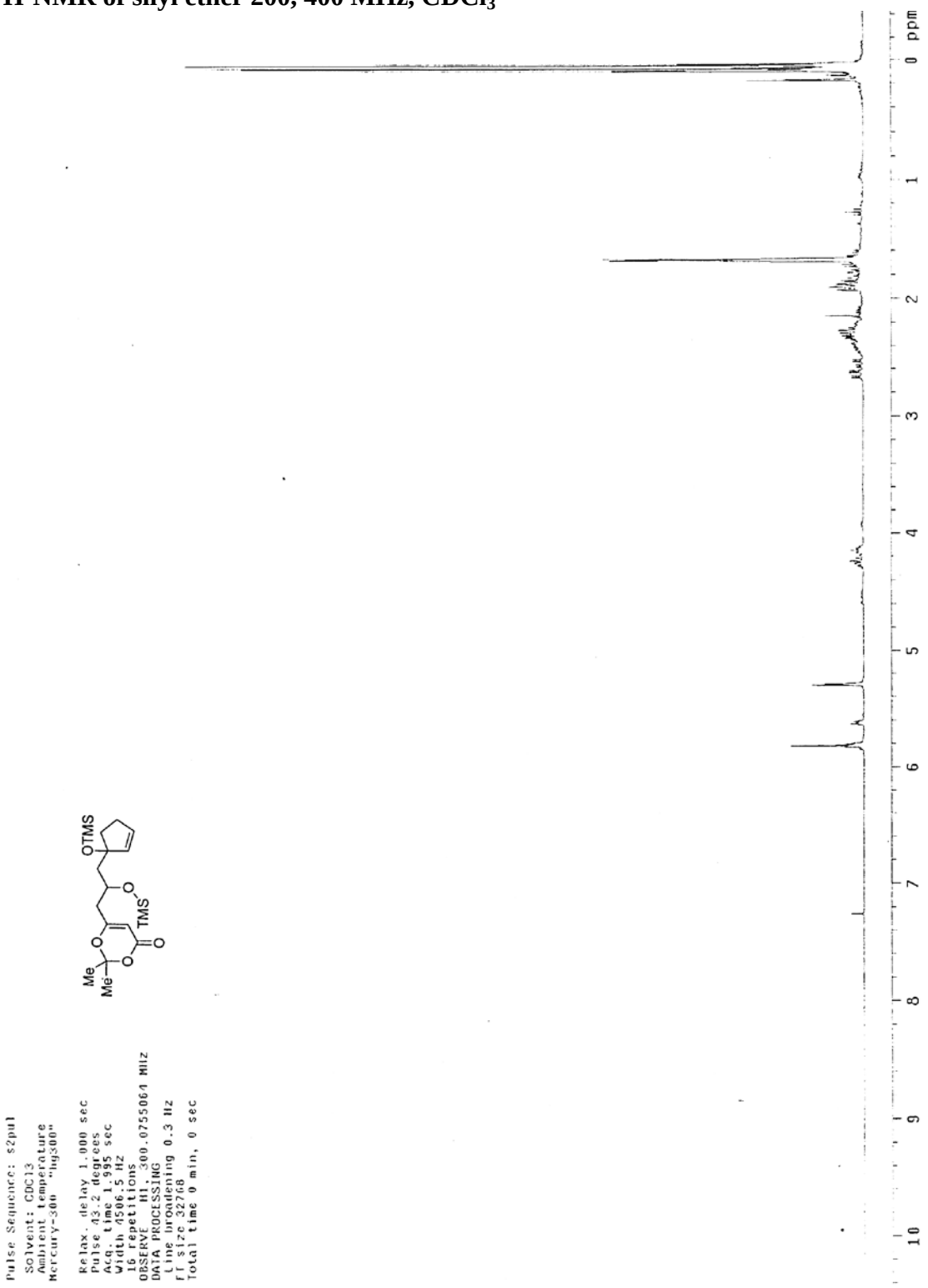

^{13}C-NMR of silyl ether 200, 100 MHz, $CDCl_3$

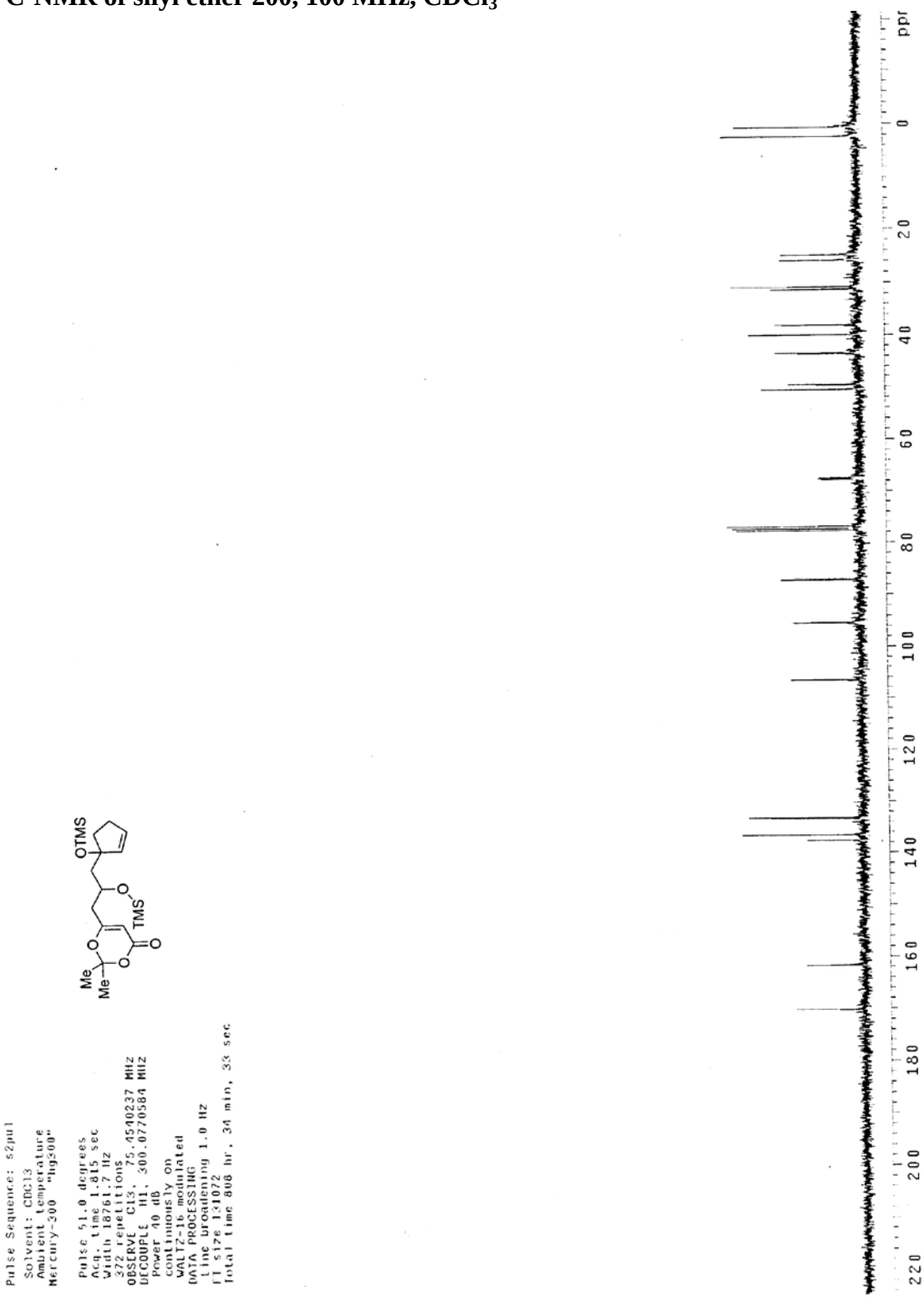

^{1}H-NMR of acetate 201, 400 MHz, $CDCl_3$

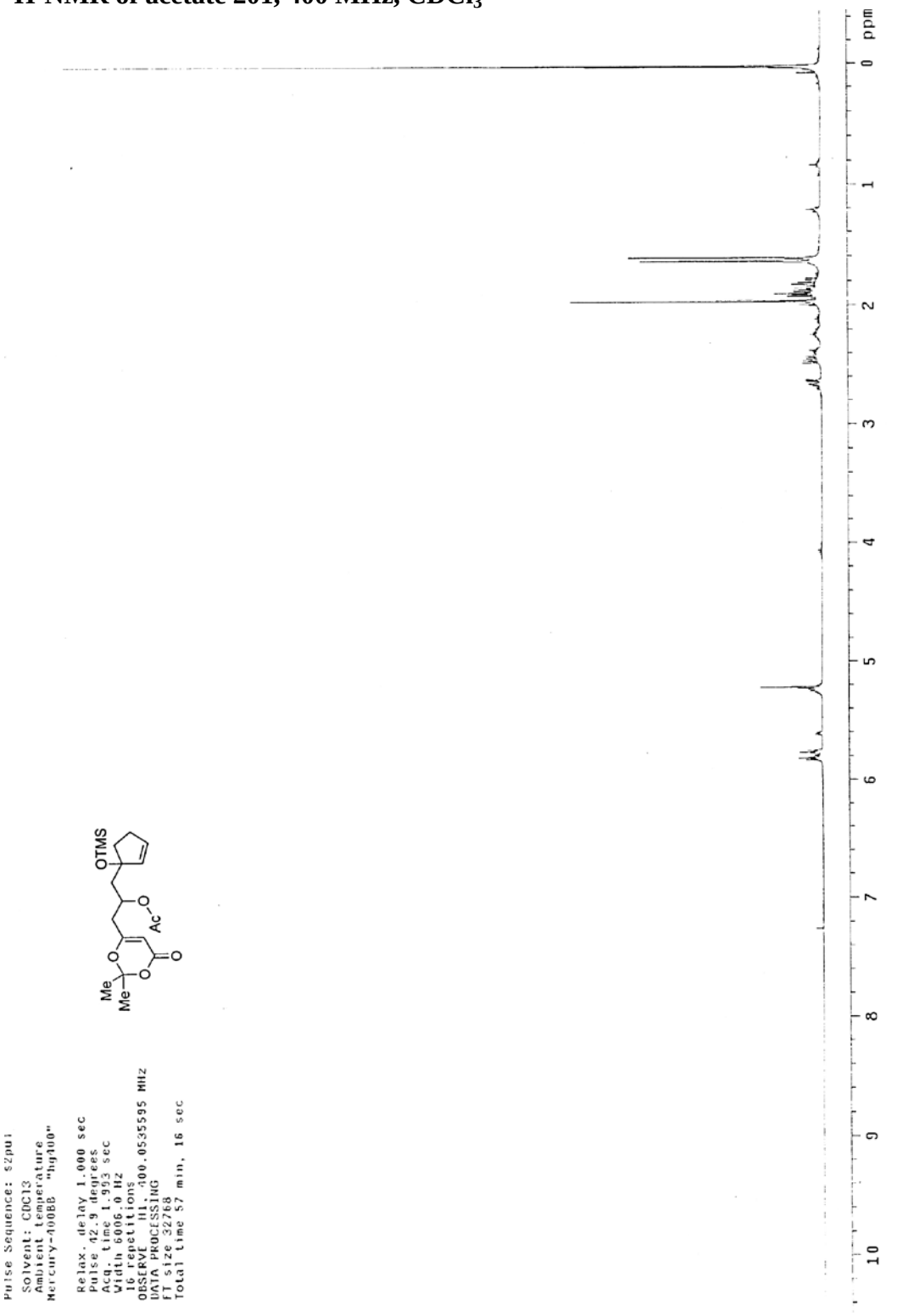

^{13}C-NMR of acetate 201, 100 MHz, $CDCl_3$

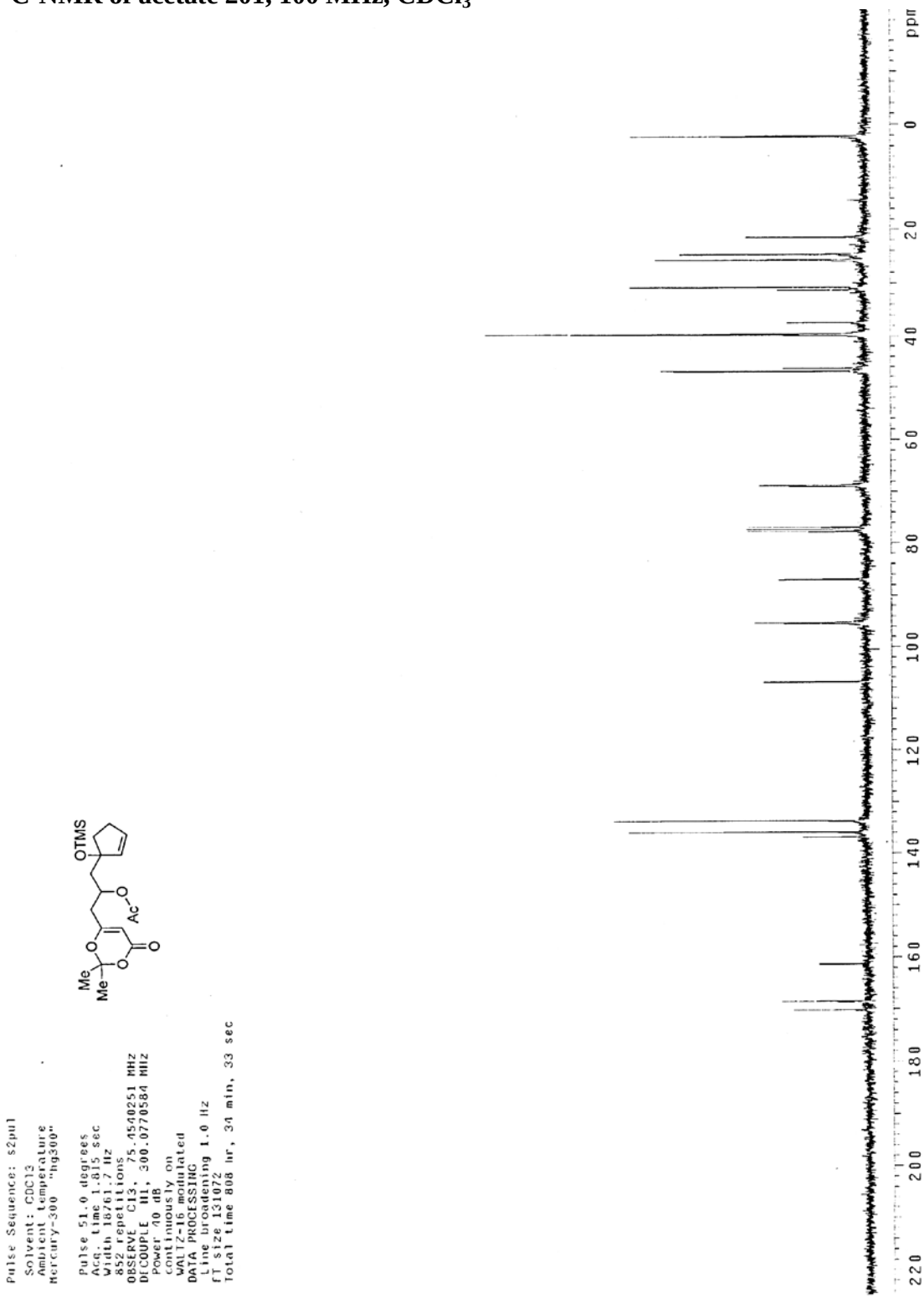

^{1}H-NMR of cyclopentenone 202, 400 MHz, $CDCl_3$

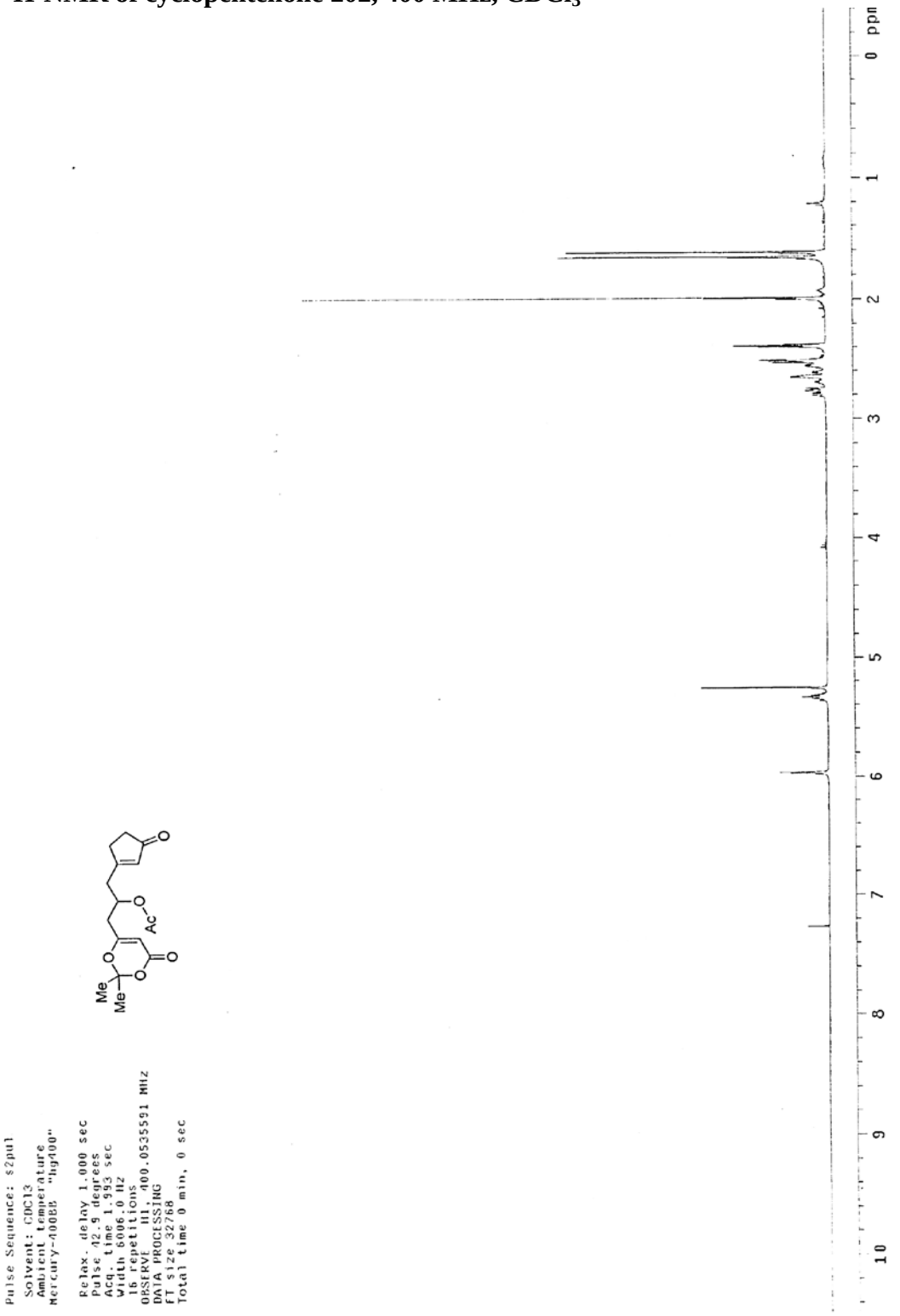

^{13}C-NMR of cyclopentenone 202, 100 MHz, $CDCl_3$

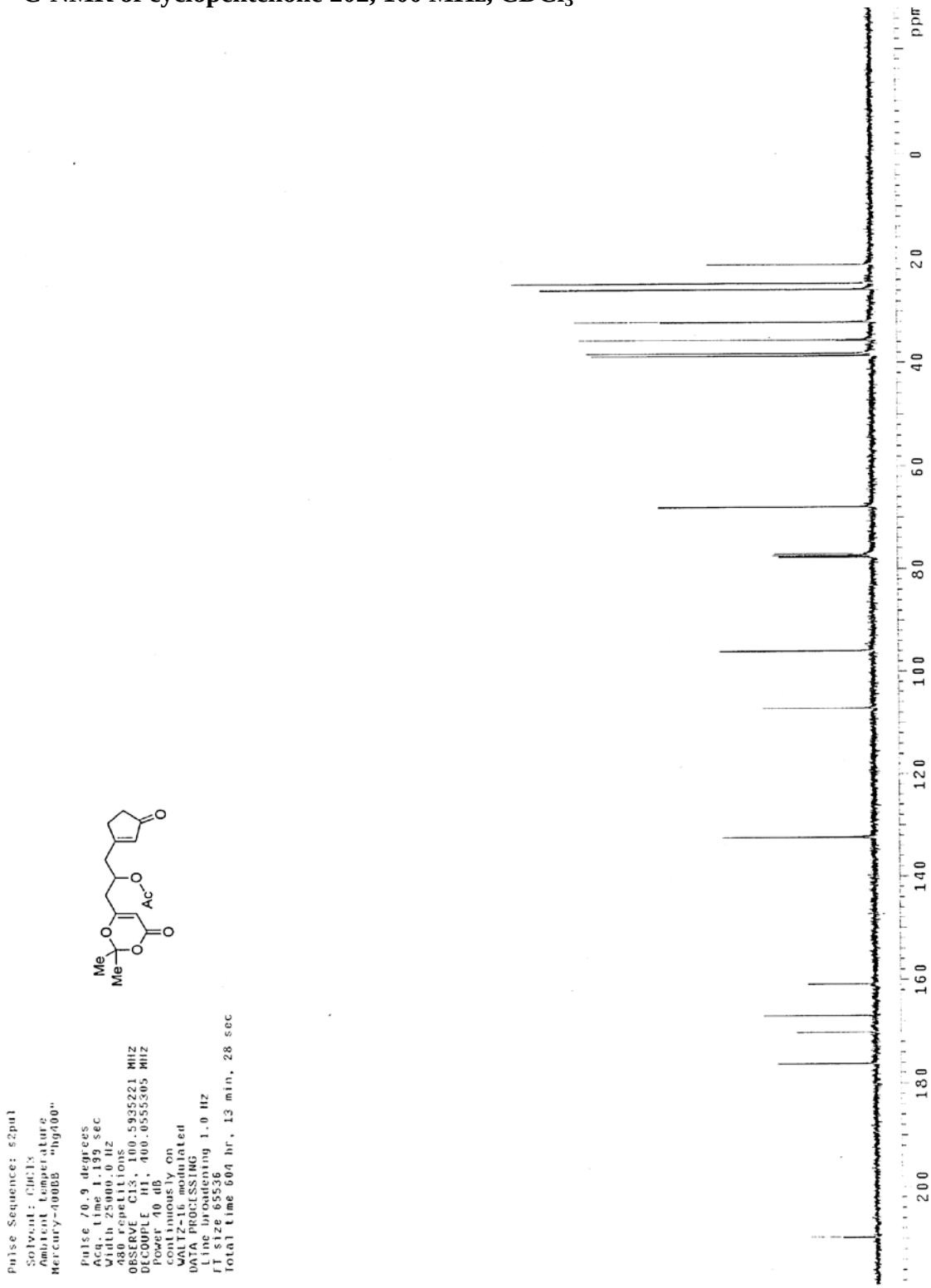

^{1}H-NMR of cyclobutane 203, 400 MHz, $CDCl_3$

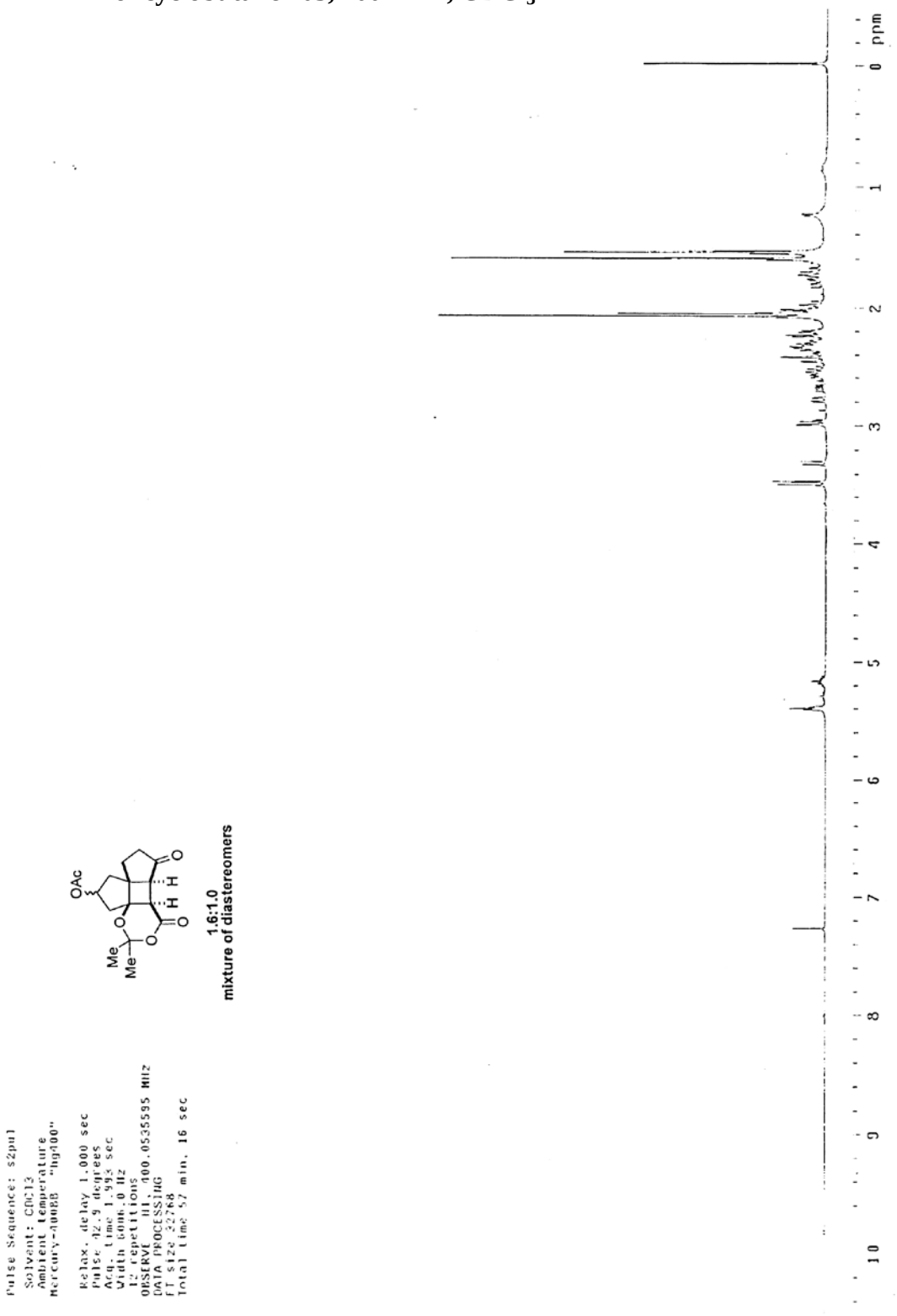

^{13}C-NMR of cyclobutane 203, 100 MHz, $CDCl_3$

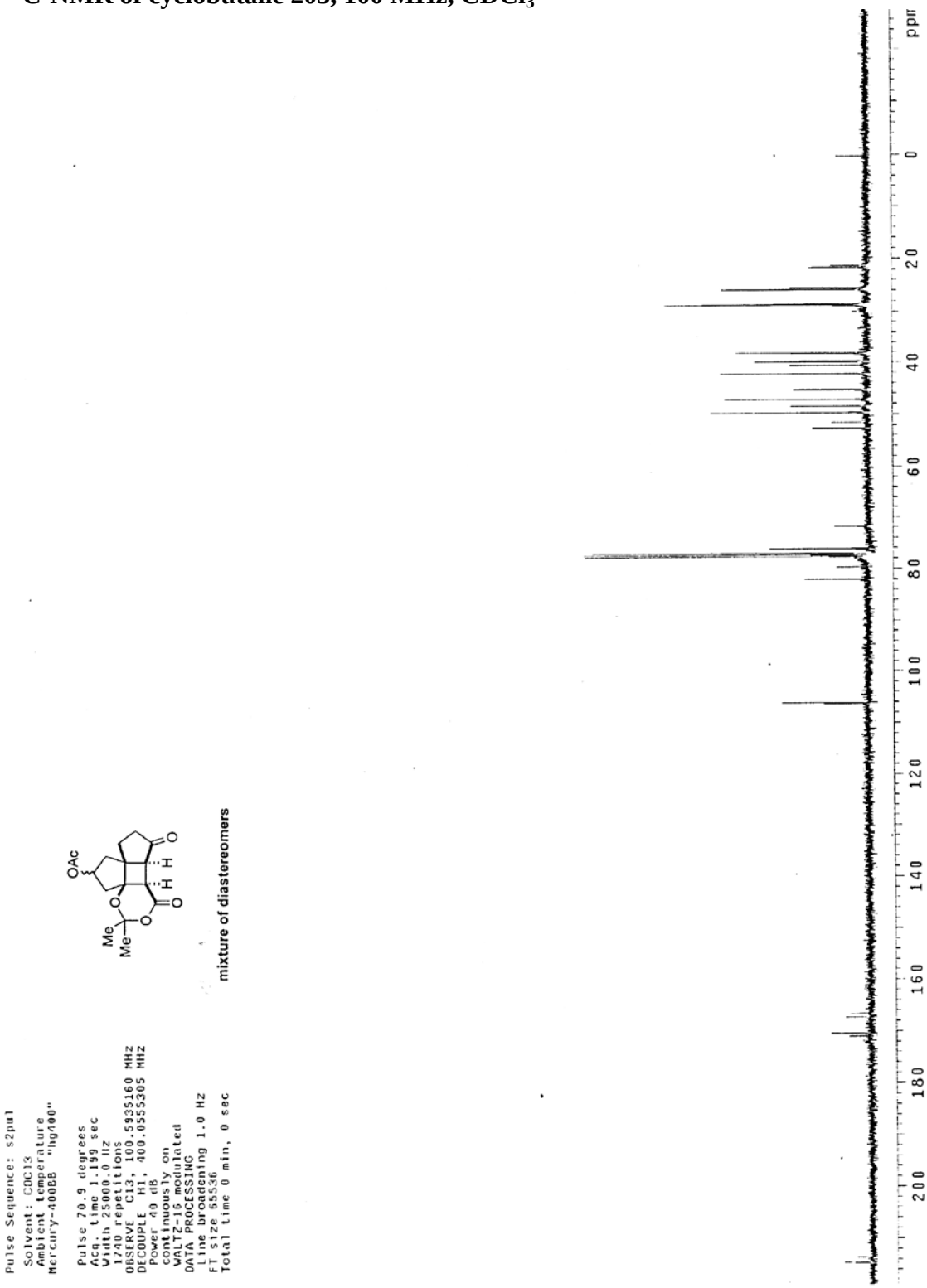

^{1}H-NMR of methyl enol ether 206, 400 MHz, $CDCl_3$

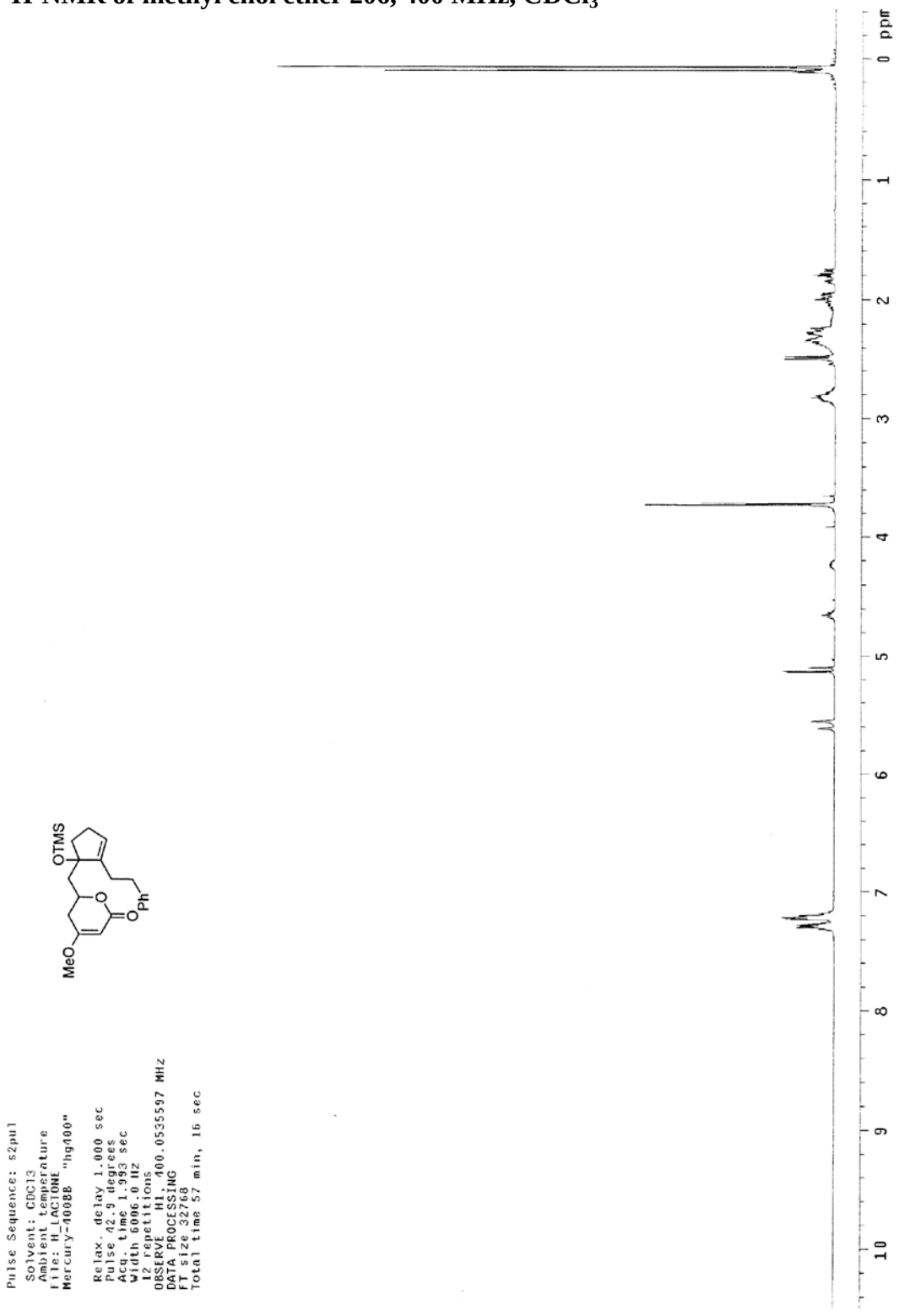

^{13}C-NMR of methyl enol ether 206, 100 MHz, $CDCl_3$

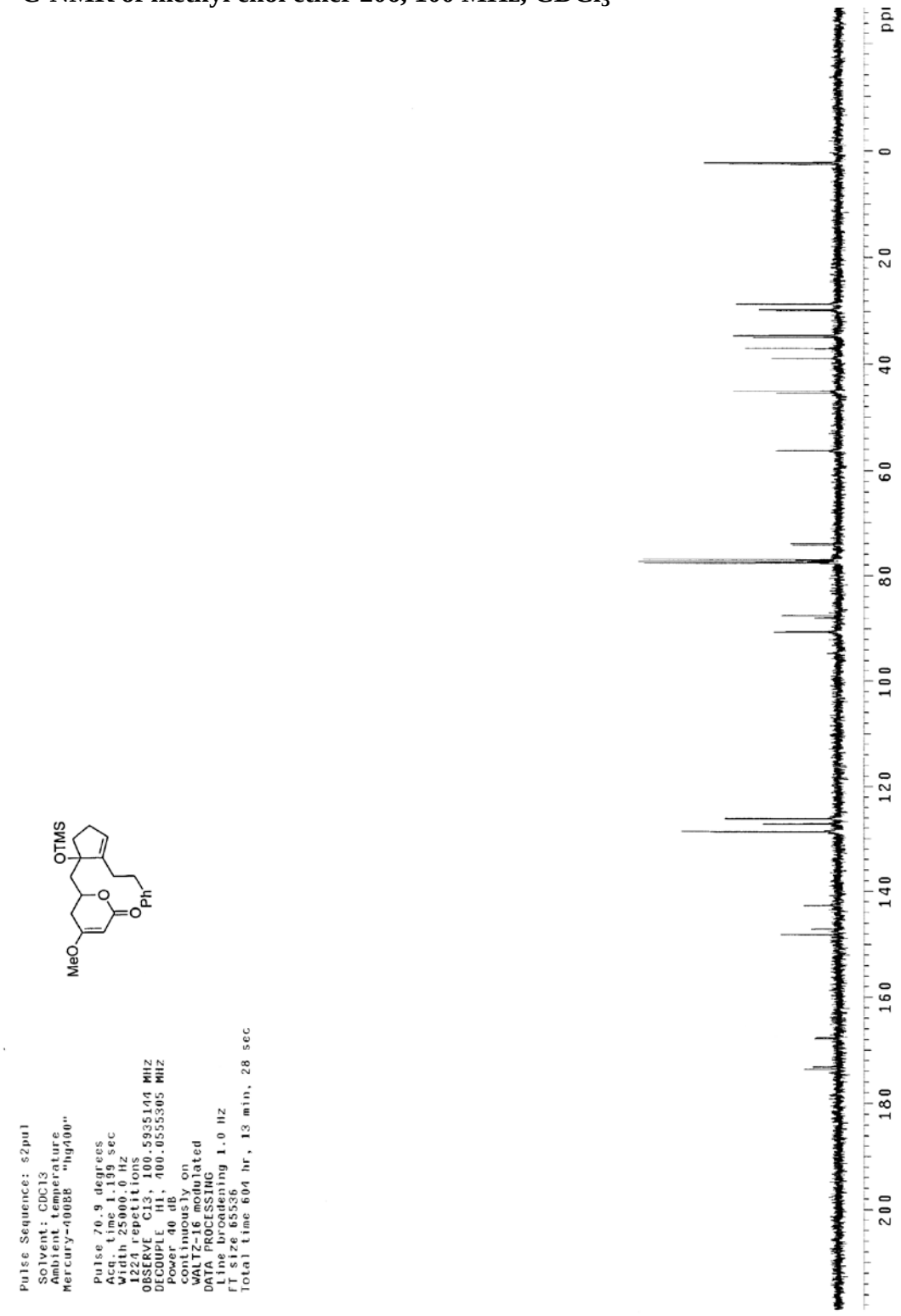

^{1}H-NMR of cyclopentenone 147, 400 MHz, $CDCl_3$

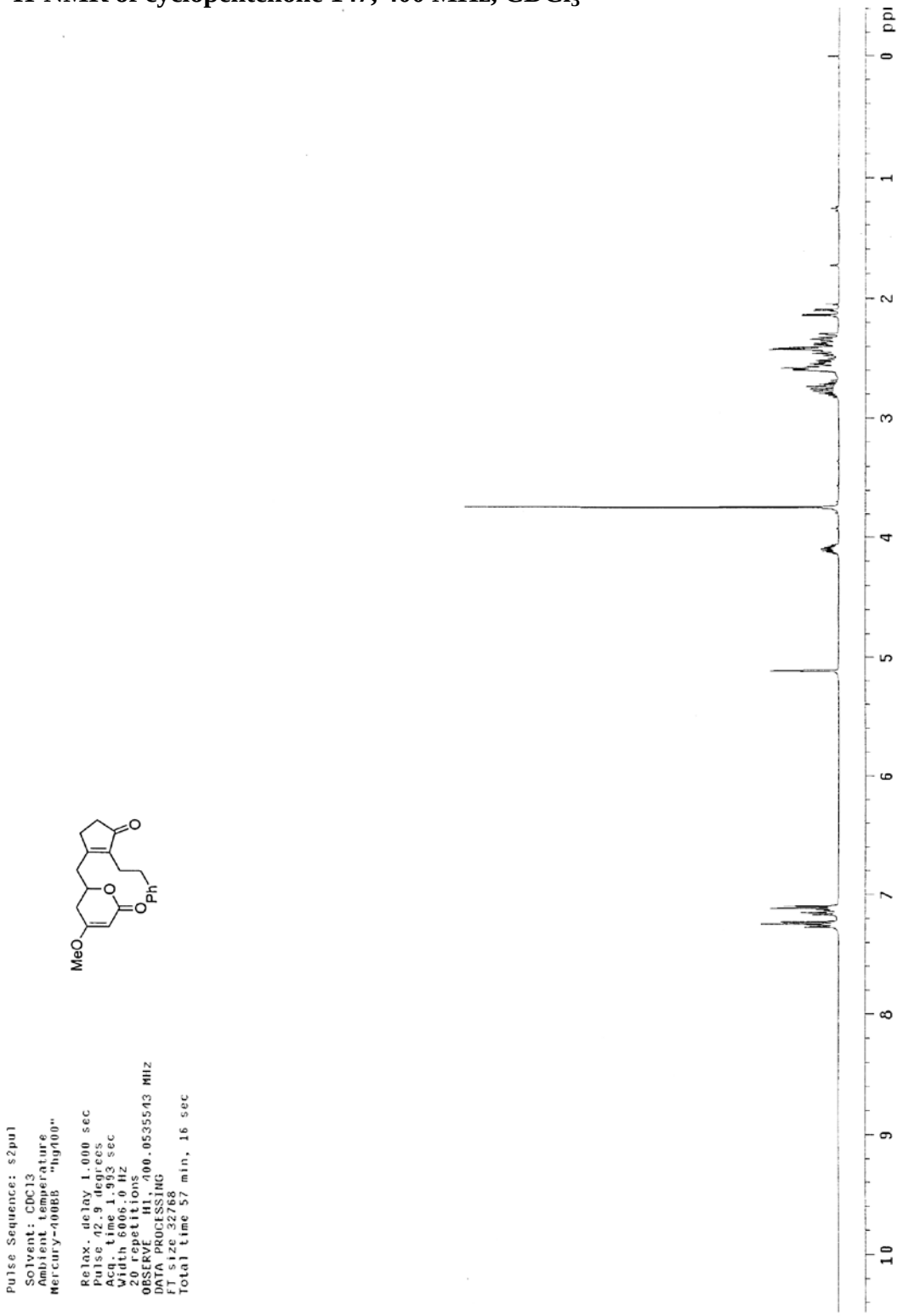

^{13}C-NMR of cyclopentenone 147, 100 MHz, $CDCl_3$

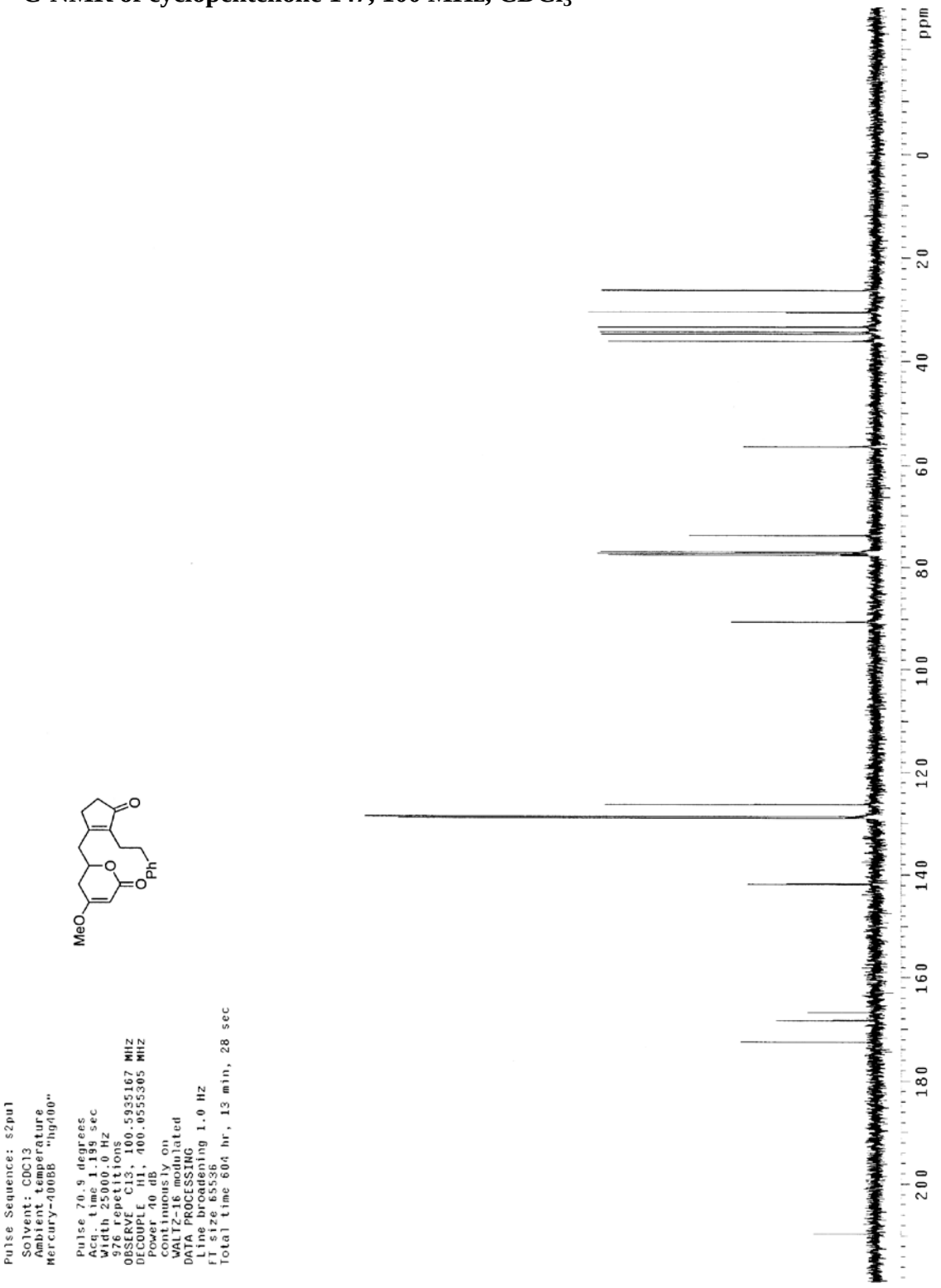

^{1}H-NMR of cyclobutane 207, 400 MHz, $CDCl_3$

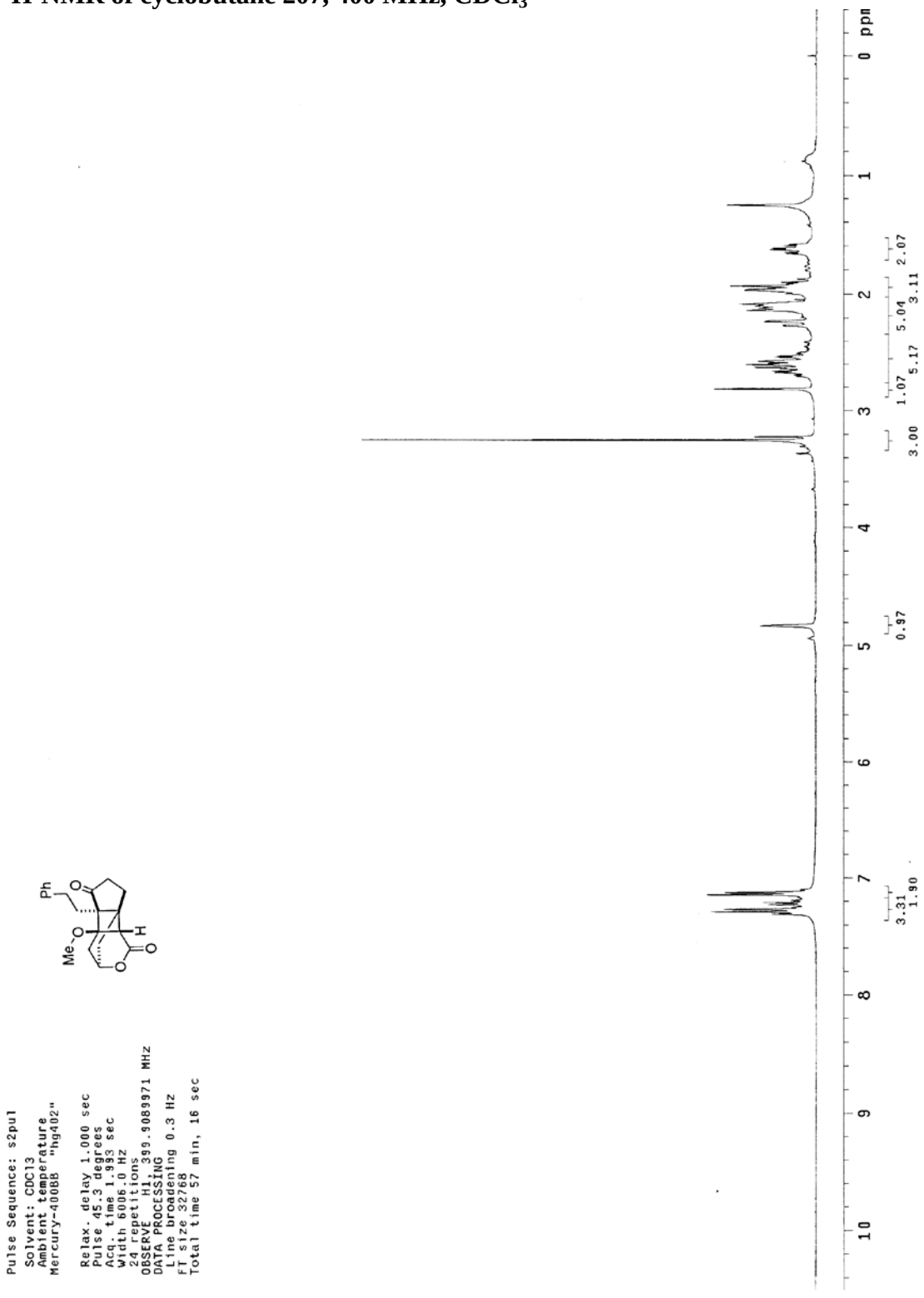

^{13}C-NMR of cyclobutane 207, 100 MHz, $CDCl_3$

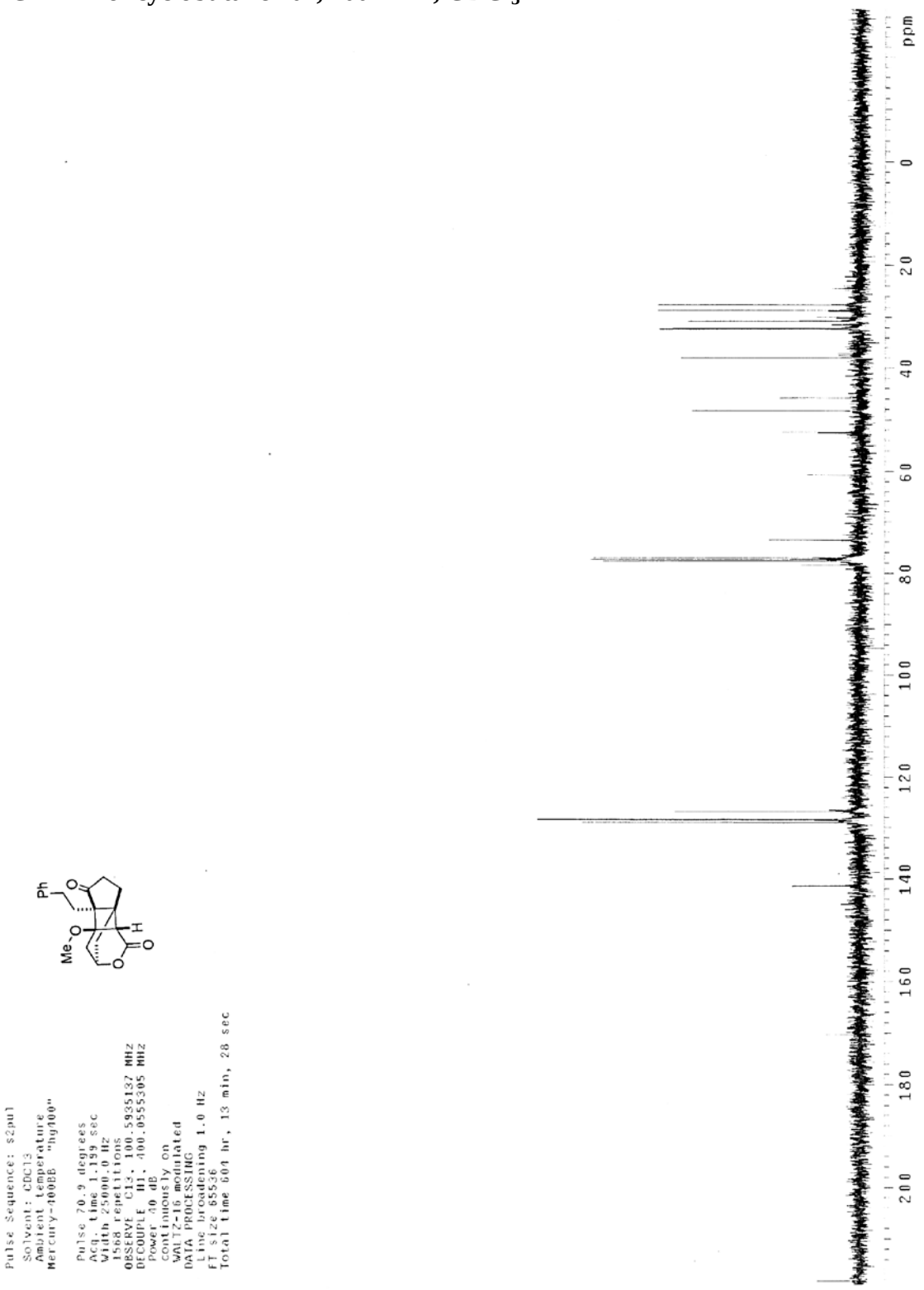

^{1}H-NMR of 2-Phenethyl-1-vinylcyclopent-2-enol 168, 400 MHz, $CDCl_3$

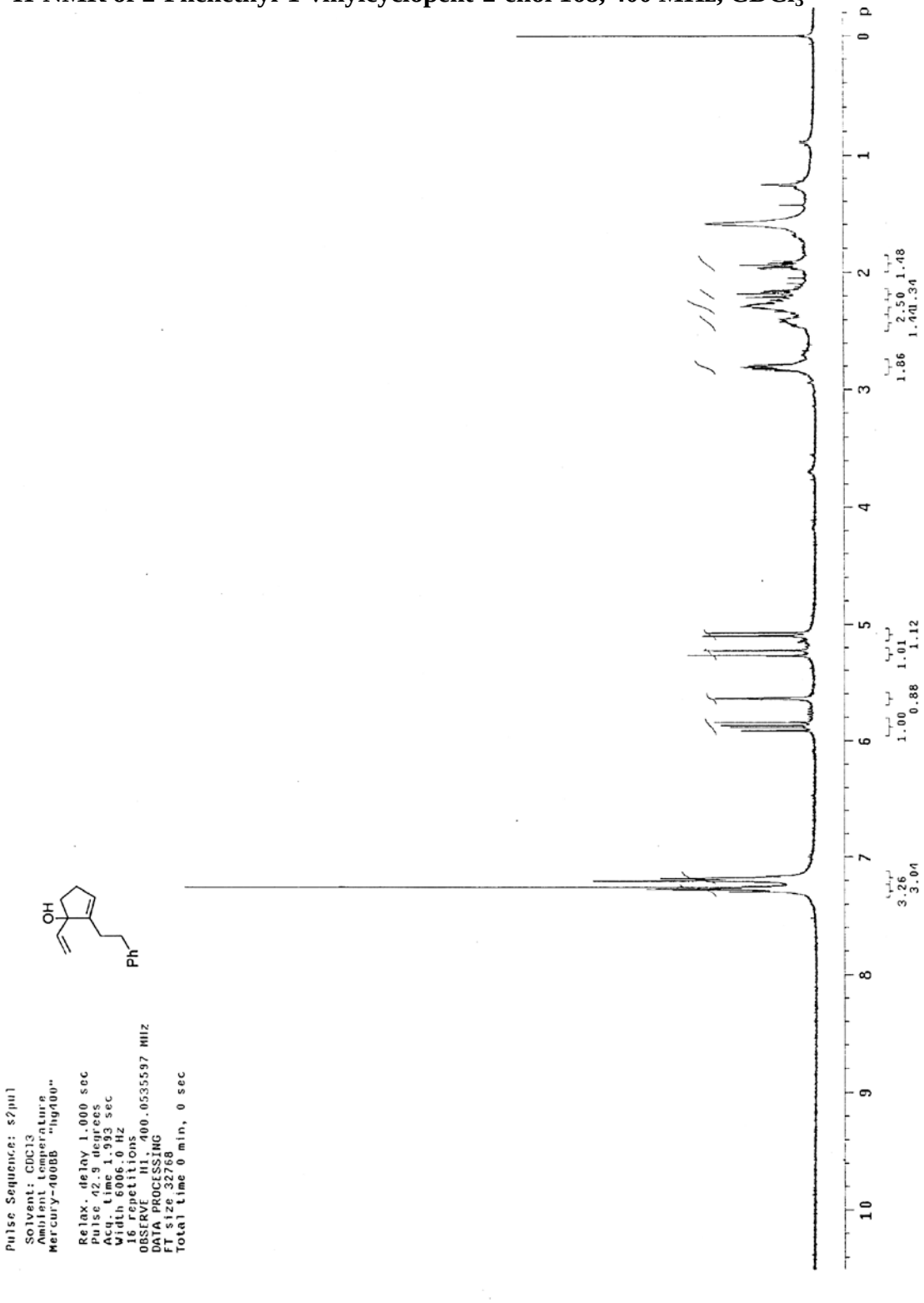

^{1}H-NMR of 2-phenethyl-3-vinylcyclopent-2-enone 169, 300 MHz, $CDCl_3$

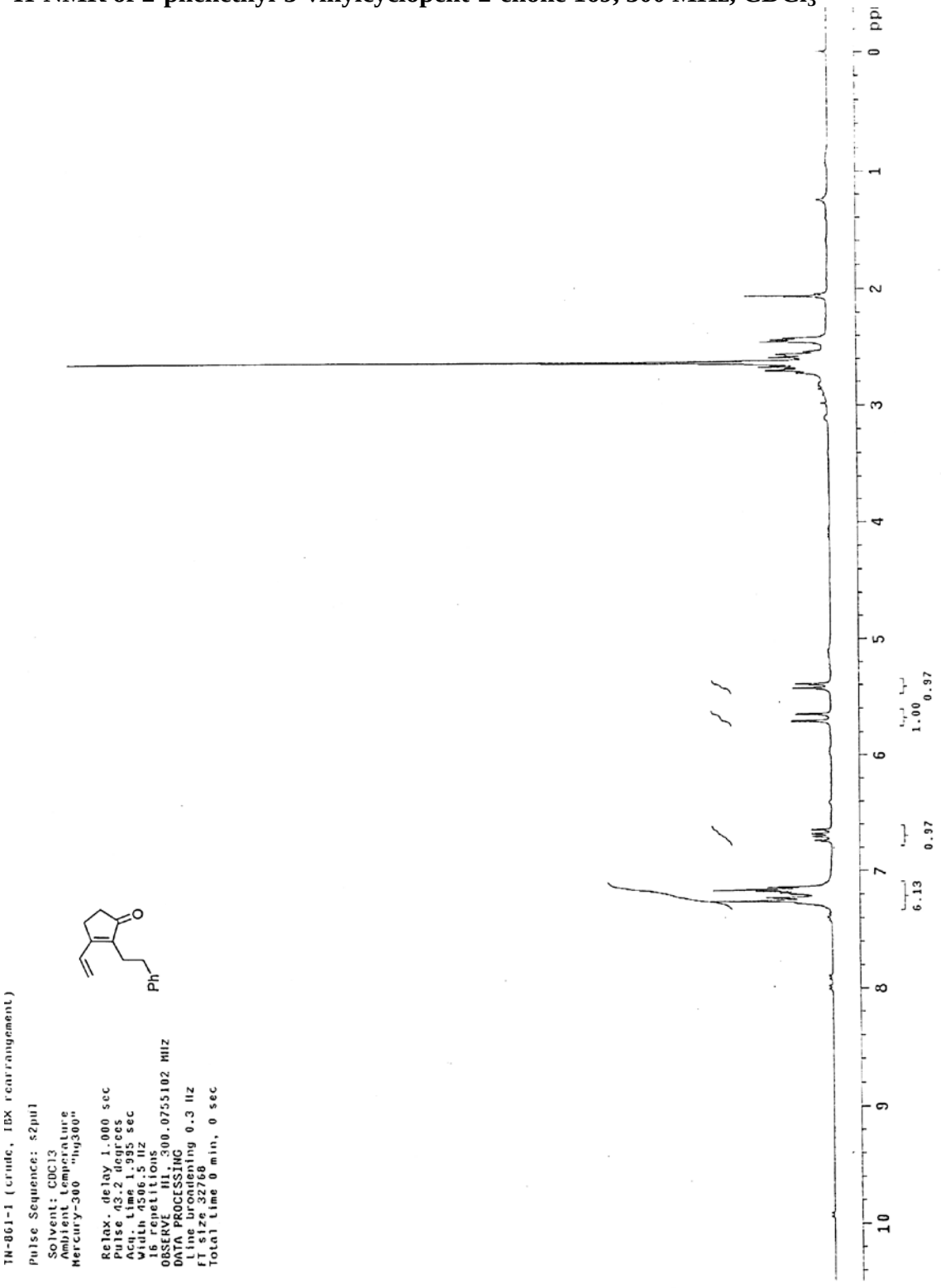

3-(1,2-Dihydroxyethyl)-2-phenethylcyclopent-2-enone 170, 400 MHz, $CDCl_3$

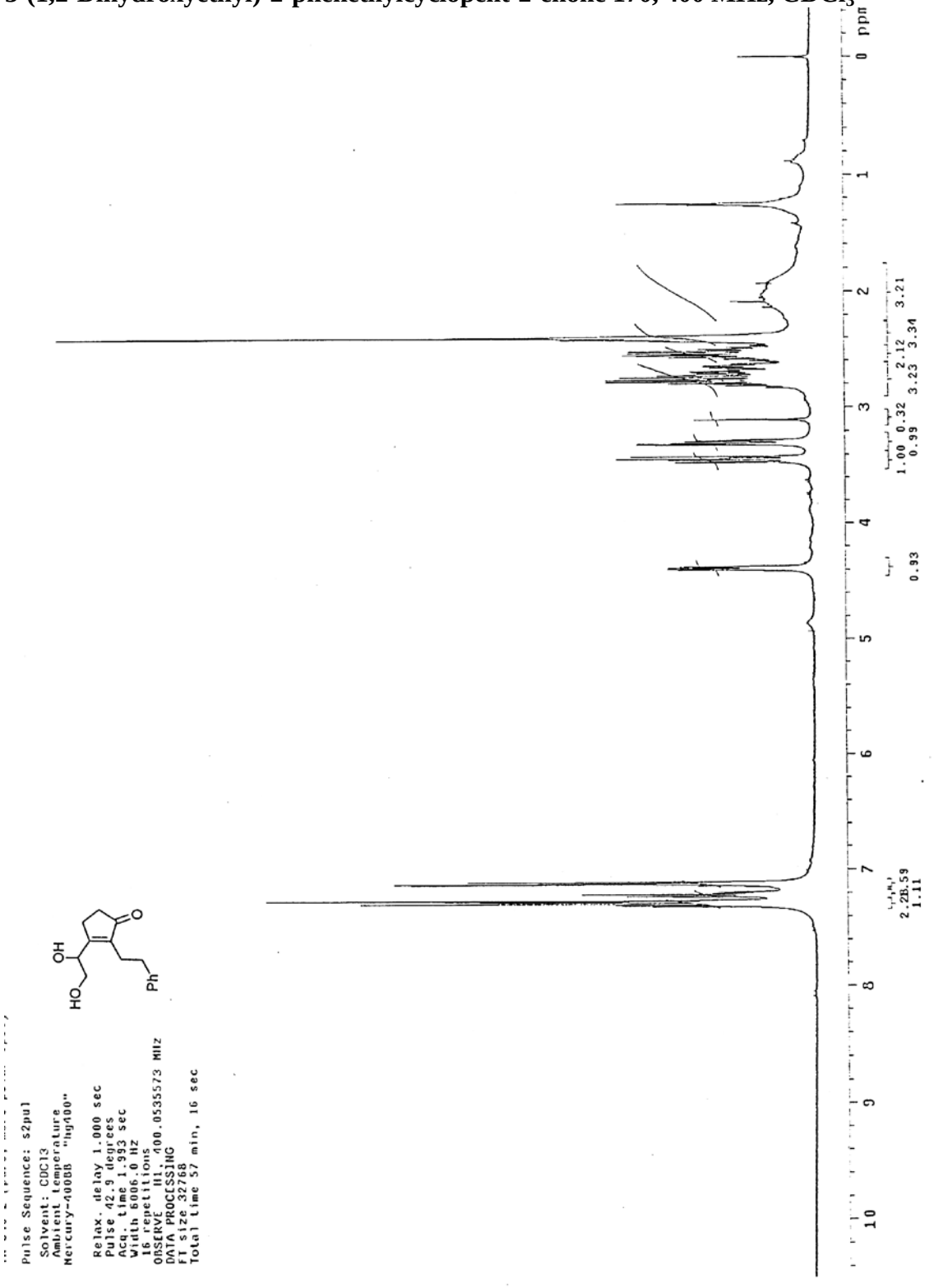

^{1}H-NMR of pivaloate 209, 400 MHz, $CDCl_3$

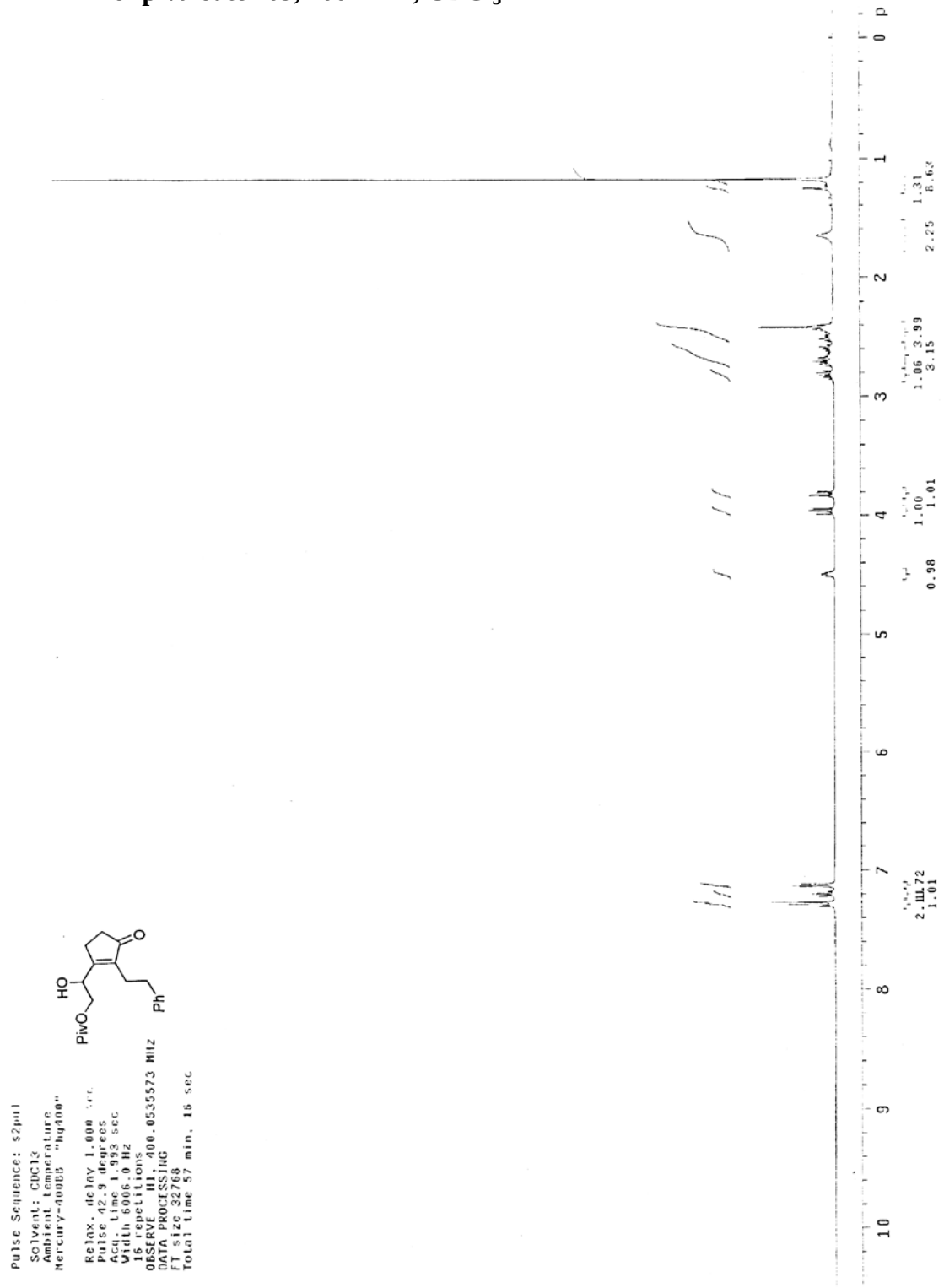

^{1}H-NMR of methyl ether 171, 300 MHz, $CDCl_3$

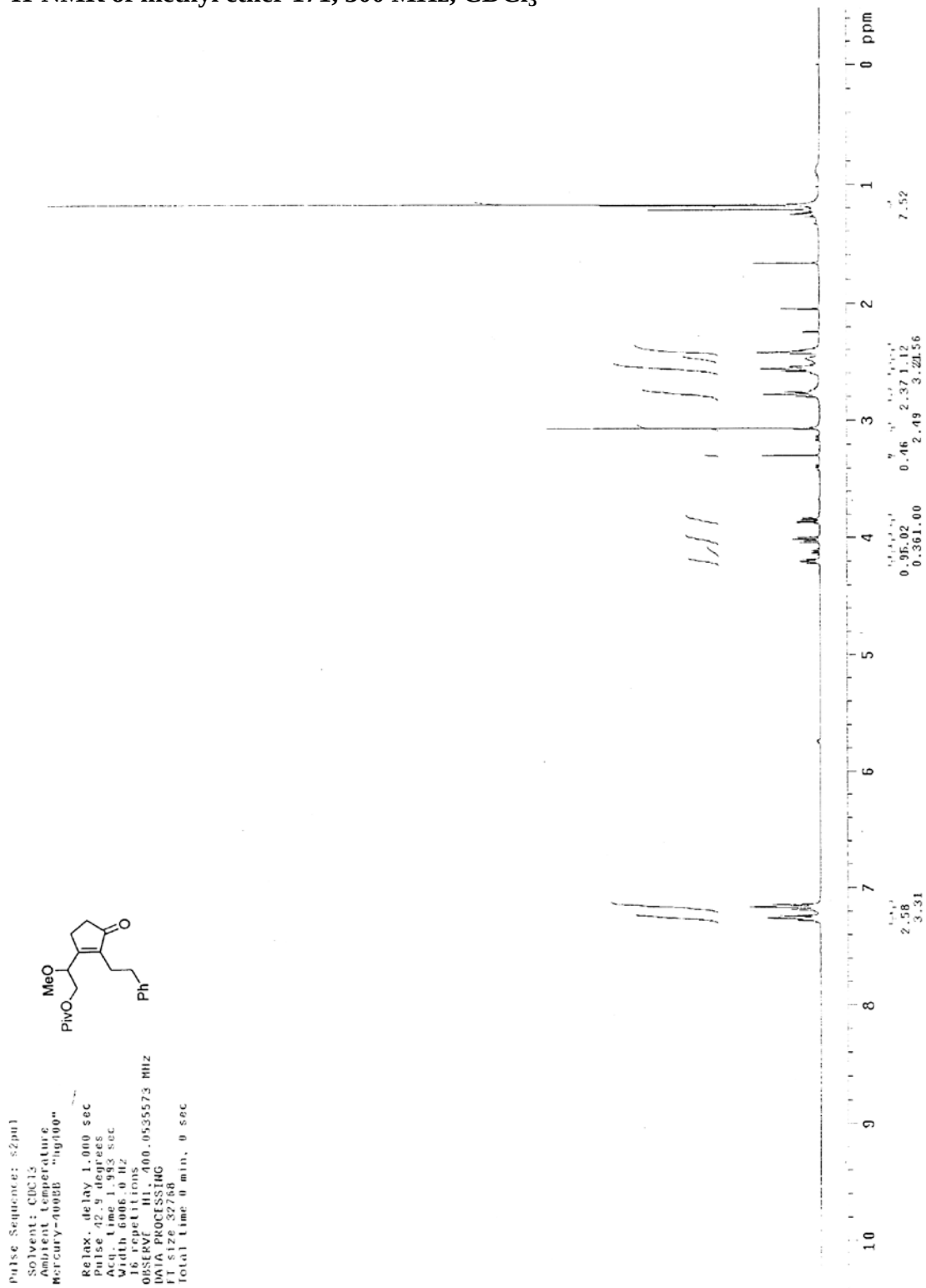

^{1}H-NMR of dienone 173, 300 MHz, $CDCl_3$

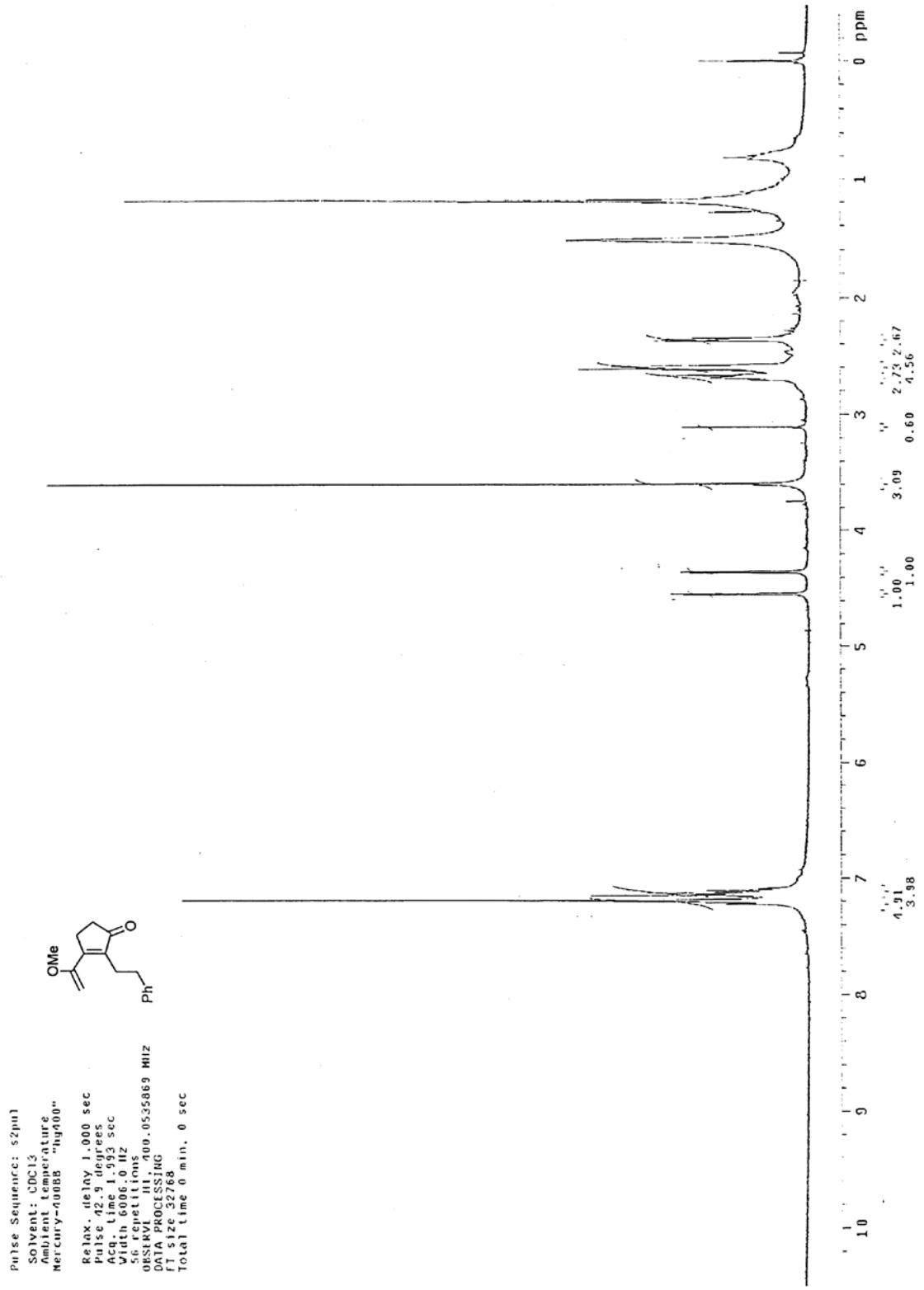

^{1}H-NMR of silyl ether 174, 300 MHz, $CDCl_3$

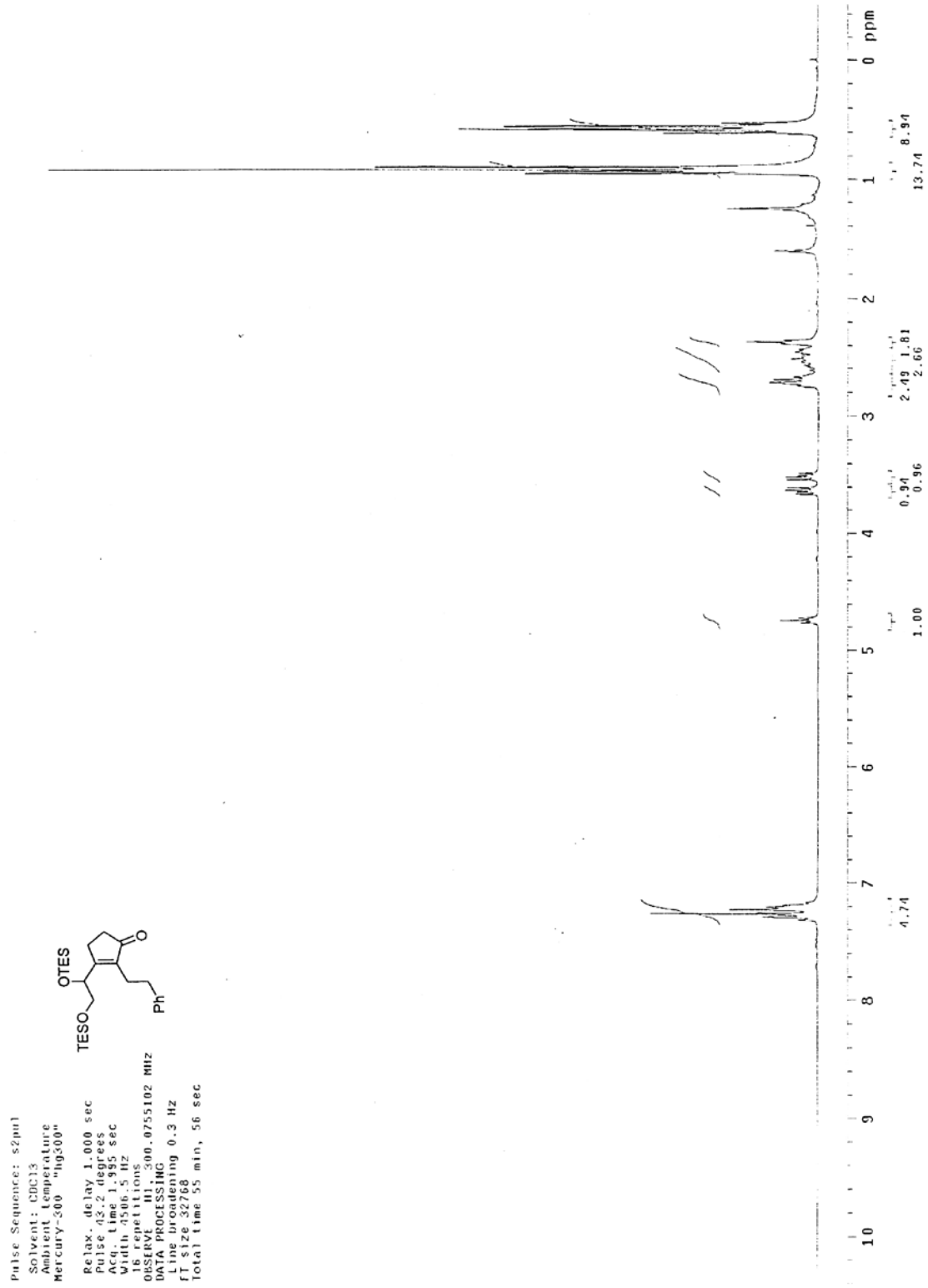

^{1}H-NMR of allylic alcohol 176, 400 MHz, $CDCl_3$

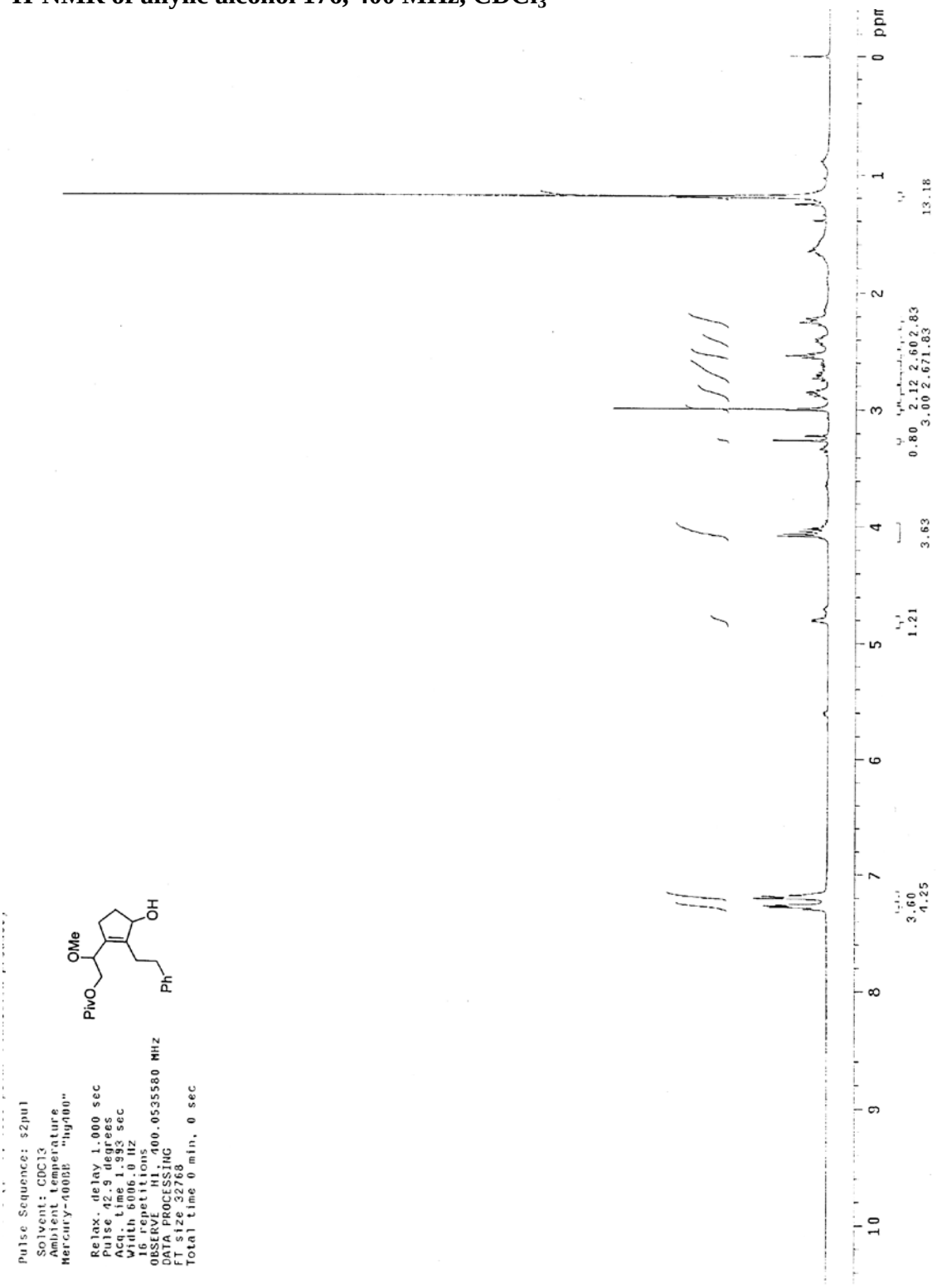

^{1}H-NMR of allylic alcohol 176b, 400 MHz, $CDCl_3$

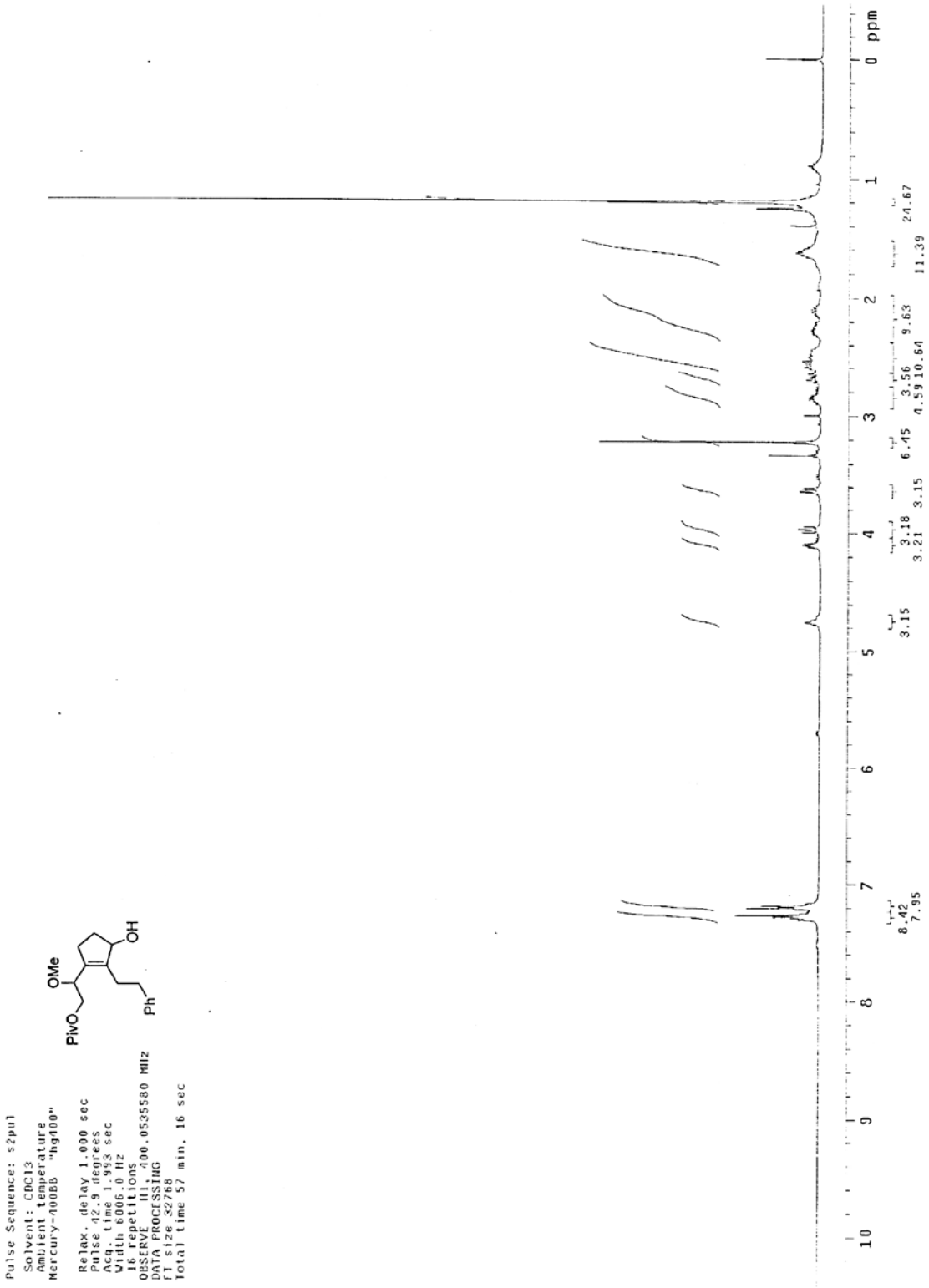

^{1}H-NMR of methyl ether 177, 300 MHz, $CDCl_3$

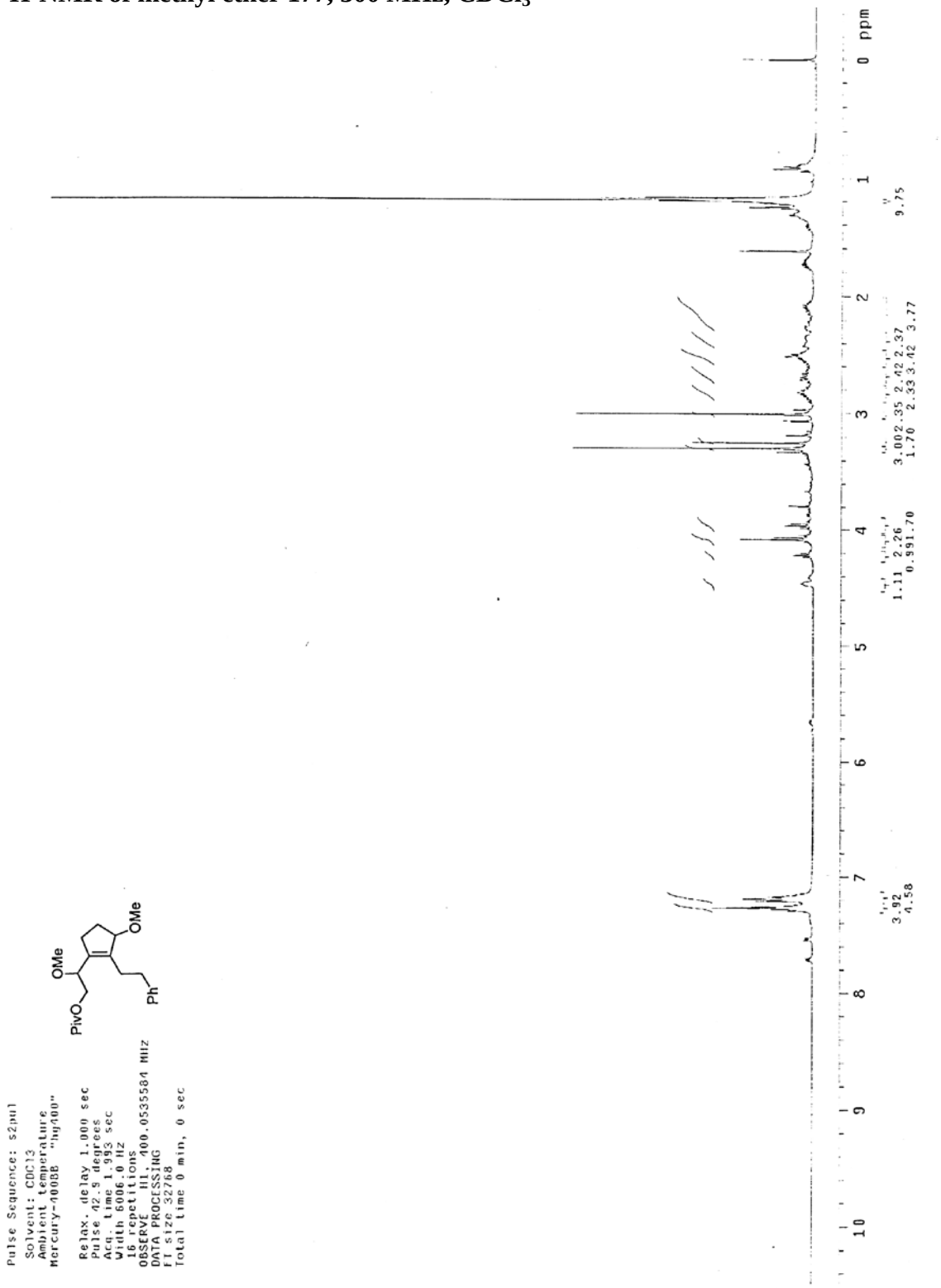

^{1}H-NMR of methyl ether 177b, 400 MHz, $CDCl_3$

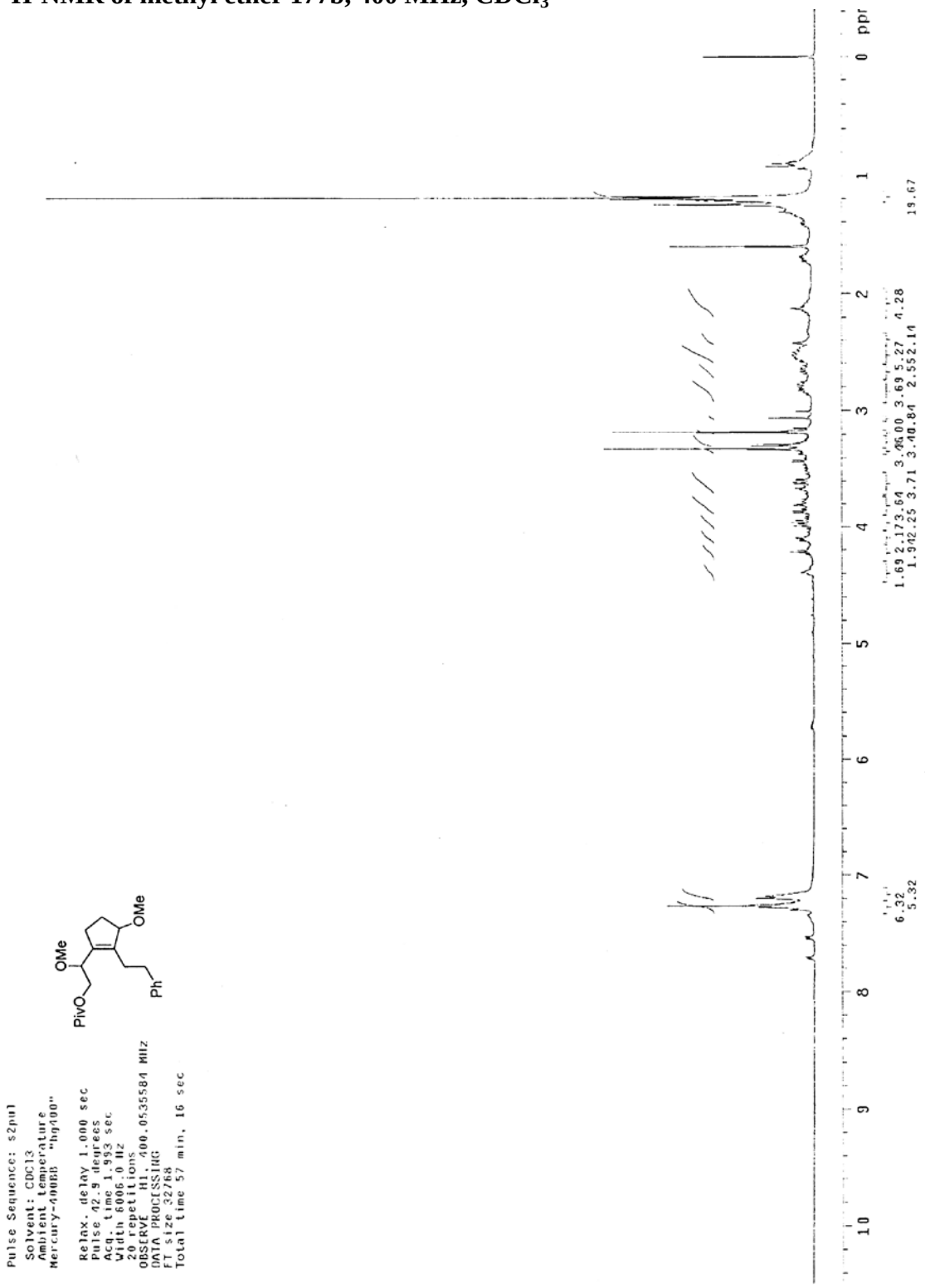

^{1}H-NMR of alcohol 178, 400 MHz, $CDCl_3$

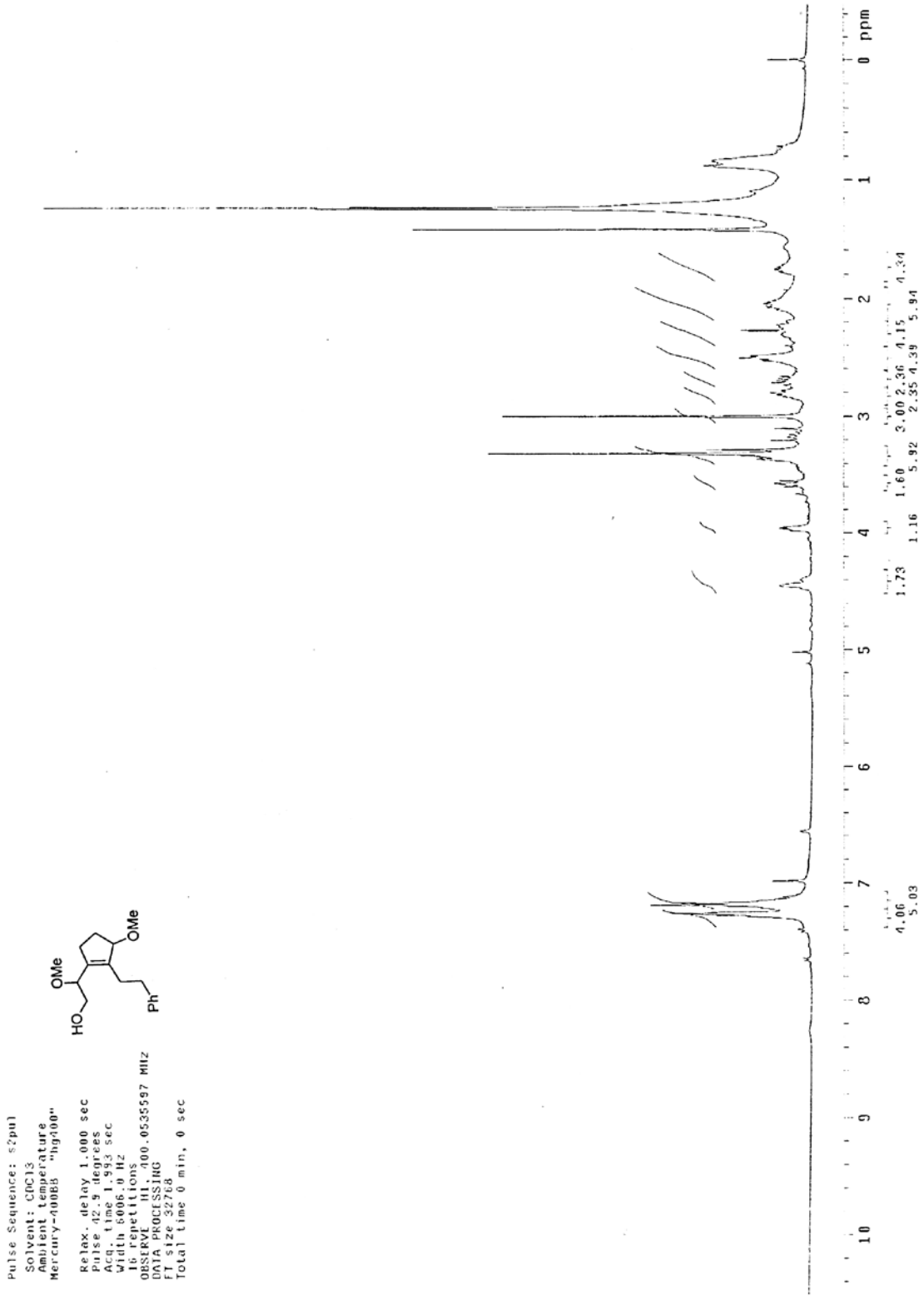

^{1}H-NMR of methyl ether 178b, 400 MHz, $CDCl_3$

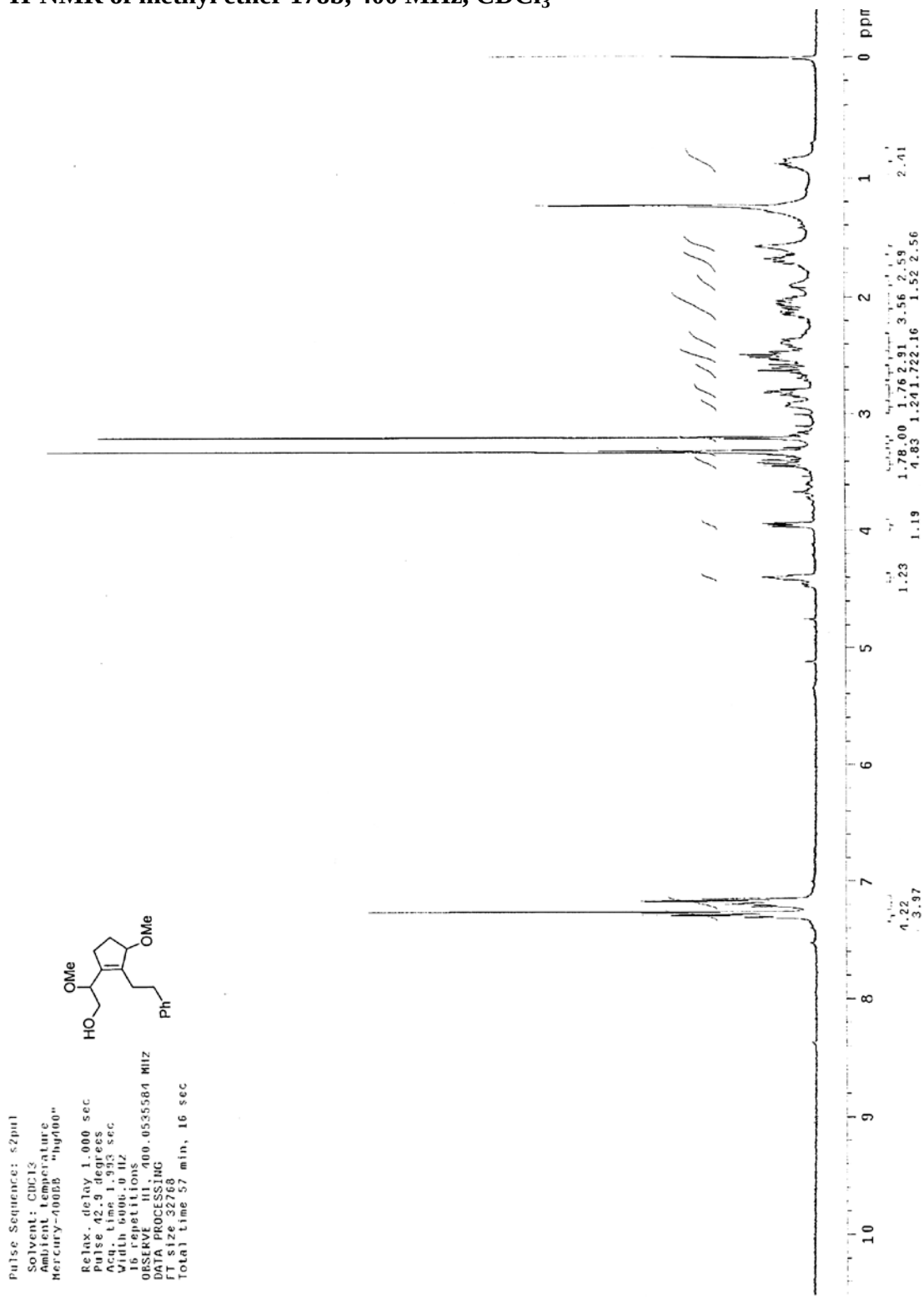

^{1}H-NMR of aldehyde 179, 400 MHz, $CDCl_3$

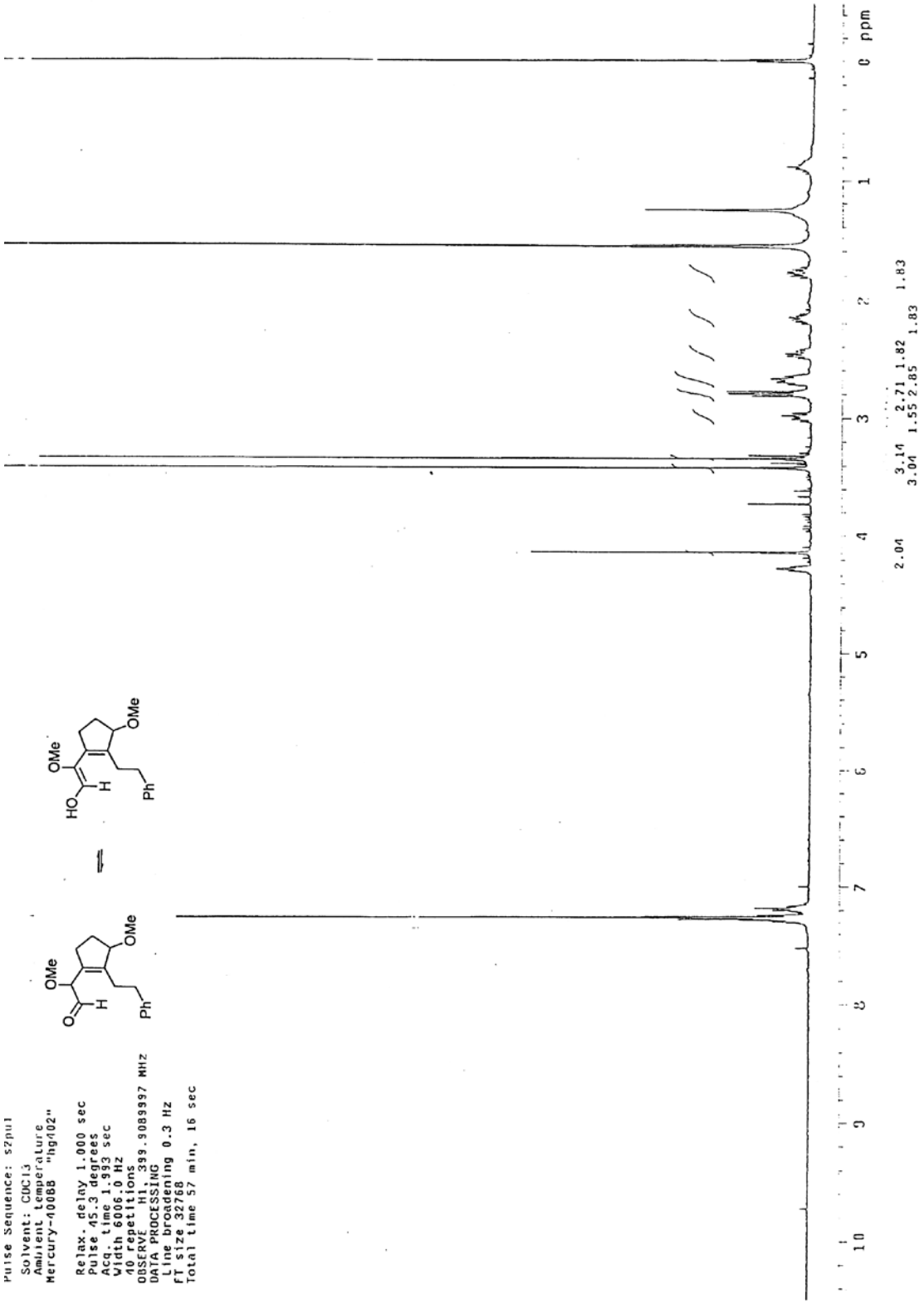

^{1}H-NMR of cyclobutane 208, 400 MHz, $CDCl_3$

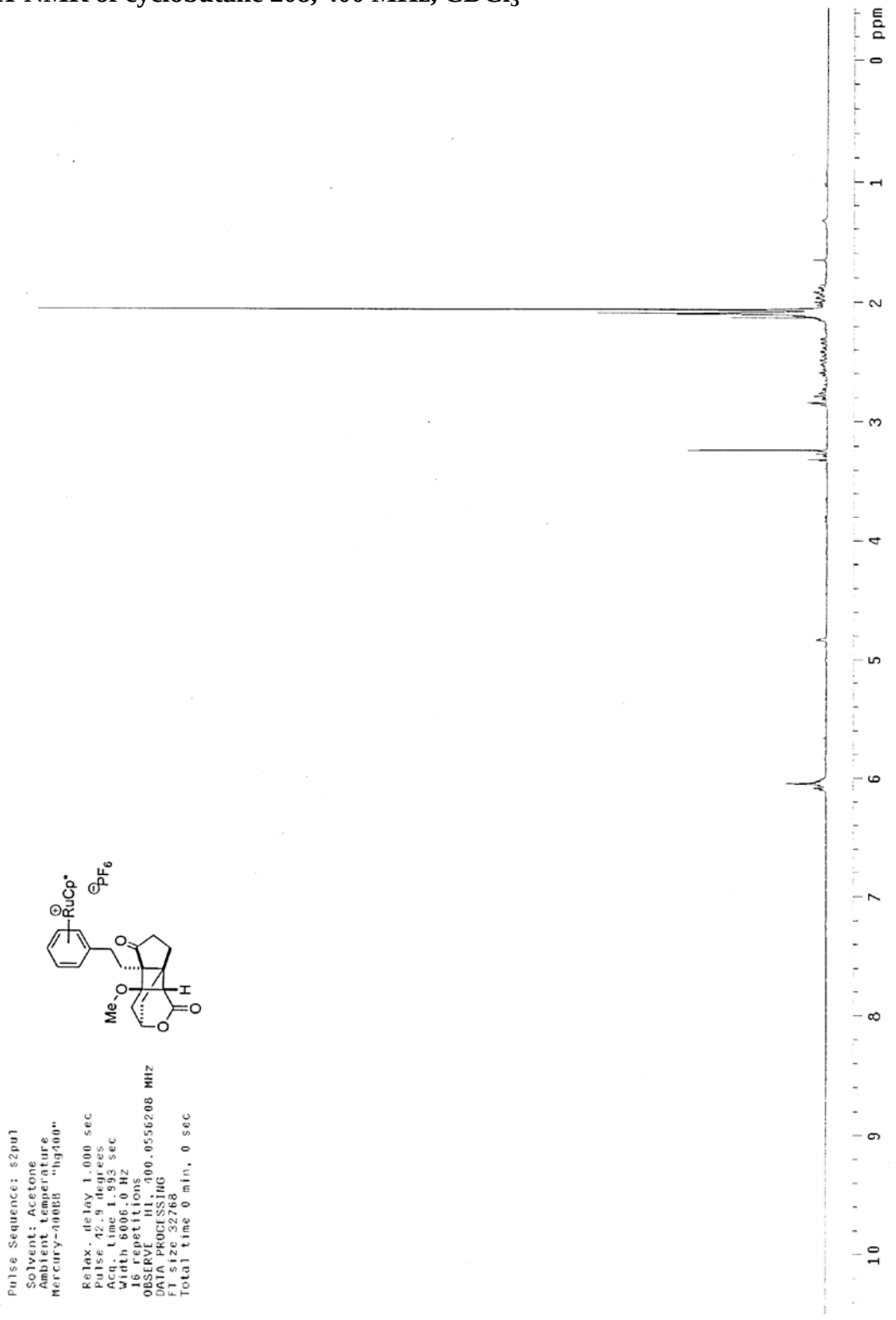

3.15 APPENDIX TWO: X-Ray Crystallography Reports Relevant to Chapter Three

X-ray Crystal Structure Report of Cyclobutane **208**

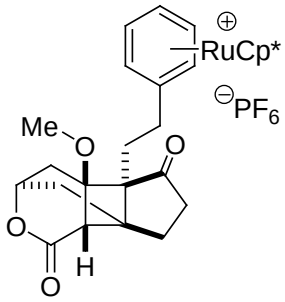

208

A colorless rod 0.33 x 0.22 x 0.11 mm in size was mounted on a Cryoloop with Paratone oil. Data were collected in a nitrogen gas stream at 153(2) K using phi and omega scans. Data collection was 99.2% complete to 25.00° in θ. A total of 20671 reflections were collected covering the indices, -10<=*h*<=10, -14<=*k*<=13, -18<=*l*<=18. 5694 reflections were found to be symmetry independent, with an R_{int} of 0.0225. Indexing and unit cell refinement indicated a triclinic lattice. The space group was found to P-1. The data were integrated using the Bruker SAINT software program and scaled using the SADABS software program. Solution by direct methods (SIR-2004) produced a complete heavy-atom phasing model consistent with the proposed structure. All non-hydrogen atoms were refined anisotropically by full-matrix least-squares (SHELXL-97). All hydrogen atoms were placed using a riding model. Their positions were constrained relative to their parent atom using the appropriate HFIX command in SHELXL-97.

Table 3.15.1 Crystal data and structure refinement for **208**.

X-ray ID	kob16	
Sample/notebook ID	KOB16	
Empirical formula	C30.50 H38 Cl F6 O4 P Ru	
Formula weight	750.10	
Temperature	153(2) K	
Wavelength	0.71073 Å	
Crystal system	Triclinic	
Space group	P-1	
Unit cell dimensions	a = 8.3487(7) Å	α= 92.7540(10)°
	b = 12.1778(11) Å	β= 91.4300(10)°
	c = 15.5732(14) Å	γ = 100.4910(10)°
Volume	1554.1(2) $Å^3$	
Z	2	
Density (calculated)	1.603 g/cm^3	
Absorption coefficient	0.713 mm^{-1}	
F(000)	766	
Crystal size	0.33 x 0.22 x 0.11 mm^3	
Theta range for data collection	1.70 to 25.46°	
Index ranges	-10<=h<=10, -14<=k<=13, -18<=l<=18	
Reflections collected	20671	
Independent reflections	5694 [R(int) = 0.0225]	
Completeness to theta = 25.00°	99.2 %	
Absorption correction	Multi-scan	
Refinement method	Full-matrix least-squares on F^2	
Data / restraints / parameters	5694 / 0 / 379	
Goodness-of-fit on F^2	1.076	
Final R indices [I>2sigma(I)]	R1 = 0.0267, wR2 = 0.0627	
R indices (all data)	R1 = 0.0291, wR2 = 0.0638	
Largest diff. peak and hole	0.556 and -0.347 e $Å^{-3}$	
SQUEEZE	0.5 mol. CH_2Cl_2/asymm unit	

Table 3.15.2 Atomic coordinates (x 10^4) and equivalent isotropic displacement parameters ($Å^2$x 10^3) for **208**. U(eq) is defined as one third of the trace of the orthogonalized U^{ij} tensor.

	x	y	z	U(eq)
Ru(1)	5491(1)	-1866(1)	6749(1)	15(1)
P(1)	1043(1)	2224(1)	6413(1)	23(1)
F(1)	1548(2)	3360(1)	6995(1)	41(1)
F(2)	-784(2)	2448(1)	6314(1)	36(1)
F(3)	1535(2)	2892(1)	5568(1)	38(1)
F(4)	2862(2)	1987(1)	6520(1)	34(1)
F(5)	560(2)	1553(1)	7260(1)	35(1)
F(6)	538(2)	1091(1)	5830(1)	32(1)
O(2)	7678(2)	5149(1)	8168(1)	34(1)
O(3)	6351(2)	5910(1)	9179(1)	33(1)
O(1)	5979(2)	1289(1)	10363(1)	31(1)
O(4)	8680(2)	3499(1)	10181(1)	29(1)
C(9)	3013(3)	-3598(2)	7905(2)	39(1)
C(30)	9815(3)	2780(2)	10337(2)	40(1)
C(8)	2152(3)	-1201(2)	7540(2)	35(1)
C(7)	2905(3)	-730(2)	5576(2)	31(1)
C(21)	3885(3)	1899(2)	9499(2)	30(1)
C(10)	4489(3)	-4523(2)	6212(2)	33(1)
C(25)	8116(3)	4071(2)	7888(2)	31(1)
C(22)	3984(3)	2479(2)	8644(2)	28(1)
C(28)	9117(3)	3719(2)	8624(2)	28(1)
C(24)	6498(3)	3262(2)	7697(1)	27(1)
C(27)	6500(3)	3950(2)	9238(1)	24(1)
C(6)	4368(3)	-2753(2)	4757(1)	27(1)
C(14)	8050(3)	-2057(2)	6557(2)	23(1)
C(26)	7966(3)	3348(2)	9348(1)	24(1)
C(29)	6807(3)	5086(2)	8893(2)	26(1)
C(18)	7454(3)	1265(2)	8593(1)	23(1)
C(5)	3930(3)	-3424(2)	6318(1)	21(1)

Table 3.15.2 (Continued)

C(17)	6092(3)	390(2)	8146(1)	22(1)
C(4)	3290(3)	-3000(2)	7087(1)	23(1)
C(3)	2886(3)	-1935(2)	6918(1)	23(1)
C(23)	5788(3)	2955(2)	8567(1)	23(1)
C(13)	7646(3)	-2280(2)	7414(2)	23(1)
C(20)	5605(3)	1748(2)	9742(1)	24(1)
C(12)	7021(3)	-1484(2)	7938(1)	22(1)
C(2)	3246(3)	-1710(2)	6043(1)	20(1)
C(19)	6806(3)	2224(2)	9057(1)	20(1)
C(16)	7221(3)	-240(2)	6748(1)	19(1)
C(11)	6793(3)	-454(2)	7609(1)	19(1)
C(1)	3887(2)	-2631(2)	5671(1)	19(1)
C(15)	7845(3)	-1033(2)	6224(1)	21(1)

Table 3.15.3 Bond lengths [Å] and angles [°] for **208**.

Ru(1)-C(5)	2.164(2)	C(10)-C(5)	1.500(3)
Ru(1)-C(4)	2.180(2)	C(25)-C(28)	1.526(4)
Ru(1)-C(1)	2.183(2)	C(25)-C(24)	1.534(4)
Ru(1)-C(3)	2.184(2)	C(22)-C(23)	1.523(3)
Ru(1)-C(2)	2.192(2)	C(28)-C(26)	1.530(3)
Ru(1)-C(13)	2.204(2)	C(24)-C(23)	1.527(3)
Ru(1)-C(12)	2.204(2)	C(27)-C(29)	1.489(3)
Ru(1)-C(14)	2.217(2)	C(27)-C(26)	1.547(3)
Ru(1)-C(11)	2.227(2)	C(27)-C(23)	1.581(3)
Ru(1)-C(16)	2.228(2)	C(6)-C(1)	1.497(3)
Ru(1)-C(15)	2.234(2)	C(14)-C(15)	1.409(3)
P(1)-F(6)	1.5982(14)	C(14)-C(13)	1.412(3)
P(1)-F(1)	1.5999(15)	C(26)-C(19)	1.566(3)
P(1)-F(4)	1.6020(14)	C(18)-C(19)	1.532(3)
P(1)-F(2)	1.6032(15)	C(18)-C(17)	1.536(3)
P(1)-F(3)	1.6039(15)	C(5)-C(4)	1.434(3)
P(1)-F(5)	1.6046(14)	C(5)-C(1)	1.434(3)
O(2)-C(29)	1.356(3)	C(17)-C(11)	1.502(3)
O(2)-C(25)	1.474(3)	C(4)-C(3)	1.433(3)
O(3)-C(29)	1.205(3)	C(3)-C(2)	1.432(3)
O(1)-C(20)	1.203(3)	C(23)-C(19)	1.551(3)
O(4)-C(26)	1.404(3)	C(13)-C(12)	1.417(3)
O(4)-C(30)	1.426(3)	C(20)-C(19)	1.542(3)
C(9)-C(4)	1.499(3)	C(12)-C(11)	1.419(3)
C(8)-C(3)	1.503(3)	C(2)-C(1)	1.433(3)
C(7)-C(2)	1.493(3)	C(16)-C(15)	1.415(3)
C(21)-C(20)	1.522(3)	C(16)-C(11)	1.420(3)
C(21)-C(22)	1.533(3)		

C(5)-Ru(1)-C(4)	38.55(8)	C(4)-Ru(1)-C(3)	38.33(9)
C(5)-Ru(1)-C(1)	38.51(8)	C(1)-Ru(1)-C(3)	64.12(8)
C(4)-Ru(1)-C(1)	64.23(8)	C(5)-Ru(1)-C(2)	64.31(8)
C(5)-Ru(1)-C(3)	64.44(8)	C(4)-Ru(1)-C(2)	64.05(8)

Table 3.15.3 (Continued)

C(1)-Ru(1)-C(2)	38.22(8)	C(14)-Ru(1)-C(16)	66.69(8)
C(3)-Ru(1)-C(2)	38.21(8)	C(11)-Ru(1)-C(16)	37.18(7)
C(5)-Ru(1)-C(13)	107.55(8)	C(5)-Ru(1)-C(15)	129.15(8)
C(4)-Ru(1)-C(13)	110.39(8)	C(4)-Ru(1)-C(15)	167.20(8)
C(1)-Ru(1)-C(13)	134.67(8)	C(1)-Ru(1)-C(15)	108.21(8)
C(3)-Ru(1)-C(13)	140.51(9)	C(3)-Ru(1)-C(15)	149.79(9)
C(2)-Ru(1)-C(13)	171.82(8)	C(2)-Ru(1)-C(15)	117.19(8)
C(5)-Ru(1)-C(12)	128.53(8)	C(13)-Ru(1)-C(15)	66.78(8)
C(4)-Ru(1)-C(12)	106.42(8)	C(12)-Ru(1)-C(15)	79.12(8)
C(1)-Ru(1)-C(12)	166.94(8)	C(14)-Ru(1)-C(15)	36.92(8)
C(3)-Ru(1)-C(12)	114.95(8)	C(11)-Ru(1)-C(15)	67.23(8)
C(2)-Ru(1)-C(12)	148.01(8)	C(16)-Ru(1)-C(15)	36.97(7)
C(13)-Ru(1)-C(12)	37.50(8)	F(6)-P(1)-F(1)	179.79(10)
C(5)-Ru(1)-C(14)	107.83(8)	F(6)-P(1)-F(4)	90.02(8)
C(4)-Ru(1)-C(14)	134.00(9)	F(1)-P(1)-F(4)	90.07(8)
C(1)-Ru(1)-C(14)	111.72(8)	F(6)-P(1)-F(2)	89.78(8)
C(3)-Ru(1)-C(14)	171.91(8)	F(1)-P(1)-F(2)	90.13(8)
C(2)-Ru(1)-C(14)	142.18(8)	F(4)-P(1)-F(2)	179.32(9)
C(13)-Ru(1)-C(14)	37.26(8)	F(6)-P(1)-F(3)	89.77(8)
C(12)-Ru(1)-C(14)	67.38(8)	F(1)-P(1)-F(3)	90.04(9)
C(5)-Ru(1)-C(11)	160.94(8)	F(4)-P(1)-F(3)	90.21(8)
C(4)-Ru(1)-C(11)	124.14(8)	F(2)-P(1)-F(3)	90.44(8)
C(1)-Ru(1)-C(11)	155.30(8)	F(6)-P(1)-F(5)	90.20(8)
C(3)-Ru(1)-C(11)	106.83(8)	F(1)-P(1)-F(5)	89.99(8)
C(2)-Ru(1)-C(11)	120.33(8)	F(4)-P(1)-F(5)	89.51(8)
C(13)-Ru(1)-C(11)	67.57(8)	F(2)-P(1)-F(5)	89.84(8)
C(12)-Ru(1)-C(11)	37.35(8)	F(3)-P(1)-F(5)	179.72(9)
C(14)-Ru(1)-C(11)	79.78(8)	C(29)-O(2)-C(25)	112.84(17)
C(5)-Ru(1)-C(16)	161.88(8)	C(26)-O(4)-C(30)	113.61(18)
C(4)-Ru(1)-C(16)	155.81(8)	C(20)-C(21)-C(22)	106.83(19)
C(1)-Ru(1)-C(16)	125.60(8)	O(2)-C(25)-C(28)	107.05(19)
C(3)-Ru(1)-C(16)	121.40(8)	O(2)-C(25)-C(24)	105.9(2)
C(2)-Ru(1)-C(16)	108.63(8)	C(28)-C(25)-C(24)	112.88(19)
C(13)-Ru(1)-C(16)	78.89(8)	C(23)-C(22)-C(21)	104.46(19)
C(12)-Ru(1)-C(16)	66.75(8)	C(25)-C(28)-C(26)	108.2(2)

Table 3.15.3 (Continued)

C(23)-C(24)-C(25)	106.58(18)	C(8)-C(3)-Ru(1)	125.54(16)
C(29)-C(27)-C(26)	118.00(19)	C(22)-C(23)-C(24)	121.1(2)
C(29)-C(27)-C(23)	115.78(19)	C(22)-C(23)-C(19)	109.13(18)
C(26)-C(27)-C(23)	85.75(16)	C(24)-C(23)-C(19)	111.80(18)
C(15)-C(14)-C(13)	119.89(19)	C(22)-C(23)-C(27)	114.97(18)
C(15)-C(14)-Ru(1)	72.22(12)	C(24)-C(23)-C(27)	107.26(18)
C(13)-C(14)-Ru(1)	70.86(12)	C(19)-C(23)-C(27)	87.66(16)
O(4)-C(26)-C(28)	115.31(19)	C(14)-C(13)-C(12)	120.2(2)
O(4)-C(26)-C(27)	113.26(17)	C(14)-C(13)-Ru(1)	71.88(13)
C(28)-C(26)-C(27)	106.39(19)	C(12)-C(13)-Ru(1)	71.27(12)
O(4)-C(26)-C(19)	120.25(18)	O(1)-C(20)-C(21)	125.2(2)
C(28)-C(26)-C(19)	109.53(17)	O(1)-C(20)-C(19)	124.3(2)
C(27)-C(26)-C(19)	88.35(17)	C(21)-C(20)-C(19)	110.45(19)
O(3)-C(29)-O(2)	119.2(2)	C(13)-C(12)-C(11)	120.6(2)
O(3)-C(29)-C(27)	127.3(2)	C(13)-C(12)-Ru(1)	71.23(12)
O(2)-C(29)-C(27)	113.51(18)	C(11)-C(12)-Ru(1)	72.19(12)
C(19)-C(18)-C(17)	112.67(18)	C(3)-C(2)-C(1)	108.03(19)
C(4)-C(5)-C(1)	108.00(19)	C(3)-C(2)-C(7)	126.3(2)
C(4)-C(5)-C(10)	125.5(2)	C(1)-C(2)-C(7)	125.6(2)
C(1)-C(5)-C(10)	126.5(2)	C(3)-C(2)-Ru(1)	70.59(12)
C(4)-C(5)-Ru(1)	71.36(12)	C(1)-C(2)-Ru(1)	70.54(12)
C(1)-C(5)-Ru(1)	71.48(12)	C(7)-C(2)-Ru(1)	127.74(16)
C(10)-C(5)-Ru(1)	124.36(16)	C(18)-C(19)-C(20)	109.42(18)
C(11)-C(17)-C(18)	110.83(18)	C(18)-C(19)-C(23)	121.26(18)
C(3)-C(4)-C(5)	107.93(19)	C(20)-C(19)-C(23)	101.29(18)
C(3)-C(4)-C(9)	126.2(2)	C(18)-C(19)-C(26)	121.30(19)
C(5)-C(4)-C(9)	125.8(2)	C(20)-C(19)-C(26)	114.47(17)
C(3)-C(4)-Ru(1)	70.98(12)	C(23)-C(19)-C(26)	86.13(16)
C(5)-C(4)-Ru(1)	70.09(12)	C(15)-C(16)-C(11)	121.2(2)
C(9)-C(4)-Ru(1)	126.93(16)	C(15)-C(16)-Ru(1)	71.76(12)
C(2)-C(3)-C(4)	108.06(18)	C(11)-C(16)-Ru(1)	71.36(12)
C(2)-C(3)-C(8)	125.8(2)	C(12)-C(11)-C(16)	118.35(19)
C(4)-C(3)-C(8)	126.1(2)	C(12)-C(11)-C(17)	121.48(19)
C(2)-C(3)-Ru(1)	71.20(12)	C(16)-C(11)-C(17)	120.16(19)
C(4)-C(3)-Ru(1)	70.69(12)	C(12)-C(11)-Ru(1)	70.46(12)

Table 3.15.3 (Continued)

C(16)-C(11)-Ru(1)	71.46(12)	C(2)-C(1)-Ru(1)	71.23(12)
C(17)-C(11)-Ru(1)	128.70(15)	C(5)-C(1)-Ru(1)	70.01(12)
C(2)-C(1)-C(5)	107.97(18)	C(6)-C(1)-Ru(1)	125.89(15)
C(2)-C(1)-C(6)	125.6(2)	C(14)-C(15)-C(16)	119.8(2)
C(5)-C(1)-C(6)	126.4(2)	C(14)-C(15)-Ru(1)	70.86(12)
		C(16)-C(15)-Ru(1)	71.27(12)

Table 3.15.4 Anisotropic displacement parameters ($Å^2 x\ 10^3$) for **208**. The anisotropic displacement factor exponent takes the form: $-2\pi^2[\ h^2 a^{*2} U^{11} + ... + 2\ h\ k\ a^*\ b^*\ U^{12}\ ]$.

U^{11}	U^{22}	U^{33}	U^{23}	U^{13}	U^{12}
Ru(1)15(1)	15(1)	15(1)	-2(1)	1(1)	1(1)
P(1)21(1)	26(1)	23(1)	-1(1)	5(1)	2(1)
F(1)43(1)	33(1)	42(1)	-11(1)	7(1)	-5(1)
F(2)26(1)	36(1)	48(1)	-2(1)	5(1)	12(1)
F(3)40(1)	45(1)	30(1)	12(1)	6(1)	6(1)
F(4)21(1)	51(1)	28(1)	3(1)	4(1)	5(1)
F(5)34(1)	41(1)	28(1)	7(1)	12(1)	2(1)
F(6)31(1)	30(1)	33(1)	-8(1)	0(1)	8(1)
O(2)53(1)	19(1)	29(1)	2(1)	17(1)	5(1)
O(3)39(1)	22(1)	38(1)	-5(1)	8(1)	7(1)
O(1)36(1)	30(1)	21(1)	4(1)	2(1)	-5(1)
O(4)30(1)	30(1)	24(1)	-7(1)	-1(1)	-2(1)
C(9)34(2)	50(2)	26(1)	11(1)	0(1)	-11(1)
C(30)32(1)	53(2)	34(1)	-4(1)	-6(1)	10(1)
C(8)21(1)	52(2)	32(1)	-15(1)	2(1)	9(1)
C(7)29(1)	28(1)	35(1)	1(1)	-8(1)	9(1)
C(21)28(1)	31(1)	30(1)	-6(1)	6(1)	1(1)
C(10)32(1)	18(1)	47(2)	-3(1)	-7(1)	1(1)
C(25)48(2)	18(1)	27(1)	0(1)	20(1)	2(1)
C(22)27(1)	28(1)	28(1)	-6(1)	1(1)	3(1)
C(28)30(1)	18(1)	35(1)	-6(1)	9(1)	-2(1)
C(24)42(2)	24(1)	16(1)	1(1)	5(1)	8(1)
C(27)30(1)	20(1)	20(1)	-4(1)	7(1)	1(1)
C(6)25(1)	35(1)	18(1)	-5(1)	2(1)	0(1)
C(14)15(1)	21(1)	31(1)	-8(1)	-1(1)	3(1)
C(26)28(1)	19(1)	21(1)	-4(1)	2(1)	-2(1)
C(29)32(1)	21(1)	24(1)	-3(1)	5(1)	1(1)
C(18)24(1)	19(1)	23(1)	-4(1)	3(1)	1(1)
C(5)19(1)	19(1)	22(1)	-1(1)	-1(1)	-3(1)
C(17)24(1)	19(1)	21(1)	-4(1)	5(1)	-2(1)
C(4)15(1)	30(1)	21(1)	1(1)	0(1)	-7(1)

Table 3.15.4 (Continued)

C(3)12(1)	31(1)	22(1)	-7(1)	0(1)	0(1)
C(23)29(1)	20(1)	18(1)	-4(1)	4(1)	2(1)
C(13)17(1)	18(1)	32(1)	1(1)	-7(1)	-1(1)
C(20)29(1)	20(1)	20(1)	-6(1)	5(1)	-2(1)
C(12)20(1)	24(1)	18(1)	2(1)	-4(1)	-4(1)
C(2)15(1)	22(1)	23(1)	-3(1)	-1(1)	2(1)
C(19)25(1)	19(1)	15(1)	-2(1)	3(1)	-1(1)
C(16)18(1)	16(1)	20(1)	0(1)	1(1)	0(1)
C(11)19(1)	16(1)	18(1)	-3(1)	0(1)	-3(1)
C(1)14(1)	22(1)	19(1)	-4(1)	-1(1)	-1(1)
C(15)17(1)	23(1)	20(1)	-3(1)	1(1)	-2(1)

Table 3.15.5 Hydrogen coordinates (x 10^4) and isotropic displacement parameters ($Å^2$x 10^3) for **208**.

	x	y	z	U(eq)
H(9A)	1916	-4054	7882	58
H(9B)	3120	-3049	8393	58
H(9C)	3822	-4081	7972	58
H(30A)	10267	2927	10927	59
H(30B)	10698	2919	9932	59
H(30C)	9258	1998	10261	59
H(8A)	960	-1398	7489	53
H(8B)	2500	-416	7409	53
H(8C)	2515	-1310	8128	53
H(7A)	1800	-904	5317	46
H(7B)	3695	-564	5123	46
H(7C)	2997	-79	5981	46
H(21A)	3468	2364	9949	36
H(21B)	3144	1165	9433	36
H(10A)	3567	-5106	6014	49
H(10B)	4923	-4714	6765	49
H(10C)	5344	-4468	5787	49
H(25A)	8770	4156	7358	38
H(22A)	3581	1936	8158	33
H(22B)	3333	3082	8654	33
H(28A)	9974	4354	8835	34
H(28B)	9651	3095	8423	34
H(24A)	5742	3624	7357	33
H(24B)	6684	2584	7366	33
H(27A)	5844	3928	9767	29
H(6A)	3419	-3124	4402	40
H(6B)	5228	-3204	4724	40
H(6C)	4773	-2012	4545	40
H(14A)	8285	-2673	6159	28
H(18A)	8054	894	9015	27

Table 3.15.5 (Continued)

H(18B)	8232	1575	8158	27
H(17A)	5393	4	8585	27
H(17B)	5405	768	7775	27
H(13A)	7605	-3053	7615	28
H(12A)	6542	-1708	8499	26
H(16A)	6858	403	6473	22
H(15A)	7924	-936	5591	25